Fixed-Pole Concept in 3D Beam Finite Elements - Relationship to Standard Approaches and Analysis of Different Interpolations

Gaćeša, Maja

University of Rijeka
Faculty of Civil Engineering

Maja Gaćeša

Fixed-Pole Concept in 3D Beam Finite Elements - Relationship to Standard Approaches and Analysis of Different Interpolations

Doctoral thesis

Supervisor: Prof. dr. sc. Gordan Jelenić

Rijeka, 2015

Mentor rada: dr. sc. Gordan Jelenić

Doktorski rad obranjen je dana 16. travnja 2015. na Građevinskome fakultetu Sveučilišta u Rijeci, pred povjerenstvom u sastavu:

1. Prof. dr. sc. Nenad Bićanić, predsjednik,
2. Prof. dr. sc. Goran Turkalj, Tehnički fakultet Sveučilišta u Rijeci, član,
3. Doc. dr. sc. Dragan Ribarić, član,
4. Prof. dr. sc. Miran Saje, član,
5. Prof. dr. sc. Dejan Zupan, Univerza v Ljubljani, Fakulteta za Gradbeništvo in geodezijo, vanjski član.

Acknowledgements

Tanja and Srećko – I love you so much. Since I was a little kid you have always let me make my own choices and supported me unconditionally. That's what parents are for, you would say. Thank you for teaching me of love and responsibility towards myself and others. Finally, thank you for providing me with food and comfort when I needed it most. Nina, my sweet little sister, thank you for being so patient and always helpful!

Maja, Domenika, Jelena, Nela, Josipa, Vedran – thank you for being there for me, thank you for always believing in me. I am truly grateful to have you in my life.

Miran, thank you for sharing with me this chapter of my life. It was pretty, pretty, pretty... pretty good.

Edita, Paulo and Leo – thank you for helping without being asked. Without your support in crucial moments, I would have been lost.

And finally, Gordan –

> *"In an ideal world your advisor would be a mentor, an expert in your field, a coach, an editor, and a career counsellor; someone to guide, teach and encourage you from the first glimmer of "the Right Topic" to your happy acceptance of a job offer from the institution of your choice. There are, however, few human beings who can fill that entire job description."*
>
> –Joan Bolker

– thank you for being one of the few.

I dedicate this thesis to the memory of my dear friend and colleague Nikola.

Your warm company and sarcastic comments will be missed.

Abstract

A family of geometrically exact spatial beam finite elements based on the fixed-pole approach is developed and presented in this thesis. All the proposed elements are derived from the principle of virtual work by interpolating the virtual spins (or virtual configurational spins).

The fixed-pole element is derived from the configuration-tensor approach. By utilising the standard Galerkin approach this element turns out to have non-standard six-dimensional system unknowns. In order to reap the benefits of the fixed-pole approach, but still be able to have standard system unknowns, a modification of the fixed-pole approach is proposed: the non-standard and standard virtual quantities are related at the nodal level. This results in a family of modified-fixed pole elements, consisting of three interpolation options.

The fixed-pole and the modified fixed-pole formulations are tested with respect to their accuracy, strain-invariance, path-independence and robustness on a number of planar and spatial numerical examples. The results show that non-invariance and path-dependence is present in all formulations – in some formulations even in the planar case.

In the case of the modified-fixed pole formulation, these problems are overcome by (i) interpolating only the relative rotations between two nodes and (ii) implementing the generalised shape-functions. The repeated numerical tests show that results are strain-invariant, path-independent and that the solution procedure is more robust. Although the results obtained by employing Interpolation option 3 are somewhat improved in comparison to those before this intervention, they still exhibit some non-invariant and path-dependent behaviour.

In the case of the fixed-pole formulation, strain-invariance and path-independence is achieved by (i) interpolating only the relative configurations between two nodes and and (ii) by deriving and implementing six-dimensional shape functions. The results of the repeated numerical tests confirm that this intervention leads to strain-invariant, path-independent and more robust elements.

Keywords: geometrically exact beam theory, fixed-pole approach, strain invariance, path dependence

Sažetak

U disertaciji je predložena familija geometrijski točnih prostornih grednih elemenata koji su temeljeni na tzv. konceptu nepomičnog pola (fixed-pole approach). Sve predložene formulacije izvedene su iz principa virtualnoga rada uz interpolaciju virtualnih spinova (ili virtualnih konfiguracijskih spinova).

Fixed-pole element izveden je iz pristupa temeljenog na konfiguracijskome tenzoru. Primjenjujući standardnu Galerkinovu metodu diskretizacije, takav pristup rezultira nestandardnim stupnjevima slobode. Kako bi se zadržale prednosti fixed-pole pristupa uz istovremeno zadržavanje standardnih stupnjeva slobode, predlaže se modifikacija fixed-pole formulacije temeljena na povezivanju standardnih i nestandardnih virtualnih veličina na razini čvorova. Takva modifikacija rezultira familijom modificiranih fixed-pole elemenata koja se sastoji od tri interpolacijske opcije.

Kod svih predloženih formulacija ispitana je njihova točnost, objektivnost deformacija s obzirom na pomak krutoga tijela, ovisnost o putanji ka rješenju te robustnost. Zaključak numeričkih primjera je da sve predložene formulacije iskazuju nepovoljna svojstva neobjektivnosti i ovisnosti o putanji ka rješenju te da im je smanjena robustnost u odnosu na standardne formulacije.

U slučaju modificirane fixed-pole formulacije, problemi neobjektivnosti, ovisnosti o putanji ka rješenju te robustnosti rješeni su (i) interpolacijom relativnih rotacija između dva čvora te (ii) ugrađivanjem generaliziranih funkcija oblika. Ponovljeni numerički testovi pokazuju da su rezultati objektivni, ne ovise o putanji ka rješenju te da je povećana robustnost same procedure. Iako su i rezultati dobiveni korištenjem treće interpolacijske opcije poboljšani u odnosu na one prije ove intervencije, oni i dalje pokazuju znakove neobjektivnosti i ovisnosti o putanji ka rješenju, no u manjoj mjeri.

U slučaju fixed-pole formulacije, problem je otklonjen (i) interpolacijom relativnih konfiguracija između dva čvora te (ii) izvođenjem te ugrađivanjem novih, šesterodimenzionalnih funkcija oblika. Ponovljenim numeričkim testovima potvrđeno je da ovakva intervencija dovodi do objektivnih, neovisnih o putanji ka rješenju te robustnijih elemenata.

Ključne riječi: geometrijski točna gredna teorija, pristup nepomičnog pola, neobjektivnost mjera deformacije, ovisnost o putanji ka rješenju

Contents

Chapter 1

Introduction and motivation

1.1 Literature overview

The topic of this thesis is the development of a family of spatial beam finite elements based on the geometrically exact beam theory given by Reissner [1] for 2D beams and extended to 3D beams by Simo [2]. Implementation of this theory in a finite-element framework becomes non-trivial because of the properties of rotations in 3D. These are defined by orientation matrices, elements of a special orthogonal group SO(3), which is also a Lie group (see eg. [3]). By definition, a Lie group is also a differentiable manifold, and in order for the solution to stay on the manifold, we must acknowledge existence of the so-called exponential map, a specific operation between a Lie group and a related Lie algebra (in this case the algebra so(3) of 3D skew-symmetric tensors). This theory was first implemented by Simo and Vu-Quoc, interpolating the infinitesimal rotations, the so-called spin vectors [4]. Similar results can be obtained interpolating the incremental rotational changes (between two converged configurations) as proposed by e.g. Cardona and Géradin [5], or the total rotations (the change between the initial and current configuration) as given by e.g. Ibrahimbegović et. al. in [6].

In this thesis we want to shed more light on the fascinating and highly promising fixed-pole concept, emphasise some of its potentials and investigate alternative options of its implementation into the geometrically exact 3D beam theory to those currently available. Certain shortcomings of the currently available implementations are not well-known and here we address them and propose techniques to overcome them. In the context of this theory, the fixed-pole concept was first introduced by Borri and Bottasso in 1994 [7] and thoroughly researched in a series of subsequent papers [8–11]. In the context of simple-material and polar-material elastomechanics,

the concept was presented in [12, 13].

It appears that Borri and Bottasso were concerned with modelling curved mechanical elements such as wind or helicopter blades, for which it ceased to be obvious how to define a "proper" reference axis. In [7–9] they approached this problem by interpolating the kinematic quantities along the beam arc-length: the authors assumed that the reference axis of the beam element had a shape of a spatial helix and that both the translational and the rotational strain measures along it should be constant. This resulted in a so-called helicoidal interpolation. Although it does not appear that this was their chief motivation, such interpolation also solved the problem of non-invariance of the strain measures but it was naturally applied only to two-node elements [14]. Their idea has been recently explored and generalised to an element of arbitrary order by Papa Dukić et. al. [15].

In [10, 11] Bottasso and Borri with co-workers managed to merge the displacement and the rotation fields and introduced a configuration tensor which uniquely determined both the position and the orientation of a cross-section under consideration. This tensor turned out to be an element of what the authors called the special group of rigid motions SR(6), a matrix representation of the special Euclidean group SE(3) [11] and a Lie group. They further proved the existence of a closed form of the exponential map between SR(6) and the related Lie algebra sr(6), which, in contrast to the earlier helicoidal interpolation, they now interpolated using Lagrangian polynomials. By employing all this, they obtained a very elegant formulation which used a unique operation for updating the kinematic fields. In the same paper [10] they have also proposed a modified Runge-Kutta integration scheme for the exponential map of motion – an algorithm that, by design, remains on the manifold SR(6) but can very easily be applied to the pure rotational dynamics problems in SO(3) by replacing the configuration tensor with the orientation matrix. This was the reason this paper has gained a lot of attention, especially in the field of flexible multi-body dynamics [16–19], modelling various contact conditions in multi-body systems [20–23], modelling shells in multi-body systems [24–26], as well as rigid body dynamics [27], although most attention was received in the field of energy conserving/decaying algorithms for structural and multi-body dynamics [28–38]. The complexities associated with simultaneous conservation of energy and momenta in 3D beams were explored in [39–42].

However, the configuration-tensor approach was researched only by Sonneville and co-workers [43–46] where they proposed a formulation for static and dynamic analysis of geometrically exact beams and multi-body systems which combined the ideas of the configuration tensor and

helicoidal interpolation based on a 4D matrix representation of SE(3) [7]. We emphasise the two distinct novelties proposed by Borri, Bottasso and their co-workers: the helicoidal interpolation and the configuration-tensor approach. Although they may go together, as they do in e.g. [44], there is no reason not to address (and implement) them separately. In our recent work [15] we have proposed a possible generalisation of the helicoidal interpolation [7] to higher-order elements without any reference to the configuration-tensor aspect of the fixed-pole approach. In this thesis, we identify the term fixed-pole approach with the use of the configuration tensor, and not with the use of the helicoidal interpolation.

Given the earlier-mentioned parallelism between the kinematics of 3D rotations in SO(3) and that of the rigid motions in SR(6) it becomes important to investigate the configuration-tensor approach in the light of certain implementational complexities present in the mechanical problems with large 3D rotations. In particular, Crisfield and Jelenić [47] detected that in such problems the approximated strain measures are non-invariant whenever the rotational variables are interpolated additively, regardless of the choice of the interpolated quantities – being it the iterative [4,48], the incremental [5,49] or the total rotations [6], and that this problem is present only in 3D. The relationship between the choice of the interpolated quantity and the strain-invariance of the underlying formulations was thoroughly researched by Romero in [50]. An invariant formulation was proposed in [51] which not only solved the problem of non-invariance of the strain measures but also the problem of path dependence which also existed in some of those formulations, by interpolating only the relative rotations between specific nodes i.e. the rotations from which the rigid-rotation is removed. Ibrahimbegović and Taylor [52] proposed a formulation based on the reparametrisation of the rotational vector while a similar approach was given recently by Ghosh and Roy in [53]. Quaternion-based invariant formulations were proposed in [54, 55]. Other authors approached this problem by avoiding the interpolation of the rotational variables altogether. For example Betsch and Steinmann [56] and Romero and Armero [57] interpolated the director fields defining the motion of the rod's cross-section, i.e. the base-vector triad. On the other hand, Zupan and Saje decided to interpolate the strain measures [58] or only curvatures [59], which resulted not only in an objective formulation, but also with increased accuracy of the formulation compared to standard approaches. Strain-invariant formulations were also proposed in [60, 61], and in the context of thin-walled beams in [62] as well as for solid finite elements in [13].

Obviously, the non-linearity of the rotational manifold SO(3) turns out to be incompatible

with the standard additive interpolation techniques of the finite-element method - the techniques designed to respect the properties of the linear (vector) spaces. For this reason, any formulation utilising an additive interpolation for the problems where the unknown functions are elements of any other non-linear manifold is also potentially prone to exhibit non-invariance and path-dependence and in this thesis special attention is devoted to investigating the extent to which it also applies to the configuration-tensor approach with the unknown functions belonging to SR(6). This potential short-coming of the configuration-tensor approach has not been systematically investigated so far, although the recent works of Sonneville and co-workers [43–46] address this issue for a two-node beam elements formulated in a 4D matrix representation of SE(3).

Additionally, the system unknowns in the fixed-pole approach formulated using the configuration-tensor representation are not the standard displacement and rotation vectors and as a consequence (i) the finite elements based on this approach cannot be combined with meshes of standard elements (with displacements and rotations as the system unknowns) and, (ii) the boundary conditions also have to be imposed in a specific non-standard manner. In this thesis, in order to re-cast the formulation into a new procedure using the standard degrees of freedom, a nodal-level projection of the non-standard degrees of freedom is presented, implemented and again investigated with respect to strain-invariance and path-independence.

1.2 Thesis overview

In Chapter 2 we summarise the kinematics of motion in 3D space, with emphasis on specific treatment of rotations in 3D. We introduce the configuration tensor and show that there are many analogies between the configuration tensor and the orientation matrix, stemming from the fact that they are both elements of Lie groups. A short overview of the properties of matrix Lie groups is given in order to introduce the exponential map needed for the parametrisation of rotation and of complete motion (a combination of translation and rotation).

In Chapter 3 we give an overview of the 3D beam theory in the material, spatial and fixed-pole description. Using the principle of virtual work and the standard Galerkin approximation, we derive the fixed-pole nodal residual, based on the fixed-pole equations of motion. We also derive a modified fixed-pole nodal residual as an alternative approach where standard virtual quantities are interpolated.

In Chapter 4 we present the solution procedures for the formulations derived in Chapter

3. Robustness, accuracy as well as strain-invariance and path-independence are tested within a number of numerical examples.

In Chapter 5 we present the generalised fixed-pole elements. The modified fixes-pole elements are enhanced by interpolating only the relative rotations as well as using the generalised shape functions. Numerical examples are repeated and results compared to the ones in Chapter 4. Additionally, using an analogous procedure, a generalised approach is derived for the fixed-pole elements. By interpolating only the relative "configurations" between nodes we propose a strain-invariant formulation in SR(6). We also derive the 6D generalised shape functions. We repeat the numerical examples and compare the results to those from Chapter 4.

Finally, in Chapter 6 we summarise the work presented and give some ideas for future work.

Chapter 2

Kinematics of motion in 3D space

2.1 Material, spatial and fixed-pole description

2.1.1 Bases and frames

A **basis** for an Euclidean 3D space is a set of three linearly independent vectors. An **orthonormal basis** is a set of three vectors, here denoted $\mathbf{e}_1$, $\mathbf{e}_2$, $\mathbf{e}_3$ and collectively by $\{\mathbf{e}_i\}$, such that [63]

$$\mathbf{e}_i \cdot \mathbf{e}_j = \delta_{ij} = \begin{cases} 1, & i = j \\ 0, & i \neq j \end{cases}, \quad i,\, j = 1, 2, 3\,, \tag{2.1}$$

where δ_{ij} is the so-called Kronecker symbol, for any pair of indices i, j. We consider the right-handed bases, i.e. the ones for which $\mathbf{e}_i \times \mathbf{e}_j = \mathbf{e}_k$, for a cyclic permutation of i, j, k. Using the orthonormal basis, we can write any vector $\mathbf{a}$ with respect to it, i.e. with its components along the base vectors as

$$\mathbf{a} = a_1\mathbf{e}_1 + a_2\mathbf{e}_2 + a_3\mathbf{e}_3\,.$$

Imagine now another right-handed orthonormal basis, $\{\mathbf{t}_i\}$, as shown in Figure 2.1. The **change of basis**, is an important tool in deriving relationship between objects expressed with respect to different bases. As shown in [63], since $\{\mathbf{e}_i\}$ is a basis, each $\mathbf{t}_i$ $(i = 1, 2, 3)$ can be expressed as a linear combination of $\mathbf{e}_1$, $\mathbf{e}_2$ and $\mathbf{e}_3$ as

$$\mathbf{t}_i = \Lambda_{ip}\mathbf{e}_p\,, \quad i, p = 1, 2, 3\,, \tag{2.2}$$

where a summation over repeated indices is implied. Taking the dot product of (2.2) with $\mathbf{e}_j$

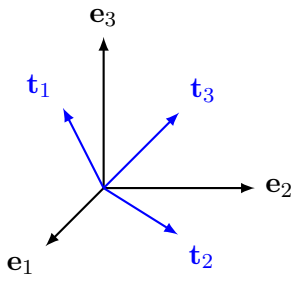

Figure 2.1: Change of basis – pure rotation

we have

$$\mathbf{t}_i \cdot \mathbf{e}_j = \Lambda_{ip}\mathbf{e}_p \cdot \mathbf{e}_j \,,$$

from where, because of (2.1), we can see that the coefficients Λ_{ij} are given as

$$\Lambda_{ij} = \mathbf{t}_i \cdot \mathbf{e}_j \,. \tag{2.3}$$

Comparing (2.3) with the definition of the dot product

$$\mathbf{a} \cdot \mathbf{b} = |\mathbf{a}|\,|\mathbf{b}|\,\cos\sphericalangle(\mathbf{a},\,\mathbf{b})\,, \tag{2.4}$$

and recalling from (2.1) that the base vectors are unit vectors we can conclude that the coefficients Λ_{ij} are in fact the direction cosines of the vectors $\mathbf{t}_i$ relative to $\mathbf{e}_j$ and can be written collectively as the **orientation matrix** or the **rotation matrix** $\mathbf{\Lambda}$. Also, using (2.2) and (2.3) we get

$$\delta_{ij} = \mathbf{t}_i \cdot \mathbf{t}_j = \Lambda_{ik}\mathbf{e}_k \cdot \mathbf{t}_j = \Lambda_{ik}\Lambda_{jk} = \Lambda_{i1}\Lambda_{j1} + \Lambda_{i2}\Lambda_{j2} + \Lambda_{i3}\Lambda_{j3}\,, \tag{2.5}$$

which reveals that $\mathbf{\Lambda}^T$ is the inverse of $\mathbf{\Lambda}$

$$\mathbf{\Lambda\Lambda}^T = \begin{bmatrix} \Lambda_{11} & \Lambda_{12} & \Lambda_{13} \\ \Lambda_{21} & \Lambda_{22} & \Lambda_{23} \\ \Lambda_{31} & \Lambda_{32} & \Lambda_{33} \end{bmatrix} \begin{bmatrix} \Lambda_{11} & \Lambda_{21} & \Lambda_{31} \\ \Lambda_{12} & \Lambda_{22} & \Lambda_{32} \\ \Lambda_{13} & \Lambda_{23} & \Lambda_{33} \end{bmatrix} = \begin{bmatrix} \Lambda_{1k}\Lambda_{1k} & \Lambda_{1k}\Lambda_{2k} & \Lambda_{1k}\Lambda_{3k} \\ \Lambda_{2k}\Lambda_{1k} & \Lambda_{2k}\Lambda_{2k} & \Lambda_{2k}\Lambda_{3k} \\ \Lambda_{3k}\Lambda_{1k} & \Lambda_{3k}\Lambda_{2k} & \Lambda_{3k}\Lambda_{3k} \end{bmatrix} = \begin{bmatrix} 1 & 0 & 0 \\ 0 & 1 & 0 \\ 0 & 0 & 1 \end{bmatrix}, \tag{2.6}$$

i.e. the orientation matrix is **orthogonal**

$$\mathbf{\Lambda}^{-1} = \mathbf{\Lambda}^T \quad \Leftrightarrow \quad \mathbf{\Lambda\Lambda}^T = \mathbf{\Lambda}^T\mathbf{\Lambda} = \mathbf{I}\,. \tag{2.7}$$

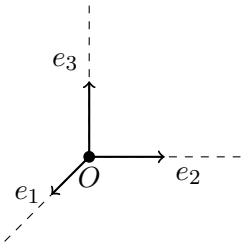

Figure 2.2: Frame – orthogonal vector basis at a known origin

Taking the determinant of (2.6) we get

$$\det(\mathbf{\Lambda}\mathbf{\Lambda}^T) = \det\mathbf{\Lambda}\det\mathbf{\Lambda}^T = \det\mathbf{I} \quad \Leftrightarrow \quad (\det\mathbf{\Lambda})^2 = 1 \quad \Rightarrow \det\mathbf{\Lambda} = \pm 1\,,$$

but we limit our attention only to such matrices $\mathbf{\Lambda}$ which have a positive unit determinant

$$\det\mathbf{\Lambda} = +1\,, \tag{2.8}$$

which corresponds to the case of **pure rotation** of the basis (i.e. the right-handedness of the basis is preserved) [63]. Such matrices are also called **proper orthogonal**, but throughout this thesis, and especially with respect to the matrix group theory given in Section 2.2, we refer to these matrices as **special orthogonal** as they in fact form the special orthogonal group SO(3) [3].

An orthonormal basis together with a placement of its origin uniquely determines the position and the orientation of an observer and is throughout this work referred to as a **frame** (shown in Figure 2.2). The orientation matrix is used to define the orientation of one frame with respect to another as it will be demonstrated in following subsections.

2.1.2 Spatial and material description

The description of any vector can be expressed with respect to a material or a spatial frame. First we introduce the **material frame**, $\{\mathbf{E}_i\}$ (also called the body frame), which is rigidly attached to an observed body at a particular point (see Figure 2.4). The notion of a material frame comes as particularly useful in continuum mechanics, where it is often convenient to express physical quantities of interest in some reference configuration rather than the current configuration [64]. However, in order to analyse the motion of a body, the material frame needs to be mapped into the ambient space. To do so, we first introduce the **inertial frame** defined by the **fixed** origin O in space and the **fixed** orthonormal basis $\{\mathbf{e}_i\}$. Then, we introduce a **moving frame**, attached to the moving body, with origin P and the **moving** orthonormal basis

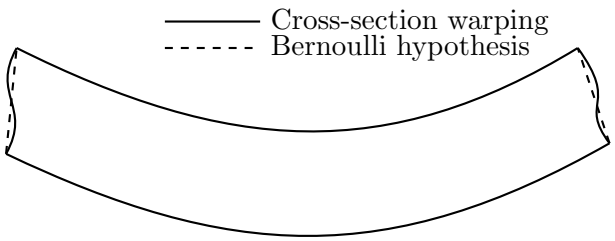

Figure 2.3: Beam deformation

$\{\mathbf{t}_i\}$. If, for the sake of simplicity, we take that $\{\mathbf{E}_i\}$ and $\{\mathbf{e}_i\}$ to coincide, any configuration of a beam[1] in ambient space is fully defined with $\mathbf{r}$ as its **position vector** defined as the position of P with respect to O, and $\mathbf{\Lambda}$ as its **orientation matrix** which is defined as the rotation of the moving basis with respect to the inertial basis, using (2.2) as

$$\mathbf{t}_i = \mathbf{\Lambda}\mathbf{e}_i \,. \tag{2.9}$$

This is the relationship which enables us to relate the so-called spatial and material objects (i.e. the physical fields with either the body or the space as the domain) using the pull-back/push-forward mappings with the orthogonal transformation $\mathbf{\Lambda}$ [2,65] as illustrated in Figure 2.5 for an arbitrary spatial vector $\mathbf{b}$. Here and throughout the thesis, the material vectors will be denoted with upper case boldface letters and the spatial ones with lower-case boldface letters. General relationship between a spatial vector $\mathbf{b}$ and its material counterpart $\mathbf{B}$ is given as

$$\mathbf{B} = \mathbf{\Lambda}^T\mathbf{b} \quad \Leftrightarrow \quad \mathbf{b} = \mathbf{\Lambda}\mathbf{B} \,. \tag{2.10}$$

To illustrate this relationship we consider a vector $\mathbf{b}$ in the ambient space (Figure 2.5). Its components with respect to the inertial frame $\{\mathbf{e}_i\}$ are b_i so that $\mathbf{b} = b_i\mathbf{e}_i$. Its components with respect to the material frame $\{\mathbf{E}_i\}$ are B_i so that $\mathbf{B} = B_i\mathbf{E}_i = B_i\mathbf{e}_i$. Using (2.9) we have $\mathbf{b} = \mathbf{\Lambda}\mathbf{B} = B_i\mathbf{\Lambda}\mathbf{E}_i = B_i\mathbf{t}_i$, which means that the vector $\mathbf{B}$ is merely a "rotated version" of $\mathbf{b}$ by $\mathbf{\Lambda}^T$, i.e. the scalar components B_i of this vector with respect to basis $\{\mathbf{E}_i\}$ are equal to the scalar components of vector $\mathbf{b}$ with respect to basis $\{\mathbf{t}_i\}$ [2, 65].

[1] A distintion between a body and a beam must be made at this point. A beam is such a body with one dimension (length) dominant to other two (height and width). In such a manner we can define the beam via only one parameter – its arc length x and define the cross section as a function of x. The fact that the length of the beam is much greater thatn its cross-sectional dimensions is a foundation for the assumption that the cross-sections remain planar during motion, i.e. the Bernoulli hypothesis is valid as illustrated in Figure 2.3.

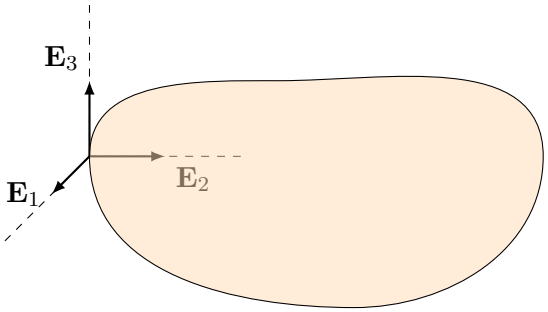

Figure 2.4: Body with the attached material frame

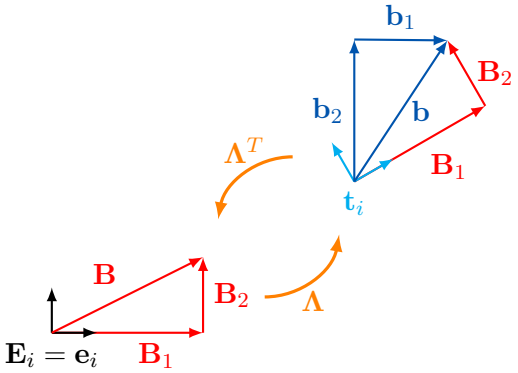

Figure 2.5: The pull-back/push-forward mapping of $\mathbf{b}$ to $\mathbf{B}$ and vice-versa via the orthogonal transformation $\boldsymbol{\Lambda}^T$ / $\boldsymbol{\Lambda}$

Velocities Given the position vector $\mathbf{r}$ of a point of a body, its **translational velocity** is a spatial object defined as its infinitesimal change in time

$$\mathbf{v} = \frac{\mathrm{d}}{\mathrm{d}t}\mathbf{r} = \dot{\mathbf{r}}\,. \tag{2.11}$$

The infinitesimal change of the orientation matrix in time yields [66, 67]

$$\dot{\mathbf{\Lambda}} = \widehat{\mathbf{w}}\mathbf{\Lambda}\,, \tag{2.12}$$

with $\widehat{\mathbf{w}} = \mathbf{w}\times = \dot{\mathbf{\Lambda}}\mathbf{\Lambda}^T$ as the skew-symmetric matrix corresponding to the cross product by a vector $\mathbf{w}$. That this matrix in (2.12) is indeed skew-symmetric follows by noting that $\mathbf{\Lambda}\mathbf{\Lambda}^T = \mathbf{I} \Rightarrow \left(\mathbf{\Lambda}\dot{\mathbf{\Lambda}}^T\right) = \mathbf{0}$. Since $\left(\mathbf{\Lambda}\dot{\mathbf{\Lambda}}^T\right) = \dot{\mathbf{\Lambda}}\mathbf{\Lambda}^T + \mathbf{\Lambda}\dot{\mathbf{\Lambda}}^T = \dot{\mathbf{\Lambda}}\mathbf{\Lambda}^T + \left(\dot{\mathbf{\Lambda}}\mathbf{\Lambda}^T\right)^T$, it follows that $\widehat{\mathbf{w}} = \dot{\mathbf{\Lambda}}\mathbf{\Lambda}^T = -\left(\dot{\mathbf{\Lambda}}\mathbf{\Lambda}^T\right)^T = -\widehat{\mathbf{w}}^T$. To qualify this vector physically, let us take the time derivative of (2.9) to get

$$\dot{\mathbf{t}}_i = \dot{\mathbf{\Lambda}}\mathbf{e}_i + \underbrace{\mathbf{\Lambda}\dot{\mathbf{e}}_i}_{\mathbf{0}}\,,$$

where we note that the time derivative of $\mathbf{e}_i$ is zero because basis $\{\mathbf{e}_i\}$ is fixed. Then, using (2.12), we get

$$\dot{\mathbf{t}}_i = \widehat{\mathbf{w}}\mathbf{\Lambda}\mathbf{e}_i = \widehat{\mathbf{w}}\mathbf{t}_i = \mathbf{w}\times\mathbf{t}_i\,, \tag{2.13}$$

which reveals that the vector $\mathbf{w}$ is in fact the **spatial angular velocity**, as the definition of the cross product is that it rotates a vector – the infinitesimal change of vector $\mathbf{t}_i$ in time results with a rotated vector $\mathbf{t}_i$ by $\mathbf{w}$.

2.1.3 Fixed-pole and spatial description

When Borri and Bottasso developed their helicoidal interpolation [7], they also introduced the fixed-pole description of kinematic quantities. In later publications, Bottasso and Borri [10] and Borri and co-workers [11] presented the fixed-pole concept by relating two definitions of velocity. They started from the definition of the position vector $\mathbf{r}$, as the position of point P with respect to point O. Naturally, we express this vector with respect to the basis of the inertial frame, using scalar components as $\mathbf{r} = r_i\mathbf{e}_i$. However, we may express this same vector using the basis of the moving frame $\{\mathbf{t}_i\}$ and its adequate scalar components as $\mathbf{r} = R_i\mathbf{t}_i$. Since these are merely two descriptions of the same vector $\mathbf{r}$ we can write

$$\mathbf{r} = r_i\mathbf{e}_i = R_i\mathbf{t}_i\,. \tag{2.14}$$

Taking the time derivative of (2.14) gives

$$\mathbf{v} = \dot{\mathbf{r}} = \dot{r}_i \mathbf{e}_i + \underbrace{r_i \dot{\mathbf{e}}_i}_{\mathbf{0}} = \dot{R}_i \mathbf{t}_i + R_i \dot{\mathbf{t}}_i \,. \tag{2.15}$$

The left hand side of (2.15) is equal to the definition of the spatial translational velocity (2.11). In the right-hand side of (2.15), we use (2.13) to compute the derivative of the moving basis $\{\mathbf{t}_i\}$, which leads to

$$\mathbf{v} = \dot{r}_i \mathbf{e}_i = \dot{R}_i \mathbf{t}_i + \widehat{\mathbf{w}} R_i \mathbf{t}_i \,.$$

This can, after recognising (2.14) and introducing $\overline{\mathbf{v}} = \dot{R}_i \mathbf{t}_i$, be written as

$$\mathbf{v} = \overline{\mathbf{v}} + \mathbf{w} \times \mathbf{r} \,. \tag{2.16}$$

The "new" velocity $\overline{\mathbf{v}}$ is called **the fixed-pole velocity** [10, 11]. It is the time derivative of the position taken by an observer rigidly attached to the moving frame $\{\mathbf{t}_i\}$. Both $\mathbf{v}$ and $\overline{\mathbf{v}}$ are spatial quantities, but we refer to the former as the **spatial velocity** and to the latter as the **fixed-pole velocity**.

Since the angular velocity $\mathbf{w}$ of the moving triad does not depend on the position vector $\mathbf{r}$, it is defined in the same way regardless where the observer taking the time derivative is. In that sense, the **fixed-pole angular velocity** is equal to the spatial angular velocity

$$\mathbf{w} = \overline{\mathbf{w}} \,. \tag{2.17}$$

Combining (2.16) and (2.17) by stacking them into a generalised velocities vector we get the relationship between the fixed-pole and spatial translational and angular velocities

$$\begin{Bmatrix} \overline{\mathbf{v}} \\ \overline{\mathbf{w}} \end{Bmatrix} = \begin{bmatrix} \mathbf{I} & \widehat{\mathbf{r}} \\ \mathbf{0} & \mathbf{I} \end{bmatrix} \begin{Bmatrix} \mathbf{v} \\ \mathbf{w} \end{Bmatrix} . \tag{2.18}$$

The matrix in (2.18) was termed the **transport operator** by Bottasso and Borri [10].

2.1.4 Fixed-pole and material description: the configuration tensor

Relationship (2.10) may be used to define material counterparts of our spatial translational and angular velocities. Substituting it in (2.18) we get the relationship between the fixed-pole, the

spatial and the material velocities defined in this way as

$$\begin{Bmatrix} \overline{\mathbf{v}} \\ \overline{\mathbf{w}} \end{Bmatrix} = \begin{bmatrix} \mathbf{I} & \widehat{\mathbf{r}} \\ \mathbf{0} & \mathbf{I} \end{bmatrix} \begin{Bmatrix} \mathbf{v} \\ \mathbf{w} \end{Bmatrix} = \begin{bmatrix} \mathbf{I} & \widehat{\mathbf{r}} \\ \mathbf{0} & \mathbf{I} \end{bmatrix} \begin{bmatrix} \mathbf{\Lambda} & \mathbf{0} \\ \mathbf{0} & \mathbf{\Lambda} \end{bmatrix} \begin{Bmatrix} \mathbf{V} \\ \mathbf{W} \end{Bmatrix} . \tag{2.19}$$

Remark 1. The nomenclature used here is not in full accordance with the one used in [64] where the infinitesimal change of a position in time is termed the *material velocity*.

We emphasise here that the standard duality of spatial vs. material description is now enriched and becomes a trinity of the fixed-pole, spatial and material description. Here we introduce the **configuration tensor** [10]

$$\mathbf{C} = \begin{bmatrix} \mathbf{I} & \widehat{\mathbf{r}} \\ \mathbf{0} & \mathbf{I} \end{bmatrix} \begin{bmatrix} \mathbf{\Lambda} & \mathbf{0} \\ \mathbf{0} & \mathbf{\Lambda} \end{bmatrix} = \begin{bmatrix} \mathbf{\Lambda} & \widehat{\mathbf{r}}\mathbf{\Lambda} \\ \mathbf{0} & \mathbf{\Lambda} \end{bmatrix} , \tag{2.20}$$

which relates the fixed-pole kinematic quantities to the material ones. Introducing the fixed-pole and material 6D vectors of **generalised velocities**

$$\overline{\boldsymbol{\omega}} = \begin{Bmatrix} \overline{\mathbf{v}} \\ \overline{\mathbf{w}} \end{Bmatrix} \quad \text{and} \quad \mathbf{\Omega} = \begin{Bmatrix} \mathbf{V} \\ \mathbf{W} \end{Bmatrix} , \tag{2.21}$$

relationship (2.19) may be written in a more compact form as

$$\overline{\boldsymbol{\omega}} = \mathbf{C}\mathbf{\Omega} \Leftrightarrow \mathbf{\Omega} = \mathbf{C}^{-1}\overline{\boldsymbol{\omega}} , \tag{2.22}$$

with

$$\mathbf{C}^{-1} = \begin{bmatrix} \mathbf{\Lambda}^T & \mathbf{0} \\ \mathbf{0} & \mathbf{\Lambda}^T \end{bmatrix} \begin{bmatrix} \mathbf{I} & -\widehat{\mathbf{r}} \\ \mathbf{0} & \mathbf{I} \end{bmatrix} = \begin{bmatrix} \mathbf{\Lambda}^T & -\mathbf{\Lambda}^T\widehat{\mathbf{r}} \\ \mathbf{0} & \mathbf{\Lambda}^T \end{bmatrix} . \tag{2.23}$$

We note here that this relationship is valid for any vectorial quantity, i.e. in the same way in which the relationship (2.10) relates spatial and material objects, (2.22) relates **fixed-pole** and **material** objects.

Relationship between velocities and time derivative of the configuration tensor Taking the time derivative of (2.20) while making use of (2.12) we have

$$\dot{\mathbf{C}} = \begin{bmatrix} \dot{\mathbf{\Lambda}} & \dot{\widehat{\mathbf{r}}}\mathbf{\Lambda} + \widehat{\mathbf{r}}\dot{\mathbf{\Lambda}} \\ \mathbf{0} & \dot{\mathbf{\Lambda}} \end{bmatrix} = \begin{bmatrix} \widehat{\mathbf{w}} & \dot{\widehat{\mathbf{r}}} + \widehat{\mathbf{r}}\widehat{\mathbf{w}} \\ \mathbf{0} & \widehat{\mathbf{w}} \end{bmatrix} \begin{bmatrix} \mathbf{\Lambda} & \mathbf{0} \\ \mathbf{0} & \mathbf{\Lambda} \end{bmatrix} ,$$

which, after noting that $\widehat{\mathbf{r}}\widehat{\mathbf{w}} - \widehat{\mathbf{w}}\widehat{\mathbf{r}} = \widehat{\mathbf{r} \times \mathbf{w}}$, turns into

$$\dot{\mathbf{C}} = \begin{bmatrix} \widehat{\mathbf{w}} & \dot{\widehat{\mathbf{r}}} + \widehat{\mathbf{r} \times \mathbf{w}} \\ \mathbf{0} & \widehat{\mathbf{w}} \end{bmatrix} \begin{bmatrix} \mathbf{I} & \widehat{\mathbf{r}} \\ \mathbf{0} & \mathbf{I} \end{bmatrix} \begin{bmatrix} \mathbf{\Lambda} & \mathbf{0} \\ \mathbf{0} & \mathbf{\Lambda} \end{bmatrix} = \begin{bmatrix} \widehat{\overline{\mathbf{w}}} & \widehat{\overline{\mathbf{v}}} \\ \mathbf{0} & \widehat{\overline{\mathbf{w}}} \end{bmatrix} \begin{bmatrix} \mathbf{\Lambda} & \widehat{\mathbf{r}}\mathbf{\Lambda} \\ \mathbf{0} & \mathbf{\Lambda} \end{bmatrix}, \tag{2.24}$$

where the first matrix in the right-hand side is called the rate tensor [11]. Introducing the **generalised cross product** (or as Borri and Bottasso [7] named it – the "north-east cross product") of a general 6D vector $\mathbf{a} = \langle \mathbf{a}_1^T \ \mathbf{a}_2^T \rangle^T$, where $\mathbf{a}_1$, $\mathbf{a}_2$ are 3D vectors, as

$$\widehat{\mathbf{a}} = \begin{bmatrix} \widehat{\mathbf{a}}_2 & \widehat{\mathbf{a}}_1 \\ \mathbf{0} & \widehat{\mathbf{a}}_2 \end{bmatrix}, \tag{2.25}$$

the above result (2.24) can be written as

$$\dot{\mathbf{C}} = \widehat{\overline{\boldsymbol{\omega}}}\mathbf{C}, \tag{2.26}$$

which can be interpreted as a generalisation of the relationship between the time derivative of the orientation matrix and the angular velocity (2.12). Furthermore, analogously to $\mathbf{w} = \mathbf{\Lambda}\mathbf{W} \Leftrightarrow \widehat{\mathbf{w}} = \mathbf{\Lambda}\widehat{\mathbf{W}}\mathbf{\Lambda}^T = \widehat{\mathbf{\Lambda}\mathbf{W}}$, as shown in (A.1) we have

$$\overline{\boldsymbol{\omega}} = \mathbf{C}\boldsymbol{\Omega} \Leftrightarrow \widehat{\overline{\boldsymbol{\omega}}} = \mathbf{C}\widehat{\boldsymbol{\Omega}}\mathbf{C}^{-1} = \widehat{\mathbf{C}\boldsymbol{\Omega}}, \tag{2.27}$$

which enables us to write the time derivative of the configuration tensor with respect to the material velocities as

$$\dot{\mathbf{C}} = \mathbf{C}\widehat{\boldsymbol{\Omega}}. \tag{2.28}$$

Remark 2. As it was shown in [11], configuration tensor (2.20) is merely a *matrix representation* of the special Euclidean group SE(3) [68]. Another possible matrix representation of SE(3) is a 4D configuration tensor given as

$$\mathbf{C}_4 = \begin{bmatrix} \mathbf{\Lambda} & \mathbf{r} \\ \mathbf{0}_{3\times 1}^T & 1 \end{bmatrix}. \tag{2.29}$$

Taking the time derivative of (2.29) reveals a result similar to (2.24), i.e.

$$\dot{\mathbf{C}}_4 = \begin{bmatrix} \widehat{\mathbf{w}} & \overline{\mathbf{v}} \\ \mathbf{0}_{3\times 1}^T & 1 \end{bmatrix} \begin{bmatrix} \mathbf{\Lambda} & \mathbf{r} \\ \mathbf{0}_{3\times 1}^T & 1 \end{bmatrix}, \tag{2.30}$$

with the first matrix in the right-hand side as the 4D version of the rate tensor. It is very important to note that while there exists a certain analogy between (2.30) and (2.24) – the

particular form of the configuration tensor is in both cases pre-multiplied by a corresponding rate tensor – with the 4D representation there is no analogue result to (2.22). This is the reason why Bottasso and Borri [10] and Borri and co-workers [11] found the 6D version of the configuration tensor (2.20) more suitable, despite its being less compact then (2.29).

2.2 Matrix Lie groups

2.2.1 Properties of groups

Definition 1. *[3] A group is a set G, together with a map of $G \times G$ into G (denoted $g_1 * g_2$) with the following properties:*

- *Closure. For all $g_1, g_2 \in G$,*

$$g_1 * g_2 \in G$$

- *Associativity. For all $g_1, g_2, g_3 \in G$,*

$$g_1 * (g_2 * g_3) = (g_1 * g_2) * g_3$$

- *Identity element. There exists an identity element $e \in G$ such that for all $g \in G$,*

$$g * e = e * g = g$$

- *Inverse element. There exists an inverse element $g^{-1} \in G$ for all $g \in G$ such that*

$$g * g^{-1} = g^{-1} * g = e$$

*If $g * h = h * g$ for all $g, h \in G$, then the group is said to be **commutative** (or **abelian**).*

Definition 2. *[3] A subgroup of a group G is a subset H of G with the following properties:*

- *The identity is an element of H;*
- *If $h \in H$ then $h^{-1} \in H$;*
- *If $h_1, h_2 \in H$, then $h_1 * h_2 \in H$*

Examples of groups range from the trivial group i.e. a set with one element, sets of integers with group operation of addition and so on.

Remark 3. Definition 1 and Definition 2 are valid in general group theory. However, we emphasise here that some parts of the group theory presented from this point on are valid **only for matrix groups**. The main reason for considering only matrix groups is to avoid abstract manifold theory and therefore simplify definition of the Lie algebra [3], but also the fact that the groups of our interest are matrix groups anyway (the special orthogonal group and the special group of rigid motions).

2.2.2 General linear group $\mathrm{GL}(n)$ and some of its interesting subgroups

The group formed of a set of all $n \times n$ (where n is any positive integer) invertible matrices with real entries and the operation of matrix multiplication is called **the general linear group**, $\mathrm{GL}(n)$. Let us check the group properties:

- Closure

  For any two invertible matrices $\mathbf{A}$, $\mathbf{B} \in \mathrm{GL}(n)$, their product $\mathbf{AB} \in \mathrm{GL}(n)$ is invertible since $(\mathbf{AB})^{-1} = \mathbf{B}^{-1}\mathbf{A}^{-1}$

- Associativity.

  Matrix multiplication is associative: $\mathbf{A}(\mathbf{BC}) = (\mathbf{AB})\mathbf{C}$;

- Identity element

  Identity matrix $\mathbf{I}$ defined as an $n \times n$ matrix with unities on the diagonal and zeros elsewhere is the identity element: $\mathbf{AI} = \mathbf{IA} = \mathbf{A}$

- Inverse element.

  By definition, an invertible matrix has an inverse.

In the following we present some interesting subgroups of $\mathrm{GL}(n)$. They all satisfy the conditions given in Definition 1 and Definition 2, therefore they indeed *are groups* and *are subgroups* of $\mathrm{GL}(n)$.

The special linear group $\mathrm{SL}(n)$

A set of all $n \times n$ real matrices with the determinant equal to $+1$ is called the **special linear group**, $\mathrm{SL}(n)$. Since any matrix with non-zero determinant is invertible, $\mathrm{SL}(n)$ is a subgroup of $\mathrm{GL}(n)$.

The special orthogonal group SO(n)

A subset of SL(n) of all the $n \times n$ real matrices with a positive unit determinant is called the **special orthogonal group**, SO(n). In the geometrical sense the elements of the special orthogonal group represent pure **rotations**[2]. We now limit our attention to two special cases: $n = 2$ and $n = 3$. If $n = 2$ we have SO(2) i.e. the group of rotations in 2D. If $n = 3$, SO(3) is the group of rotations in 3D – the orientation matrix as given in Section 2.1 is an element of this group.

The special group of rigid motions SR(6)

As it was shown by Bottasso and Borri [10], the configuration tensor (2.20) and an orientation matrix share many analogies. They all stem from the fact that the configuration tensor is also an element of a group. This group was named "the special group of rigid motions" by Bottasso and Borri and here we consider only the specific case of our interest, i.e. the 6D case. To show that SR(6) is a group, we first check if matrices of the form (2.20) satisfy conditions given in Definition 1. Matrix multiplication is **associative** by definition. The **identity element** exists on the group as a 6×6 identity matrix (just imagine a case when $\mathbf{r} = \mathbf{0}$ and $\mathbf{\Lambda} = \mathbf{I}$). The **inverse element** of $\mathbf{C}$ exists

$$\begin{bmatrix} \mathbf{\Lambda} & \widehat{\mathbf{r}}\mathbf{\Lambda} \\ \mathbf{0} & \mathbf{\Lambda} \end{bmatrix}^{-1} = \begin{bmatrix} \mathbf{\Lambda}^T & -\mathbf{\Lambda}^T\widehat{\mathbf{r}} \\ \mathbf{0} & \mathbf{\Lambda}^T \end{bmatrix} = \begin{bmatrix} \mathbf{\Lambda}^T & -\widehat{\mathbf{\Lambda}^T\mathbf{r}}\mathbf{\Lambda}^T \\ \mathbf{0} & \mathbf{\Lambda}^T \end{bmatrix},$$

and remains on the group (because $\mathbf{\Lambda}^T\widehat{\mathbf{r}} = \mathbf{\Lambda}^T\widehat{\mathbf{r}}\mathbf{\Lambda}\mathbf{\Lambda}^T = \widehat{\mathbf{\Lambda}^T\mathbf{r}}\mathbf{\Lambda}^T$). And finally to check **closure** we multiply two matrices $\mathbf{C}_1$ and $\mathbf{C}_2$

$$\begin{bmatrix} \mathbf{\Lambda}_1 & \widehat{\mathbf{r}}_1\mathbf{\Lambda}_1 \\ \mathbf{0} & \mathbf{\Lambda}_1 \end{bmatrix} \begin{bmatrix} \mathbf{\Lambda}_2 & \widehat{\mathbf{r}}_2\mathbf{\Lambda}_2 \\ \mathbf{0} & \mathbf{\Lambda}_2 \end{bmatrix} = \begin{bmatrix} \mathbf{\Lambda}_1\mathbf{\Lambda}_2 & \mathbf{\Lambda}_1\widehat{\mathbf{r}}_2\mathbf{\Lambda}_2 + \widehat{\mathbf{r}}_1\mathbf{\Lambda}_1\mathbf{\Lambda}_2 \\ \mathbf{0} & \mathbf{\Lambda}_1\mathbf{\Lambda}_2 \end{bmatrix} = \begin{bmatrix} \mathbf{\Lambda}_1\mathbf{\Lambda}_2 & \left(\widehat{\mathbf{\Lambda}_1\mathbf{r}_2} + \widehat{\mathbf{r}}_1\right)\mathbf{\Lambda}_1\mathbf{\Lambda}_2 \\ \mathbf{0} & \mathbf{\Lambda}_1\mathbf{\Lambda}_2 \end{bmatrix},$$

and, noting that $\mathbf{\Lambda}_1\widehat{\mathbf{r}}_2\mathbf{\Lambda}_2 = \mathbf{\Lambda}_1\widehat{\mathbf{r}}_2\mathbf{\Lambda}_1^T\mathbf{\Lambda}_1\mathbf{\Lambda}_2 = \widehat{\mathbf{\Lambda}_1\mathbf{r}_2}\mathbf{\Lambda}_1\mathbf{\Lambda}_2$, see that their product also remains on the group. Furthermore, the determinant of matrices in SR(6) is

$$\det \begin{bmatrix} \mathbf{\Lambda} & \widehat{\mathbf{r}}\mathbf{\Lambda} \\ \mathbf{0} & \mathbf{\Lambda} \end{bmatrix} = \det \mathbf{\Lambda} \det \mathbf{\Lambda} = +1\,, \tag{2.31}$$

since $\mathbf{\Lambda} \in$ SO(3), which means that SR(6) is a subgroup of SL(6).

[2] A group representing *both* rotations and reflections is a subgroup of GL(n) of all the $n \times n$ real matrices with determinant equal to ± 1, called the **orhtogonal group**, O(n).

2.2.3 Lie groups, Lie algebras and the matrix exponentials

Definition 3. *[3] A Lie group is a differentiable manifold G which is also a group and such that the group product $G \times G \to G$ and the inverse map $g \to g^{-1}$ are differentiable.*

It follows from the definition of the general linear group (and consequently, all of its subgroups) that both the group product and the group inverse (since for any $\mathbf{A} \in \mathrm{GL}(n)$, $\det \mathbf{A} \neq 0$) are infinitely many times continuously differentiable thus making the group a differentiable manifold. This means that the general linear group and its subgroups are also Lie groups [3].

Definition 4. *[3] A finite dimensional Lie algebra is a finite-dimensional vector space $\mathfrak{g}$ together with a map $[\cdot, \cdot]$ from $\mathfrak{g} \times \mathfrak{g} \to \mathfrak{g}$, with the following properties:*

1. *$[\cdot, \cdot]$ is bilinear.*
2. *$[X, Y] = -[Y, X]$ for all $X, Y \in \mathfrak{g}$*
3. *$[X, [Y, Z]] + [Y, [Z, X]] + [Z, [X, Y]] = 0$ for all $X, Y, Z \in \mathfrak{g}$.*

The property 2 in Definition 4 defines an additional structure, an operation called the **Lie bracket** which is a law of composition that is not associative. However, this law of composition does satisfy the **Jacobi identity** (property 3 od Definition 4) which is a substitute for the associative law [3].

Definition 5. *[3] Let G be a matrix Lie group. The **Lie algebra of** G, denoted $\mathfrak{g}$, is the set of all matrices X such that e^{tX} is in G for all real numbers t.*

Here we use Definition 5 to present the relationship between a Lie group and a Lie algebra via matrix exponential and show how is the internal structure of a Lie algebra determined for previously shown subgroups of $\mathrm{GL}(n)$. In order to define a Lie algebra, the matrix exponential first must be introduced because it plays a crucial role in the theory of Lie groups – it is the mechanism for passing information from the Lie algebra to the Lie group. Since many computations are done much more easily at the level of the Lie algebra, the exponential is indispensable in studying matrix Lie groups [3]. For any real or complex $n \times n$ matrix $\mathbf{A}$, the matrix exponential is given as an infinite series

$$\exp \mathbf{A} := \sum_{k=0}^{\infty} \frac{\mathbf{A}^k}{k!} \,. \tag{2.32}$$

The series (2.32) converges for any real or complex $n \times n$ matrix $\mathbf{A}$ and is also a continuous function of $\mathbf{A}$ [3]. For an element of a matrix Lie group, an $n \times n$ matrix, there always exists an element in a corresponding Lie algebra, $\mathfrak{a}$. These two are related via **exponential mapping** via map $\exp : \mathfrak{a} \to \mathrm{SO}(3)$.

Lie algebra so(3)

Consider a matrix $\mathbf{\Lambda}_\epsilon \in \mathrm{SO}(3)$ close to identity, i.e.

$$\mathbf{\Lambda}_\epsilon = \mathbf{I} + \epsilon \mathbf{X}\,,$$

where ϵ is an infinitesimally small positive number and $\mathbf{X}$ is a 3×3 matrix representing an element in the Lie algebra for the group SO(3). Using the condition of orthogonality $\mathbf{\Lambda}_\epsilon^{-1} = \mathbf{\Lambda}_\epsilon^T$ we can write $\mathbf{\Lambda}_\epsilon \mathbf{\Lambda}_\epsilon^T = \mathbf{I}$ so that

$$(\mathbf{I} + \epsilon \mathbf{X})(\mathbf{I} + \epsilon \mathbf{X})^T = \mathbf{I}\,,$$

from where

$$\mathbf{I} + \epsilon(\mathbf{X} + \mathbf{X}^T) = \mathbf{I}\,,$$

since ϵ is infinitesimally small. This shows that $\mathbf{X} + \mathbf{X}^T = \mathbf{0}$, i.e. $\mathbf{X} = -\mathbf{X}^T$, therefore $\mathbf{X}$ is a 3×3 **skew-symmetric** matrix. Since we have already introduced the notation for skew-symmetric matrices using a superimposed hat we identify $\mathbf{X}$ with $\widehat{\boldsymbol{\psi}}$ i.e.

$$\mathbf{X} = \widehat{\boldsymbol{\psi}} = -\widehat{\boldsymbol{\psi}}^T = \begin{bmatrix} 0 & -\psi_3 & \psi_2 \\ \psi_3 & 0 & -\psi_1 \\ -\psi_2 & \psi_1 & 0 \end{bmatrix} \quad \Leftrightarrow \quad \boldsymbol{\psi} = \begin{Bmatrix} \psi_1 \\ \psi_2 \\ \psi_3 \end{Bmatrix}. \tag{2.33}$$

Obviously, a 3×3 skew-symmetric matrix has three independent parameters ψ_1, ψ_3, ψ_3, forming a vector $\boldsymbol{\psi}$, an element of the vector space $\mathbb{R}^3$ with an additional operation of the vector product. This vector space is thus also an algebra, in particular a Lie algebra with the vector product as the Lie bracket, which is topologically equivalent to so(3). This correspondence between the dimension of a Lie algebra and the number of parameters for orthogonal groups happens **only in the 3D case**.

Lie algebra so(1)

Now we consider a planar case, i.e. a matrix $\mathbf{\Lambda}_\epsilon \in \mathrm{SO}(2)$ close to identity and by the same token as before arrive at

$$\mathbf{X} = \widehat{\boldsymbol{\theta}} = \begin{bmatrix} 0 & -\theta \\ \theta & 0 \end{bmatrix} . \tag{2.34}$$

Obviously, the element of the Lie algebra for SO(2) has *only one independent parameter*. We thus denote it with so(1), a Lie algebra topologically equivalent to the algebra of real numbers. As a consequence, $\mathbf{\Lambda}(\theta_1)\mathbf{\Lambda}(\theta_2) = \mathbf{\Lambda}(\theta_1 + \theta_2)$, i.e. **the rotational parameters are additive** (and therefore commutative)

$$\begin{bmatrix} \cos\theta_1 & -\sin\theta_1 \\ \sin\theta_1 & \cos\theta_1 \end{bmatrix} \begin{bmatrix} \cos\theta_2 & -\sin\theta_2 \\ \sin\theta_2 & \cos\theta_2 \end{bmatrix} = \begin{bmatrix} \cos(\theta_1+\theta_2) & -\sin(\theta_1+\theta_2) \\ \sin(\theta_1+\theta_2) & \cos(\theta_1+\theta_2) \end{bmatrix} ,$$

which is a specific property of planar rotations that does not exist in 3D. Although seemingly contradictory, the fact that the Lie group SO(2) has a corresponding Lie algebra which is one-dimensional, is in fact in agreement with a rotation in plane, which is completely defined by a twist around a normal to the plane.

Lie algebra sr(6)

Consider a matrix $\mathbf{C}_\epsilon \in \mathrm{SR}(6)$, close to identity

$$\mathbf{C}_\epsilon = \mathbf{I} + \epsilon\mathbf{X} , \tag{2.35}$$

where ϵ is an infinitesimally small positive number and $\mathbf{X}$ is a 6×6 matrix representing a Lie algebra for the group SR(6). Since by definition, the determinant of matrices in SR(6) is equal to $+1$, taking the determinant of (2.35) we have

$$\det \mathbf{C}_\epsilon = \det \mathbf{I} + \epsilon \det \mathbf{X} = +1 .$$

However, we cannot use the same procedure as when finding the Lie algebra of the SO(n) group. This is because $\mathbf{C}_\epsilon^{-1} \neq \mathbf{C}_\epsilon^T$, i.e. we cannot use the property of orthogonality as in the previous cases. To deduce the form of $\mathbf{X}$, we must look into the blockwise structure of matrices in SR(6)

as given in (2.20) and write it close to identity as

$$\mathbf{C}_\epsilon = \begin{bmatrix} \mathbf{\Lambda}_\epsilon & \widehat{\mathbf{r}}_\epsilon \mathbf{\Lambda}_\epsilon \\ \mathbf{0} & \mathbf{\Lambda}_\epsilon \end{bmatrix} . \tag{2.36}$$

Using (2.33) and introducing $\widehat{\mathbf{r}}_\epsilon = \epsilon\widehat{\boldsymbol{\rho}}$, we can rewrite the above result as

$$\mathbf{C}_\epsilon = \begin{bmatrix} \mathbf{I} + \epsilon\widehat{\boldsymbol{\psi}} & \epsilon\widehat{\boldsymbol{\rho}}\left(\mathbf{I} + \epsilon\widehat{\boldsymbol{\psi}}\right) \\ \mathbf{0} & \mathbf{I} + \epsilon\widehat{\boldsymbol{\psi}} \end{bmatrix} = \begin{bmatrix} \mathbf{I} & \mathbf{0} \\ \mathbf{0} & \mathbf{I} \end{bmatrix} + \epsilon \begin{bmatrix} \widehat{\boldsymbol{\psi}} & \widehat{\boldsymbol{\rho}} \\ \mathbf{0} & \widehat{\boldsymbol{\psi}} \end{bmatrix} + \epsilon^2 \begin{bmatrix} \mathbf{0} & \widehat{\boldsymbol{\rho}}\widehat{\boldsymbol{\psi}} \\ \mathbf{0} & \mathbf{0} \end{bmatrix} .$$

Since ϵ is infinitesimally small,

$$\mathbf{C}_\epsilon = \begin{bmatrix} \mathbf{I} & \mathbf{0} \\ \mathbf{0} & \mathbf{I} \end{bmatrix} + \epsilon \begin{bmatrix} \widehat{\boldsymbol{\psi}} & \widehat{\boldsymbol{\rho}} \\ \mathbf{0} & \widehat{\boldsymbol{\psi}} \end{bmatrix} . \tag{2.37}$$

Comparing (2.37) and (2.35) reveals that the corresponding Lie algebra has the same blockwise form as does the generalised cross product introduced in Section 2.1.4, i.e. instead of $\mathbf{X}$ we can use $\widehat{\boldsymbol{\nu}}$ as

$$\mathbf{X} = \widehat{\boldsymbol{\nu}} = \begin{bmatrix} \widehat{\boldsymbol{\psi}} & \widehat{\boldsymbol{\rho}} \\ \mathbf{0} & \widehat{\boldsymbol{\psi}} \end{bmatrix} \quad \Leftrightarrow \quad \boldsymbol{\nu} = \begin{Bmatrix} \boldsymbol{\rho} \\ \boldsymbol{\psi} \end{Bmatrix} . \tag{2.38}$$

Since both $\widehat{\boldsymbol{\psi}}$ and $\widehat{\boldsymbol{\rho}}$ are 3×3 skew-symmetric matrices, each of them has three independent parameters as shown in (2.33). This means that the Lie algebra corresponding to the Lie group SR(6) has *six independent parameters*, i.e. the Lie algebra sr(6) corresponds to the Lie group SR(6). This reveals an analogy between the Lie groups SR(6) and SO(3), which both have the corresponding Lie algebras of a dimension equal to the number of group parameters.

2.3 Vectorial parametrisations of motion

We begin this section with a quote by Bauchau and Trainelli [69]:

> In fact, rotation may be described as the motion of a point on a three-dimensional non-linear manifold, the Lie group of special orthogonal transformations of the three-dimensional space. The various parametrisations of rotation are, in differential geometry terminology, different charts available for this particular manifold.

These "charts" have been well researched (see eg. [50,69–71]) and can roughly be divided into two categories, depending on what the actual parameter is – **a vector** or **a quaternion**, although other parametrisations are also possible [50, 56]. In the course of this thesis we focus on the

vectorial parametrisation. We give a detailed description of vectorial parametrisation of rotation and follow an analogous procedure to define a vectorial parametrisation of complete motion as presented in [10].

2.3.1 Vectorial parametrisation of rotation

The vector $\boldsymbol{\psi}$ in (2.33) is (in the context of three dimensional rotations) called **the rotational vector** and it represents the simplest vectorial parameter of rotation. Two orientations represented with orientation matrices, $\mathbf{\Lambda}_0$ and $\mathbf{\Lambda}$, are related via exponential map of $\widehat{\boldsymbol{\psi}}$ as

$$\mathbf{\Lambda} = \exp \widehat{\boldsymbol{\psi}} \mathbf{\Lambda}_0 \,, \tag{2.39}$$

where the exponential map of $\widehat{\boldsymbol{\psi}}$ is written using (2.32) as

$$\exp \widehat{\boldsymbol{\psi}} = \mathbf{I} + \widehat{\boldsymbol{\psi}} + \frac{1}{2}\widehat{\boldsymbol{\psi}}^2 + \frac{1}{6}\widehat{\boldsymbol{\psi}}^3 + \frac{1}{24}\widehat{\boldsymbol{\psi}}^4 + \dots \,. \tag{2.40}$$

The fact that the three-dimensional skew-symmetric matrices have recursive properties

$$\begin{aligned} \widehat{\boldsymbol{\psi}}^{2k-1} &= (-1)^{k-1}\psi^{2(k-1)}\widehat{\boldsymbol{\psi}} \,, \\ \widehat{\boldsymbol{\psi}}^{2k} &= (-1)^{k-1}\psi^{2(k-1)}\widehat{\boldsymbol{\psi}}^2 \,, \end{aligned} \tag{2.41}$$

which can easily be confirmed by a direct calculation, enables us to rewrite (2.40) as

$$\begin{aligned} \exp \widehat{\boldsymbol{\psi}} = \mathbf{I} &+ \left(1 - \frac{1}{3!}\psi^2 + \frac{1}{5!}\psi^4 - \frac{1}{7!}\psi^6 + \dots\right)\widehat{\boldsymbol{\psi}} + \\ &+ \left(\frac{1}{2!} - \frac{1}{4!}\psi^2 + \frac{1}{6!}\psi^4 - \frac{1}{8!}\psi^6 + \dots\right)\widehat{\boldsymbol{\psi}}^2 \,. \end{aligned} \tag{2.42}$$

The infinite sums in the parentheses are in fact series expansions of the following functions

$$\frac{\sin\psi}{\psi} = \sum_{n=0}^{\infty} \frac{(-1)^n}{(2n+1)!}\psi^{2n} \,, \tag{2.43}$$

$$\frac{1-\cos\psi}{\psi^2} = \sum_{n=0}^{\infty} \frac{(-1)^n}{(2n+2)!}\psi^{2n} \,. \tag{2.44}$$

Consequently, we conclude that the exponential map of elements in so(3) has a closed form

$$\exp \widehat{\boldsymbol{\psi}} = \mathbf{I} + \alpha_1 \widehat{\boldsymbol{\psi}} + \alpha_2 \widehat{\boldsymbol{\psi}}^2 \,, \tag{2.45}$$

where

$$\alpha_1 = \frac{\sin\psi}{\psi} \,, \quad \text{and} \quad \alpha_2 = \frac{1-\cos\psi}{\psi^2} \,. \tag{2.46}$$

Expression (2.45) is in literature often referred to as the Rodrigues formula [72] and it represents one of the most used parametrisations of rotations. The same result can be obtained using pure geometrical observations, as Agryris did in [73].

Variation of the orientation matrix The variation of the orientation matrix $\mathbf{\Lambda}$ is defined as its directional derivative in the direction of a superimposed infinitesimally small perturbation $\delta\boldsymbol{\vartheta}$ (usually termed the **spin vector**) as

$$\delta\mathbf{\Lambda} = \frac{\mathrm{d}}{\mathrm{d}\epsilon}\Big|_{\epsilon=0} \mathbf{\Lambda}_\epsilon = \frac{\mathrm{d}}{\mathrm{d}\epsilon}\Big|_{\epsilon=0} \exp\left(\epsilon\widehat{\delta\boldsymbol{\vartheta}}\right)\mathbf{\Lambda} = \delta\widehat{\boldsymbol{\vartheta}}\mathbf{\Lambda}\,, \tag{2.47}$$

due to (A.5) derived in Appendix A.2.1. Also, we may vary (2.39) as

$$\delta\mathbf{\Lambda} = \delta\left(\exp\widehat{\boldsymbol{\psi}}\right)\mathbf{\Lambda}_0\,. \tag{2.48}$$

Then, combining (2.47) and (2.48) as demonstrated in Appendix A.2.2 we get

$$\delta\boldsymbol{\vartheta} = \mathbf{H}(\boldsymbol{\psi})\delta\boldsymbol{\psi}\,, \tag{2.49}$$

as the relationship between the spin vector $\delta\boldsymbol{\vartheta}$ and the variation of the rotational vector $\boldsymbol{\psi}$, with the function $\mathbf{H}(\boldsymbol{\psi})$ and its inverse obtained as

$$\mathbf{H}(\boldsymbol{\psi}) = \mathbf{I} + \beta_1\widehat{\boldsymbol{\psi}} + \beta_2\widehat{\boldsymbol{\psi}}^2\,, \tag{2.50}$$

$$\mathbf{H}^{-1}(\boldsymbol{\psi}) = \mathbf{I} + \gamma_1\widehat{\boldsymbol{\psi}} + \gamma_2\widehat{\boldsymbol{\psi}}^2\,, \tag{2.51}$$

where

$$\begin{aligned} \beta_1 &= \frac{1-\cos\psi}{\psi^2}\,, \quad \beta_2 = \frac{\psi-\sin\psi}{\psi^3}\,, \\ \gamma_1 &= -\frac{1}{2}\,, \quad \gamma_2 = \frac{1}{\psi^2}\left(1 - \frac{1}{2}\frac{\psi\sin\psi}{1-\cos\psi}\right)\,. \end{aligned} \tag{2.52}$$

Remark 4. Although $\delta\boldsymbol{\psi}$ follows as the variation of the rotational vector $\boldsymbol{\psi}$, the spin vector $\delta\boldsymbol{\vartheta}$ **does not** follow from the variation of $\boldsymbol{\vartheta}$ (existence of such $\boldsymbol{\vartheta}$ is never implied), but from the variation of $\mathbf{\Lambda}$ (2.47). We also note that the analogy of results (2.12) and (2.47).

2.3.2 Vectorial parametrisation of complete motion

In analogy to the previous case, we start by defining the parameter of complete motion. Using (2.38) we can define a parameter of complete motion as $\boldsymbol{\nu} = \left\langle \boldsymbol{\rho}^T \quad \boldsymbol{\psi}^T \right\rangle^T$, with $\boldsymbol{\psi}$ as the rotational vector and $\boldsymbol{\rho}$ as a quantity which will be defined after the closed form of the exponential

map is deduced. Using (2.32), we write the exponential map of matrices in sr(6) as

$$\exp\widehat{\boldsymbol{\nu}} = \mathbf{I} + \widehat{\boldsymbol{\nu}} + \frac{1}{2}\widehat{\boldsymbol{\nu}}^2 + \frac{1}{6}\widehat{\boldsymbol{\nu}}^3 + \frac{1}{24}\widehat{\boldsymbol{\nu}}^4 + \frac{1}{120}\widehat{\boldsymbol{\nu}}^5 + \frac{1}{720}\widehat{\boldsymbol{\nu}}^6 + \dots \tag{2.53}$$

The powers of elements of sr(6) (matrix $\widehat{\boldsymbol{\nu}}$) also have recursive properties. This is the foundation upon which Bottasso and Borri [10] derived the closed form of the exponential map of matrices in sr(6), which we present here in detail. We calculate the first four odd powers of $\widehat{\boldsymbol{\nu}}$ while also using (2.41) and get the following results

$$\begin{aligned}
\widehat{\boldsymbol{\nu}} &= \begin{bmatrix} \widehat{\boldsymbol{\psi}} & \widehat{\boldsymbol{\rho}} \\ \mathbf{0} & \widehat{\boldsymbol{\psi}} \end{bmatrix}, \\
\widehat{\boldsymbol{\nu}}^3 &= -\psi^2 \begin{bmatrix} \widehat{\boldsymbol{\psi}} & \widehat{\boldsymbol{\rho}} \\ \mathbf{0} & \widehat{\boldsymbol{\psi}} \end{bmatrix} - 2\left(\boldsymbol{\rho}\cdot\boldsymbol{\psi}\right) \begin{bmatrix} \mathbf{0} & \widehat{\boldsymbol{\psi}} \\ \mathbf{0} & \mathbf{0} \end{bmatrix}, \\
\widehat{\boldsymbol{\nu}}^5 &= \psi^4 \begin{bmatrix} \widehat{\boldsymbol{\psi}} & \widehat{\boldsymbol{\rho}} \\ \mathbf{0} & \widehat{\boldsymbol{\psi}} \end{bmatrix} + 4\psi^2\left(\boldsymbol{\rho}\cdot\boldsymbol{\psi}\right) \begin{bmatrix} \mathbf{0} & \widehat{\boldsymbol{\psi}} \\ \mathbf{0} & \mathbf{0} \end{bmatrix}, \\
\widehat{\boldsymbol{\nu}}^7 &= -\psi^6 \begin{bmatrix} \widehat{\boldsymbol{\psi}} & \widehat{\boldsymbol{\rho}} \\ \mathbf{0} & \widehat{\boldsymbol{\psi}} \end{bmatrix} - 6\psi^4\left(\boldsymbol{\rho}\cdot\boldsymbol{\psi}\right) \begin{bmatrix} \mathbf{0} & \widehat{\boldsymbol{\psi}} \\ \mathbf{0} & \mathbf{0} \end{bmatrix}, \dots
\end{aligned} \tag{2.54}$$

which can be written in a general form as

$$\widehat{\boldsymbol{\nu}}^{2n-1} = (-1)^{n-1}\psi^{2(n-1)} \begin{bmatrix} \widehat{\boldsymbol{\psi}} & \widehat{\boldsymbol{\rho}} \\ \mathbf{0} & \widehat{\boldsymbol{\psi}} \end{bmatrix} + 2(n-1)(-1)^{n-1}\psi^{2(n-2)}\left(\boldsymbol{\rho}\cdot\boldsymbol{\psi}\right) \begin{bmatrix} \mathbf{0} & \widehat{\boldsymbol{\psi}} \\ \mathbf{0} & \mathbf{0} \end{bmatrix}, \quad n = 2, 3\dots \tag{2.55}$$

Then, we calculate the first four even powers of $\widehat{\boldsymbol{\nu}}$ while also using (2.41) and get the following results

$$\begin{aligned}
\widehat{\boldsymbol{\nu}}^2 &= \begin{bmatrix} \widehat{\boldsymbol{\psi}}^2 & \widehat{\boldsymbol{\rho}}\widehat{\boldsymbol{\psi}} + \widehat{\boldsymbol{\psi}}\widehat{\boldsymbol{\rho}} \\ \mathbf{0} & \widehat{\boldsymbol{\psi}}^2 \end{bmatrix}, \\
\widehat{\boldsymbol{\nu}}^4 &= -\psi^2 \begin{bmatrix} \widehat{\boldsymbol{\psi}}^2 & \widehat{\boldsymbol{\rho}}\widehat{\boldsymbol{\psi}} + \widehat{\boldsymbol{\psi}}\widehat{\boldsymbol{\rho}} \\ \mathbf{0} & \widehat{\boldsymbol{\psi}}^2 \end{bmatrix} - 2\left(\boldsymbol{\rho}\cdot\boldsymbol{\psi}\right) \begin{bmatrix} \mathbf{0} & \widehat{\boldsymbol{\psi}}^2 \\ \mathbf{0} & \mathbf{0} \end{bmatrix}, \\
\widehat{\boldsymbol{\nu}}^6 &= \psi^4 \begin{bmatrix} \widehat{\boldsymbol{\psi}}^2 & \widehat{\boldsymbol{\rho}}\widehat{\boldsymbol{\psi}} + \widehat{\boldsymbol{\psi}}\widehat{\boldsymbol{\rho}} \\ \mathbf{0} & \widehat{\boldsymbol{\psi}}^2 \end{bmatrix} + 4\psi^2\left(\boldsymbol{\rho}\cdot\boldsymbol{\psi}\right) \begin{bmatrix} \mathbf{0} & \widehat{\boldsymbol{\psi}}^2 \\ \mathbf{0} & \mathbf{0} \end{bmatrix}, \\
\widehat{\boldsymbol{\nu}}^8 &= -\psi^6 \begin{bmatrix} \widehat{\boldsymbol{\psi}}^2 & \widehat{\boldsymbol{\rho}}\widehat{\boldsymbol{\psi}} + \widehat{\boldsymbol{\psi}}\widehat{\boldsymbol{\rho}} \\ \mathbf{0} & \widehat{\boldsymbol{\psi}}^2 \end{bmatrix} - 6\psi^4\left(\boldsymbol{\rho}\cdot\boldsymbol{\psi}\right) \begin{bmatrix} \mathbf{0} & \widehat{\boldsymbol{\psi}}^2 \\ \mathbf{0} & \mathbf{0} \end{bmatrix}, \dots
\end{aligned} \tag{2.56}$$

which can similarly be written in a general form as

$$\widehat{\boldsymbol{\nu}}^{2n} = (-1)^{n-1}\psi^{2(n-1)} \begin{bmatrix} \widehat{\boldsymbol{\psi}}^2 & \widehat{\boldsymbol{\rho}}\widehat{\boldsymbol{\psi}} + \widehat{\boldsymbol{\psi}}\widehat{\boldsymbol{\rho}} \\ \mathbf{0} & \widehat{\boldsymbol{\psi}}^2 \end{bmatrix} + 2(n-1)(-1)^{n-1}\psi^{2(n-2)} \, (\boldsymbol{\rho}\cdot\boldsymbol{\psi}) \begin{bmatrix} \mathbf{0} & \widehat{\boldsymbol{\psi}}^2 \\ \mathbf{0} & \mathbf{0} \end{bmatrix}, \quad n = 2, 3, \dots \tag{2.57}$$

Substituting (2.55) and (2.57) into (2.53) we get

$$\begin{aligned} \exp\widehat{\boldsymbol{\nu}} = \mathbf{I} &+ \left(1 - \frac{\psi^2}{3!} + \frac{\psi^4}{5!} - \frac{\psi^6}{7!} + \frac{\psi^8}{9!} - \dots\right) \begin{bmatrix} \widehat{\boldsymbol{\psi}} & \widehat{\boldsymbol{\rho}} \\ \mathbf{0} & \widehat{\boldsymbol{\psi}} \end{bmatrix} + \\ &+ \left(\frac{1}{2} - \frac{\psi^2}{4!} + \frac{\psi^4}{6!} - \frac{\psi^6}{8!} + \frac{\psi^8}{10!} - \dots\right) \begin{bmatrix} \widehat{\boldsymbol{\psi}}^2 & \widehat{\boldsymbol{\rho}}\widehat{\boldsymbol{\psi}} + \widehat{\boldsymbol{\psi}}\widehat{\boldsymbol{\rho}} \\ \mathbf{0} & \widehat{\boldsymbol{\psi}}^2 \end{bmatrix} + \\ &+ \left(-\frac{2}{3!} + \frac{4\psi^2}{5!} - \frac{6\psi^4}{7!} + \frac{8\psi^6}{9!} - \dots\right) (\boldsymbol{\rho}\cdot\boldsymbol{\psi}) \begin{bmatrix} \mathbf{0} & \widehat{\boldsymbol{\psi}} \\ \mathbf{0} & \mathbf{0} \end{bmatrix} + \\ &+ \left(-\frac{2}{4!} + \frac{4\psi^2}{6!} - \frac{6\psi^4}{8!} + \frac{8\psi^6}{10!} - \dots\right) (\boldsymbol{\rho}\cdot\boldsymbol{\psi}) \begin{bmatrix} \mathbf{0} & \widehat{\boldsymbol{\psi}}^2 \\ \mathbf{0} & \mathbf{0} \end{bmatrix}. \end{aligned} \tag{2.58}$$

The sums of the infinite series in the parentheses above are

$$\begin{aligned} 1 - \frac{\psi^2}{3!} + \frac{\psi^4}{5!} - \frac{\psi^6}{7!} + \frac{\psi^8}{9!} - \dots &= \sum_{n=0}^{\infty} \frac{(-1)^n\psi^{2n}}{(2n+1)!} = \alpha_1 \,, \\ \frac{1}{2} - \frac{\psi^2}{4!} + \frac{\psi^4}{6!} - \frac{\psi^6}{8!} + \frac{\psi^8}{10!} - \dots &= \sum_{n=0}^{\infty} \frac{(-1)^n\psi^{2n}}{(2n+2)!} = \alpha_2 \,, \\ -\frac{2}{3!} + \frac{4\psi^2}{5!} - \frac{6\psi^4}{7!} + \frac{8\psi^6}{9!} - \dots &= \sum_{n=0}^{\infty} \frac{2(n+1)(-1)^{n+1}\psi^{2n}}{(2n+3)!} = -\alpha_2 + \beta_2 \,, \\ -\frac{2}{4!} + \frac{4\psi^2}{6!} - \frac{6\psi^4}{8!} + \frac{8\psi^6}{10!} - \dots &= \sum_{n=0}^{\infty} \frac{2(n+1)(-1)^{n+1}\psi^{2n}}{(2n+4)!} = \frac{\alpha_1 - 2\alpha_2}{\psi^2} \,, \end{aligned}$$

which means we can rewrite (2.58) in a closed form as

$$\exp\widehat{\boldsymbol{\nu}} = \begin{bmatrix} \exp\widehat{\boldsymbol{\psi}} & \mathbf{Q}(\boldsymbol{\nu}) \\ \mathbf{0} & \exp\widehat{\boldsymbol{\psi}} \end{bmatrix}, \tag{2.59}$$

with

$$\mathbf{Q}(\boldsymbol{\nu}) = \alpha_1\widehat{\boldsymbol{\rho}} + \alpha_2(\widehat{\boldsymbol{\rho}}\widehat{\boldsymbol{\psi}} + \widehat{\boldsymbol{\psi}}\widehat{\boldsymbol{\rho}}) - (\alpha_2 - \beta_2)\,(\boldsymbol{\psi}\cdot\boldsymbol{\rho})\,\widehat{\boldsymbol{\psi}} + \frac{\alpha_1 - 2\alpha_2}{\psi^2}\,(\boldsymbol{\psi}\cdot\boldsymbol{\rho})\,\widehat{\boldsymbol{\psi}}^2 \,. \tag{2.60}$$

As it is shown in Appendix A.2.3, (2.60) can be written in a more compact form as

$$\mathbf{Q}(\boldsymbol{\nu}) = \widehat{\mathbf{H}(\boldsymbol{\psi})\boldsymbol{\rho}}\exp\widehat{\boldsymbol{\psi}} \,. \tag{2.61}$$

We have now shown that the exponential map of matrices in sr(6) has a closed form. The next step is to deduce what exactly is the upper part of the parameter of the configuration, $\boldsymbol{\rho}$. Since two configurations defined by configuration tensors $\mathbf{C}_0$ and $\mathbf{C}$ are related via the exponential map (2.59) of $\boldsymbol{\nu}$, we can write

$$\begin{bmatrix} \boldsymbol{\Lambda} & \widehat{\mathbf{r}}\boldsymbol{\Lambda} \\ \mathbf{0} & \boldsymbol{\Lambda} \end{bmatrix} = \exp \widehat{\boldsymbol{\nu}} \begin{bmatrix} \boldsymbol{\Lambda}_0 & \widehat{\mathbf{r}}_0\boldsymbol{\Lambda}_0 \\ \mathbf{0} & \boldsymbol{\Lambda}_0 \end{bmatrix} = \begin{bmatrix} \exp \widehat{\boldsymbol{\psi}} & \mathbf{Q}(\boldsymbol{\nu}) \\ \mathbf{0} & \exp \widehat{\boldsymbol{\psi}} \end{bmatrix} \begin{bmatrix} \boldsymbol{\Lambda}_0 & \widehat{\mathbf{r}}_0\boldsymbol{\Lambda}_0 \\ \mathbf{0} & \boldsymbol{\Lambda}_0 \end{bmatrix} . \tag{2.62}$$

Equating the upper-right blocks gives

$$\widehat{\mathbf{r}}\boldsymbol{\Lambda} = \left(\exp \widehat{\boldsymbol{\psi}}\widehat{\mathbf{r}}_0 + \mathbf{Q}(\boldsymbol{\nu})\right) \boldsymbol{\Lambda}_0 \,,$$

from where it follows

$$\begin{aligned} \widehat{\mathbf{r}} &= \left(\exp \widehat{\boldsymbol{\psi}}\widehat{\mathbf{r}}_0 + \mathbf{Q}(\boldsymbol{\nu})\right) \boldsymbol{\Lambda}_0\boldsymbol{\Lambda}_0^T (\exp \widehat{\boldsymbol{\psi}})^T \\ &= \exp \widehat{\boldsymbol{\psi}}\widehat{\mathbf{r}}_0 (\exp \widehat{\boldsymbol{\psi}})^T + \widehat{\mathbf{H}(\boldsymbol{\psi})\boldsymbol{\rho}} \exp \widehat{\boldsymbol{\psi}} (\exp \widehat{\boldsymbol{\psi}})^T \,. \end{aligned}$$

Since both sides of the equation are skew-symmetric we finally have

$$\mathbf{r} = \exp \widehat{\boldsymbol{\psi}}\mathbf{r}_0 + \mathbf{H}(\boldsymbol{\psi})\boldsymbol{\rho} \,, \tag{2.63}$$

from where we get $\boldsymbol{\rho}$ as

$$\begin{aligned} \boldsymbol{\rho} &= \mathbf{H}^{-1}(\boldsymbol{\psi}) \left(\mathbf{r} - \exp \widehat{\boldsymbol{\psi}}\mathbf{r}_0\right) \\ &= \mathbf{H}^{-1}(\boldsymbol{\psi})\mathbf{r} - \mathbf{H}^{-T}(\boldsymbol{\psi})\mathbf{r}_0 \,, \end{aligned} \tag{2.64}$$

because, due to (A.13), $\mathbf{H}^{-1}(\boldsymbol{\psi}) \exp \widehat{\boldsymbol{\psi}} = \mathbf{H}^{-T}(\boldsymbol{\psi})$. Finally we have

$$\boldsymbol{\nu} = \left\{ \begin{matrix} \mathbf{H}^{-1}(\boldsymbol{\psi})\mathbf{r} - \mathbf{H}^{-T}(\boldsymbol{\psi})\mathbf{r}_0 \\ \boldsymbol{\psi} \end{matrix} \right\} \tag{2.65}$$

completely defined as the topological equivalent to the corresponding element $\widehat{\boldsymbol{\nu}}$ of the Lie algebra sr(6) which we will call **the configuration parameter** or the vectorial parameter of complete motion.

Variation of the configuration tensor The variation of $\mathbf{C}$ is its directional derivative in the direction of a superimposed infinitesimally small perturbation $\delta\boldsymbol{\varsigma} = \left\langle \delta\boldsymbol{\xi}^T \; \delta\boldsymbol{\vartheta}^T \right\rangle^T$ which we

term the **configurational spin vector** as

$$\delta\mathbf{C} = \frac{\mathrm{d}}{\mathrm{d}\epsilon}\Big|_{\epsilon=0} \mathbf{C}_\epsilon = \frac{\mathrm{d}}{\mathrm{d}\epsilon}\Big|_{\epsilon=0} \exp \epsilon\widehat{\delta\boldsymbol{\varsigma}}\mathbf{C} = \widehat{\delta\boldsymbol{\varsigma}}\mathbf{C}\,, \tag{2.66}$$

due to (A.5), as well as (A.15) and (A.16) derived in Appendix A.2.4. Also, we may vary the relationship $\mathbf{C} = \exp\widehat{\boldsymbol{\nu}}\mathbf{C}_0$ as

$$\delta\mathbf{C} = \delta\left(\exp\widehat{\boldsymbol{\nu}}\right)\mathbf{C}_0\,. \tag{2.67}$$

Then, combining (2.66) and (2.67) as demonstrated in Appendix A.2.5 we get

$$\delta\boldsymbol{\varsigma} = \mathbf{H_6}(\boldsymbol{\nu})\delta\boldsymbol{\nu}\,, \tag{2.68}$$

as the relationship between the configurational spin vector $\delta\boldsymbol{\varsigma}$ and the variation of the configuration vector $\boldsymbol{\nu}$, with the function $\mathbf{H_6}(\boldsymbol{\nu})$ derived as

$$\mathbf{H_6}(\boldsymbol{\nu}) = \begin{bmatrix} \mathbf{H}(\boldsymbol{\psi}) & \mathbf{B}(\boldsymbol{\nu}) \\ \mathbf{0} & \mathbf{H}(\boldsymbol{\psi}) \end{bmatrix}, \tag{2.69}$$

and function $\mathbf{B}(\boldsymbol{\nu})$ derived as (see Appendix A.2.5)

$$\mathbf{B}(\boldsymbol{\nu}) = \alpha_2\widehat{\boldsymbol{\rho}} + \frac{\alpha_1 - 2\alpha_2}{\psi^2}\left(\boldsymbol{\rho}\cdot\boldsymbol{\psi}\right)\widehat{\boldsymbol{\psi}} + \frac{\alpha_2 - 3\beta_2}{\psi^2}\left(\boldsymbol{\rho}\cdot\boldsymbol{\psi}\right)\widehat{\boldsymbol{\psi}}^2 + \beta_2\left(\widehat{\boldsymbol{\psi}}\widehat{\boldsymbol{\rho}} + \widehat{\boldsymbol{\rho}}\widehat{\boldsymbol{\psi}}\right) \tag{2.70}$$

Remark 5. Although $\delta\boldsymbol{\nu}$ follows as the variation of the configuration vector $\boldsymbol{\nu}$, the configurational spin vector $\delta\boldsymbol{\varsigma}$ **does not** follow from the variation of $\boldsymbol{\varsigma}$ (existence of such $\boldsymbol{\varsigma}$ is never implied), but from the variation of $\mathbf{C}$ (2.66). We also note that the analogy of results (2.26) and (2.66).

Chapter 3

Geometrically exact 3D beam theory and finite-element discretisation: material, spatial and fixed-pole approach

In order to formulate a beam problem, three sets of equations are required. **Kinematic equations** are the equations which relate the strain measures to the displacements and rotations. **Constitutive equations** relate the strain measures to the stress resultants via a constitutive law. In this dissertation the emphasis is on geometrical non-linearity, so the constitutive law is taken as linear. The final set of equations are the **equations of motion** which are derived from the Newton's second law of motion which states that the acceleration of a body is directly proportional to, and in the same direction as the force acting on that body and inversely proportional to the mass of the body. In order to make use of this law in terms of spatial beam theory, we must apply it to all the forces and accelerations that act at a cross-section of the beam. The equations of motion can be given in their **strong form**, which means that they are given as differential equations, or in their **weak form**, which means they are given as an integral over a specified domain. The latter is a suitable form for employing the finite element method [74].

The general concept of obtaining the weak form is that the differential equations of motion are dot multiplied by some arbitrary *test* functions, which are (i) continuous, (ii) at least once continuously differentiable and (iii) identically equal to zero at all co-ordinates x with prescribed

essential (kinematic) boundary conditions [74]. This approach is equivalent to formulating the well-known virtual work principle in which we do not need to know the strong form of equations of motion, and where the set of arbitrary test functions are identified with admissible variations of the system unknowns, i.e. the infinitesimally small perturbations of displacements and rotations, which we call the *virtual* displacements and rotations.

3.1 Standard approach

We first consider the theory given by Simo in [2] and its finite-element implementation given by Simo and Vu-Quoc in [4], which we here refer to as the *standard approach*. In this section we give an overview of this theory concluding in the nodal dynamic residual which makes a basis for a finite-element solution procedure.

3.1.1 Kinematic and constitutive equations

The basic kinematic assumption which enables the formulation of the beam as a 1D problem is the Bernoulli hypothesis which states that the plane cross sections remain planar after deformation and retain their shape and area. With this assumption, we can identify the beam with the line of cross section centroids (in this case, initially straight) called the **reference axis**. Then, the position vector of an *arbitrary* point (x, y, z) in the deformed beam continuum can be expressed as [2, 51]

$$\mathbf{r}(x, y, z) = \mathbf{r}(x) + \mathbf{\Lambda}(x) \begin{Bmatrix} 0 \\ y \\ z \end{Bmatrix}, \tag{3.1}$$

with $\mathbf{r}(x)$ as the position vector of a reference axis at the cross section and $\mathbf{\Lambda}(x)$ as the orientation matrix defining the orientation of the orthonormal triad $\{\mathbf{t}_i\}$ at the cross section.

The spatial translational and rotational strain measures are derived in [2] by evaluating the internal power (stress power) which is equal to the integral of the inner product of the Piola-Kirchhoff stress tensor and the deformation gradient [75] and is equivalent to the virtual work of the internal forces with the translational and angular velocities taken as the virtual displacements and rotations. The kinematic assumption (3.1) enabled Simo to reduce the general 3D expression of the internal power which resulted in the appropriate definition of strain measures conjugate to the resultant force and moment in the spatial as in the fully material description [2]. The

spatial translational and rotational strain measures follow as

$$\boldsymbol{\gamma} = \mathbf{r}' - \mathbf{t}_1 \tag{3.2}$$

$$\widehat{\boldsymbol{\kappa}} = \boldsymbol{\Lambda}'\boldsymbol{\Lambda}^T\,, \tag{3.3}$$

where $\boldsymbol{\gamma} = \langle \epsilon\ \gamma_2\ \gamma_3 \rangle^T$ is the spatial vector of translational strains consisting of one axial (ϵ) and two shear (γ_2, γ_3) strains, while $\boldsymbol{\kappa} = \langle \kappa_1\ \kappa_2\ \kappa_3 \rangle^T$ is the spatial vector of rotational strain measures with one torsional (κ_1) and two bending (κ_2, κ_3) strains. Their material counterparts are obtained using (2.10) as

$$\boldsymbol{\Gamma} = \boldsymbol{\Lambda}^T\boldsymbol{\gamma} = \boldsymbol{\Lambda}^T\mathbf{r}' - \mathbf{E}_1\,, \tag{3.4}$$

$$\widehat{\mathbf{K}} = \boldsymbol{\Lambda}^T\widehat{\boldsymbol{\kappa}}\boldsymbol{\Lambda} = \boldsymbol{\Lambda}^T\boldsymbol{\Lambda}'\,. \tag{3.5}$$

When developing the geometrically exact planar beam theory, Reissner [1] derived the material strain measures from the stipulation that the virtual work equation and the equations of motion are valid independently. Crisfield and Jelenić [47] have used this principle to derive the 3D material strain measures and this approach is presented in Appendix A.3.

A linearly elastic material is considered, where the material stress and stress-couple resultants are defined as

$$\begin{Bmatrix} \mathbf{N} \\ \mathbf{M} \end{Bmatrix} = \mathbf{D} \begin{Bmatrix} \boldsymbol{\Gamma} \\ \mathbf{K} \end{Bmatrix}\,, \tag{3.6}$$

with

$$\mathbf{D} = \begin{bmatrix} \mathbf{C}_N & \mathbf{0} \\ \mathbf{0} & \mathbf{C}_M \end{bmatrix}\,,$$

as well as

$$\mathbf{C}_N = \begin{bmatrix} EA_1 & 0 & 0 \\ 0 & GA_2 & 0 \\ 0 & 0 & GA_3 \end{bmatrix} \quad \text{and} \quad \mathbf{C}_M = \begin{bmatrix} GJ & 0 & 0 \\ 0 & EI_2 & 0 \\ 0 & 0 & EI_3 \end{bmatrix}\,,$$

as the translational and rotational constitutive matrices. Here, A_1, A_2, A_3 denote the cross-sectional and shear areas and J, I_2, I_3 denote the torsional constant and cross-sectional second moments of area, while G and E are the shear and Young's modulus, respectively. The constitutive matrices are, obviously, constant for a linear elastic material considered here.

3.1.2 Equations of motion

Strong form of the equations of motion

The spatial translational and angular momenta per unit length of a beam are defined as

$$\mathbf{l} = A\rho\mathbf{v}\,, \tag{3.7}$$

$$\boldsymbol{\pi} = \mathbf{j}_\rho\mathbf{w}\,, \tag{3.8}$$

with $\mathbf{v}$ as the translational velocity (2.11), $\mathbf{w}$ as the angular velocity (2.12) of the cross section and $\mathbf{j}_\rho$ as the spatial tensor of the mass moment of inertia, which is related to its material counterpart, $\mathbf{J}_\rho$ via orthogonal transformation $\boldsymbol{\Lambda}$ as

$$\mathbf{j}_\rho = \boldsymbol{\Lambda}\mathbf{J}_\rho\boldsymbol{\Lambda}^T\,, \tag{3.9}$$

and the material tensor of the mass moments of inertia given as

$$\mathbf{J}_\rho = \rho\begin{bmatrix} I_2+I_3 & 0 & 0 \\ 0 & I_2 & 0 \\ 0 & 0 & I_3 \end{bmatrix}. \tag{3.10}$$

We note here that while $\mathbf{J}_\rho$ is configuration-independent, $\mathbf{j}_\rho$ is not, because it depends on $\boldsymbol{\Lambda}$. Substituting (3.9) into (3.8), we have

$$\boldsymbol{\pi} = \boldsymbol{\Lambda}\mathbf{J}_\rho\boldsymbol{\Lambda}^T\mathbf{w} = \boldsymbol{\Lambda}\mathbf{J}_\rho\mathbf{W}\,. \tag{3.11}$$

Taking the time derivative of (3.7) we obtain

$$\dot{\mathbf{l}} = A\rho\ddot{\mathbf{r}}\,, \tag{3.12}$$

as the change of translational momentum per unit of beam length. We may obtain the differential equations of motion by observing a differential segment of a beam (Figure 3.1). The Newton's second law of dynamics states that the total force acting upon a body is equal to the body's mass times acceleration. The mass of the differential segment shown in Figure 3.1 is the specific mass multiplied by the length of the observed segment, $m = A\,\rho\,\mathrm{d}x$. We define the position vector of the left cross section as $\mathbf{r}$ and the position vector of the right cross section as $\mathbf{r} + \mathrm{d}\mathbf{r}$. The corresponding accelerations are $\ddot{\mathbf{r}}$ and $\ddot{\mathbf{r}} + \mathrm{d}\ddot{\mathbf{r}}$, with their average value defining the acceleration of the centroid of the observed segment, i.e. $\frac{1}{2}\left(\ddot{\mathbf{r}} + \ddot{\mathbf{r}} + \mathrm{d}\ddot{\mathbf{r}}\right) = \ddot{\mathbf{r}} + \frac{1}{2}\mathrm{d}\ddot{\mathbf{r}}$. Evaluating mass times

acceleration yields

$$A\,\rho\,\mathrm{d}x\left(\ddot{\mathbf{r}}+\frac{1}{2}\mathrm{d}\ddot{\mathbf{r}}\right)=A\,\rho\ddot{\mathbf{r}}\,\mathrm{d}x=\dot{\mathbf{l}}\,\mathrm{d}x\,, \tag{3.13}$$

because $\mathrm{d}x$ and $\mathrm{d}\ddot{\mathbf{r}}$ are infinitesimally small quantities. Next, we add all the forces acting upon the differential segment

$$\sum\mathbf{F}=-\mathbf{n}+\mathbf{n}+\mathrm{d}\mathbf{n}+\mathbf{n}_e\,\mathrm{d}x \tag{3.14}$$

where $\mathbf{n}_e$ is the distributed external loading taken to be acting at the reference axis (drawn with a dashed line) and $\mathbf{n}$ is the spatial translational stress resultant. The sum of all forces acting

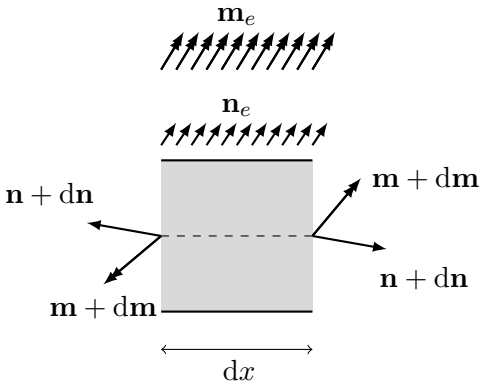

Figure 3.1: A differential segment of a beam in motion

upon the differential segment (3.14) is equal to the mass times acceleration of the differential segment (3.13), i.e.

$$\begin{aligned}\mathrm{d}\mathbf{n}+\mathbf{n}_e&=\dot{\mathbf{l}}\,\mathrm{d}x\quad\big/:\,\mathrm{d}x\\ \mathbf{n}'+\mathbf{n}_e&=\dot{\mathbf{l}}\,,\quad t\geqslant 0\,,\,x\in[0,\,L]\,.\end{aligned} \tag{3.15}$$

Correspondingly, the Newton-Euler second law states that the rate of change of angular momentum is equal to the sum of torques. Taking the time derivative of (3.8) we have

$$\begin{aligned}\dot{\boldsymbol{\pi}}&=\dot{\boldsymbol{\Lambda}}\mathbf{J}_\rho\mathbf{W}+\boldsymbol{\Lambda}\mathbf{J}_\rho\dot{\mathbf{W}}\\ &=\boldsymbol{\Lambda}\widehat{\mathbf{W}}\mathbf{J}_\rho\mathbf{W}+\boldsymbol{\Lambda}\mathbf{J}_\rho\dot{\mathbf{W}}\\ &=\boldsymbol{\Lambda}\left(\widehat{\mathbf{W}}\mathbf{J}_\rho\mathbf{W}+\mathbf{J}_\rho\dot{\mathbf{W}}\right)\\ &=\boldsymbol{\Lambda}\left[\mathbf{W}\times(\mathbf{J}_\rho\mathbf{W})+\mathbf{J}_\rho\dot{\mathbf{W}}\right]\,,\end{aligned} \tag{3.16}$$

as the temporal change of the angular momentum per unit length. Total angular momentum of the observed segment is then $\dot{\boldsymbol{\pi}}\,\mathrm{d}x$. On the other hand, the sum of all torques on the differential

$x = 0$:	$\mathbf{r} = \mathbf{r}_0\,,\ \mathbf{\Lambda} = \mathbf{\Lambda}_0$
$x = L$:	$\mathbf{r} = \mathbf{r}_L\,,\ \mathbf{\Lambda} = \mathbf{\Lambda}_L$

Table 3.1: Essential (kinematic) boundary conditions

$x = 0$:	$-\mathbf{\Lambda N} = \mathbf{F}_0\,,\ -\mathbf{\Lambda M} = \mathbf{M}_0$
$x = L$:	$\mathbf{\Lambda N} = \mathbf{F}_L\,,\quad \mathbf{\Lambda M} = \mathbf{M}_L$

Table 3.2: Natural (static) boundary conditions

segment of the beam is

$$\sum \mathbf{M} = -\mathbf{m} + \mathbf{m} + \mathrm{d}\mathbf{m} + \mathrm{d}\mathbf{r} \times \mathbf{n} + \frac{1}{2}\mathrm{d}\mathbf{r} \times \mathbf{n}_e\,\mathrm{d}x + \mathbf{m}_e\,\mathrm{d}x\,, \tag{3.17}$$

with $\mathbf{m}_e$ as the external torque per unit length, taken to be acting at the reference axis. Since $\dot{\boldsymbol{\pi}}\,\mathrm{d}x$ must be equal to (3.17) we have

$$\begin{aligned} \mathrm{d}\mathbf{m} + \mathrm{d}\mathbf{r} \times \mathbf{n} + \mathbf{m}_e\,\mathrm{d}x = \dot{\boldsymbol{\pi}}\,\mathrm{d}x \quad \big/ : \mathrm{d}x \\ \mathbf{m}' + \mathbf{r}' \times \mathbf{n} + \mathbf{m}_e = \dot{\boldsymbol{\pi}}\,, \quad t \geqslant 0\,,\ x \in [0,\, L]\,. \end{aligned} \tag{3.18}$$

Finally we can write the governing equations of motion in **strong form** as

$$\begin{aligned} (\mathbf{\Lambda N})' + \mathbf{n}_e &= \dot{\mathbf{i}}\,, \\ (\mathbf{\Lambda M})' + \widehat{\mathbf{r}}'\mathbf{\Lambda N} + \mathbf{m}_e &= \dot{\boldsymbol{\pi}}\,, \end{aligned} \qquad t \geqslant 0\,,\ x \in [0,\, L]\,. \tag{3.19}$$

In order to fully define the equations of motion, a set of boundary conditions must be imposed. There are two sets of boundary conditions which are mutually exclusive. The first is the set of **essential** (or kinematic) boundary conditions which defines the prescribed displacements or rotations on the domain boundary as shown in Table 3.1. The second set is the set of **natural** (or static) boundary conditions, which defines the forces and moments ($\mathbf{F}_0$, $\mathbf{F}_L$, $\mathbf{M}_0$, $\mathbf{M}_L$) acting at the boundary as shown in Table 3.2.

Weak form of the equations of motion

In order to obtain the weak form of equations of motion we multiply (3.19) with a set of test functions $\mathbf{f}$ and $\boldsymbol{\varphi}$ which satisfy conditions (i)-(iii) given in the introduction to this chapter to give

$$\begin{aligned} \mathbf{f}^T \left[(\mathbf{\Lambda N})' + \mathbf{n}_e - \dot{\mathbf{i}}\right] = 0\,, \\ \boldsymbol{\varphi}^T \left[(\mathbf{\Lambda M})' + \widehat{\mathbf{r}}'\,(\mathbf{\Lambda N}) + \mathbf{m}_e - \dot{\boldsymbol{\pi}}\right] = 0\,, \end{aligned}$$

which can be written as

$$\mathbf{f}^T\left[(\mathbf{\Lambda N})' + \mathbf{n}_e - \dot{\mathbf{l}}\right] + \boldsymbol{\varphi}^T\left[(\mathbf{\Lambda M})' + \widehat{\mathbf{r}}'\,(\mathbf{\Lambda N}) + \mathbf{m}_e - \dot{\boldsymbol{\pi}}\right] = 0$$

and integrated over the domain of the problem (the condition (i) implies integrability of the test functions) so we have

$$\int_0^L \left[\mathbf{f}^T\dot{\mathbf{l}} + \boldsymbol{\varphi}^T\dot{\boldsymbol{\pi}}\right]\,\mathrm{d}x = \int_0^L \left\{\mathbf{f}^T\left[(\mathbf{\Lambda N})' + \mathbf{n}_e\right] + \boldsymbol{\varphi}^T\left[(\mathbf{\Lambda M})' + \widehat{\mathbf{r}}'\,(\mathbf{\Lambda N}) + \mathbf{m}_e\right]\right\}\,\mathrm{d}x\,.$$

Integrating by parts the terms which contain $(\mathbf{\Lambda N})'$ and $(\mathbf{\Lambda M})'$ we obtain

$$\int_0^L \left(\mathbf{f}'^T(\mathbf{\Lambda N}) - \boldsymbol{\varphi}^T\widehat{\mathbf{r}}'\mathbf{\Lambda N} + \mathbf{f}^T\dot{\mathbf{l}}\right)\,\mathrm{d}x + \int_0^L \left[\boldsymbol{\varphi}'^T(\mathbf{\Lambda M}) + \boldsymbol{\varphi}^T\dot{\boldsymbol{\pi}}\right]\,\mathrm{d}x = \int_0^L \left(\mathbf{f}^T\mathbf{n}_e + \boldsymbol{\varphi}^T\mathbf{m}_e\right)\,\mathrm{d}x + \left(\mathbf{f}^T\mathbf{\Lambda N} + \boldsymbol{\varphi}^T\mathbf{\Lambda M}\right)|_0^L\,. \tag{3.20}$$

The term $\left(\mathbf{f}^T\mathbf{\Lambda N} + \boldsymbol{\varphi}^T\mathbf{\Lambda M}\right)|_0^L$ has to be complemented with the appropriate, predefined boundary conditions (Table 3.2): the stress resultants $\mathbf{\Lambda N}$ and $\mathbf{\Lambda M}$ at $x = 0$ and $x = L$ are zero in case of unloaded ends or equal to the applied end loads $\mathbf{F}_0$, $\mathbf{F}_L$ and $\mathbf{M}_0$, $\mathbf{M}_L$ (natural boundary conditions) or are equal to the reactions in which case the essential boundary conditions are defined. In that case, due to (iii) the test functions are zero and the term vanishes. Since the essential and natural boundary conditions are mutually exclusive, equation (3.20) finally gives the weak form of equation (3.19) as

$$\int_0^L \left(\left\langle \mathbf{f}^T \quad \boldsymbol{\varphi}^T\right\rangle \begin{bmatrix} \mathbf{I}\frac{\mathrm{d}}{\mathrm{d}x} & \mathbf{0} \\ -\widehat{\mathbf{r}}' & \mathbf{I}\frac{\mathrm{d}}{\mathrm{d}x}\end{bmatrix}\right)\begin{Bmatrix}\mathbf{n}\\ \mathbf{m}\end{Bmatrix}\,\mathrm{d}x + \int_0^L \left\langle \mathbf{f}^T \quad \boldsymbol{\varphi}^T\right\rangle\left(\begin{Bmatrix}\dot{\mathbf{k}}\\ \dot{\boldsymbol{\pi}}\end{Bmatrix} - \begin{Bmatrix}\mathbf{n}_e\\ \mathbf{m}_e\end{Bmatrix}\right)\,\mathrm{d}x - \left\langle \mathbf{f}_0^T \quad \boldsymbol{\varphi}_0^T\right\rangle\begin{Bmatrix}\mathbf{F}_0\\ \mathbf{M}_0\end{Bmatrix} - \left\langle \mathbf{f}_L^T \quad \boldsymbol{\varphi}_L^T\right\rangle\begin{Bmatrix}\mathbf{F}_L\\ \mathbf{M}_L\end{Bmatrix} = 0\,. \tag{3.21}$$

Virtual work principle and objective strain rates

The virtual work principle states that the virtual work of the internal and the inertial forces must be equal to the virtual work of the external loading, i.e.

$$V_i + V_m = V_e \tag{3.22}$$

where V_i is the virtual work of internal forces, V_m the virtual work of inertial forces and V_e the virtual work of external loading. The **virtual work** is defined either as the scalar product of a **virtual displacement** and a force, or a **virtual force** and a displacement (or some other

mutually conjugate quantities). In this thesis, in line with the displacement-based approach, we employ the former definition.

The virtual work of internal forces is thus defined as the work of stress resultants on virtual strains, i.e.

$$V_i = \int_0^L (\delta\boldsymbol{\Gamma} \cdot \mathbf{N} + \delta\mathbf{K} \cdot \mathbf{M}) \, \mathrm{d}x \,. \tag{3.23}$$

We note that this can also be obtained by varying the strain energy

$$\phi = \frac{1}{2}\int_0^L (\boldsymbol{\Gamma} \cdot \mathbf{N} + \mathbf{K} \cdot \mathbf{M}) \, \mathrm{d}x = \frac{1}{2}\int_0^L (\boldsymbol{\gamma} \cdot \mathbf{n} + \boldsymbol{\kappa} \cdot \mathbf{m}) \, \mathrm{d}x \,, \tag{3.24}$$

giving

$$\delta\phi = \frac{1}{2}\int_0^L (\delta\boldsymbol{\Gamma} \cdot \mathbf{N} + \boldsymbol{\Gamma} \cdot \delta\mathbf{N} + \delta\mathbf{K} \cdot \mathbf{M} + \mathbf{K} \cdot \delta\mathbf{M}) \, \mathrm{d}x = \int_0^L (\delta\boldsymbol{\Gamma} \cdot \mathbf{N} + \delta\mathbf{K} \cdot \mathbf{M}) \, \mathrm{d}x = V_i \,,$$

where we note that the variation of the material stress resultants $\mathbf{N}$ and $\mathbf{M}$ yields $\delta\mathbf{N} = \mathbf{C}_N\delta\boldsymbol{\Gamma}$ and $\delta\mathbf{M} = \mathbf{C}_M\delta\mathbf{K}$.

We now focus on a very important property which will be necessary in further investigation of the fixed-pole approach. Let us use the right-hand side of (3.24) and vary it to obtain the internal virtual work expressed in terms of the spatial quantities

$$\begin{aligned}
V_i &= \frac{1}{2}\int_0^L (\delta\boldsymbol{\gamma} \cdot \mathbf{n} + \boldsymbol{\gamma} \cdot \delta\mathbf{n} + \delta\boldsymbol{\kappa} \cdot \mathbf{m} + \boldsymbol{\kappa} \cdot \delta\mathbf{m}) \, \mathrm{d}x \\
&= \frac{1}{2}\int_0^L (\delta\boldsymbol{\gamma} \cdot \mathbf{n} + \boldsymbol{\gamma} \cdot \delta(\boldsymbol{\Lambda}\mathbf{N}) + \delta\boldsymbol{\kappa} \cdot \mathbf{m} + \boldsymbol{\kappa} \cdot \delta(\boldsymbol{\Lambda}\mathbf{M})) \, \mathrm{d}x \\
&= \frac{1}{2}\int_0^L \left[\delta\boldsymbol{\gamma} \cdot \mathbf{n} + \boldsymbol{\gamma} \cdot (\widehat{\delta\boldsymbol{\vartheta}}\boldsymbol{\Lambda}\mathbf{N} + \boldsymbol{\Lambda}\mathbf{C}_\mathbf{N} \underbrace{\delta\boldsymbol{\Gamma}}_{\delta(\boldsymbol{\Lambda}^T\boldsymbol{\gamma})}) + \delta\boldsymbol{\kappa} \cdot \mathbf{m} + \boldsymbol{\kappa} \cdot (\widehat{\delta\boldsymbol{\vartheta}}\boldsymbol{\Lambda}\mathbf{M} + \boldsymbol{\Lambda}\mathbf{C}_\mathbf{M} \underbrace{\delta\mathbf{K}}_{\delta(\boldsymbol{\Lambda}^T\boldsymbol{\kappa})}) \right] \mathrm{d}x \\
&= \frac{1}{2}\int_0^L \Bigg[\delta\boldsymbol{\gamma} \cdot \mathbf{n} + \boldsymbol{\gamma} \cdot (\delta\boldsymbol{\vartheta} \times \mathbf{n}) - \underbrace{\boldsymbol{\gamma} \cdot (\boldsymbol{\Lambda}\mathbf{C}_N\boldsymbol{\Lambda}^T\widehat{\delta\boldsymbol{\vartheta}}\boldsymbol{\gamma})}_{\mathbf{n}\cdot(\delta\boldsymbol{\vartheta}\times\boldsymbol{\gamma})} + \underbrace{\boldsymbol{\gamma} \cdot (\boldsymbol{\Lambda}\mathbf{C}_N\boldsymbol{\Lambda}^T\delta\boldsymbol{\gamma})}_{\mathbf{n}\cdot\delta\boldsymbol{\gamma}} \\
&\quad + \delta\boldsymbol{\kappa} \cdot \mathbf{m} + \boldsymbol{\kappa} \cdot (\delta\boldsymbol{\vartheta} \times \mathbf{m}) - \underbrace{\boldsymbol{\kappa} \cdot (\boldsymbol{\Lambda}\mathbf{C}_M\boldsymbol{\Lambda}^T\widehat{\delta\boldsymbol{\vartheta}}\boldsymbol{\kappa})}_{\mathbf{m}\cdot(\delta\boldsymbol{\vartheta}\times\boldsymbol{\kappa})} + \underbrace{\boldsymbol{\kappa} \cdot (\boldsymbol{\Lambda}\mathbf{C}_M\boldsymbol{\Lambda}^T\delta\boldsymbol{\kappa})}_{\mathbf{m}\cdot\delta\boldsymbol{\kappa}} \Bigg] \mathrm{d}x \\
&= \int_0^L [(\delta\boldsymbol{\gamma} + \boldsymbol{\gamma} \times \delta\boldsymbol{\vartheta}) \cdot \mathbf{n} + (\delta\boldsymbol{\kappa} + \boldsymbol{\kappa} \times \delta\boldsymbol{\vartheta}) \cdot \mathbf{m}] \, \mathrm{d}x \,.
\end{aligned} \tag{3.25}$$

It is obvious that the elegant form of (3.23) is not sustained when internal virtual work is expressed in terms of the spatial quantities, but such a form may be restored by defining the

objective spatial strain rates

$$\overset{\triangledown}{\delta\boldsymbol{\gamma}} = \delta\boldsymbol{\gamma} + \boldsymbol{\gamma} \times \delta\boldsymbol{\vartheta}$$
$$\overset{\triangledown}{\delta\boldsymbol{\kappa}} = \delta\boldsymbol{\kappa} + \boldsymbol{\kappa} \times \delta\boldsymbol{\vartheta}$$

leading to

$$V_i = \int_0^L \left(\overset{\triangledown}{\delta\boldsymbol{\gamma}} \cdot \mathbf{n} + \overset{\triangledown}{\delta\boldsymbol{\kappa}} \cdot \mathbf{m} \right) \mathrm{d}x \,. \tag{3.26}$$

The virtual change of the translational strain measure follows as

$$\delta\boldsymbol{\Gamma} = \delta\left(\boldsymbol{\Lambda}^T\mathbf{r}' - \mathbf{E}_1\right) = \delta\boldsymbol{\Lambda}^T\mathbf{r}' + \boldsymbol{\Lambda}^T\delta\mathbf{r}' = \boldsymbol{\Lambda}^T\left(\delta\mathbf{r}' + \mathbf{r}' \times \delta\boldsymbol{\vartheta}\right) . \tag{3.27}$$

The virtual change of the rotational strain measure follows as

$$\begin{aligned} \delta\widehat{\mathbf{K}} = \delta\left(\boldsymbol{\Lambda}^T\boldsymbol{\Lambda}'\right) &= \left(\widehat{\delta\boldsymbol{\vartheta}}\boldsymbol{\Lambda}\right)^T\boldsymbol{\Lambda}' + \boldsymbol{\Lambda}^T\left(\widehat{\delta\boldsymbol{\vartheta}}\boldsymbol{\Lambda}\right)' \\ &= \boldsymbol{\Lambda}^T\widehat{\delta\boldsymbol{\vartheta}}^T\boldsymbol{\Lambda}' + \boldsymbol{\Lambda}^T\widehat{\delta\boldsymbol{\vartheta}}'\boldsymbol{\Lambda} + \boldsymbol{\Lambda}^T\widehat{\delta\boldsymbol{\vartheta}}\boldsymbol{\Lambda}' = \boldsymbol{\Lambda}^T\delta\widehat{\boldsymbol{\vartheta}}'\boldsymbol{\Lambda} \\ \Rightarrow \quad \delta\mathbf{K} &= \boldsymbol{\Lambda}^T\delta\boldsymbol{\vartheta}' \,. \end{aligned} \tag{3.28}$$

On the other hand, taking the total variation of the spatial strain measures (3.2) and (3.3) we get

$$\delta\boldsymbol{\gamma} = \delta(\mathbf{r}' - \mathbf{t}_1) = \delta\mathbf{r}' - \widehat{\delta\boldsymbol{\vartheta}}\mathbf{t}_1 = \delta\mathbf{r}' - \delta\boldsymbol{\vartheta} \times (\mathbf{r}' - \boldsymbol{\gamma}) = \delta\mathbf{r}' + \mathbf{r}' \times \delta\boldsymbol{\vartheta} - \boldsymbol{\gamma} \times \delta\boldsymbol{\vartheta} \,, \tag{3.29}$$

$$\begin{aligned} \delta\widehat{\boldsymbol{\kappa}} = \delta(\boldsymbol{\Lambda}'\boldsymbol{\Lambda}^T) &= \widehat{\delta\boldsymbol{\vartheta}}'\boldsymbol{\Lambda}\boldsymbol{\Lambda}^T + \widehat{\delta\boldsymbol{\vartheta}}\boldsymbol{\Lambda}'\boldsymbol{\Lambda}^T + \boldsymbol{\Lambda}'\boldsymbol{\Lambda}^T\widehat{\delta\boldsymbol{\vartheta}}^T = \widehat{\delta\boldsymbol{\vartheta}}' + \widehat{\delta\boldsymbol{\vartheta}}\widehat{\boldsymbol{\kappa}} - \widehat{\boldsymbol{\kappa}}\widehat{\delta\boldsymbol{\vartheta}} = \widehat{\delta\boldsymbol{\vartheta}}' + \widehat{\delta\boldsymbol{\vartheta} \times \boldsymbol{\kappa}} \\ &= \widehat{\delta\boldsymbol{\vartheta}' + \delta\boldsymbol{\vartheta} \times \boldsymbol{\kappa}} \Rightarrow \delta\boldsymbol{\kappa} = \delta\boldsymbol{\vartheta}' - \boldsymbol{\kappa} \times \delta\boldsymbol{\vartheta} \,. \end{aligned} \tag{3.30}$$

Comparing (3.27) and (3.28) with (3.29) and (3.30) reveals the following relationship between the material and objective spatial strain rates

$$\begin{aligned} \overset{\triangledown}{\delta\boldsymbol{\gamma}} &= \delta\boldsymbol{\gamma} + \boldsymbol{\gamma} \times \delta\boldsymbol{\vartheta} = \delta\mathbf{r}' + \mathbf{r}' \times \delta\boldsymbol{\vartheta} = \boldsymbol{\Lambda}\delta\boldsymbol{\Gamma} \,, \\ \overset{\triangledown}{\delta\boldsymbol{\kappa}} &= \delta\boldsymbol{\kappa} + \boldsymbol{\kappa} \times \delta\boldsymbol{\vartheta} = \delta\boldsymbol{\vartheta}' = \boldsymbol{\Lambda}\delta\mathbf{K} \,. \end{aligned} \tag{3.31}$$

The specific virtual work of internal forces can therefore be written as

$$\delta\boldsymbol{\Gamma} \cdot \mathbf{N} + \delta\mathbf{K} \cdot \mathbf{M} = \overset{\triangledown}{\delta\boldsymbol{\gamma}} \cdot \mathbf{n} + \overset{\triangledown}{\delta\boldsymbol{\kappa}} \cdot \mathbf{m} \,, \tag{3.32}$$

but $\overset{\triangledown}{\delta\boldsymbol{\gamma}} \cdot \mathbf{n} + \overset{\triangledown}{\delta\boldsymbol{\kappa}} \cdot \mathbf{m} \neq \delta\boldsymbol{\gamma} \cdot \mathbf{n} + \delta\boldsymbol{\kappa} \cdot \mathbf{m}$. In other words, while ($\boldsymbol{\Gamma}$, $\mathbf{K}$) and ($\boldsymbol{\gamma}$, $\boldsymbol{\kappa}$) are both the

respective strain-energy conjugates to ($\mathbf{N}$, $\mathbf{M}$) and ($\mathbf{n}$, $\mathbf{m}$), i.e.

$$\phi = \frac{1}{2}\int_0^L (\boldsymbol{\Gamma}\cdot\mathbf{N} + \mathbf{K}\cdot\mathbf{M})\,\mathrm{d}x = \frac{1}{2}\int_0^L (\boldsymbol{\gamma}\cdot\mathbf{n} + \boldsymbol{\kappa}\cdot\mathbf{m})\,\mathrm{d}x\,, \tag{3.33}$$

only ($\delta\boldsymbol{\Gamma}$, $\delta\mathbf{K}$) are the virtual-work conjugates to ($\mathbf{N}$, $\mathbf{M}$), while the virtual-work conjugates to ($\mathbf{n}$, $\mathbf{m}$) are ($\overset{\triangledown}{\delta}\boldsymbol{\gamma}$, $\overset{\triangledown}{\delta}\boldsymbol{\kappa}$) rather than ($\delta\boldsymbol{\gamma}$, $\delta\boldsymbol{\kappa}$).

The virtual work of inertial forces is defined as the product between the virtual displacements and virtual rotations, respectively, with the change of specific momenta, $\dot{\mathbf{l}}$ and $\dot{\boldsymbol{\pi}}$

$$V_m = \int_0^L \left(\delta\mathbf{r}\cdot\dot{\mathbf{l}} + \delta\boldsymbol{\vartheta}\cdot\dot{\boldsymbol{\pi}}\right)\mathrm{d}x\,. \tag{3.34}$$

Finally, the virtual work of external loading is given as the work of distributed forces acting on virtual displacements and virtual rotations

$$V_e = \int_0^L (\delta\mathbf{r}\cdot\mathbf{n}_e + \delta\boldsymbol{\vartheta}\cdot\mathbf{m}_e)\,\mathrm{d}x + \delta\mathbf{r}_0\cdot\mathbf{F}_0 + \delta\boldsymbol{\vartheta}_0\cdot\mathbf{M}_0 + \delta\mathbf{r}_L\cdot\mathbf{F}_L + \delta\boldsymbol{\vartheta}_L\cdot\mathbf{M}_L\,, \tag{3.35}$$

Inserting (3.23), (3.27), (3.27), (3.34) and (3.35) into (3.22) we get $G = V_i + V_m - V_e = 0$ or

$$\begin{aligned} G \equiv \int_0^L \left(\left\langle \delta\mathbf{r}^T \quad \delta\boldsymbol{\vartheta}^T \right\rangle \begin{bmatrix} \mathbf{I}\frac{\mathrm{d}}{\mathrm{d}x} & \mathbf{0} \\ -\widehat{\mathbf{r}}' & \mathbf{I}\frac{\mathrm{d}}{\mathrm{d}x} \end{bmatrix} \right) \begin{Bmatrix} \mathbf{n} \\ \mathbf{m} \end{Bmatrix} \mathrm{d}x + \int_0^L \left\langle \delta\mathbf{r}^T \quad \delta\boldsymbol{\vartheta}^T \right\rangle \left(\begin{Bmatrix} \dot{\mathbf{k}} \\ \dot{\boldsymbol{\pi}} \end{Bmatrix} - \begin{Bmatrix} \mathbf{n}_e \\ \mathbf{m}_e \end{Bmatrix} \right) \mathrm{d}x \\ - \left\langle \delta\mathbf{r}_0^T \quad \delta\boldsymbol{\vartheta}_0^T \right\rangle \begin{Bmatrix} \mathbf{F}_0 \\ \mathbf{M}_0 \end{Bmatrix} - \left\langle \delta\mathbf{r}_L^T \quad \delta\boldsymbol{\vartheta}_L^T \right\rangle \begin{Bmatrix} \mathbf{F}_L \\ \mathbf{M}_L \end{Bmatrix} = 0\,. \end{aligned} \tag{3.36}$$

Comparing (3.36) to (3.21) we see that for $\mathbf{f} = \delta\mathbf{r}$ and $\boldsymbol{\varphi} = \delta\boldsymbol{\vartheta}$ these results are identical. This means that the virtual work principle can (and will) be used as a substitute for equation of motion.

Standard dynamic nodal residual

In order to implement the finite element method we must define the position of the so-called nodes (see Figure 3.2) and interpolate the virtual displacements and rotations $\delta\mathbf{r}$ and $\delta\boldsymbol{\vartheta}$. In the standard approach [4] these functions are interpolated using Lagrange polynomials. The i-th Lagrange polynomial $I^i(x)$ is equal to one at $x = x_i$ and zero at x_j for $i \neq j$. Also, $\sum_{i=1}^N I^i(x) = 1$ and $\sum_{i=1}^N I^{i'}(x) = 0$. In this way, the approximated values for the virtual displacements and

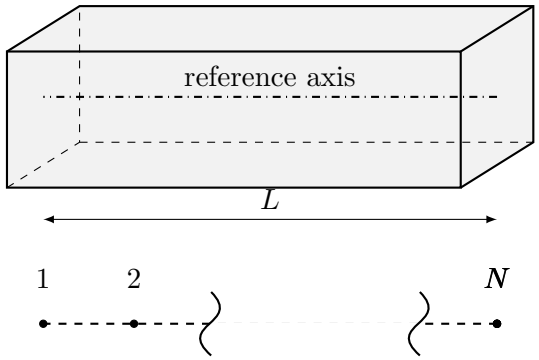

Figure 3.2: A beam of length L discretised into an N node element

rotations are

$$\delta\mathbf{r} \doteq \delta\mathbf{r}^h = \sum_{i=1}^{N} I^i(x)\delta\mathbf{r}_i \quad \text{and} \quad \delta\boldsymbol{\vartheta} \doteq \delta\boldsymbol{\vartheta}^h = \sum_{i=1}^{N} I^i(x)\delta\boldsymbol{\vartheta}_i\,, \tag{3.37}$$

as well as their derivatives

$$\delta\mathbf{r}' \doteq \delta\mathbf{r}^h = \sum_{i=1}^{N} I^{i'}(x)\delta\mathbf{r}_i \quad \text{and} \quad \delta\boldsymbol{\vartheta}' \doteq \delta\boldsymbol{\vartheta}^h = \sum_{i=1}^{N} I^{i'}(x)\delta\boldsymbol{\vartheta}_i\,. \tag{3.38}$$

Substituting (3.37) and (3.38) into (3.36) we get

$$G^h \equiv \sum_{i=1}^{N} \left\langle \delta\mathbf{r}_i^T \quad \delta\boldsymbol{\vartheta}_i^T \right\rangle \mathbf{g}^i = 0\,, \tag{3.39}$$

with $\mathbf{g}^i$ as the nodal dynamic residual

$$\mathbf{g}^i = \mathbf{q}_i^i + \mathbf{q}_m^i - \mathbf{q}_e^i\,, \tag{3.40}$$

and

$$\mathbf{q}_i^i = \int_0^L \begin{bmatrix} I^{i\prime}\mathbf{I} & \mathbf{0} \\ -I^{i\prime}\widehat{\mathbf{r}}' & I^{i\prime}\mathbf{I} \end{bmatrix} \begin{Bmatrix} \mathbf{n} \\ \mathbf{m} \end{Bmatrix} \mathrm{d}x \tag{3.41}$$

$$\mathbf{q}_m^i = \int_0^L I^i \begin{Bmatrix} \dot{\mathbf{k}} \\ \dot{\boldsymbol{\pi}} \end{Bmatrix} \mathrm{d}x \tag{3.42}$$

$$\mathbf{q}_e^i = \int_0^L I^i \begin{Bmatrix} \mathbf{n}_e \\ \mathbf{m}_e \end{Bmatrix} \mathrm{d}x + \delta_1^i \begin{Bmatrix} \mathbf{F}_0 \\ \mathbf{M}_0 \end{Bmatrix} + \delta_N^i \begin{Bmatrix} \mathbf{F}_L \\ \mathbf{M}_L \end{Bmatrix} \tag{3.43}$$

as the nodal vectors of internal, inertial and external loads, respectively, where δ_j^i is the Kronecker delta which is equal to one for $i = j$ and zero otherwise. Since (3.39) must be satisfied for

arbitrary values of $\delta\mathbf{r}_i$ and $\delta\boldsymbol{\vartheta}_i$, we have

$$\mathbf{g}^i = \mathbf{0}\,, \quad i = 1,\, 2,\, ..,\, N\,, \tag{3.44}$$

as the non-linear equation defining dynamic equilibrium of the beam element. We will refer to $\mathbf{g}^i$ as the standard nodal dynamic residual. Note that there exists a matrix operator containing $I^{i'}\mathbf{I}$ and $I^i\widehat{\mathbf{r}}'$ acting on the vector of spatial stress resultants in $\mathbf{q}_i^i$ (shaded area in (3.41)) as opposed to $\mathbf{q}_m^i$ and $\mathbf{q}_e^i$ where the vectors within the integrals are only multiplied by I^i.

3.2 Fixed-pole approach

In this section we use the fixed-pole approach given in [7, 10, 11] along with the configuration-tensor approach used in [10] and presented in Chapter 2. In [10], Bottasso and Borri have interpolated the incremental configuration vectors, while in the present case we interpolate the **iterative configuration vectors** (which is analogous to the approach given in the previous section where spin vectors are interpolated). We derive the governing equations and conclude with the fixed-pole dynamic residual.

3.2.1 Kinematic and constitutive equations

The spatial strain measures $\boldsymbol{\gamma}$ and $\boldsymbol{\kappa}$ can be stacked as

$$\begin{Bmatrix} \boldsymbol{\gamma} \\ \boldsymbol{\kappa} \end{Bmatrix} = \boldsymbol{\chi} - \boldsymbol{\chi}_N\,, \tag{3.45}$$

with

$$\boldsymbol{\chi} = \begin{Bmatrix} \mathbf{r}' \\ \boldsymbol{\kappa} \end{Bmatrix}\,,$$

as the strain parameter or the "local configuration parameter", and

$$\boldsymbol{\chi}_N = \begin{Bmatrix} \mathbf{t}_1 \\ \mathbf{0} \end{Bmatrix}$$

as the "natural configuration parameter" as termed in [7, 10]. The reason for dividing strain measures in two parts $\boldsymbol{\chi}$ and $\boldsymbol{\chi}_N$ becomes evident when taking the derivative of the configuration

tensor with respect to the beam arc-length x

$$\mathbf{C}' = \frac{\mathrm{d}}{\mathrm{d}x}\begin{bmatrix}\mathbf{\Lambda} & \widehat{\mathbf{r}}\mathbf{\Lambda} \\ \mathbf{0} & \mathbf{\Lambda}\end{bmatrix} = \begin{bmatrix}\mathbf{\Lambda}' & \widehat{\mathbf{r}}'\mathbf{\Lambda} + \widehat{\mathbf{r}}\mathbf{\Lambda}' \\ \mathbf{0} & \mathbf{\Lambda}'\end{bmatrix}.$$

Noting from (3.3) that $\mathbf{\Lambda}'\mathbf{\Lambda}^T = \widehat{\boldsymbol{\kappa}}$ we obtain an analogous result to (2.26)

$$\mathbf{C}' = \begin{bmatrix}\widehat{\boldsymbol{\kappa}} & \widehat{\mathbf{r}}' + \widehat{\mathbf{r}\times\boldsymbol{\kappa}} + \widehat{\boldsymbol{\kappa}}\widehat{\mathbf{r}} \\ \mathbf{0} & \widehat{\boldsymbol{\kappa}}\end{bmatrix}\begin{bmatrix}\mathbf{\Lambda} & \mathbf{0} \\ \mathbf{0} & \mathbf{\Lambda}\end{bmatrix} = \begin{bmatrix}\widehat{\boldsymbol{\kappa}} & \widehat{\mathbf{r}}' + \widehat{\mathbf{r}\times\boldsymbol{\kappa}} \\ \mathbf{0} & \widehat{\boldsymbol{\kappa}}\end{bmatrix}\begin{bmatrix}\mathbf{I} & \widehat{\mathbf{r}} \\ \mathbf{0} & \mathbf{I}\end{bmatrix}\begin{bmatrix}\mathbf{\Lambda} & \mathbf{0} \\ \mathbf{0} & \mathbf{\Lambda}\end{bmatrix}, \tag{3.46}$$

because for $\widehat{\mathbf{r}}$, $\widehat{\boldsymbol{\kappa}} \in \mathrm{so}(3)$, $\widehat{\mathbf{r}\times\boldsymbol{\kappa}} = \widehat{\mathbf{r}}\widehat{\boldsymbol{\kappa}} - \widehat{\boldsymbol{\kappa}}\widehat{\mathbf{r}}$. Using relationship (2.18) we have the fixed-pole description of the strain parameter as

$$\overline{\boldsymbol{\chi}} = \begin{Bmatrix}\mathbf{r}' + \mathbf{r}\times\boldsymbol{\kappa} \\ \boldsymbol{\kappa}\end{Bmatrix}, \tag{3.47}$$

which enables us to recognise that (3.46) can in fact be written as

$$\mathbf{C}' = \widehat{\overline{\boldsymbol{\chi}}}\mathbf{C}. \tag{3.48}$$

Once again, we note the analogy with the derivative of the orientation matrix $\mathbf{\Lambda}$. Furthermore, noting that result (3.48) is in full accordance with result (2.26) we have

$$\mathbf{C}' = \mathbf{C}\widehat{\mathbf{X}}, \tag{3.49}$$

with $\mathbf{X} = \mathbf{C}^{-1}\overline{\boldsymbol{\chi}} = \begin{Bmatrix}\mathbf{\Lambda}^T\mathbf{r}' \\ \mathbf{K}\end{Bmatrix}$ as the material strain parameter.

The material stress resultants are related to the strain measures via linear constitutive law, so rewriting (3.6) in a stacked form we have

$$\begin{Bmatrix}\mathbf{N} \\ \mathbf{M}\end{Bmatrix} = \mathbf{D}\begin{Bmatrix}\mathbf{\Gamma} \\ \mathbf{K}\end{Bmatrix} = \mathbf{D}\left(\mathbf{X} - \mathbf{X}_N\right), \tag{3.50}$$

where $\mathbf{X}_N = \begin{Bmatrix}\mathbf{E}_1 \\ \mathbf{0}\end{Bmatrix}$.

3.2.2 Equations of motion

The strong form of equations of motion can be written in a more compact form by using the fixed-pole description of kinematic quantities. In order to simplify the notation, the material

generalised vectors of stress resultants, external loading and momenta are introduced

$$\mathbf{S} = \begin{Bmatrix} \mathbf{N} \\ \mathbf{M} \end{Bmatrix}, \quad \mathbf{S}_e = \begin{Bmatrix} \boldsymbol{\Lambda}^T \mathbf{n}_e \\ \boldsymbol{\Lambda}^T \mathbf{m}_e \end{Bmatrix} = \begin{Bmatrix} \mathbf{N}_e \\ \mathbf{M}_e \end{Bmatrix}, \quad \text{and} \quad \mathbf{P} = \begin{Bmatrix} \boldsymbol{\Lambda}^T \mathbf{l} \\ \boldsymbol{\Lambda}^T \boldsymbol{\pi} \end{Bmatrix} = \begin{Bmatrix} \mathbf{L} \\ \boldsymbol{\Pi} \end{Bmatrix}.$$

Rewriting (3.19) in a stacked form we have

$$\begin{Bmatrix} \boldsymbol{\Lambda}'\mathbf{N} + \boldsymbol{\Lambda}\mathbf{N}' \\ \boldsymbol{\Lambda}'\mathbf{M} + \boldsymbol{\Lambda}\mathbf{M}' + \widehat{\mathbf{r}}'\boldsymbol{\Lambda}\mathbf{N} \end{Bmatrix} + \begin{Bmatrix} \boldsymbol{\Lambda}\mathbf{N}_e \\ \boldsymbol{\Lambda}\mathbf{M}_e \end{Bmatrix} = \begin{Bmatrix} \dot{\boldsymbol{\Lambda}}\mathbf{L} + \boldsymbol{\Lambda}\dot{\mathbf{L}} \\ \dot{\boldsymbol{\Lambda}}\boldsymbol{\Pi} + \boldsymbol{\Lambda}\dot{\boldsymbol{\Pi}} \end{Bmatrix}.$$

Using the relationships $\boldsymbol{\Lambda}' = \boldsymbol{\Lambda}\widehat{\mathbf{K}}$ and $\dot{\boldsymbol{\Lambda}} = \boldsymbol{\Lambda}\widehat{\mathbf{W}}$ and also rewriting $\widehat{\mathbf{r}}'$ as $\boldsymbol{\Lambda}\widehat{\boldsymbol{\Lambda}^T\mathbf{r}'}\boldsymbol{\Lambda}^T$ as well as noting that $(\boldsymbol{\Lambda}^T\mathbf{v}) \times \mathbf{L} = \mathbf{0}$ (because $\mathbf{l} = A\rho\mathbf{v}$, i.e. $\mathbf{v} \times \mathbf{v} = \mathbf{0}$) the above equation turns into

$$\begin{bmatrix} \boldsymbol{\Lambda} & \mathbf{0} \\ \mathbf{0} & \boldsymbol{\Lambda} \end{bmatrix} \left(\begin{Bmatrix} \mathbf{N}' \\ \mathbf{M}' \end{Bmatrix} + \begin{bmatrix} \widehat{\mathbf{K}} & \mathbf{0} \\ \widehat{\boldsymbol{\Lambda}^T\mathbf{r}'} & \widehat{\mathbf{K}} \end{bmatrix} \begin{Bmatrix} \mathbf{N} \\ \mathbf{M} \end{Bmatrix} + \begin{Bmatrix} \mathbf{N}_e \\ \mathbf{M}_e \end{Bmatrix} \right) = \begin{bmatrix} \boldsymbol{\Lambda} & \mathbf{0} \\ \mathbf{0} & \boldsymbol{\Lambda} \end{bmatrix} \left(\begin{Bmatrix} \dot{\mathbf{L}} \\ \dot{\boldsymbol{\Pi}} \end{Bmatrix} + \begin{bmatrix} \widehat{\mathbf{W}} & \mathbf{0} \\ \widehat{\mathbf{V}} & \widehat{\mathbf{W}} \end{bmatrix} \begin{Bmatrix} \mathbf{L} \\ \boldsymbol{\Pi} \end{Bmatrix} \right),$$

i.e.,

$$\begin{Bmatrix} \mathbf{N}' \\ \mathbf{M}' \end{Bmatrix} + \underbrace{\begin{bmatrix} \widehat{\mathbf{K}} & \mathbf{0} \\ \widehat{\boldsymbol{\Lambda}^T\mathbf{r}'} & \widehat{\mathbf{K}} \end{bmatrix}}_{-\widehat{\mathbf{X}}^T} \begin{Bmatrix} \mathbf{N} \\ \mathbf{M} \end{Bmatrix} + \begin{Bmatrix} \mathbf{N}_e \\ \mathbf{M}_e \end{Bmatrix} = \begin{Bmatrix} \dot{\mathbf{L}} \\ \dot{\boldsymbol{\Pi}} \end{Bmatrix} + \underbrace{\begin{bmatrix} \widehat{\mathbf{W}} & \mathbf{0} \\ \widehat{\mathbf{V}} & \widehat{\mathbf{W}} \end{bmatrix}}_{-\widehat{\boldsymbol{\Omega}}^T} \begin{Bmatrix} \mathbf{L} \\ \boldsymbol{\Pi} \end{Bmatrix}, \tag{3.51}$$

where we recognise the material strain parameter $\mathbf{X}$ as well as the material generalised velocities $\boldsymbol{\Omega}$ as given in (2.21) in the form of the generalised cross product. This enables us to rewrite (3.51) as

$$\mathbf{S}' - \widehat{\mathbf{X}}^T\mathbf{S} + \mathbf{S}_e = \dot{\mathbf{P}} - \widehat{\boldsymbol{\Omega}}^T\mathbf{P}. \tag{3.52}$$

The next step is finding the relationship between the fixed-pole and the material generalised stress resultants, external loading and momenta. Since the specific work of stress resultants must remain invariant to the choice of the kinematic description, the fixed-pole stress resultants are introduced as a conjugate quantity to the fixed-pole strain measures, i.e.

$$(\mathbf{X} - \mathbf{X}_N) \cdot \mathbf{S} = (\overline{\boldsymbol{\chi}} - \overline{\boldsymbol{\chi}}_N) \cdot \overline{\mathbf{s}}.$$

Substituting the relationship between the fixed-pole and the material strain measures using (2.19), $\overline{\boldsymbol{\chi}} - \overline{\boldsymbol{\chi}}_N = \mathbf{C}(\mathbf{X} - \mathbf{X}_N)$ the above equation turns into

$$(\mathbf{X} - \mathbf{X}_N) \cdot \mathbf{S} = [\mathbf{C}(\mathbf{X} - \mathbf{X}_N)] \cdot \overline{\mathbf{s}},$$

$x = 0$:	$\mathbf{C} = \mathbf{C}_0$
$x = L$:	$\mathbf{C} = \mathbf{C}_L$

Table 3.3: Essential (kinematic) boundary conditions – fixed pole approach

$x = 0$:	$-\overline{\mathbf{s}} = \overline{\mathbf{s}}_0$
$x = L$:	$\overline{\mathbf{s}} = \overline{\mathbf{s}}_L$

Table 3.4: Natural (static) boundary conditions – fixed pole approach

from where we obtain

$$\overline{\mathbf{s}} = \mathbf{C}^{-T}\mathbf{S}\,. \tag{3.53}$$

An analogous relationship holds for the external forces and specific momenta [10]

$$\overline{\mathbf{p}} = \mathbf{C}^{-T}\mathbf{P}\,, \tag{3.54}$$

$$\overline{\mathbf{s}}_e = \mathbf{C}^{-T}\mathbf{S}_e\,. \tag{3.55}$$

Substituting (3.53)-(3.55) into (3.52) we have

$$(\mathbf{C}^T\overline{\mathbf{s}})' - \widehat{\mathbf{X}}^T\mathbf{C}^T\overline{\mathbf{s}} + \mathbf{C}^T\overline{\mathbf{s}}_e = (\mathbf{C}^{\dot{T}}\overline{\mathbf{p}}) - \widehat{\mathbf{\Omega}}^T\mathbf{C}^T\overline{\mathbf{p}}$$
$$\widehat{\mathbf{X}}^T\mathbf{C}^T\overline{\mathbf{s}} + \mathbf{C}^T\overline{\mathbf{s}}' - \widehat{\mathbf{X}}^T\mathbf{C}^T\overline{\mathbf{s}} + \mathbf{C}^T\overline{\mathbf{s}}_e = \widehat{\mathbf{\Omega}}^T\mathbf{C}^T\overline{\mathbf{p}} + \mathbf{C}^T\dot{\overline{\mathbf{p}}} - \widehat{\mathbf{\Omega}}^T\mathbf{C}^T\overline{\mathbf{p}}\,,$$

which, since $\mathbf{C} \neq \mathbf{0}$, gives

$$\overline{\mathbf{s}}' + \overline{\mathbf{s}}_e = \dot{\overline{\mathbf{p}}}\,, \tag{3.56}$$

as the strong form of the equations of motion. Obviously, the approach which combines the fixed-pole description of kinematic quantities along with the configuration tensor results in an extremely elegant equation. Of course, in order for the problem to be fully defined we need to couple (3.56) with the appropriate essential and natural boundary conditions as given in Table 3.3 and Table 3.4. These boundary conditions are equivalent to the ones given in Table 3.1 and Table 3.2, but are written in a compact form using the configuration tensor.

Weak form of equations of motion

In order to obtain the weak form of the equation of motion (3.56) we multiply it with a test function $\boldsymbol{\zeta}$ which satisfies conditions (i)-(iii) given in the introduction to this chapter and integrate

it over the domain of the problem

$$\int_0^L \boldsymbol{\zeta} \cdot \left(\dot{\overline{\mathbf{p}}} - \overline{\mathbf{s}}' - \overline{\mathbf{s}}_e \right) \mathrm{d}x = 0 \,. \tag{3.57}$$

Integrating by parts the term $\int_0^L \boldsymbol{\zeta} \cdot \overline{\mathbf{s}}' \, \mathrm{d}x$ we get

$$\int_0^L \boldsymbol{\zeta} \cdot \dot{\overline{\mathbf{p}}} \, \mathrm{d}x + \int_0^L \mathbf{f}' \cdot \overline{\mathbf{s}} \, \mathrm{d}x - \int_0^L \mathbf{f} \cdot \overline{\mathbf{s}}_e \, \mathrm{d}x = \boldsymbol{\zeta} \cdot \overline{\mathbf{s}}|_0^L \tag{3.58}$$

The term $\boldsymbol{\zeta} \cdot \overline{\mathbf{s}}|_0^L$ has to be complemented with the appropriate, predefined boundary conditions (Table 3.3 or Table 3.4): the stress resultants $\overline{\mathbf{s}}$ at $x = 0$ and $x = L$ are zero in case of unloaded ends or equal to the applied end loads $\overline{\mathbf{s}}_0$ and $\overline{\mathbf{s}}_L$ (natural boundary conditions) or are equal to the reactions in which case the essential boundary conditions are defined. In that case, due to condition (iii) the test function is zero and the term vanishes. Since the essential and natural boundary conditions are mutually exclusive, equation (3.58) finally gives the weak form of equation (3.56) as

$$\int_0^L \left(\boldsymbol{\zeta} \cdot \dot{\overline{\mathbf{p}}} + \boldsymbol{\zeta}' \cdot \overline{\mathbf{s}} - \boldsymbol{\zeta} \cdot \overline{\mathbf{s}}_e \right) \mathrm{d}x = \boldsymbol{\zeta}_L \cdot \overline{\mathbf{s}}_L + \boldsymbol{\zeta}_0 \cdot \overline{\mathbf{s}}_0 \,. \tag{3.59}$$

Virtual work principle

The strain energy (3.24) may now be written as

$$\phi = \frac{1}{2} \int_0^L (\mathbf{X} - \mathbf{X}_N) \cdot \mathbf{S} \, \mathrm{d}x \,. \tag{3.60}$$

Variation of the strain energy is equal to the virtual work of internal forces

$$V_i = \delta\phi = \frac{1}{2} \int_0^L \delta\mathbf{X} \cdot \mathbf{S} \, \mathrm{d}x + \frac{1}{2} \int_0^L (\mathbf{X} - \mathbf{X}_N) \cdot \delta\mathbf{S} \, \mathrm{d}x = \int_0^L \delta\mathbf{X} \cdot \mathbf{S} \, \mathrm{d}x \,, \tag{3.61}$$

because

$$\delta\mathbf{S} = \delta \left[\mathbf{D}(\mathbf{X} - \mathbf{X}_N) \right] = \mathbf{D}\delta\mathbf{X} \,.$$

From (3.49) we have $\widehat{\mathbf{X}} = \mathbf{C}^{-1}\mathbf{C}'$, therefore, using (2.66) and due to (A.2) we obtain the variation of the material strain parameter as

$$\begin{aligned} \delta\widehat{\mathbf{X}} &= \delta\mathbf{C}^{-1}\mathbf{C}' + \mathbf{C}^{-1}\delta\mathbf{C}' \\ &= -\mathbf{C}^{-1}\widehat{\delta\boldsymbol{\zeta}}\mathbf{C}' + \mathbf{C}^{-1}\left(\widehat{\delta\boldsymbol{\zeta}}\mathbf{C}\right)' \\ &= -\mathbf{C}^{-1}\widehat{\delta\boldsymbol{\zeta}}\mathbf{C}' + \mathbf{C}^{-1}\widehat{\delta\boldsymbol{\zeta}}'\mathbf{C} + \mathbf{C}^{-1}\widehat{\delta\boldsymbol{\zeta}}\mathbf{C}' = \mathbf{C}^{-1}\widehat{\delta\boldsymbol{\zeta}}'\mathbf{C} \\ \Rightarrow \quad \delta\mathbf{X} &= \mathbf{C}^{-1}\delta\boldsymbol{\zeta}' \,. \end{aligned} \tag{3.62}$$

Inserting (3.62) into (3.61) we get the virtual work of internal forces

$$V_i = \int_0^L \delta\boldsymbol{\varsigma}' \cdot \mathbf{C}^{-T}\mathbf{S}\,\mathrm{d}x = \int_0^L \delta\boldsymbol{\varsigma}' \cdot \bar{\mathbf{s}}\,\mathrm{d}x\,. \tag{3.63}$$

Since the virtual work of inertial and external forces is done on virtual displacements $\delta\mathbf{r}$ and virtual rotations $\delta\boldsymbol{\vartheta}$, we need to relate these quantities to the configurational spin vector (virtual configuration vector) $\delta\boldsymbol{\varsigma}$ as it is demonstrated in Appendix A.2.6.

From (3.54) we have the relationship between the generalised vectors of fixed-pole and spatial momenta

$$\overline{\mathbf{p}} = \begin{bmatrix} \mathbf{I} & \mathbf{0} \\ \widehat{\mathbf{r}} & \mathbf{I} \end{bmatrix} \mathbf{p}.$$

Taking the time-derivative of the above relationship yields

$$\dot{\overline{\mathbf{p}}} = \begin{bmatrix} \mathbf{0} & \mathbf{0} \\ \widehat{\mathbf{v}} & \mathbf{0} \end{bmatrix} \begin{Bmatrix} \mathbf{l} \\ \boldsymbol{\pi} \end{Bmatrix} + \begin{bmatrix} \mathbf{I} & \mathbf{0} \\ \widehat{\mathbf{r}} & \mathbf{I} \end{bmatrix} \dot{\mathbf{p}} = \begin{bmatrix} \mathbf{I} & \mathbf{0} \\ \widehat{\mathbf{r}} & \mathbf{I} \end{bmatrix} \dot{\mathbf{p}}\,, \tag{3.64}$$

because $\mathbf{v} \times \mathbf{l} = \mathbf{v} \times A\rho\mathbf{v} = \mathbf{0}$. Substituting (A.37) and recognising (3.64) we can rewrite the virtual work of inertial forces (3.34) as

$$V_m = \int_0^L \delta\boldsymbol{\varsigma} \cdot \begin{bmatrix} \mathbf{I} & \mathbf{0} \\ \widehat{\mathbf{r}} & \mathbf{I} \end{bmatrix} \begin{Bmatrix} \dot{\mathbf{l}} \\ \dot{\boldsymbol{\pi}} \end{Bmatrix} \mathrm{d}x = \int_0^L \delta\boldsymbol{\varsigma} \cdot \dot{\overline{\mathbf{p}}}\,\mathrm{d}x\,, \tag{3.65}$$

Substituting (A.37) into (3.35), the standard form of the virtual work of external forces transforms to

$$\begin{aligned} V_e &= \int_0^L \delta\boldsymbol{\varsigma} \cdot \begin{bmatrix} \mathbf{I} & \mathbf{0} \\ \widehat{\mathbf{r}} & \mathbf{I} \end{bmatrix} \begin{Bmatrix} \mathbf{n}_e \\ \mathbf{m}_e \end{Bmatrix} \mathrm{d}x + \delta\boldsymbol{\varsigma}_0 \cdot \begin{bmatrix} \mathbf{I} & \mathbf{0} \\ \widehat{\mathbf{r}}_0 & \mathbf{I} \end{bmatrix} \begin{Bmatrix} \mathbf{F}_0 \\ \mathbf{M}_0 \end{Bmatrix} + \delta\boldsymbol{\varsigma}_L \cdot \begin{bmatrix} \mathbf{I} & \mathbf{0} \\ \widehat{\mathbf{r}}_L & \mathbf{I} \end{bmatrix} \begin{Bmatrix} \mathbf{F}_L \\ \mathbf{M}_L \end{Bmatrix} \\ &= \int_0^L \delta\boldsymbol{\varsigma} \cdot \bar{\mathbf{s}}_e\,\mathrm{d}x + \delta\boldsymbol{\varsigma}_0 \cdot \bar{\mathbf{s}}_0 + \delta\boldsymbol{\varsigma}_L \cdot \bar{\mathbf{s}}_L\,. \end{aligned} \tag{3.66}$$

Inserting (3.63), (3.65) and (3.66) into the virtual work principle (3.22) we have

$$\overline{G} \equiv \int_0^L \left(\delta\boldsymbol{\varsigma}' \cdot \bar{\mathbf{s}} + \delta\boldsymbol{\varsigma} \cdot \dot{\overline{\mathbf{p}}} - \delta\boldsymbol{\varsigma} \cdot \bar{\mathbf{s}}_e\right) \mathrm{d}x = \delta\boldsymbol{\varsigma}_1 \cdot \bar{\mathbf{s}}_0 + \delta\boldsymbol{\varsigma}_N \cdot \bar{\mathbf{s}}_L\,, \tag{3.67}$$

which is a result identical to (3.59) for $\delta\boldsymbol{\varsigma} = \boldsymbol{\zeta}$.

Fixed-pole dynamic nodal residual

Using a standard finite-element discretisation in a sense that $\delta\boldsymbol{\varsigma}$ in (3.67) is interpolated using Lagrange polynomials we have

$$\delta\boldsymbol{\varsigma} \doteq \sum_{i=1}^{N} I^i(x)\delta\boldsymbol{\varsigma}_i \quad \text{and} \quad \delta\boldsymbol{\varsigma}' \doteq \sum_{i=1}^{N} I^{i'}(x)\delta\boldsymbol{\varsigma}_i \,. \tag{3.68}$$

Substituting (3.68) into (3.67) we get

$$\overline{G}^h \equiv \sum_{i=1}^{N} \delta\boldsymbol{\varsigma}_i^T \overline{\mathbf{g}}^i = 0 \,, \tag{3.69}$$

with $\overline{\mathbf{g}}^i$ as the nodal dynamic residual

$$\overline{\mathbf{g}}^i = \overline{\mathbf{q}}^i_m + \overline{\mathbf{q}}^i_i - \overline{\mathbf{q}}^i_e \,, \tag{3.70}$$

and

$$\overline{\mathbf{q}}^i_m = \int_0^L I^i \dot{\overline{\mathbf{p}}} \, \mathrm{d}x \,, \tag{3.71}$$

$$\overline{\mathbf{q}}^i_i = \int_0^L I^{i\prime} \overline{\mathbf{s}} \, \mathrm{d}x \,, \tag{3.72}$$

$$\overline{\mathbf{q}}^i_e = \int_0^L I^i \overline{\mathbf{s}}_e \, \mathrm{d}x + \delta^i_1 \overline{\mathbf{s}}_0 + \delta^i_N \overline{\mathbf{s}}_L \,, \tag{3.73}$$

as the nodal vectors of inertial, internal and external forces, respectively. Since (3.69) must be satisfied for arbitrary values of $\delta\boldsymbol{\varsigma}_i$, the non-linear equation of our problem is

$$\overline{\mathbf{g}}^i = \mathbf{0} \,, \quad i = 1, 2, .., N \,. \tag{3.74}$$

3.2.3 Alternative fixed-pole description

The fixed-pole theory can be given in an alternative manner, completely circumventing the use of the configuration tensor (in its explicit sense) and its properties related to its being an element of the special group of rigid motions SR(6). This approach was described in [76] and starts from the fact that the stress resultants at a cross section can be statically reduced (as shown in Figure 3.3) to the force and couple system at the fixed pole, O resulting in a new set of stress resultants

$$\begin{Bmatrix} \overline{\mathbf{n}} \\ \overline{\mathbf{m}} \end{Bmatrix} = \begin{Bmatrix} \mathbf{n} \\ \mathbf{m} + \mathbf{r} \times \mathbf{n} \end{Bmatrix} = \begin{bmatrix} \mathbf{I} & \mathbf{0} \\ \widehat{\mathbf{r}} & \mathbf{I} \end{bmatrix} \begin{Bmatrix} \mathbf{n} \\ \mathbf{m} \end{Bmatrix} . \tag{3.75}$$

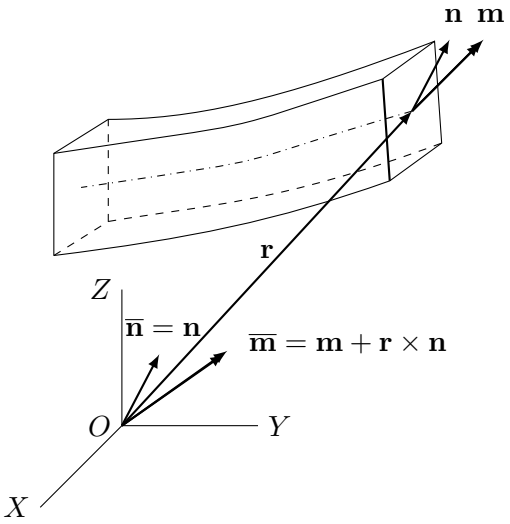

Figure 3.3: Reduction of the spatial stress resultants the fixed-pole stress resultants at O

Since the strain energy (3.33) must remain invariant to the choice of stress resultants, from the requirement

$$\phi = \frac{1}{2}\int_0^L (\boldsymbol{\gamma}\cdot\mathbf{n} + \boldsymbol{\kappa}\cdot\mathbf{m})\,\mathrm{d}x = \frac{1}{2}\int_0^L (\overline{\boldsymbol{\gamma}}\cdot\overline{\mathbf{n}} + \overline{\boldsymbol{\kappa}}\cdot\overline{\mathbf{m}})\,\mathrm{d}x\,. \tag{3.76}$$

we find the conjugate strain measures as

$$\begin{aligned}
\overline{\boldsymbol{\gamma}}\cdot\overline{\mathbf{n}} + \overline{\boldsymbol{\kappa}}\cdot\overline{\mathbf{m}} &= \boldsymbol{\gamma}\cdot\mathbf{n} + \boldsymbol{\kappa}\cdot\mathbf{m} \\
\overline{\boldsymbol{\gamma}}\cdot\mathbf{n} + \overline{\boldsymbol{\kappa}}\cdot(\mathbf{m} + \mathbf{r}\times\mathbf{n}) &= \boldsymbol{\gamma}\cdot\mathbf{n} + \boldsymbol{\kappa}\cdot\mathbf{m} \\
\Rightarrow \overline{\boldsymbol{\kappa}} &= \boldsymbol{\kappa} \\
\overline{\boldsymbol{\gamma}} &= \boldsymbol{\gamma} + \mathbf{r}\times\boldsymbol{\kappa}\,,
\end{aligned}$$

which can be written as

$$\begin{Bmatrix} \overline{\boldsymbol{\gamma}} \\ \overline{\boldsymbol{\kappa}} \end{Bmatrix} = \begin{bmatrix} \mathbf{I} & \widehat{\mathbf{r}} \\ \mathbf{0} & \mathbf{I} \end{bmatrix} \begin{Bmatrix} \boldsymbol{\gamma} \\ \boldsymbol{\kappa} \end{Bmatrix}, \tag{3.77}$$

where we recognise relationship (2.18) between spatial and fixed-pole objects.

Virtual work principle and objective fixed-pole strain rates

In order to write the virtual work of internal forces we must find the corresponding strain rates. As shown in Section 3.1, the **objective spatial strain rates** are virtual-work conjugate to the spatial stress resultants. Since the fixed-pole strain measures are derived from the spatial strain measures, it is logical to stipulate that the conjugate strain rates to the fixed-pole stress resul-

tants are also not the total variations of the fixed-pole strain measures. This can be illustrated very easily by rewriting the right-hand side of (3.32) and substituting (3.75) so that

$$\overset{\triangledown}{\delta}\boldsymbol{\gamma}\cdot\mathbf{n}+\overset{\triangledown}{\delta}\boldsymbol{\kappa}\cdot\mathbf{m}=\overset{\triangledown}{\delta}\boldsymbol{\gamma}\cdot\overline{\mathbf{n}}+\overset{\triangledown}{\delta}\boldsymbol{\kappa}\cdot(\overline{\mathbf{m}}-\mathbf{r}\times\overline{\mathbf{n}})\,,$$

which gives

$$\overset{\triangledown}{\delta}\boldsymbol{\gamma}\cdot\mathbf{n}+\overset{\triangledown}{\delta}\boldsymbol{\kappa}\cdot\mathbf{m}=\underbrace{(\overset{\triangledown}{\delta}\boldsymbol{\gamma}+\mathbf{r}\times\overset{\triangledown}{\delta}\boldsymbol{\kappa})}_{\overset{\diamondsuit}{\delta}\overline{\boldsymbol{\gamma}}}\cdot\overline{\mathbf{n}}+\overset{\triangledown}{\delta}\boldsymbol{\kappa}\cdot\overline{\mathbf{m}}\,,$$

with $\overset{\diamondsuit}{\delta}\overline{\boldsymbol{\gamma}}=\overset{\triangledown}{\delta}\boldsymbol{\gamma}+\mathbf{r}\times\overset{\triangledown}{\delta}\boldsymbol{\kappa}$ and $\overset{\diamondsuit}{\delta}\overline{\boldsymbol{\kappa}}=\overset{\triangledown}{\delta}\boldsymbol{\kappa}$ as the **objective fixed-pole strain rates**. Substituting (3.31) in this result we get the relationship between the material, spatial and fixed-pole objective strain rates

$$\begin{Bmatrix}\overset{\diamondsuit}{\delta}\overline{\boldsymbol{\gamma}}\\ \overset{\diamondsuit}{\delta}\overline{\boldsymbol{\kappa}}\end{Bmatrix}=\begin{bmatrix}\mathbf{I}&\widehat{\mathbf{r}}\\ \mathbf{0}&\mathbf{I}\end{bmatrix}\begin{Bmatrix}\overset{\triangledown}{\delta}\boldsymbol{\gamma}\\ \overset{\triangledown}{\delta}\boldsymbol{\kappa}\end{Bmatrix}=\underbrace{\begin{bmatrix}\mathbf{I}&\widehat{\mathbf{r}}\\ \mathbf{0}&\mathbf{I}\end{bmatrix}\begin{bmatrix}\boldsymbol{\Lambda}&\mathbf{0}\\ \mathbf{0}&\boldsymbol{\Lambda}\end{bmatrix}}_{\mathbf{C}}\begin{Bmatrix}\delta\boldsymbol{\Gamma}\\ \delta\mathbf{K}\end{Bmatrix}\,,\tag{3.78}$$

which is identical to the relationship between the material, spatial and fixed-pole objects as given in (2.19). This in turn enables us to write the virtual work of internal forces in the fixed-pole description as

$$V_i=\int_0^L\left(\overset{\diamondsuit}{\delta}\overline{\boldsymbol{\gamma}}\cdot\overline{\mathbf{n}}+\overset{\diamondsuit}{\delta}\overline{\boldsymbol{\kappa}}\cdot\overline{\mathbf{m}}\right)\,\mathrm{d}x\,,\tag{3.79}$$

which, after introducing the fixed-pole virtual displacements (note that this relationship is analogous to (A.37))

$$\overline{\delta\mathbf{r}}=\delta\mathbf{r}+\mathbf{r}\times\delta\boldsymbol{\vartheta}\,,\tag{3.80}$$

and recognizing that

$$\overset{\diamondsuit}{\delta}\overline{\boldsymbol{\gamma}}=\delta\mathbf{r}'+\mathbf{r}'\times\delta\boldsymbol{\vartheta}+\mathbf{r}\times\delta\boldsymbol{\vartheta}'=\overline{\delta\mathbf{r}}'\qquad\text{and}\qquad\overset{\diamondsuit}{\delta}\overline{\boldsymbol{\kappa}}=\delta\boldsymbol{\vartheta}'\,,\tag{3.81}$$

gives an extremely elegant form of the virtual work of internal forces

$$V_i=\int_0^L\left(\overline{\delta\mathbf{r}}'\cdot\overline{\mathbf{n}}+\delta\boldsymbol{\vartheta}'\cdot\overline{\mathbf{m}}\right)\,\mathrm{d}x.\tag{3.82}$$

Note that the fixed-pole virtual displacement vector $\overline{\delta\mathbf{r}}$ in (3.80) is fully consistent with the fixed-pole velocity $\overline{\mathbf{v}}$ in (2.19), where $\overline{\mathbf{v}}=\overline{\delta\mathbf{r}}/\delta t$, $\mathbf{v}=\delta\mathbf{r}/\delta t$ and $\mathbf{w}=\delta\boldsymbol{\vartheta}/\delta t$.

Since all the forces can be transported to the fixed-pole, the fixed-pole distributed loading and

specific inertial forces can be defined in an analogous manner to the fixed-pole stress resultants in (3.75), i.e.

$$\begin{Bmatrix} \overline{\mathbf{n}}_e \\ \overline{\mathbf{m}}_e \end{Bmatrix} = \begin{Bmatrix} \mathbf{n}_e \\ \mathbf{r} \times \mathbf{n}_e + \mathbf{m}_e \end{Bmatrix} = \begin{bmatrix} \mathbf{I} & \mathbf{0} \\ \widehat{\mathbf{r}} & \mathbf{I} \end{bmatrix} \begin{Bmatrix} \mathbf{n}_e \\ \mathbf{m}_e \end{Bmatrix}, \tag{3.83}$$

$$\begin{Bmatrix} \dot{\overline{\mathbf{l}}} \\ \dot{\overline{\boldsymbol{\pi}}} \end{Bmatrix} = \begin{Bmatrix} \dot{\mathbf{l}} \\ \mathbf{r} \times \dot{\mathbf{l}} + \dot{\boldsymbol{\pi}} \end{Bmatrix} = \begin{bmatrix} \mathbf{I} & \mathbf{0} \\ \widehat{\mathbf{r}} & \mathbf{I} \end{bmatrix} \begin{Bmatrix} \dot{\mathbf{l}} \\ \dot{\boldsymbol{\pi}} \end{Bmatrix}, \tag{3.84}$$

and so can the point loading

$$\begin{Bmatrix} \overline{\mathbf{F}}_0 \\ \overline{\mathbf{M}}_0 \end{Bmatrix} = \begin{bmatrix} \mathbf{I} & \mathbf{0} \\ \widehat{\mathbf{r}} & \mathbf{I} \end{bmatrix} \begin{Bmatrix} \mathbf{F}_0 \\ \mathbf{M}_0 \end{Bmatrix} \qquad \text{and} \qquad \begin{Bmatrix} \overline{\mathbf{F}}_L \\ \overline{\mathbf{M}}_L \end{Bmatrix} = \begin{bmatrix} \mathbf{I} & \mathbf{0} \\ \widehat{\mathbf{r}} & \mathbf{I} \end{bmatrix} \begin{Bmatrix} \mathbf{F}_L \\ \mathbf{M}_L \end{Bmatrix} \tag{3.85}$$

which enables us to define the virtual work of the inertial forces as

$$V_m = \int_0^L \left(\overline{\delta \mathbf{r}} \cdot \dot{\overline{\mathbf{l}}} + \delta \boldsymbol{\vartheta} \cdot \dot{\overline{\boldsymbol{\pi}}} \right) \mathrm{d}x \tag{3.86}$$

and the virtual work of the external forces as

$$V_e = \int_0^L \left(\overline{\delta \mathbf{r}} \cdot \overline{\mathbf{n}}_e + \delta \boldsymbol{\vartheta} \cdot \overline{\mathbf{m}}_e \right) \mathrm{d}x + \overline{\delta \mathbf{r}}_0 \cdot \mathbf{F}_0 + \delta \boldsymbol{\vartheta}_0 \cdot \mathbf{M}_0 + \overline{\delta \mathbf{r}}_L \cdot \mathbf{F}_L + \delta \boldsymbol{\vartheta}_L \cdot \mathbf{M}_L \,. \tag{3.87}$$

Substituting (3.82), (3.86) and (3.87) into (3.22) we get an alternative "unstacked" version of (3.69) as

$$\begin{aligned} \overline{G} \equiv \int_0^L \left\langle \overline{\delta \mathbf{r}}^T \quad \delta \boldsymbol{\vartheta}^T \right\rangle' \begin{Bmatrix} \overline{\mathbf{n}} \\ \overline{\mathbf{m}} \end{Bmatrix} \mathrm{d}x + \int_0^L \left\langle \overline{\delta \mathbf{r}}^T \quad \delta \boldsymbol{\vartheta}^T \right\rangle \left(\begin{Bmatrix} \dot{\overline{\mathbf{l}}} \\ \dot{\overline{\boldsymbol{\pi}}} \end{Bmatrix} - \begin{Bmatrix} \overline{\mathbf{n}}_e \\ \overline{\mathbf{m}}_e \end{Bmatrix} \right) \mathrm{d}x \\ - \left\langle \overline{\delta \mathbf{r}}_0^T \quad \delta \boldsymbol{\vartheta}_0^T \right\rangle \begin{Bmatrix} \overline{\mathbf{F}}_0 \\ \overline{\mathbf{M}}_0 \end{Bmatrix} - \left\langle \overline{\delta \mathbf{r}}_L^T \quad \delta \boldsymbol{\vartheta}_L^T \right\rangle \begin{Bmatrix} \overline{\mathbf{F}}_L \\ \overline{\mathbf{M}}_L \end{Bmatrix} = 0 \,. \end{aligned} \tag{3.88}$$

Fixed-pole dynamic nodal residual (alternative approach)

Since (3.88) is equivalent to (3.67), interpolating $\overline{\delta \mathbf{r}}$ and $\delta \boldsymbol{\vartheta}$ using Lagrange polynomials results in the same results as those given in (3.69)-(3.74) which we present here in their unstacked form. Substituting interpolated values

$$\overline{\delta \mathbf{r}} \doteq \sum_{i=1}^{N} I^i \overline{\delta \mathbf{r}}_i \,, \quad \text{and} \quad \delta \boldsymbol{\vartheta} \doteq \sum_{i=1}^{N} I^i \delta \boldsymbol{\vartheta}_i \tag{3.89}$$

into (3.88) we get

$$\overline{G}^h \equiv \sum_{i=1}^{N} \left\langle \overline{\delta \mathbf{r}}_i^T \quad \delta \boldsymbol{\vartheta}_i^T \right\rangle \overline{\mathbf{g}}^i = 0 \quad \Rightarrow \quad \overline{\mathbf{g}}^i = \mathbf{0} \,, \tag{3.90}$$

with $\overline{\mathbf{g}}^i$ as the fixed-pole nodal residual

$$\overline{\mathbf{g}}^i \equiv \overline{\mathbf{q}}^i_i + \overline{\mathbf{q}}^i_m - \overline{\mathbf{q}}^i_e = \mathbf{0}\,, \tag{3.91}$$

and

$$\overline{\mathbf{q}}^i_i = \int_0^L I^{i\prime} \begin{Bmatrix} \overline{\mathbf{n}} \\ \overline{\mathbf{m}} \end{Bmatrix} \mathrm{d}x\,, \tag{3.92}$$

$$\overline{\mathbf{q}}^i_m = \int_0^L I^i \begin{Bmatrix} \dot{\overline{\mathbf{l}}} \\ \dot{\overline{\boldsymbol{\pi}}} \end{Bmatrix} \mathrm{d}x\,, \tag{3.93}$$

$$\overline{\mathbf{q}}^i_e = \int_0^L I^i \begin{Bmatrix} \overline{\mathbf{n}}_e \\ \overline{\mathbf{m}}_e \end{Bmatrix} \mathrm{d}x + \delta^i_1 \begin{Bmatrix} \overline{\mathbf{F}}_0 \\ \overline{\mathbf{M}}_0 \end{Bmatrix} + \delta^i_N \begin{Bmatrix} \overline{\mathbf{F}}_L \\ \overline{\mathbf{M}}_L \end{Bmatrix}\,, \tag{3.94}$$

as the nodal vectors of internal, inertial and external forces, respectively.

3.3 Modified fixed-pole approach

In Section 3.2 we gave an overview of the fixed-pole approach as given by Borri and Bottasso [7], Bottasso and Borri [10] as well as its alternative description [76]. Unfortunately, as it is seen from (A.37) and (3.80), the virtual quantities in this approach are not the standard virtual displacements and rotations. Utilising the standard Bubnov–Galerkin approach [74], where same interpolations are used both for the virtual quantities (test functions) and for their iterative changes (trial functions), would result in a finite element which has non-standard degrees of freedom. Consequently, such a type of element cannot be combined with standard finite-element meshes. This inspired us to define a modified residual where standard virtual quantities are interpolated.

Modified fixed-pole dynamic nodal residual

Trying to keep the spirit of the fixed-pole approach, but also keep the standard system unknowns, we use relationship (3.80) at the nodal level

$$\overline{\delta\mathbf{r}}_i = \delta\mathbf{r}_i + \mathbf{r}_i \times \delta\boldsymbol{\vartheta}_i\,, \tag{3.95}$$

and simply substitute it in (3.69) so that the virtual work equation becomes

$$\overline{G}^h \equiv \sum_{i=1}^{N} \left\langle \delta\mathbf{r}_i^T \quad \delta\boldsymbol{\vartheta}_i^T \right\rangle \begin{bmatrix} \mathbf{I} & \mathbf{0} \\ -\widehat{\mathbf{r}}_i & \mathbf{I} \end{bmatrix} \overline{\mathbf{g}}^i = \sum_{i=1}^{N} \left\langle \delta\mathbf{r}_i^T \quad \delta\boldsymbol{\vartheta}_i^T \right\rangle \tilde{\mathbf{g}}^i = 0 \quad \Rightarrow \quad \tilde{\mathbf{g}}^i = \mathbf{0}\,, \tag{3.96}$$

with

$$\tilde{\mathbf{g}}^i \equiv \tilde{\mathbf{q}}_i^i + \tilde{\mathbf{q}}_m^i - \tilde{\mathbf{q}}_e^i = \mathbf{0}\,, \tag{3.97}$$

as the modified fixed-pole dynamic nodal residual and

$$\tilde{\mathbf{q}}_i^i = \int_0^L I^{i'} \begin{bmatrix} \mathbf{I} & \mathbf{0} \\ -\widehat{\mathbf{r}}_i & \mathbf{I} \end{bmatrix} \begin{Bmatrix} \overline{\mathbf{n}} \\ \overline{\mathbf{m}} \end{Bmatrix} \mathrm{d}x = \int_0^L I^{i'} \begin{bmatrix} \mathbf{I} & \mathbf{0} \\ \widehat{\mathbf{r} - \mathbf{r}_i} & \mathbf{I} \end{bmatrix} \begin{Bmatrix} \mathbf{n} \\ \mathbf{m} \end{Bmatrix} \mathrm{d}x \tag{3.98}$$

$$\tilde{\mathbf{q}}_m^i = \int_0^L I^i \begin{bmatrix} \mathbf{I} & \mathbf{0} \\ -\widehat{\mathbf{r}}_i & \mathbf{I} \end{bmatrix} \begin{Bmatrix} \dot{\overline{\mathbf{k}}} \\ \dot{\overline{\boldsymbol{\pi}}} \end{Bmatrix} \mathrm{d}x = \int_0^L I^i \begin{bmatrix} \mathbf{I} & \mathbf{0} \\ \widehat{\mathbf{r} - \mathbf{r}_i} & \mathbf{I} \end{bmatrix} \begin{Bmatrix} \dot{\mathbf{k}} \\ \dot{\boldsymbol{\pi}} \end{Bmatrix} \mathrm{d}x \tag{3.99}$$

$$\begin{aligned} \tilde{\mathbf{q}}_e^i &= \int_0^L I^i \begin{bmatrix} \mathbf{I} & \mathbf{0} \\ -\widehat{\mathbf{r}}_i & \mathbf{I} \end{bmatrix} \begin{Bmatrix} \overline{\mathbf{n}}_e \\ \overline{\mathbf{m}}_e \end{Bmatrix} \mathrm{d}x + \delta_1^i \begin{Bmatrix} \overline{\mathbf{F}}_0 \\ \overline{\mathbf{M}}_0 \end{Bmatrix} + \delta_N^i \begin{Bmatrix} \overline{\mathbf{F}}_L \\ \overline{\mathbf{M}}_L \end{Bmatrix} \\ &= \int_0^L I^i \begin{bmatrix} \mathbf{I} & \mathbf{0} \\ \widehat{\mathbf{r} - \mathbf{r}_i} & \mathbf{I} \end{bmatrix} \begin{Bmatrix} \mathbf{n}_e \\ \mathbf{m}_e \end{Bmatrix} \mathrm{d}x + \delta_1^i \begin{Bmatrix} \mathbf{F}_0 \\ \mathbf{M}_0 \end{Bmatrix} + \delta_N^i \begin{Bmatrix} \mathbf{F}_L \\ \mathbf{M}_L \end{Bmatrix}, \end{aligned} \tag{3.100}$$

as the modified fixed-pole nodal vectors of internal, inertial and external forces, respectively. This is a foundation upon we build the family of modified fixed-pole elements which use the standard unknowns and are therefore combinable with any displacement-based finite element mesh.

Relationship to configuration-dependent interpolation

An interesting result follows by substituting results (3.98)–(3.100) into $\tilde{\mathbf{g}}^i$ and then back in (3.96):

$$\begin{aligned} \overline{G}^h \equiv \sum_{i=1}^{N} \int_0^L \left\langle \delta\mathbf{r}_i^T \quad \delta\boldsymbol{\vartheta}_i^T \right\rangle \left(I^{i'} \begin{bmatrix} \mathbf{I} & \mathbf{0} \\ \widehat{\mathbf{r} - \mathbf{r}_i} & \mathbf{I} \end{bmatrix} \begin{Bmatrix} \mathbf{n} \\ \mathbf{m} \end{Bmatrix} + I^i \begin{bmatrix} \mathbf{I} & \mathbf{0} \\ \widehat{\mathbf{r} - \mathbf{r}_i} & \mathbf{I} \end{bmatrix} \left(\begin{Bmatrix} \dot{\mathbf{k}} \\ \dot{\boldsymbol{\pi}} \end{Bmatrix} - \begin{Bmatrix} \mathbf{n}_e \\ \mathbf{m}_e \end{Bmatrix} \right) \right) \mathrm{d}x - \\ - \sum_{i=1}^{N} \left\langle \delta\mathbf{r}_i^T \quad \delta\boldsymbol{\vartheta}_i^T \right\rangle \left(\delta_1^i \begin{Bmatrix} \mathbf{F}_0 \\ \mathbf{M}_0 \end{Bmatrix} + \delta_N^i \begin{Bmatrix} \mathbf{F}_L \\ \mathbf{M}_L \end{Bmatrix} \right) = 0\,. \end{aligned}$$

From here we have

$$\overline{G}^h \equiv \int_0^L \left(\sum_{i=1}^N I^i \begin{Bmatrix} \delta\mathbf{r}_i - (\mathbf{r}-\mathbf{r}_i)\times\delta\boldsymbol{\vartheta}_i \\ \delta\boldsymbol{\vartheta}_i \end{Bmatrix}^T \right)' \begin{Bmatrix} \mathbf{n} \\ \mathbf{m} \end{Bmatrix} \mathrm{d}x - \int_0^L \sum_{i=1}^N I^i \left\langle \delta\boldsymbol{\vartheta}_i^T\widehat{\mathbf{r}}' \quad \mathbf{0}^T \right\rangle \begin{Bmatrix} \mathbf{n} \\ \mathbf{m} \end{Bmatrix} \mathrm{d}x +$$
$$+ \int_0^L \left(\sum_{i=1}^N I^i \begin{Bmatrix} \delta\mathbf{r}_i - (\mathbf{r}-\mathbf{r}_i)\times\delta\boldsymbol{\vartheta}_i \\ \delta\boldsymbol{\vartheta}_i \end{Bmatrix}^T \right) \left(\begin{Bmatrix} \dot{\mathbf{k}} \\ \dot{\boldsymbol{\pi}} \end{Bmatrix} - \begin{Bmatrix} \mathbf{n}_e \\ \mathbf{m}_e \end{Bmatrix} \right) \mathrm{d}x -$$
$$- \left\langle \delta\mathbf{r}_1^T \quad \delta\boldsymbol{\vartheta}_1^T \right\rangle \begin{Bmatrix} \mathbf{F}_0 \\ \mathbf{M}_0 \end{Bmatrix} - \left\langle \delta\mathbf{r}_N^T \quad \delta\boldsymbol{\vartheta}_N^T \right\rangle \begin{Bmatrix} \mathbf{F}_L \\ \mathbf{M}_L \end{Bmatrix} = 0\,,$$

and finally

$$\begin{aligned} \overline{G}^h \equiv & \int_0^L \left(\sum_{i=1}^N I^i \begin{Bmatrix} \delta\mathbf{r}_i + (\mathbf{r}_i-\mathbf{r})\times\delta\boldsymbol{\vartheta}_i \\ \delta\boldsymbol{\vartheta}_i \end{Bmatrix}^T \begin{bmatrix} \mathbf{I}\frac{\mathrm{d}}{\mathrm{d}x} & \mathbf{0} \\ -\widehat{\mathbf{r}}' & \mathbf{I}\frac{\mathrm{d}}{\mathrm{d}x} \end{bmatrix} \right) \begin{Bmatrix} \mathbf{n} \\ \mathbf{m} \end{Bmatrix} \mathrm{d}x + \\ & + \int_0^L \left(\sum_{i=1}^N I^i \begin{Bmatrix} \delta\mathbf{r}_i + (\mathbf{r}_i-\mathbf{r})\times\delta\boldsymbol{\vartheta}_i \\ \delta\boldsymbol{\vartheta}_i \end{Bmatrix}^T \right) \left(\begin{Bmatrix} \dot{\mathbf{k}} \\ \dot{\boldsymbol{\pi}} \end{Bmatrix} - \begin{Bmatrix} \mathbf{n}_e \\ \mathbf{m}_e \end{Bmatrix} \right) \mathrm{d}x - \\ & - \left\langle \delta\mathbf{r}_1^T \quad \delta\boldsymbol{\vartheta}_1^T \right\rangle \begin{Bmatrix} \mathbf{F}_0 \\ \mathbf{M}_0 \end{Bmatrix} - \left\langle \delta\mathbf{r}_N^T \quad \delta\boldsymbol{\vartheta}_N^T \right\rangle \begin{Bmatrix} \mathbf{F}_L \\ \mathbf{M}_L \end{Bmatrix} = 0\,. \end{aligned} \tag{3.101}$$

Clearly, for a non-linear interpolation of the type

$$\begin{aligned} \delta\mathbf{r} &= \sum_{i=1}^N I^i(x)\left[\delta\mathbf{r}_i + (\mathbf{r}_i - \mathbf{r}(x))\times\delta\boldsymbol{\vartheta}_i\right]\,, \\ \delta\boldsymbol{\vartheta} &= \sum_{i=1}^N I^i(x)\delta\boldsymbol{\vartheta}_i\,, \end{aligned} \tag{3.102}$$

we get back to the form of G as given in (3.36). In other words, comparing (3.96) with (3.101) we may conclude that the standard (Lagrange) interpolation of the fixed-pole virtual displacements and rotations $\overline{\delta\mathbf{r}}$, $\delta\boldsymbol{\vartheta}$ (or simply $\delta\boldsymbol{\varsigma}$) is equivalent to the **configuration-dependent** interpolation of the standard virtual displacements and rotations (3.102).

Chapter 4

Fixed-pole family of finite elements

4.1 Fixed-pole element

In this section we present a novel finite element, based on the non-linear equation (3.74) developed from the virtual work principle. In order to concentrate on the issues that arise when attempting to utilise a fixed-pole approach, we proceed by considering only the static case, i.e. $\overline{\mathbf{q}}_m^i = \mathbf{0}$.

4.1.1 Solution procedure

Linearisation

The non-linear equation (3.74) is solved iteratively using the Newton-Raphson solution procedure: the equation is first linearised (written in a Taylor series around a known configuration with the higher-order terms omitted) and then solved iteratively until a certain convergence criterion is achieved. The first-order Taylor series expansion of (3.74) is

$$\overline{\mathbf{g}}^i + \Delta\overline{\mathbf{g}}^i = \mathbf{0}\,, \tag{4.1}$$

with $\Delta(\bullet) = \frac{\mathrm{d}}{\mathrm{d}\epsilon}|_{\epsilon=0}(\bullet)_\epsilon$ as a directional derivative in the direction of the perturbation $\Delta\boldsymbol{\varsigma}$ and

$$\Delta\overline{\mathbf{g}}^i = \Delta\overline{\mathbf{q}}_i^i - \Delta\overline{\mathbf{q}}_e^i\,. \tag{4.2}$$

Linearising the nodal internal force vector we get

$$\Delta\overline{\mathbf{q}}_i^i = \int_0^L I^{i'}\,\Delta\overline{\mathbf{s}}\,\mathrm{d}x = \int_0^L I^{i'}\,\Delta\left(\mathbf{C}^{-T}\mathbf{S}\right)\,\mathrm{d}x = \int_0^L I^{i'}\left(\Delta\mathbf{C}^{-T}\mathbf{S} + \mathbf{C}^{-T}\Delta\mathbf{S}\right)\,\mathrm{d}x\,.$$

Using results (A.19) and (3.62) we have

$$\begin{aligned}\Delta\overline{\mathbf{q}}_i^i &= \int_0^L I^{i'}\left(-\widehat{\Delta\boldsymbol{\varsigma}}^T\mathbf{C}^{-T}\mathbf{S} + \mathbf{C}^{-T}\mathbf{D}\mathbf{C}^{-1}\Delta\boldsymbol{\varsigma}'\right)\mathrm{d}x \\ &= \int_0^L I^{i'}\left(-\widehat{\Delta\boldsymbol{\varsigma}}^T\overline{\mathbf{s}} + \mathbf{C}^{-T}\mathbf{D}\mathbf{C}^{-1}\Delta\boldsymbol{\varsigma}'\right)\mathrm{d}x\,. \end{aligned} \tag{4.3}$$

Introducing a new generalised-cross product matrix $\overset{\triangledown}{\mathbf{a}}$, where $\mathbf{a}_1$, $\mathbf{a}_2$ are 3D vectors,

$$\overset{\triangledown}{\mathbf{a}} = \begin{bmatrix}\mathbf{0} & \widehat{\mathbf{a}}_1 \\ \widehat{\mathbf{a}}_1 & \widehat{\mathbf{a}}_2\end{bmatrix}, \tag{4.4}$$

we can rewrite (4.3) as

$$\begin{aligned}\Delta\overline{\mathbf{q}}_i^i &= \int_0^L I^{i'}\left(-\overset{\triangledown}{\overline{\mathbf{s}}}\Delta\boldsymbol{\varsigma} + \mathbf{C}^{-T}\mathbf{D}\mathbf{C}^{-1}\Delta\boldsymbol{\varsigma}'\right)\mathrm{d}x \\ &= \int_0^L I^{i'}\left(-\mathbf{C}^{-T}\overset{\triangledown}{\mathbf{S}}\mathbf{C}^{-1}\Delta\boldsymbol{\varsigma} + \mathbf{C}^{-T}\mathbf{D}\mathbf{C}^{-1}\Delta\boldsymbol{\varsigma}'\right)\mathrm{d}x\,, \end{aligned} \tag{4.5}$$

due to (A.3).

Unlike most standard procedures with conservative loading, in case of the fixed-pole solution procedure the linearisation of the external loading vector is not zero. This is because both the distributed loading $\overline{\mathbf{s}}_e$ and the nodal loads $\overline{\mathbf{s}}_0$, $\overline{\mathbf{s}}_L$ are configuration dependent. During the implementation, we divide the nodal external forces vector (3.73) into the local part $\overline{\mathbf{q}}^i_{e,\,\mathrm{local}} = \int_0^L I^i\overline{\mathbf{s}}_e\,\mathrm{d}x$ and the nodal part $\overline{\mathbf{q}}^i_{e,\,\mathrm{nodal}} = \overline{\mathbf{s}}_i$, because it is more convenient to add the local effects in the element loops and the nodal effects in the global loops. We do the same for their respective linearised values $\Delta\overline{\mathbf{q}}_{e,\,\mathrm{local}}$ and $\Delta\overline{\mathbf{q}}_{e,\,\mathrm{nodal}}$. Linearisation of the local part is

$$\Delta\overline{\mathbf{q}}^i_{e,\,\mathrm{local}} = \Delta\int_0^L I^i\overline{\mathbf{s}}_e\,\mathrm{d}x = \int_0^L I^i\begin{bmatrix}\mathbf{0} & \mathbf{0} \\ \Delta\widehat{\mathbf{r}} & \mathbf{0}\end{bmatrix}\mathbf{s}_e\,\mathrm{d}x\,. \tag{4.6}$$

However, there is no $\Delta\boldsymbol{\varsigma}$ in (4.6) which means that we need to relate $\Delta\mathbf{r}$ to $\Delta\boldsymbol{\varsigma}$, which is performed using (A.37) as

$$\Delta\boldsymbol{\varsigma} = \begin{bmatrix}\mathbf{I} & \widehat{\mathbf{r}} \\ \mathbf{0} & \mathbf{I}\end{bmatrix}\begin{Bmatrix}\Delta\mathbf{r} \\ \Delta\boldsymbol{\vartheta}\end{Bmatrix}. \tag{4.7}$$

Now we can rewrite (4.6) as

$$\Delta\overline{\mathbf{q}}^i_{e,\,\mathrm{local}} = \int_0^L I^i\begin{bmatrix}\mathbf{0} & \mathbf{0} \\ -\widehat{\mathbf{n}}_e & \widehat{\mathbf{n}}_e\widehat{\mathbf{r}}\end{bmatrix}\Delta\boldsymbol{\varsigma}\,\mathrm{d}x\,. \tag{4.8}$$

For any loaded node i, the nodal part of the external loading is given as

$$\overline{\mathbf{q}}^{i}_{e,\,\mathrm{nodal}} = \overline{\mathbf{s}}_{e,\,i} = \begin{bmatrix} \mathbf{I} & \mathbf{0} \\ \widehat{\mathbf{r}}_i & \mathbf{I} \end{bmatrix} \mathbf{s}_{e,\,i}\,. \tag{4.9}$$

Using (4.7) at the nodal level and linearising (4.9) we get

$$\Delta\overline{\mathbf{q}}^{i}_{e,\,\mathrm{nodal}} = \begin{cases} \begin{bmatrix} \mathbf{0} & \mathbf{0} \\ -\widehat{\mathbf{F}}_i & \widehat{\mathbf{F}}_i\widehat{\mathbf{r}}_i \end{bmatrix} \Delta\boldsymbol{\varsigma}_j & \text{if} \quad i = j\,, \\ \begin{Bmatrix} \mathbf{0} \\ \mathbf{0} \end{Bmatrix} & \text{if} \quad i \neq j\,. \end{cases} \tag{4.10}$$

Configuration update

We interpolate $\Delta\boldsymbol{\varsigma}$ using Lagrange polynomials via

$$\Delta\boldsymbol{\varsigma} \doteq \sum_{j=1}^{N} I^j \Delta\boldsymbol{\varsigma}_j \quad \text{and} \quad \Delta\boldsymbol{\varsigma}' \doteq \sum_{j=1}^{N} I^{j'} \Delta\boldsymbol{\varsigma}_j\,. \tag{4.11}$$

Substituting (4.11) into (4.5), (4.8) and (4.10) we can rewrite (4.1) using the nodal iterative values of $\Delta\boldsymbol{\varsigma}_j$ as

$$\overline{\mathbf{g}}^{i} + \sum_{j=1}^{N} \mathbf{K}_{ij} \Delta\boldsymbol{\varsigma}_j = \mathbf{0}\,, \tag{4.12}$$

with

$$\mathbf{K}^{ij} = \mathbf{K}^{i}_{ij} - \mathbf{K}^{e,\,\mathrm{local}}_{ij} - \mathbf{K}^{e,\,\mathrm{nodal}}_{ij}\,, \tag{4.13}$$

and

$$\mathbf{K}^{i}_{ij} = \int_0^L I^{i'} \mathbf{C}^{-T} \left(I^{j'} \mathbf{D} - I^{j} \overset{\triangledown}{\mathbf{S}} \right) \mathbf{C}^{-1}\, \mathrm{d}x\,, \tag{4.14}$$

$$\mathbf{K}^{e,\,\mathrm{local}}_{ij} = \int_0^L I^i I^j \begin{bmatrix} \mathbf{0} & \mathbf{0} \\ -\widehat{\mathbf{n}}_e & \widehat{\mathbf{n}}_e\widehat{\mathbf{r}} \end{bmatrix} \mathrm{d}x\,, \tag{4.15}$$

$$\mathbf{K}^{e,\,\mathrm{nodal}}_{ij} = \begin{cases} \begin{bmatrix} \mathbf{0} & \mathbf{0} \\ -\widehat{\mathbf{F}}_i & \widehat{\mathbf{F}}_i\widehat{\mathbf{r}}_i \end{bmatrix} & \text{if} \quad i = j\,, \\ \begin{bmatrix} \mathbf{0} & \mathbf{0} \\ \mathbf{0} & \mathbf{0} \end{bmatrix} & \text{if} \quad i \neq j\,. \end{cases} \tag{4.16}$$

The matrix (4.13) is the tangent stiffness matrix at node i due to node j. The stiffness matrix of the whole element is thus an $N \times N$ matrix consisting of blocks $\mathbf{K}_{ij}$. In order to obtain the solution for the whole structure, we need to know the assembly conditions (at which nodes are the elements connected) and the boundary conditions (which nodes have prescribed displacements and/or rotations). The assembly conditions allow us to construct the global residual vector and the global stiffness matrix by relating the element nodes i, j to the corresponding global nodes m, n. Then the element nodal residual $\overline{\mathbf{g}}^i$ is added to the position m of the global residual vector. Likewise, the block matrix $\mathbf{K}_{ij}$ is added to the position (m, n) of the global matrix. Finally, by imposing boundary conditions we ensure the unique solution of the problem as described in [77] which leads to

$$\Delta\boldsymbol{\varsigma}_{\text{global}} = -\mathbf{K}^{-1}\overline{\mathbf{g}}\,,$$

with $\Delta\boldsymbol{\varsigma}_{\text{global}}$ as the global vector of nodal unknowns, $\mathbf{K}$ as the global tangent stiffness matrix and $\overline{\mathbf{g}}$ as the global residual. From (A.37) we see that the nodal unknowns are non-standard

$$\Delta\boldsymbol{\varsigma}_m = \begin{Bmatrix} \Delta\boldsymbol{\xi}_m \\ \Delta\boldsymbol{\vartheta}_m \end{Bmatrix} = \begin{Bmatrix} \Delta\mathbf{r}_m + \mathbf{r}_m \times \Delta\boldsymbol{\vartheta}_m \\ \Delta\boldsymbol{\vartheta}_m \end{Bmatrix}, \tag{4.17}$$

which in some cases complicates imposing of the boundary conditions. For instance, defining a pinned support at node m means that the translational increment must be zero, i.e.

$$\Delta\boldsymbol{\varsigma}_{m,\text{pinned}} = \begin{Bmatrix} \mathbf{r}_m \times \Delta\boldsymbol{\vartheta}_m \\ \Delta\boldsymbol{\vartheta}_m \end{Bmatrix}, .$$

The standard procedure [77] for imposing of the boundary conditions may still be used, but when interpolating values of $\Delta\boldsymbol{\varsigma}$ we need to take into account that $\Delta\boldsymbol{\xi}_m = \mathbf{r}_m \times \Delta\boldsymbol{\vartheta}_m$ and not zero (as it is in the standard procedures where $\Delta\mathbf{r}_m$ is the nodal unknown). However, defining a clamped end is very straightforward: substituting $\Delta\mathbf{r}_m = \mathbf{0}$ and $\Delta\boldsymbol{\vartheta}_m = \mathbf{0}$ into (4.17) reveals

$$\Delta\boldsymbol{\varsigma}_{m,\text{clamped}} = \begin{Bmatrix} \mathbf{0} \\ \mathbf{0} \end{Bmatrix}.$$

We note here that the above discussion is here only to show that there are some additional complexities related to the implementation of the fixed-pole approach, which can be overcome by some additional algorithmic interventions. However, such nodal unknowns (4.17) also prevent combining these elements with the standard displacement-based finite-element meshes, which is

a much greater issue which serves as a motivation to develop the modified fixed-pole family of elements described in Section 4.2.

Update of the residual vector and the tangent stiffness matrix

Since (4.1) is solved iteratively, we need to find the updated values of the residual (3.70) and the tangent stiffness matrix (4.13), which are both evaluated as integrals over the length of the element. The non-constant terms in these integrals are the configuration tensor $\mathbf{C}(x)$ and the strain parameter $\mathbf{X}(x)$. By updating their values we obtain the residual and the tangent stiffness matrix needed for the completion of the next iteration.

Using interpolation (4.11) we obtain the values of $\Delta\boldsymbol{\varsigma}(x)$. Then the updated value of the configuration tensor is evaluated using the exponential map[1]

$$\mathbf{C} = \exp\widehat{\Delta\boldsymbol{\varsigma}}\mathbf{C}_{\text{old}}\,, \tag{4.18}$$

where $\mathbf{C}_{\text{old}}$ is the value of $\mathbf{C}$ from the last iteration.

Next, following a process described below we obtain the updated values of the strain parameter $\mathbf{X}$. From (4.18) we have

$$\exp\widehat{\Delta\boldsymbol{\varsigma}} = \mathbf{C}\mathbf{C}_{\text{old}}^{-1}\,, \tag{4.19}$$

$$\left(\exp\widehat{\Delta\boldsymbol{\varsigma}}\right)^{-1} = \mathbf{C}_{\text{old}}\mathbf{C}^{-1}. \tag{4.20}$$

Taking the derivative of (4.19) with respect to the beam arc-length parameter x we obtain

$$\left(\exp\widehat{\Delta\boldsymbol{\varsigma}}\right)' = \mathbf{C}'\mathbf{C}_{\text{old}}^{-1} + \mathbf{C}\mathbf{C}_{\text{old}}^{-1'}. \tag{4.21}$$

Then, using (4.21) and (4.20) we can write

$$\left(\exp\widehat{\Delta\boldsymbol{\varsigma}}\right)'\left(\exp\widehat{\Delta\boldsymbol{\varsigma}}\right)^{-1} = \mathbf{C}'\underbrace{\mathbf{C}_{\text{old}}^{-1}\mathbf{C}_{\text{old}}}_{\mathbf{I}}\mathbf{C}^{-1} + \mathbf{C}\mathbf{C}_{\text{old}}^{-1'}\mathbf{C}_{\text{old}}\mathbf{C}^{-1}\,. \tag{4.22}$$

The derivative of $\mathbf{C}_{\text{old}}^{-1}$ with respect to x is

$$\mathbf{C}_{\text{old}}^{-1'} = \begin{bmatrix} \boldsymbol{\Lambda}_{\text{old}}^{T} & -\boldsymbol{\Lambda}_{\text{old}}^{T}\widehat{\mathbf{r}}_{\text{old}} \\ \mathbf{0} & \boldsymbol{\Lambda}_{\text{old}}^{T} \end{bmatrix}' = \begin{bmatrix} \boldsymbol{\Lambda}_{\text{old}}^{T'} & -\boldsymbol{\Lambda}_{\text{old}}^{T'}\widehat{\mathbf{r}}_{\text{old}} - \boldsymbol{\Lambda}_{\text{old}}^{T}\widehat{\mathbf{r}}'_{\text{old}} \\ \mathbf{0} & \boldsymbol{\Lambda}_{\text{old}}^{T'} \end{bmatrix} = \begin{bmatrix} \boldsymbol{\Lambda}'_{\text{old}} & \mathbf{0} \\ \widehat{\mathbf{r}}_{\text{old}}\boldsymbol{\Lambda}'_{\text{old}} + \widehat{\mathbf{r}}'_{\text{old}}\boldsymbol{\Lambda}_{\text{old}} & \boldsymbol{\Lambda}'_{\text{old}} \end{bmatrix}^{T}.$$

[1] we omit the functional dependence on (x) to simplify notation

Using property (A.4) the above result can be rewritten as

$$\mathbf{C}_{\text{old}}^{-1'} = \left(\begin{bmatrix} \mathbf{0} & \mathbf{I} \\ \mathbf{I} & \mathbf{0} \end{bmatrix} \mathbf{C}'_{\text{old}} \begin{bmatrix} \mathbf{0} & \mathbf{I} \\ \mathbf{I} & \mathbf{0} \end{bmatrix} \right)^T = \begin{bmatrix} \mathbf{0} & \mathbf{I} \\ \mathbf{I} & \mathbf{0} \end{bmatrix} \left(\mathbf{C}'_{\text{old}}\right)^T \begin{bmatrix} \mathbf{0} & \mathbf{I} \\ \mathbf{I} & \mathbf{0} \end{bmatrix}.$$

Recalling (3.49), we substitute $\mathbf{C}'_{\text{old}} = \mathbf{C}_{\text{old}}\widehat{\widehat{\mathbf{X}}}_{\text{old}}$ into the above equation to obtain

$$\begin{aligned}
\mathbf{C}_{\text{old}}^{-1'}\mathbf{C}_{\text{old}} &= \begin{bmatrix} \mathbf{0} & \mathbf{I} \\ \mathbf{I} & \mathbf{0} \end{bmatrix} \widehat{\widehat{\mathbf{X}}}_{\text{old}}^T \mathbf{C}_{\text{old}}^T \begin{bmatrix} \mathbf{0} & \mathbf{I} \\ \mathbf{I} & \mathbf{0} \end{bmatrix} \mathbf{C}_{\text{old}} \\
&= \begin{bmatrix} \mathbf{0} & \mathbf{I} \\ \mathbf{I} & \mathbf{0} \end{bmatrix} \begin{bmatrix} -\widehat{\mathbf{K}}_{\text{old}} & \mathbf{0} \\ -\widehat{\boldsymbol{\Lambda}_{\text{old}}\mathbf{r}'_{\text{old}}} & -\widehat{\mathbf{K}}_{\text{old}} \end{bmatrix} \begin{bmatrix} \boldsymbol{\Lambda}_{\text{old}}^T & \mathbf{0} \\ -\boldsymbol{\Lambda}_{\text{old}}^T\widehat{\mathbf{r}}_{\text{old}} & \boldsymbol{\Lambda}_{\text{old}}^T \end{bmatrix} \begin{bmatrix} \mathbf{0} & \mathbf{I} \\ \mathbf{I} & \mathbf{0} \end{bmatrix} \begin{bmatrix} \boldsymbol{\Lambda}_{\text{old}} & \widehat{\mathbf{r}}_{\text{old}}\boldsymbol{\Lambda}_{\text{old}} \\ \mathbf{0} & \boldsymbol{\Lambda}_{\text{old}} \end{bmatrix} \\
&= \begin{bmatrix} -\widehat{\boldsymbol{\Lambda}_{\text{old}}\mathbf{r}'_{\text{old}}} & -\widehat{\mathbf{K}}_{\text{old}} \\ -\widehat{\mathbf{K}}_{\text{old}} & \mathbf{0} \end{bmatrix} \begin{bmatrix} \boldsymbol{\Lambda}_{\text{old}}^T & \mathbf{0} \\ -\boldsymbol{\Lambda}_{\text{old}}^T\widehat{\mathbf{r}}_{\text{old}} & \boldsymbol{\Lambda}_{\text{old}}^T \end{bmatrix} \begin{bmatrix} \mathbf{0} & \boldsymbol{\Lambda}_{\text{old}} \\ \boldsymbol{\Lambda}_{\text{old}} & \widehat{\mathbf{r}}_{\text{old}}\boldsymbol{\Lambda}_{\text{old}} \end{bmatrix} \\
&= \begin{bmatrix} -\widehat{\boldsymbol{\Lambda}_{\text{old}}\mathbf{r}'_{\text{old}}} & -\widehat{\mathbf{K}}_{\text{old}} \\ -\widehat{\mathbf{K}}_{\text{old}} & \mathbf{0} \end{bmatrix} \begin{bmatrix} \mathbf{0} & \mathbf{I} \\ \mathbf{I} & \mathbf{0} \end{bmatrix} = -\widehat{\widehat{\mathbf{X}}}_{\text{old}}\,.
\end{aligned}$$

Substituting the above result along with $\mathbf{C}' = \mathbf{C}\widehat{\widehat{\mathbf{X}}}$ into (4.22) we have

$$\left(\exp\widehat{\Delta\boldsymbol{\varsigma}}\right)'\left(\exp\widehat{\Delta\boldsymbol{\varsigma}}\right)^{-1} = \mathbf{C}\widehat{\widehat{\mathbf{X}}}\mathbf{C}^{-1} - \mathbf{C}\widehat{\widehat{\mathbf{X}}}_{\text{old}}\mathbf{C}^{-1} = \mathbf{C}\left(\widehat{\widehat{\mathbf{X}}} - \widehat{\widehat{\mathbf{X}}}_{\text{old}}\right)\mathbf{C}^{-1} = \widehat{\mathbf{C}(\mathbf{X} - \mathbf{X}_{\text{old}})}\,.$$

Using results obtained in Appendix A.2.5 we recognise that the left-hand side of the above equation can be expressed as

$$\left(\exp\widehat{\Delta\boldsymbol{\varsigma}}\right)'\left(\exp\widehat{\Delta\boldsymbol{\varsigma}}\right)^{-1} = \widehat{\mathbf{H}_{\mathbf{6}}(\Delta\boldsymbol{\varsigma})\Delta\boldsymbol{\varsigma}'}\,. \tag{4.23}$$

Finally we have

$$\widehat{\mathbf{C}(\mathbf{X} - \mathbf{X}_{\text{old}})} = \widehat{\mathbf{H}_{\mathbf{6}}(\Delta\boldsymbol{\varsigma})\Delta\boldsymbol{\varsigma}'} \quad \Rightarrow \mathbf{C}(\mathbf{X} - \mathbf{X}_{\text{old}}) = \mathbf{H}_{\mathbf{6}}(\Delta\boldsymbol{\varsigma})\Delta\boldsymbol{\varsigma}'\,,$$

i.e. the updated value of the strain parameter is given as

$$\mathbf{X} = \mathbf{X}_{\text{old}} + \mathbf{C}^{-1}\mathbf{H}_{\mathbf{6}}(\Delta\boldsymbol{\varsigma})\Delta\boldsymbol{\varsigma}'\,, \tag{4.24}$$

Compared to the standard approach where translational and rotational strain measures are updated separately, equation (4.24) enables a unified update of strain measures, which is algorithmically more elegant.

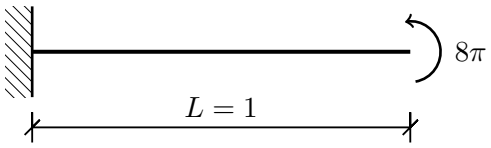

Figure 4.1: Cantilever beam subject to concentrated moment at the free end [4]

4.1.2 Numerical examples

In all of the numerical examples $N-1$ point Gaussian quadrature is used for evaluating the internal forces vector and its stiffness matrix. The Newton-Raphson solution procedure is used for obtaining solutions inside each load increment with the convergence criterion defined as

$$\sqrt{\sum_{i=1}^{M} \Delta\boldsymbol{\varsigma}_i \cdot \Delta\boldsymbol{\varsigma}_i} < \delta_u \,,$$

where M is the number of all nodes in the structure and δ_u is the prescribed tolerance (in examples presented within this section, $\delta_u = 10^{-10}$. All the examples were run using self-made programs coded in *Wolfram Mathematica*.

Cantilever beam subject to pure bending

We analyse a well-known example of a planar cantilever beam subject to pure bending shown in Figure 4.1. The beam has the following geometric and material properties: $A_1 = A_2 = A_3 = 1$, $J = 1$, $I_2 = I_3 = 2$, $E = G = 1$. The length of the beam is 1 and it is modelled using five linear elements. This example is known as the "roll-up manoeuvre" as the beam rolls up twice with the tip of the beam coinciding with the clamped end. It is known to converge in one load increment in only 3 iterations using the standard beam elements [4]. However, when using the fixed-pole elements described in previous section, this problem gives very inaccurate results. After increasing the number of equally sized load increments we found that the results are **very path dependent** as it is seen in Table 4.1. We assume that the reason for this behaviour is the fact that the special group of rigid motions is not commutative in 2D. The results in Table 4.1 show that the accuracy is increased as the number of load increments is increased. Also, the results are improved as the mesh becomes more refined, as shown in Table 4.2. Improvement of results with respect to the number of load increments as well as with respect to the mesh refinement is typical of path-dependent formulations.

Increments	r_1	r_2
1 [4]	0	0
1	-0.15772	-0.06808
2	-0.09691	-0.03109
5	-0.01847	-0.01101
10	-0.00429	-0.00341
20	-0.00102	-0.00094

Table 4.1: Cantilever beam subject to pure bending: tip position components obtained using different load incrementation

Elements	r_1	r_2
1 [4]	0	0
5	-0.15772	-0.06808
10	-0.03322	-0.01472
20	-0.00798	-0.00355

Table 4.2: Cantilever beam subject to pure bending: tip position components obtained using meshes of different refinement

45° cantilever bend

Next we analyse a well-known spatial problem of a planar curved cantilever loaded with a vertical out-of-plane concentrated force of magnitude $F = 600$ at its tip, as shown in Figure 4.2. The geometric and material characteristics are given as follows: $A = A_2 = A_3 = 1$, $J_1 = 16.656 \times 10^{-2}$, $I_2 = I_3 = 8.3333 \times 10^{-2}$, $E = 10^7$ and $G = 0.5 \times 10^7$. The cantilever is in the horizontal plane and it represents one eighth of a circle of radius $R = 100$ and is modelled using eight equally long straight linear elements. Again, we have path-dependent results as shown in Table 4.3. Additionally, the procedure does not converge unless the loading is split in at least ten equally sized increments, and is thus considerably less robust than e.g. that of Simo and Vu-Quoc [4] where the same example is solved using only three load increments.

Increments	u_1	u_2	u_3
10	13.47712	-23.53199	53.10212
20	13.47917	-23.53181	53.10235
50	13.47917	-23.53180	53.10233

Table 4.3: Tip displacement components obtained using different load incrementation

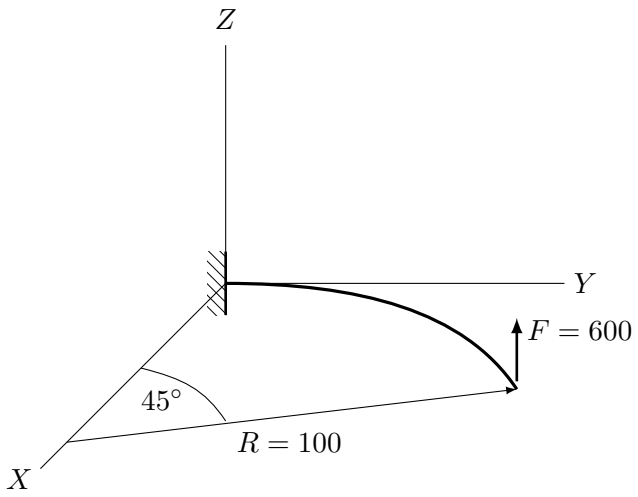

Figure 4.2: 45° cantilever bend

4.2 Modified fixed-pole elements

In this section we present a modification of the fixed-pole element, which uses standard degrees of freedom. The family of elements presented in this section is based on solving the non-linear equation (3.97) derived from the virtual work principle. We limit our attention to the case when $\tilde{\mathbf{q}}_m^i = \mathbf{0}$ in order to concentrate on issues that arise when attempting to utilise a fixed-pole approach in the modified manner presented here, in which the standard displacement and rotation quantities have been kept as the problem unknowns.

4.2.1 Solution procedures

Linearisation

The non-linear equation (3.97) is solved using the Newton-Raphson solution procedure. Expanding it into a Taylor series around a known configuration and omitting higher-order terms we have

$$\tilde{\mathbf{g}}^i + \Delta\tilde{\mathbf{g}}^i = \mathbf{0}\,, \tag{4.25}$$

where

$$\Delta\tilde{\mathbf{g}}^i = \Delta\tilde{\mathbf{q}}_i^i - \Delta\tilde{\mathbf{q}}_e^i\,. \tag{4.26}$$

Linearisation of the modified nodal internal force vector (3.98) follows as

$$\Delta\tilde{\mathbf{q}}_i^i \int_0^L I^{i'} \begin{bmatrix} \mathbf{I} & \mathbf{0} \\ \Delta\widehat{\mathbf{r}} - \Delta\widehat{\mathbf{r}}_i & \mathbf{I} \end{bmatrix} \begin{Bmatrix} \mathbf{n} \\ \mathbf{m} \end{Bmatrix} \mathrm{d}x + \int_0^L I^{i'} \begin{bmatrix} \mathbf{I} & \mathbf{0} \\ \widehat{\mathbf{r} - \mathbf{r}_i} & \mathbf{I} \end{bmatrix} \begin{Bmatrix} \Delta\mathbf{n} \\ \Delta\mathbf{m} \end{Bmatrix} \mathrm{d}x\,.$$

Noting that we can use results (2.47), (3.27) and (3.28) to linearise the orientation matrix and the strain measures, the spatial stress resultants are linearised as

$$\begin{aligned} \begin{Bmatrix} \Delta\mathbf{n} \\ \Delta\mathbf{m} \end{Bmatrix} &= \begin{Bmatrix} \Delta\boldsymbol{\Lambda}\mathbf{N} + \boldsymbol{\Lambda}\Delta\mathbf{N} \\ \Delta\boldsymbol{\Lambda}\mathbf{M} + \boldsymbol{\Lambda}\Delta\mathbf{M} \end{Bmatrix} = \begin{Bmatrix} \widehat{\Delta\boldsymbol{\vartheta}}\boldsymbol{\Lambda}\mathbf{N} + \boldsymbol{\Lambda}\mathbf{C}_N\Delta\boldsymbol{\Gamma} \\ \widehat{\Delta\boldsymbol{\vartheta}}\boldsymbol{\Lambda}\mathbf{M} + \boldsymbol{\Lambda}\mathbf{C}_M\Delta\mathbf{K} \end{Bmatrix} \\ &= \begin{Bmatrix} -\widehat{\mathbf{n}}\Delta\boldsymbol{\vartheta} \\ -\widehat{\mathbf{m}}\Delta\boldsymbol{\vartheta} \end{Bmatrix} + \begin{Bmatrix} \boldsymbol{\Lambda}\mathbf{C}_N\boldsymbol{\Lambda}^T(\Delta\mathbf{r}' + \mathbf{r}' \times \Delta\boldsymbol{\vartheta}) \\ \boldsymbol{\Lambda}\mathbf{C}_M\boldsymbol{\Lambda}^T\Delta\boldsymbol{\vartheta}' \end{Bmatrix}. \end{aligned}$$

Finally we have

$$\begin{aligned} \Delta\tilde{\mathbf{q}}_i^i = &\int_0^L I^{i'} \begin{bmatrix} \mathbf{0} & \mathbf{0} \\ \widehat{\mathbf{n}} & \mathbf{0} \end{bmatrix} \begin{Bmatrix} \Delta\mathbf{r}_i - \Delta\mathbf{r} \\ \Delta\boldsymbol{\vartheta}_i - \Delta\boldsymbol{\vartheta} \end{Bmatrix} \mathrm{d}x + \int_0^L I^{i'} \begin{bmatrix} \mathbf{I} & \mathbf{0} \\ \widehat{\mathbf{r}} - \widehat{\mathbf{r}_i} & \mathbf{I} \end{bmatrix} \begin{bmatrix} \mathbf{0} & -\widehat{\mathbf{n}} \\ \mathbf{0} & -\widehat{\mathbf{m}} \end{bmatrix} \begin{Bmatrix} \Delta\mathbf{r} \\ \Delta\boldsymbol{\vartheta} \end{Bmatrix} \mathrm{d}x + \\ &+ \int_0^L I^{i'} \begin{bmatrix} \mathbf{I} & \mathbf{0} \\ \widehat{\mathbf{r}} - \widehat{\mathbf{r}_i} & \mathbf{I} \end{bmatrix} \begin{bmatrix} \boldsymbol{\Lambda}\mathbf{C}_N\boldsymbol{\Lambda}^T & \mathbf{0} \\ \mathbf{0} & \boldsymbol{\Lambda}\mathbf{C}_M\boldsymbol{\Lambda}^T \end{bmatrix} \begin{Bmatrix} \Delta\mathbf{r}' + \mathbf{r}' \times \Delta\boldsymbol{\vartheta} \\ \Delta\boldsymbol{\vartheta}' \end{Bmatrix} \mathrm{d}x\,. \end{aligned} \tag{4.27}$$

Linearising the modified nodal external force vector (3.100) we obtain

$$\Delta\tilde{\mathbf{q}}_e^i = \int_0^L I^i \begin{bmatrix} \mathbf{0} & \mathbf{0} \\ \widehat{\mathbf{n}}_e & \mathbf{0} \end{bmatrix} \begin{Bmatrix} \Delta\mathbf{r}_i - \Delta\mathbf{r} \\ \Delta\boldsymbol{\vartheta}_i - \Delta\boldsymbol{\vartheta} \end{Bmatrix} \mathrm{d}x\,. \tag{4.28}$$

As mentioned before, an interesting phenomenon occurs when linearising the external force vector, which is a direct consequence of the use of the fixed-pole virtual quantities and their conversion back to standard virtual quantities: even though the external loading is configuration-independent, the modified nodal external loading vector (3.100) is not. As a result of this, the stiffness matrix will have an additional part as a result of the linearisation of $\tilde{\mathbf{q}}_e^i$. Here, though, this happens only in the presence of the distributed force loading, i.e. no contribution to the tangent stiffness matrix exists due to point loadings and distributed moment loading, in contrast to the fixed-pole element presented in the previous section.

Configuration update

In order to complete the solution procedure, the unknown functions and/or their iterative changes must be interpolated in some way. We propose three different interpolation options,

which arise as a consequence of the fact that the virtual position vector has been interpolated in a non-linear manner, dependent on the actual position vector not only at the nodal points, but also at x. The basic solution procedure is the same for all interpolation options, with differences arising in the structure of the stiffness matrices. Following the process described in Section 4.1 we obtain the global fixed-pole modified residual $\tilde{\mathbf{g}}$ and the global stiffness matrix $\mathbf{K}$. After imposing the boundary conditions (which is standard [77]), we obtain the global vector of nodal unknowns $\Delta\mathbf{p}$ as

$$\Delta\mathbf{p} = -\mathbf{K}^{-1}\tilde{\mathbf{g}}\,, \tag{4.29}$$

where the m-th subblock of $\Delta\mathbf{p}$ is $\mathbf{p}_m = \left\langle \Delta\mathbf{r}_m^T\, \Delta\boldsymbol{\vartheta}_m^T \right\rangle^T$. Then, the nodal position vectors and nodal orientation matrices are updated via

$$\mathbf{r}_m = \mathbf{r}_{m,\,\mathrm{old}} + \Delta\mathbf{r}_m\,, \tag{4.30}$$

$$\boldsymbol{\Lambda}_m = \exp\widehat{\Delta\boldsymbol{\vartheta}}_m \boldsymbol{\Lambda}_{m,\,\mathrm{old}}\,. \tag{4.31}$$

Update of the residual vector and the tangent stiffness matrix

In the present formulation, besides the orientation matrix $\boldsymbol{\Lambda}$ and the material strain measures $\boldsymbol{\Gamma}$, $\mathbf{K}$, the position vector $\mathbf{r}$ is also present in the integrals of the residual and the stiffness matrix. This revealed the necessity to compute it, which in turn made us propose three different interpolation options as given below.

Interpolation option 1 Within this option $\Delta\mathbf{r}$ and $\Delta\boldsymbol{\vartheta}$ are interpolated in the same way as the virtual displacements and rotations $\delta\mathbf{r}$ and $\delta\boldsymbol{\vartheta}$ in (3.102)

$$\begin{aligned} \Delta\mathbf{r} &\doteq \sum_{j=1}^{N} I^j [\Delta\mathbf{r}_j + (\mathbf{r}_j - \mathbf{r}) \times \Delta\boldsymbol{\vartheta}_j]\,, \\ \Delta\boldsymbol{\vartheta} &\doteq \sum_{j=1}^{N} I^j \Delta\boldsymbol{\vartheta}_j\,, \end{aligned} \tag{4.32}$$

while, in addition, the unknown displacement vector is interpolated using Lagrangian polynomials as

$$\mathbf{r} \doteq \sum_{k=1}^{N} I^k \mathbf{r}_k\,. \tag{4.33}$$

It should be noted that (4.32) obviously **does not follow** as a linearisation of (4.33). This contradiction necessarily results in loss of quadratic convergence of the Newton-Raphson solu-

tion process, and has been introduced as a simplest means of providing $\mathbf{r}(x)$ in (4.32). After introducing (4.32) into (4.27) and (4.28) we have

$$\Delta\tilde{\mathbf{q}}_i^i = \sum_{j=1}^{N} \mathbf{K}_{ij}^i \begin{Bmatrix} \Delta\mathbf{r}_j \\ \Delta\boldsymbol{\vartheta}_j \end{Bmatrix},$$

$$\Delta\tilde{\mathbf{q}}_e^i = \sum_{j=1}^{N} \mathbf{K}_{ij}^e \begin{Bmatrix} \Delta\mathbf{r}_j \\ \Delta\boldsymbol{\vartheta}_j \end{Bmatrix},$$

where

$$\mathbf{K}_{ij}^i = \int_0^L I^{i'} \begin{bmatrix} \mathbf{0} & \mathbf{0} \\ (\delta_{ij} - I^j)\widehat{\mathbf{n}} & -I^j\widehat{\mathbf{n}}(\widehat{\mathbf{r}}_j - \widehat{\mathbf{r}}) \end{bmatrix} \mathrm{d}x + \int_0^L I^{i'} I^j \begin{bmatrix} \mathbf{0} & -\widehat{\mathbf{n}} \\ \mathbf{0} & -(\widehat{\mathbf{r}} - \widehat{\mathbf{r}}_i)\widehat{\mathbf{n}} - \widehat{\mathbf{m}} \end{bmatrix} \mathrm{d}x$$
$$+ \int_0^L I^{i'} I^{j'} \begin{bmatrix} \mathbf{I} & \mathbf{0} \\ \widehat{\mathbf{r}} - \widehat{\mathbf{r}}_i & \mathbf{I} \end{bmatrix} \begin{bmatrix} \boldsymbol{\Lambda}\mathbf{C}_N\boldsymbol{\Lambda}^T & \mathbf{0} \\ \mathbf{0} & \boldsymbol{\Lambda}\mathbf{C}_M\boldsymbol{\Lambda}^T \end{bmatrix} \begin{bmatrix} \mathbf{I} & \widehat{\mathbf{r}}_j - \widehat{\mathbf{r}} \\ \mathbf{0} & \mathbf{I} \end{bmatrix} \mathrm{d}x\,, \tag{4.34}$$

and

$$\mathbf{K}_{ij}^e = -\int_0^L I^i \begin{bmatrix} \mathbf{0} & \mathbf{0} \\ (I^j - \delta_{ij})\widehat{\mathbf{n}}_e & I^j\widehat{\mathbf{n}}_e(\widehat{\mathbf{r}}_j - \widehat{\mathbf{r}}) \end{bmatrix} \mathrm{d}x\,. \tag{4.35}$$

We substitute $\mathbf{K}_{ij} = \mathbf{K}_{ij}^i - \mathbf{K}_{ij}^e$ into (4.29) to solve the system using this interpolation option. In numerical examples, we term these elements MFP1 (Modified fixed-pole – Interpolation option 1).

Interpolation option 2 Within this option, $\mathbf{r}$ is interpolated using (4.33). Interpolation of the displacement increments follows consistently by linearising $\mathbf{r}$ as

$$\Delta\mathbf{r} = \sum_{j=1}^{N} I^j \Delta\mathbf{r}_j\,, \tag{4.36}$$

while

$$\Delta\boldsymbol{\vartheta} = \sum_{j=1}^{N} I^j \Delta\boldsymbol{\vartheta}_j\,. \tag{4.37}$$

After introducing (4.36) and (4.37) into (4.27) and (4.28) we have

$$\Delta\tilde{\mathbf{q}}_i^i = \sum_{j=1}^{N} \mathbf{K}_{ij}^i \begin{Bmatrix} \Delta\mathbf{r}_j \\ \Delta\boldsymbol{\vartheta}_j \end{Bmatrix},$$

$$\Delta\tilde{\mathbf{q}}_e^i = \sum_{j=1}^{N} \mathbf{K}_{ij}^e \begin{Bmatrix} \Delta\mathbf{r}_j \\ \Delta\boldsymbol{\vartheta}_j \end{Bmatrix},$$

where

$$\mathbf{K}_{ij}^i = \int_0^L I^{i'} \begin{bmatrix} \mathbf{0} & \mathbf{0} \\ \widehat{\mathbf{n}} & \mathbf{0} \end{bmatrix} (\delta_{ij} - I^j)\,\mathrm{d}x + \int_0^L I^{i'} I^j \begin{bmatrix} \mathbf{0} & -\widehat{\mathbf{n}} \\ \mathbf{0} & -(\widehat{\mathbf{r}} - \widehat{\mathbf{r}}_i)\widehat{\mathbf{n}} - \widehat{\mathbf{m}} \end{bmatrix} \mathrm{d}x +$$
$$+ \int_0^L I^{i'} \begin{bmatrix} \mathbf{I} & \mathbf{0} \\ \widehat{\mathbf{r}} - \widehat{\mathbf{r}}_i & \mathbf{I} \end{bmatrix} \begin{bmatrix} \boldsymbol{\Lambda}\mathbf{C}_N\boldsymbol{\Lambda}^T & \mathbf{0} \\ \mathbf{0} & \boldsymbol{\Lambda}\mathbf{C}_M\boldsymbol{\Lambda}^T \end{bmatrix} \begin{bmatrix} I^{j'}\mathbf{I} & I^j\widehat{\mathbf{r}}' \\ \mathbf{0} & I^{j'}\mathbf{I} \end{bmatrix} \mathrm{d}x\,,$$

and

$$\mathbf{K}_{ij}^e = -\int_0^L I^i(I^j - \delta_{ij}) \begin{bmatrix} \mathbf{0} & \mathbf{0} \\ \widehat{\mathbf{n}}_e & \mathbf{0} \end{bmatrix} \mathrm{d}x\,. \tag{4.38}$$

We substitute $\mathbf{K}_{ij} = \mathbf{K}_{ij}^i - \mathbf{K}_{ij}^e$ into (4.29) to solve the system using this interpolation option. In numerical examples we term these elements MFP2 (Modified fixed-pole – Interpolation option 2). In this case, different interpolations have been used for the test functions and the trial functions, which is bound to make the tangent stiffness matrix even more non-symmetric.

Interpolation option 3 Within this option $\mathbf{r}$ is not interpolated, but only updated as follows:

$$\mathbf{r}(x) = \mathbf{r}_{\mathrm{old}}(x) + \Delta\mathbf{r}(x)\,, \tag{4.39}$$

where $\mathbf{r}_{\mathrm{old}}(x)$ is the last known value for $\mathbf{r}(x)$, not necessarily associated with an equilibrium state and $\Delta\mathbf{r}(x)$ following interpolation of the Newton-Raphson changes given in (4.32). This is a consistent choice which yields a tangent stiffness matrix. In this case the values of $\mathbf{r}$ at both integration and nodal points must be saved. The earlier results from Interpolation option 1 can still be used, but noting that the position vector in (4.34) and (4.35), as well as (3.98) and (3.100), must now be computed from (4.39).

Update of strain measures In order to evaluate the material strain measures $\boldsymbol{\Gamma}$ and $\mathbf{K}$ we need to compute the values of the position vector and the orientation matrix at integration points $\boldsymbol{\Lambda}(x)$. Depending on the interpolation option used, the values of the position vector derivatives at integration points are obtained by taking the derivative of either (4.33) or (4.39),

while the values of the orientation matrix are obtained via

$$\mathbf{\Lambda} = \exp\widehat{\Delta\boldsymbol{\vartheta}}\mathbf{\Lambda}_{\text{old}}\,, \tag{4.40}$$

where $\mathbf{\Lambda}_{\text{old}}$ is the orientation matrix from the previous iteration. The current material translational strain measures are then simply evaluated by substituting current values of $\mathbf{r}'$ and $\mathbf{\Lambda}$ in (3.4). From (3.5), using (4.40) we have

$$\begin{aligned}
\widehat{\mathbf{K}} &= \left(\exp\widehat{\Delta\boldsymbol{\vartheta}}\mathbf{\Lambda}_{\text{old}}\right)^T\left(\exp\widehat{\Delta\boldsymbol{\vartheta}}\mathbf{\Lambda}_{\text{old}}\right)' \\
&= \mathbf{\Lambda}_{\text{old}}^T\left(\exp\widehat{\Delta\boldsymbol{\vartheta}}\right)^T\left[\left(\exp\widehat{\Delta\boldsymbol{\vartheta}}\right)'\mathbf{\Lambda}_{\text{old}} + \exp\widehat{\Delta\boldsymbol{\vartheta}}\mathbf{\Lambda}_{\text{old}}'\right] \\
&= \mathbf{\Lambda}_{\text{old}}^T\left(\exp\widehat{\Delta\boldsymbol{\vartheta}}\right)^T\left(\exp\widehat{\Delta\boldsymbol{\vartheta}}\right)'\mathbf{\Lambda}_{\text{old}} + \mathbf{\Lambda}_{\text{old}}^T\underbrace{\left(\exp\widehat{\Delta\boldsymbol{\vartheta}}\right)^T\exp\widehat{\Delta\boldsymbol{\vartheta}}}_{\mathbf{I}}\mathbf{\Lambda}_{\text{old}}'\,.
\end{aligned}$$

We recognise that $\mathbf{\Lambda}_{\text{old}}^T\mathbf{\Lambda}_{\text{old}}' = \widehat{\mathbf{K}}_{\text{old}}$ and using (4.40) rewrite $\mathbf{\Lambda}_{\text{old}}$ as $\left(\exp\widehat{\Delta\boldsymbol{\vartheta}}\right)^T\mathbf{\Lambda}$ to obtain

$$\begin{aligned}
\widehat{\mathbf{K}} &= \mathbf{\Lambda}^T\underbrace{\exp\widehat{\Delta\boldsymbol{\vartheta}}\left(\exp\widehat{\Delta\boldsymbol{\vartheta}}\right)^T}_{\mathbf{I}}\left(\exp\widehat{\Delta\boldsymbol{\vartheta}}\right)'\left(\exp\widehat{\Delta\boldsymbol{\vartheta}}\right)^T\mathbf{\Lambda} + \widehat{\mathbf{K}}_{\text{old}} \\
&= \widehat{\mathbf{K}}_{\text{old}} + \mathbf{\Lambda}^T\left(\exp\widehat{\Delta\boldsymbol{\vartheta}}\right)'\left(\exp\widehat{\Delta\boldsymbol{\vartheta}}\right)^T\mathbf{\Lambda} \\
&= \widehat{\mathbf{K}}_{\text{old}} + \mathbf{\Lambda}^T\widehat{\mathbf{H}(\Delta\boldsymbol{\vartheta})\Delta\boldsymbol{\vartheta}'}\mathbf{\Lambda}
\end{aligned} \tag{4.41}$$

due to results from Appendix A.2.2. The update of material rotational strain measures is therefore

$$\mathbf{K} = \mathbf{K}_{\text{old}} + \mathbf{\Lambda}^T\mathbf{H}(\Delta\boldsymbol{\vartheta})\Delta\boldsymbol{\vartheta}'\,. \tag{4.42}$$

4.2.2 Numerical examples

In all of the numerical examples $N-1$ point Gaussian quadrature (reduced integration) is used for evaluating the internal forces vector and its stiffness matrix. The Newton-Raphson solution procedure is used for obtaining solutions inside each load increment, with two convergence criteria which must both be satisfied. The displacement norm is defined as the square root of the squares of nodal iterative displacements over all nodes in the structure M as a percentage of the square root of the sum of the squares of total nodal displacements $\mathbf{u}_i$, and it must be less than a prescribed tolerance δ_u [51]

$$100\sqrt{\frac{\sum_{i=1}^{M}\Delta\mathbf{u}_i\cdot\Delta\mathbf{u}_i}{\sum_{i=1}^{M}\mathbf{u}_i\cdot\mathbf{u}_i}} < \delta_u\,.$$

The residual norm is defined as the square root of the sum of the squares of the nodal residual forces $\mathbf{g}^i$ over all the nodes in the structure M as a percentage of the square root of the sum of squares of the nodal external forces vector $\mathbf{q}_e^i$, which must be less than a prescribed tolerance δ_r

$$100\sqrt{\frac{\sum_{i=1}^{M}\mathbf{g}^i\cdot\mathbf{g}^i}{\sum_{i=1}^{M}\mathbf{q}_e^i\cdot\mathbf{q}_e^i}} < \delta_r\,.$$

Unless noted otherwise, in all numerical examples the convergence criteria is set as $\delta_u = 10^{-7}$ and $\delta_r = 10^{-7}$. All the examples were run using self-made programs coded in *Wolfram Mathematica*.

Cantilever beam subject to pure bending

We analyse a well-known example of a planar cantilever beam subject to pure bending shown in Figure 4.1. The beam has the following geometric and material properties: $A_1 = A_2 = A_3 = 1$, $J = 1$, $I_2 = I_3 = 2$, $E = G = 1$. The length of the beam is 1 and it is modelled using five linear elements. All three interpolation options obtain the exact solution [4] in three iterations.

Single-element path-dependence and strain-invariance test

This is a simple example given in [51] of a single horizontal beam of length $L = 1$, of the following geometric and material properties: $A = A_2 = A_3 = 0.1$, $J_1 = 1.6\times10^{-4}$, $I_2 = I_3 = 8.3\times10^{-5}$, $E = 1.2\times10^{8}$ and Poisson's ratio $\nu = 0.3$. The convergence criterion is set as $\delta_u < 10^{-5}$. The displacements at the first node are fixed to zero, while both nodes are given prescribed end-point rotations

$$\boldsymbol{\psi}_1 = \begin{Bmatrix} 1.00 \\ -0.50 \\ 0.25 \end{Bmatrix} \qquad \text{and} \qquad \boldsymbol{\psi}_2 = \begin{Bmatrix} -0.40 \\ 0.70 \\ 0.10 \end{Bmatrix},$$

such that $\boldsymbol{\Lambda}_1 = \exp\widehat{\boldsymbol{\psi}}_1$ and $\boldsymbol{\Lambda}_2 = \exp\widehat{\boldsymbol{\psi}}_2$. The end point rotations are applied using two incrementation sequences. At first, we apply the end-point rotations in a single increment. Then, in order to simulate a general situation in which increments of the nodal unknowns may take arbitrary values, we apply the end-point rotations in two sample inrements: $0.775\,\boldsymbol{\psi}_1$, $0.4\,\boldsymbol{\psi}_2$ in the first increment and $0.225\,\boldsymbol{\psi}_1$, $0.6\,\boldsymbol{\psi}_2$ in the second increment. The rotational strain components K_i at the integration point $x = L/2$ as well as the displacements of the free node for the interpolation options MFP1, MFP2 and MFP3 and the incrementation sequences 1 and 2 are given in Table 4.4. We can see that all three proposed formulations are path dependent, where

path-dependence in the displacements for MFP3 is particularly notable. Next, we test the strain-

	K_1	K_2	K_3	u_1	u_2	u_3
MFP1, 1	-1.27464	1.26756	-0.40350	-0.02009	0.18605	-0.07187
MFP1, 2	-1.28872	1.25182	-0.41280	-0.01701	0.16401	-0.08261
MFP2, 1	-1.27464	1.26756	-0.40350	-0.02009	0.18605	-0.07187
MFP2, 2	-1.28872	1.25182	-0.41280	-0.01701	0.16401	-0.08261
MFP3, 1	-1.27464	1.26756	-0.40350	-0.02009	0.18605	-0.07187
MFP3, 2	-1.28872	1.25182	-0.41280	-0.10572	0.08642	-0.06474

Table 4.4: Components of rotational strains and the displacements of the second node using different incrementation sequences for the end-point rotations

invariance of these formulations. A rigid rotation $\boldsymbol{\psi}_R^T = \langle 0.2 \quad 1.2 \quad -0.5 \rangle^T$ is superimposed onto the prescribed rotations $\boldsymbol{\psi}_1$, $\boldsymbol{\psi}_2$ to produce

$$\underline{\boldsymbol{\psi}}_1 = \begin{Bmatrix} 1.00145\,66233\,24399 \\ 0.34679\,74254\,22351 \\ -0.83717\,18210\,05534 \end{Bmatrix} \quad \text{and} \quad \underline{\boldsymbol{\psi}}_2 = \begin{Bmatrix} 0.08849\,14860\,02004 \\ 1.93320\,47713\,48018 \\ -0.08186\,60178\,89401 \end{Bmatrix},$$

which are obtained by extraction from $\exp \widehat{\underline{\boldsymbol{\psi}}}_1 = \exp \widehat{\boldsymbol{\psi}}_R \exp \widehat{\boldsymbol{\psi}}_1$ and $\exp \widehat{\underline{\boldsymbol{\psi}}}_2 = \exp \widehat{\boldsymbol{\psi}}_R \exp \widehat{\boldsymbol{\psi}}_2$ via Spurrier's algorithm [78]. Now we subject the beam ends to the "new" rotations $\underline{\boldsymbol{\psi}}_1$ and $\underline{\boldsymbol{\psi}}_2$ in a single increment and compare the results for the obtained rotational strain components $\underline{K}_i$ to the results from Table 4.4 obtained by applying $\boldsymbol{\psi}_1$ and $\boldsymbol{\psi}_2$ in a single increment. The results in Table 4.5 show that all three proposed formulations are non-invariant with respect to a rigid body rotation.

	K_1	K_2	K_3	$\underline{K}_1$	$\underline{K}_2$	$\underline{K}_3$
MFP1	-1.27464	1.26756	-0.40350	-1.26399	1.31371	-0.33751
MFP2	-1.27464	1.26756	-0.40350	-1.26399	1.31371	-0.33751
MFP3	-1.27464	1.26756	-0.40350	-1.26399	1.31371	-0.33751

Table 4.5: Components of rotational strains for end-point rotations $\boldsymbol{\psi}_1$, $\boldsymbol{\psi}_2$ and $\underline{\boldsymbol{\psi}}_1$, $\underline{\boldsymbol{\psi}}_2$ applied in a single increment

Lee's frame

We next consider a hinged right-angle frame given in [4], with the following geometric and material properties $I_3 = 2$, $A_1 = 6$, $E = 7.2 \times 10^6$, $\nu = 0.3$, and length of each leg $L = 120$. The frame is divided into ten quadratic elements, five along each leg. The horizontal leg of the frame is loaded with a point force $F = 15000$ as shown in Figure 4.3.

The structure is first modelled using ten equally long quadratic elements to analyse the

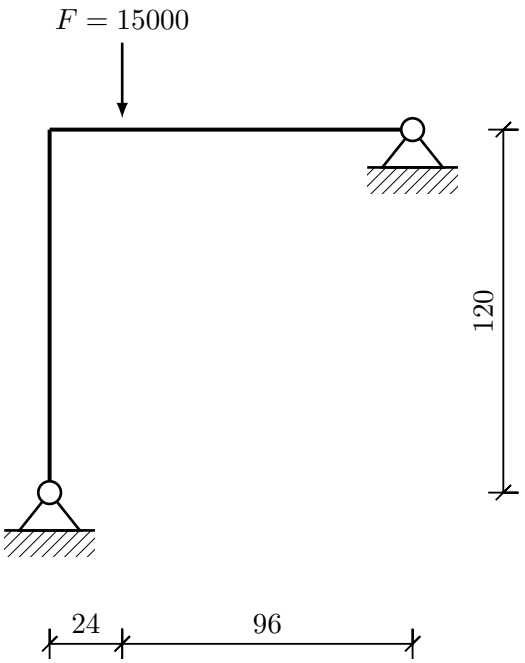

Figure 4.3: Lee's frame

accuracy, which is compared to the reference solution obtained by using 40 quadratic elements from [4]. From the results for the displacement components u_1 and u_2 of the loaded node given in Table 4.6 we can observe that formulations MFP1 and MFP2 give the same results as the formulation of Simo and Vu-Quoc [4], but MFP3 does not. Additionally, the results obtained using MFP3 appear to be less accurate. Next, path dependence of the presented formulation is

	u_1	u_2
Referent	8.02817	-25.89251
[4]	8.01638	-25.86247
MFP1	8.01638	-25.86247
MFP2	8.01638	-25.86247
MFP3	8.05463	-25.96012

Table 4.6: Displacements of the loaded node using ten quadratic elements

tested. The structure is modelled using ten linear elements because path dependence is more evident when using lower-order elements. The load is applied to the structure in 1, 2, 10, and 20 equally sized increments, as shown in Table 4.7. The results show that both MFP1 and MFP2 give path-independent results, while MFP3 gives path-dependent results. It is interesting to note, though, that the results obtained using MFP3 now appear to be the most accurate.

	MFP1		MFP2		MFP3	
	u_1	u_2	u_1	u_2	u_1	u_2
1	6.46073	-22.48634	6.46073	-22.48634	8.59392	-26.02842
2	6.46073	-22.48634	6.46073	-22.48634	8.72739	-26.12403
10	6.46073	-22.48634	6.46073	-22.48634	8.97095	-26.13286
20	6.46073	-22.48634	6.46073	-22.48634	9.00150	-26.09732

Table 4.7: Displacements of the loaded node using ten linear elements with different load incrementation

45° **cantilever bend**

Finally, we analyse a well-known spatial problem of a planar curved cantilever loaded with a vertical out-of-plane concentrated force of magnitude $F = 600$ at its tip, as shown in Figure 4.2. The geometric and material characteristics are given as follows: $A = A_2 = A_3 = 1$, $J_1 = 16.656 \times 10^{-2}$, $I_2 = I_3 = 8.3333 \times 10^{-2}$, $E = 10^7$ and $G = 0.5 \times 10^7$. The cantilever is in the horizontal plane and it represents one eighth of a circle of radius $R = 100$ and is modelled using eight equally long straight linear elements. We compare our results to the ones obtained using the invariant formulation [51], as shown in Table 4.8, using different load incrementations. The load is divided into 3, 7, 10, 15 and 20 equal load increments. Results clearly show that the robustness of the proposed formulation is reduced in comparison to [4] or [51], regardless of the interpolation option applied – in all of the proposed interpolations the minimum number of equal load increments is 7.

Formulation	Increments	u_1	u_2	u_3
MFP1	3	-	-	-
MFP1	7	13.48783	-23.47882	53.36984
MFP1	10	13.48789	-23.47877	53.36983
MFP1	15	13.48784	-23.47876	53.36980
MFP1	20	13.48782	-23.47876	53.36981
MFP2	3	-	-	-
MFP2	7	13.48784	-23.47883	53.36989
MFP2	10	13.48789	-23.47876	53.36983
MFP2	15	13.48785	-23.47877	53.36984
MFP2	20	13.48783	-23.47877	53.36985
MFP3	3	-	-	-
MFP3	7	13.48272	-23.53052	53.18321
MFP3	10	13.48194	-23.53197	53.15572
MFP3	15	13.48130	-23.53258	53.13641
MFP3	20	13.48092	-23.53273	53.12735

Table 4.8: Tip displacement components obtained using different load incrementation

Chapter 5

Generalised fixed-pole family of finite elements

5.1 Invariance of strain measures

We begin this section with a quote from [47]:

> The objectivity of material strain measures at a particular configuration is understood as their inherent ability to remain unaffected by a constant motion of the configuration. We also say that such strain measures are **invariant under a superimposed rigid body motion**.

In this section we show that the strain invariance is an inherent property, regardless of the manner in which the problem is defined. Imagine a rigid motion ($\mathbf{r}_R$, $\mathbf{\Lambda}_R$) superimposed onto a configuration ($\mathbf{r}$, $\mathbf{\Lambda}$), such that we get a new configuration ($\underline{\mathbf{r}}$, $\underline{\mathbf{\Lambda}}$) depicted in Figure 5.1 and defined as [47]

$$\underline{\mathbf{r}} = \mathbf{\Lambda}_R(\mathbf{r}_R + \mathbf{r})\,, \tag{5.1}$$

$$\underline{\mathbf{\Lambda}} = \mathbf{\Lambda}_R\mathbf{\Lambda}\,. \tag{5.2}$$

The strain measures $\mathbf{\Gamma}$ and $\mathbf{K}$ at configuration $(\mathbf{r}, \mathbf{\Lambda})$ are (i) **objective** in the sense that they are equal to the strain measures $\underline{\mathbf{\Gamma}}$ and $\underline{\mathbf{K}}$ at the configuration ($\underline{\mathbf{r}}$, $\underline{\mathbf{\Lambda}}$), defined by (5.1) and (5.2) and (ii) independent of the history of deformation [47]. This can easily be proven by evaluating the strain measures at the new configuration ($\underline{\mathbf{r}}$, $\underline{\mathbf{\Lambda}}$). Substituting (5.1) and (5.2) into (3.4) we

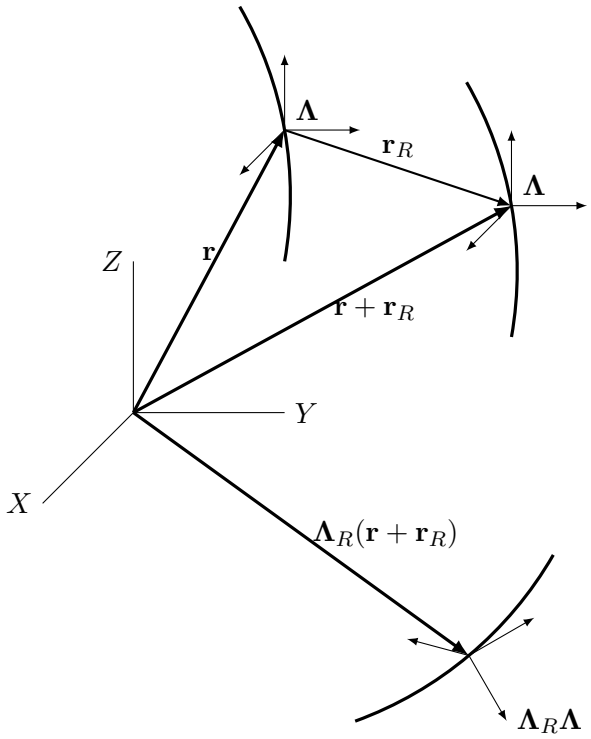

Figure 5.1: Superimposed rigid-body translation $\mathbf{r}_R$ and rotation $\mathbf{\Lambda}_R$ onto the original deformed configuration ($\mathbf{r}$, $\mathbf{\Lambda}$)

find the translational material strain measures of the new configuration as

$$\underline{\mathbf{\Gamma}} = \underline{\mathbf{\Lambda}}^T \underline{\mathbf{r}}' - \mathbf{E}_1 = \mathbf{\Lambda}^T \mathbf{\Lambda}_R^T \mathbf{\Lambda}_R' (\mathbf{r}_R + \mathbf{r}) + \mathbf{\Lambda}^T \underbrace{\mathbf{\Lambda}_R^T \mathbf{\Lambda}_R}_{\mathbf{I}} (\mathbf{r}_R' + \mathbf{r}') - \mathbf{E}_1 \,,$$

which, since $\mathbf{r}_R$ and $\mathbf{\Lambda}_R$ are constant, yields

$$\underline{\mathbf{\Gamma}} = \mathbf{\Lambda}^T \mathbf{r}' - \mathbf{E}_1 = \mathbf{\Gamma} \,. \tag{5.3}$$

Next, substituting (5.1) and (5.2) into (3.5) we find the rotational material strain measures of the new configuration as

$$\underline{\widehat{\mathbf{K}}} = \underline{\mathbf{\Lambda}}^T \underline{\mathbf{\Lambda}}' = \mathbf{\Lambda}^T \mathbf{\Lambda}_R^T \mathbf{\Lambda}_R' \mathbf{\Lambda} + \mathbf{\Lambda}^T \mathbf{\Lambda}_R^T \mathbf{\Lambda}_R \mathbf{\Lambda}' \,,$$

which in turn gives

$$\underline{\widehat{\mathbf{K}}} = \mathbf{\Lambda}^T \mathbf{\Lambda}' = \widehat{\mathbf{K}} \,. \tag{5.4}$$

Results (5.3) and (5.4) prove that the material strain measures $\mathbf{\Gamma}$ and $\mathbf{K}$ depend **only on the current configuration** ($\mathbf{r}$, $\mathbf{\Lambda}$), which makes them independent of the history of deformation.

We should obtain the same result using the configuration-tensor approach. Imagine a configuration $\mathbf{C}(\mathbf{r}, \mathbf{\Lambda})$ and a new configuration $\underline{\mathbf{C}}$, which is a result of a rigid motion $\mathbf{C}_R$ in a sense

that $\underline{\mathbf{\Lambda}} = \mathbf{\Lambda}_R\mathbf{\Lambda}$ and $\underline{\mathbf{r}} = \mathbf{r}_R + \mathbf{r}$ so that

$$\mathbf{C} = \begin{bmatrix} \mathbf{\Lambda} & \widehat{\mathbf{r}\mathbf{\Lambda}} \\ \mathbf{0} & \mathbf{\Lambda} \end{bmatrix}, \quad \underline{\mathbf{C}} = \begin{bmatrix} \underline{\mathbf{\Lambda}} & \widehat{\underline{\mathbf{r}}\underline{\mathbf{\Lambda}}} \\ \mathbf{0} & \underline{\mathbf{\Lambda}} \end{bmatrix} = \begin{bmatrix} \mathbf{\Lambda}_R\mathbf{\Lambda} & \widehat{\mathbf{\Lambda}_R(\mathbf{r}_R + \mathbf{r})} \\ \mathbf{0} & \mathbf{\Lambda}_R\mathbf{\Lambda} \end{bmatrix}.$$

Clearly, $\underline{\mathbf{C}} = \mathbf{C}_R\mathbf{C}$, i.e.

$$\begin{bmatrix} \mathbf{\Lambda}_R\mathbf{\Lambda} & \mathbf{\Lambda}_R\widehat{\mathbf{r}_R + \mathbf{r}}\mathbf{\Lambda}_R^T\mathbf{\Lambda}_R\mathbf{\Lambda} \\ \mathbf{0} & \mathbf{\Lambda}_R\mathbf{\Lambda} \end{bmatrix} = \begin{bmatrix} \mathbf{\Lambda}_R & \mathbf{\Lambda}_R\widehat{\mathbf{r}_R} \\ \mathbf{0} & \mathbf{\Lambda}_R \end{bmatrix} \begin{bmatrix} \mathbf{\Lambda} & \widehat{\mathbf{r}\mathbf{\Lambda}} \\ \mathbf{0} & \mathbf{\Lambda} \end{bmatrix},$$

which means that the rigid motion is defined as

$$\mathbf{C}_R = \begin{bmatrix} \mathbf{\Lambda}_R & \mathbf{\Lambda}_R\widehat{\mathbf{r}_R} \\ \mathbf{0} & \mathbf{\Lambda}_R \end{bmatrix}.$$

Next, let us calculate the strain parameter $\underline{\mathbf{X}}$ of the new configuration using (3.49). We start from

$$\begin{aligned} \widehat{\underline{\mathbf{X}}} &= \underline{\mathbf{C}}^{-1}\underline{\mathbf{C}}' \\ &= \mathbf{C}^{-1}\mathbf{C}_R^{-1}\mathbf{C}_R'\mathbf{C} + \mathbf{C}^{-1}\mathbf{C}_R^{-1}\mathbf{C}_R\mathbf{C}', \end{aligned}$$

which after noting that $\mathbf{C}_R$ is constant gives

$$\widehat{\underline{\mathbf{X}}} = \mathbf{C}^{-1}\mathbf{C}' = \widehat{\mathbf{X}} \quad \Leftrightarrow \quad \underline{\mathbf{X}} = \mathbf{X} \tag{5.5}$$

Result (5.5) proves that the strain measures $\mathbf{X} - \mathbf{X}_N$ are objective and independent of history of deformation as they only depend on the current configuration $\mathbf{C}$.

5.2 Generalised modified fixed-pole elements

As it was discussed in [47] and presented in the previous section, the strain measures are **invariant**. However, their approximated values do not necessarily inherit this property, as results in Section 4.2 suggest. Regardless of the choice of the interpolated quantities – being it the iterative [4, 49], the incremental [5, 48] or the total rotations [6] – the interpolation is always applied to the rotations between a particular reference configuration and the current configuration. As a consequence, the rotations interpolated in this way in general include rigid-body rotations, so that the error, introduced by the interpolation, makes the resulting strain measures dependent on the rigid-body rotation [47].

5.2.1 Solution procedure

Decomposition of the orientation matrix

After detecting what was the underlying cause of strain non-invariance, the proposed remedy is logical – elimination of rigid-body rotations from the interpolation of the rotational variables. In [47] this was achieved by decomposing the total rotational matrix $\mathbf{\Lambda}(x)$ using a reference orientation matrix $\mathbf{\Lambda}_r$ which is unique for the whole beam and rigidly attached to it, and an orientation matrix defining a local rotation $\mathbf{\Psi}^l(x)$ between the reference orientation matrix and the total orientation matrix, so that

$$\mathbf{\Lambda}(x) \doteq \mathbf{\Lambda}^h(x) = \mathbf{\Lambda}_r \exp \widehat{\mathbf{\Psi}}^{lh}(x)\,. \tag{5.6}$$

The reference orientation matrix $\mathbf{\Lambda}_r$ represents the rotation of one of the beam nodes. In the most general case, two nodes, I and J are selected and the relative rotation $\boldsymbol{\phi}_{IJ}$ between these nodes is calculated from

$$\exp \widehat{\boldsymbol{\phi}}_{IJ} = \mathbf{\Lambda}_I^T \mathbf{\Lambda}_J \rightarrow \boldsymbol{\phi}_{IJ}\,, \tag{5.7}$$

noting that $\boldsymbol{\phi}_{IJ}$ can be extracted using Spurrier's algorithm [78]. Then $\mathbf{\Lambda}_r$ is defined as the orientation matrix of a point midway between two nodes I and J as

$$\mathbf{\Lambda}_r = \mathbf{\Lambda}_I \exp\left(\frac{1}{2}\widehat{\boldsymbol{\phi}}_{IJ}\right)\,. \tag{5.8}$$

The nodal orientation matrices are updated in the usual manner during the iterative process using $\mathbf{\Lambda}_i = \exp \widehat{\Delta\boldsymbol{\vartheta}}_i \mathbf{\Lambda}_{i,\text{old}}$. Then the local nodal rotations $\mathbf{\Psi}_k^l$ (i.e. the relative rotations between the orientation matrix at node i and the reference orientation matrix $\mathbf{\Lambda}_r$) are evaluated using (5.6) as

$$\exp \widehat{\mathbf{\Psi}}_i^l = \mathbf{\Lambda}_r^T \mathbf{\Lambda}_i\,. \tag{5.9}$$

From (5.6) we see that we only need the values of the local rotations at integration points, $\mathbf{\Psi}^{lh}(x)$ in order to compute the orientation matrices at integration points. This means that the **only rotational quantities which need to be interpolated are the local rotations**, which is performed using Lagrange polynomials

$$\mathbf{\Psi}^l(x) \doteq \mathbf{\Psi}^{lh}(x) = \sum_{k=1}^{N} I^k \mathbf{\Psi}_k^l \quad \text{and} \quad \mathbf{\Psi}^{l'}(x) \doteq \mathbf{\Psi}^{lh'}(x) = \sum_{k=1}^{N} I^{k'} \mathbf{\Psi}_k^l\,. \tag{5.10}$$

Generalised shape functions

Except being strain non-invariant, the numerical examples presented in Section 4.2 suggest that the results are also path-dependent. Path-dependence is characterised by dependence on the iterative path towards a converged solution which is present in formulations where iterative or incremental rotations are interpolated (the total formulation [6] does not suffer from path-dependence). The solution to this problem is to ensure that the iterative (or incremental) rotations are interpolated in such a manner that the rigid-body rotations are eliminated. In that sense, Jelenić and Crisfield [51] proposed an appropriate interpolation for the iterative changes of the rotational parameter $\Delta\boldsymbol{\vartheta}$ based on the linearisation of (5.6). Following a process of finding a relationship between the nodal spin vectors $\Delta\boldsymbol{\vartheta}_i$ and the nodal iterative values of the local rotations $\Delta\boldsymbol{\Psi}_i^l$ we arrive at [51]

$$\begin{aligned}\Delta\boldsymbol{\vartheta}(x) \doteq \Delta\boldsymbol{\vartheta}^h(x) &= \sum_{j=1}^{N} \tilde{\mathbf{I}}^j(x)\Delta\boldsymbol{\vartheta}_j\,,\\ \Delta\boldsymbol{\vartheta}'(x) \doteq \Delta\boldsymbol{\vartheta}^{h'}(x) &= \sum_{j=1}^{N} \tilde{\mathbf{I}}^{j'}(x)\Delta\boldsymbol{\vartheta}_j\,,\end{aligned} \tag{5.11}$$

with $= \tilde{\mathbf{I}}^j(x)$ as the **generalised shape functions**. These functions and their derivatives are defined as

$$\tilde{\mathbf{I}}^j = (\delta_I^j + \delta_J^j)\boldsymbol{\Lambda}_r \left[\mathbf{I} - \mathbf{H}\left[\boldsymbol{\Psi}^{lh}(x)\right] \sum_{m=1}^{N} I^m(x)\mathbf{H}^{-1}(\boldsymbol{\Psi}_m^l)\right] \mathbf{v}_j\boldsymbol{\Lambda}_r^T + \boldsymbol{\Lambda}_r\mathbf{H}\left[\boldsymbol{\Psi}^{lh}(x)\right] I^j(x)\mathbf{H}^{-1}(\boldsymbol{\Psi}_j^l)\boldsymbol{\Lambda}_r^T\,, \tag{5.12}$$

$$\begin{aligned}\tilde{\mathbf{I}}^{j'} = (\delta_I^j + \delta_J^j)\boldsymbol{\Lambda}_r \sum_{m=1}^{N} \left\{-\mathbf{H}'\left[\boldsymbol{\Psi}^{lh}(x)\right] I^m(x)\mathbf{H}^{-1}(\boldsymbol{\Psi}_m^l) - \mathbf{H}\left[\boldsymbol{\Psi}^{lh}(x)\right] I^{m'}(x)\mathbf{H}^{-1}(\boldsymbol{\Psi}_m^l)\right\} \mathbf{v}_j\boldsymbol{\Lambda}_r^T + \\ + \boldsymbol{\Lambda}_r\left[\mathbf{H}'\left[\boldsymbol{\Psi}^{lh}(x)\right] I^j(x) + \mathbf{H}\left[\boldsymbol{\Psi}^{lh}(x)\right] I^{j'}(x)\right]\mathbf{H}^{-1}(\boldsymbol{\Psi}_j^l)\boldsymbol{\Lambda}_r^T\,,\end{aligned} \tag{5.13}$$

with

$$\mathbf{v}_j = \left(\mathbf{I} + \exp\widehat{\boldsymbol{\Psi}}_j^l\right)^{-1} = \begin{cases} \frac{1}{2}\left(\mathbf{I} + \tan\frac{\Phi_{IJ}}{4}\widehat{\boldsymbol{\Phi}}_{IJ}\right) & \text{if } j = I \\ \frac{1}{2}\left(\mathbf{I} - \tan\frac{\Phi_{IJ}}{4}\widehat{\boldsymbol{\Phi}}_{IJ}\right) & \text{if } j = J \end{cases} \tag{5.14}$$

as well as the derivative of $\mathbf{H}(\boldsymbol{\Psi})$ with respect to x derived in [49] as

$$\mathbf{H}'(\boldsymbol{\Psi}) = \boldsymbol{\Psi}^T\boldsymbol{\Psi}'\frac{\alpha_1 - 2\alpha_2}{\Psi^2}\widehat{\boldsymbol{\Psi}} + \alpha_2\widehat{\boldsymbol{\Psi}}' + \beta_2\left(\widehat{\boldsymbol{\Psi}}\widehat{\boldsymbol{\Psi}}' + \widehat{\boldsymbol{\Psi}}'\widehat{\boldsymbol{\Psi}}\right) + \boldsymbol{\Psi}^T\boldsymbol{\Psi}'\frac{3\alpha_1 - 2 - \cos\Psi}{\Psi^4}\widehat{\boldsymbol{\Psi}}^2\,. \tag{5.15}$$

Configuration update

Here we limit our attention to the simplest case of these interpolating functions, when $I = J$ so that the reference node $I = \frac{N}{2}$ for even-noded elements and $I = \frac{N+1}{2}$ for odd-noded elements. In such a case the generalised shape functions given in (5.12) and (5.13) take the following explicit form

$$\tilde{\mathbf{I}}^j(x) = \begin{cases} \mathbf{I} - \boldsymbol{\Lambda}_I \mathbf{H}\left[\boldsymbol{\Psi}^{lh}(x)\right] \sum_{m=1}^{N} (1-\delta_I^m) I^m(x) \mathbf{H}^{-1}(\boldsymbol{\Psi}_m^l) \boldsymbol{\Lambda}_I^T\,, & \text{if } j = I\,, \\ \boldsymbol{\Lambda}_I \mathbf{H}\left[\boldsymbol{\Psi}^{lh}(x)\right] I^j(x) \mathbf{H}^{-1}(\boldsymbol{\Psi}_j^l) \boldsymbol{\Lambda}_I^T\,, & \text{if } j \neq I\,. \end{cases} \tag{5.16}$$

$$\tilde{\mathbf{I}}^{j'}(x) = \begin{cases} -\boldsymbol{\Lambda}_I \left\{ \mathbf{H}'\left[\boldsymbol{\Psi}^{lh}(x)\right] \sum_{m=1}^{N} (1-\delta_I^m) I^m(x) \mathbf{H}^{-1}(\boldsymbol{\Psi}_m^l) + \right. & \\ \left. + \mathbf{H}\left[\boldsymbol{\Psi}^{lh}(x)\right] \sum_{m=1}^{N} (1-\delta_I^m) I^{m'}(x) \mathbf{H}^{-1}(\boldsymbol{\Psi}_m^l) \right\} \boldsymbol{\Lambda}_I^T\,, & \text{if } j = I\,, \\ \boldsymbol{\Lambda}_I \left\{ \mathbf{H}'\left[\boldsymbol{\Psi}^{lh}(x)\right] I^j(x) + \mathbf{H}\left[\boldsymbol{\Psi}^{lh}(x)\right] I^{j'}(x) \right\} \mathbf{H}^{-1}(\boldsymbol{\Psi}_j^l) \boldsymbol{\Lambda}_I^T\,, & \text{if } j \neq I\,. \end{cases} \tag{5.17}$$

Choosing to interpolate in the Lagrangian manner the local rotations instead of the spin vectors results in a new family of elements which we call the **generalised modified fixed-pole family** of elements. The implementation into the proposed interpolation options is straightforward: I^j is replaced with $\tilde{\mathbf{I}}^j$, although the fact that these functions are now matrices, not scalars, must be taken into account. In the following paragraphs we show the resulting changes to the formulation given in Section 4.2.

Generalised interpolation option 1 Substituting (5.11) into (4.32) we get

$$\begin{Bmatrix} \Delta\mathbf{r} \\ \Delta\boldsymbol{\vartheta} \end{Bmatrix} = \sum_{j=1}^{N} \begin{bmatrix} I^j\mathbf{I} & (\widehat{\mathbf{r}}_j - \widehat{\mathbf{r}})\,\tilde{\mathbf{I}}^j \\ \mathbf{0} & \tilde{\mathbf{I}}^j \end{bmatrix} \begin{Bmatrix} \Delta\mathbf{r}_j \\ \Delta\boldsymbol{\vartheta}_j \end{Bmatrix}. \tag{5.18}$$

Applying this interpolation to (4.27) and (4.28) alows us to rewrite $\mathbf{K}_{int}^{ij}$ and $\mathbf{K}_{ext}^{ij}$ as

$$\begin{aligned} \mathbf{K}_{int}^{ij} = & \int_0^L I^{i'} \begin{bmatrix} \mathbf{0} & \mathbf{0} \\ (\delta_{ij} - I^j)\widehat{\mathbf{n}} & -\widehat{\mathbf{n}}\,(\widehat{\mathbf{r}}_j - \widehat{\mathbf{r}})\,\tilde{\mathbf{I}}^j \end{bmatrix} \mathrm{d}x + \\ & + \int_0^L I^{i'} \begin{bmatrix} \mathbf{0} & -\widehat{\mathbf{n}}\tilde{\mathbf{I}}^j \\ \mathbf{0} & -\left[(\widehat{\mathbf{r}} - \widehat{\mathbf{r}}_i)\,\widehat{\mathbf{n}} + \widehat{\mathbf{m}}\right]\tilde{\mathbf{I}}^j \end{bmatrix} \mathrm{d}x + \\ & + \int_0^L I^{i'} \begin{bmatrix} \boldsymbol{\Lambda}\mathbf{C}_N\boldsymbol{\Lambda}^T & \mathbf{0} \\ (\widehat{\mathbf{r}} - \widehat{\mathbf{r}}_i)\,\boldsymbol{\Lambda}\mathbf{C}_N\boldsymbol{\Lambda}^T & \boldsymbol{\Lambda}\mathbf{C}_M\boldsymbol{\Lambda}^T \end{bmatrix} \begin{bmatrix} I^{j'}\mathbf{I} & (\widehat{\mathbf{r}}_j - \widehat{\mathbf{r}})\,\tilde{\mathbf{I}}^{j'} \\ \mathbf{0} & \tilde{\mathbf{I}}^{j'} \end{bmatrix} \mathrm{d}x\,, \end{aligned} \tag{5.19}$$

and

$$\mathbf{K}_{ext}^{ij} = \int_0^L I^i \begin{bmatrix} \mathbf{0} & \mathbf{0} \\ (\delta_{ij} - I^j)\widehat{\mathbf{n}}_e & -\widehat{\mathbf{n}}_e\,(\widehat{\mathbf{r}}_j - \widehat{\mathbf{r}})\,\tilde{\mathbf{I}}^j \end{bmatrix} \mathrm{d}x\,. \tag{5.20}$$

In numerical examples, we will refer to these elements as GMFP1.

Generalised interpolation option 2 Analogously to the previous case, (5.11) is substituted into (4.36) and (4.37) to obtain

$$\begin{Bmatrix} \Delta\mathbf{r} \\ \Delta\boldsymbol{\vartheta} \end{Bmatrix} = \sum_{j=1}^{N} \begin{bmatrix} I^j\mathbf{I} & \mathbf{0} \\ \mathbf{0} & \tilde{\mathbf{I}}^j \end{bmatrix} \begin{Bmatrix} \Delta\mathbf{r}_j \\ \Delta\boldsymbol{\vartheta}_j \end{Bmatrix},$$

which is applied to (4.27) and (4.28) to give

$$\mathbf{K}_{int}^{ij} = \int_0^L I^{i'}(\delta_{ij} - I^j) \begin{bmatrix} \mathbf{0} & \mathbf{0} \\ \widehat{\mathbf{n}} & \mathbf{0} \end{bmatrix} \mathrm{d}x + \int_0^L I^{i'} \begin{bmatrix} \mathbf{0} & -\widehat{\mathbf{n}}\tilde{\mathbf{I}}^j \\ \mathbf{0} & -\left[(\widehat{\mathbf{r}} - \widehat{\mathbf{r}}_i)\,\widehat{\mathbf{n}} + \widehat{\mathbf{m}}\right]\tilde{\mathbf{I}}^j \end{bmatrix} \mathrm{d}x + \tag{5.21}$$

$$+ \int_0^L I^{i'} \begin{bmatrix} I^{j'}\boldsymbol{\Lambda}\mathbf{C}_N\boldsymbol{\Lambda}^T & \boldsymbol{\Lambda}\mathbf{C}_N\boldsymbol{\Lambda}^T\widehat{\mathbf{r}}'\tilde{\mathbf{I}}^j \\ I^{j'}\,(\widehat{\mathbf{r}} - \widehat{\mathbf{r}}_i)\,\boldsymbol{\Lambda}\mathbf{C}_N\boldsymbol{\Lambda}^T & (\widehat{\mathbf{r}} - \widehat{\mathbf{r}}_i)\,\boldsymbol{\Lambda}\mathbf{C}_N\boldsymbol{\Lambda}^T\widehat{\mathbf{r}}'\tilde{\mathbf{I}}^j + \boldsymbol{\Lambda}\mathbf{C}_M\boldsymbol{\Lambda}^T\tilde{\mathbf{I}}^{j'} \end{bmatrix} \mathrm{d}x\,, \tag{5.22}$$

and

$$\mathbf{K}_{ext}^{ij} = \int_0^L I^i(\delta_{ij} - I^j) \begin{bmatrix} \mathbf{0} & \mathbf{0} \\ \widehat{\mathbf{n}}_e & \mathbf{0} \end{bmatrix} \mathrm{d}x\,. \tag{5.23}$$

In numerical examples, we will refer to these elements as GMFP2.

Generalised interpolation option 3 Implementation of generalised interpolation functions into this option requires the most coding interventions. Namely, this is the only option where we directly calculate the position vectors based on the current incremental values and this means that $\tilde{\mathbf{I}}^j$ and $\tilde{\mathbf{I}}^{j'}$ appear not only in the stiffness matrix, but also in the update procedure for $\mathbf{r}$ and $\mathbf{r}'$ at integration points. Remembering that within this option $\mathbf{r}$ is updated at integration points as

$$\mathbf{r}(x) = \mathbf{r}_{\mathrm{old}}(x) + \Delta\mathbf{r}(x)\,,$$

we use (5.18) to obtain the values of $\Delta\mathbf{r}$ at integration points. After updating $\mathbf{r}(x)$ and $\mathbf{r}'(x)$, the strain measures are updated and from there the same expressions for the stiffness matrix as in the generalised Interpolation option 1 can be used. In numerical examples, we will refer to

these elements as GMFP3.

Evaluation of strain measures

Evaluation of the approximated translational material strain measures $\boldsymbol{\Gamma}^h$ at x follows by substituting (5.6) in (3.4) as

$$\boldsymbol{\Gamma}^h = \exp \widehat{\boldsymbol{\Psi}}^{lh} \boldsymbol{\Lambda}_r^T \mathbf{r}' - \mathbf{E}_1 \,. \tag{5.24}$$

The approximated rotational material strain measures $\mathbf{K}^h$ at x are evaluated by substituting (5.6) into (3.5) to obtain

$$\begin{aligned} \widehat{\mathbf{K}}^h &= \left[\exp \widehat{\boldsymbol{\Psi}}^{lh}\right]^T \underbrace{\boldsymbol{\Lambda}_r^T \boldsymbol{\Lambda}_r}_{\mathbf{I}} \left[\exp \widehat{\boldsymbol{\Psi}}^{lh}\right]' = \widehat{\mathbf{H}^T \left[\boldsymbol{\Psi}^{lh}\right] \boldsymbol{\Psi}^{lh\prime}} \\ \Rightarrow \mathbf{K}^h &= \mathbf{H}^T \left[\boldsymbol{\Psi}^{lh}\right] \boldsymbol{\Psi}^{lh\prime} , \end{aligned} \tag{5.25}$$

due to Appendix A.2.2 and (2.50). Results (5.24) and (5.25) show that two configurations, which do not differ in current local rotations, but do differ in reference (rigid-body) rotations, **have the same approximated strain measures**. In other words, this type of formulation is strain-invariant.

5.2.2 Numerical examples

In this section, all the numerical examples from Section 4.2.2 are repeated using the generalised formulations.

Cantilever beam subject to pure bending

Using any of the three generalised interpolation options we obtain the exact solution [4] in three iterations, i.e. the same result as before the implementation of the generalised approach. This is in accordance with the fact that the effects of strain non-invariance and path-dependence are present only in 3D when standard rotational degrees of freedom are interpolated. Further numerical tests need to be conducted, however, because in this numerical example there are no translational strains present.

Single-element path-dependence and strain-invariance test

As it is seen from Tables 5.1 and 5.2, the results of this test are improved with respect to the earlier presented modified fixed-pole elements. GMFP1 and GMFP2 now give path-independent and strain-invariant results. Although comparing rotational strain measure components suggests that GMFP3 is also strain-invariant, the difference in displacement components shown in Table 5.1 implies that the translational strain measures are non-invariant for this interpolation option. To demonstrate this, consider the position vector

$$\mathbf{r} = \langle 0.97592 \quad 0.18655 \quad -0.06552 \rangle^T$$

of the free end obtained using GMFP3 in a single increment. After applying the rigid rotation to the whole structure this end takes the position

$$\exp \widehat{\boldsymbol{\psi}}_R \mathbf{r} = \langle 0.29645 \quad -0.06797 \quad -0.94816 \rangle^T \ .$$

Using GMFP3 with $\underline{\boldsymbol{\psi}}_1$ and $\underline{\boldsymbol{\psi}}_2$, however gives a different end-node position

$$\underline{\mathbf{r}} = \langle 0.28697 \quad 0.01921 \quad -0.89881 \rangle^T \ ,$$

which confirms that this interpolation option is non-invariant. In contrast, with GMFP1 and GMFP2, the end-point position vector

$$\mathbf{r} = \langle 0.97592 \quad 0.20094 \quad -0.08490 \rangle^T$$

is rotated into

$$\exp \widehat{\boldsymbol{\psi}}_R \mathbf{r} = \langle 0.28697 \quad -0.04751 \quad -0.95676 \rangle^T \ ,$$

which is identical to

$$\underline{\mathbf{r}} = \langle 0.28697 \quad -0.04751 \quad -0.95676 \rangle^T \ ,$$

obtained when $\underline{\boldsymbol{\psi}}_1$ and $\underline{\boldsymbol{\psi}}_2$ are applied for both interpolation options.

Lee's frame

Results from Table 4.7 have shown that MFP3 exhibits path-dependent behaviour, even in the planar case. In Table 5.3 we show the corresponding results using the generalised approach. The results are identical, suggesting that the path-dependence of MFP3 cannot be solved using the generalised interpolation functions for the spin vectors. Again, this does not come as a surprise

	K_1	K_2	K_3	u_1	u_2	u_3
Invariant, 1 [51]	-1.26383	1.27102	-0.42294	-0.02408	0.20094	-0.08490
Invariant, 2 [51]	-1.26383	1.27102	-0.42294	-0.02408	0.20094	-0.08490
GMFP1, 1	-1.26383	1.27102	-0.42294	-0.02408	0.20094	-0.08490
GMFP1, 2	-1.26383	1.27102	-0.42294	-0.02408	0.20094	-0.08490
GMFP2, 1	-1.26383	1.27102	-0.42294	-0.02408	0.20094	-0.08490
GMFP2, 2	-1.26383	1.27102	-0.42294	-0.02408	0.20094	-0.08490
GMFP3, 1	-1.26383	1.27102	-0.42294	-0.02408	0.18655	-0.06552
GMFP3, 2	-1.26383	1.27102	-0.42294	-0.10522	0.09523	-0.08081

Table 5.1: Components of rotational strains and the displacements of the second node using different incrementation sequences for the end-point rotations – the generalised approach

	K_1	K_2	K_3	$\underline{K}_1$	$\underline{K}_2$	$\underline{K}_3$
Invariant [51]	-1.26383	1.27102	-0.42294	-1.26383	1.27102	-0.42294
GMFP1	-1.26383	1.27102	-0.42294	-1.26383	1.27102	-0.42294
GMFP2	-1.26383	1.27102	-0.42294	-1.26383	1.27102	-0.42294
GMFP3	-1.26383	1.27102	-0.42294	-1.26383	1.27102	-0.42294

Table 5.2: Components of rotational strains for end-point rotations $\boldsymbol{\psi}_1$, $\boldsymbol{\psi}_2$ and $\underline{\boldsymbol{\psi}}_1$, $\underline{\boldsymbol{\psi}}_2$ applied in one increment – the generalised approach

as we know that in 2D this interpolation makes no difference.

	GMFP1		GMFP2		GMFP3	
	u_1	u_2	u_1	u_2	u_1	u_2
1	6.46073	-22.48634	6.46073	-22.48634	8.59392	-26.02842
2	6.46073	-22.48634	6.46073	-22.48634	8.72739	-26.12403
10	6.46073	-22.48634	6.46073	-22.48634	8.97095	-26.13286
20	6.46073	-22.48634	6.46073	-22.48634	9.00150	-26.09732

Table 5.3: Displacements of the loaded node using ten linear elements – the generalised approach

45° **cantilever bend**

Depending on the interpolation option analysed, implementation of the generalised shape functions for the spin vectors has improved robustness and path-independence in this example. The results in Table 5.4 show that, similarly to the planar example, introduction of generalised shape functions has no effect on the path-dependence of MFP3. The solutions obtained using formulation GMFP3 are different from the ones given in Table 4.8, but without obvious relationship, though the robustness of the procedure is improved and now the solution is obtained in 5 equal load increments. GMFP1 and GMFP2 now produce path independent results, while GMFP2 also has improved robustness (only 3 equal load increments) in comparison to MFP2.

Formulation	Increments	u_1	u_2	u_3
Invariant [51]	3	13.48286	-23.47949	53.37152
GMFP1	3	-	-	-
GMFP1	7	13.48286	-23.47949	53.37152
GMFP1	10	13.48286	-23.47949	53.37152
GMFP2	3	13.48286	-23.47949	53.37152
GMFP2	7	13.48286	-23.47949	53.37152
GMFP2	10	13.48286	-23.47949	53.37152
GMFP3	3	-	-	-
GMFP3	5	13.51873	-23.53052	53.33627
GMFP3	10	13.48871	-23.53052	53.15864
GMFP3	15	13.48871	-23.52958	53.15864
GMFP3	20	13.48737	-23.53049	53.13021

Table 5.4: Tip displacement components using different load incrementation – the generalised approach

5.3 Generalised fixed-pole element

In this section we propose an extension of the generalised approach given in Section 5.2 to the 6D case (the configuration-tensor approach). As the results in Section 4.1 suggest, the proposed implementation of the fixed-pole approach using iterative configuration parameters, is path-dependent. Although in the approaches which use standard degrees of freedom the problem of path-dependence and non-invariance emerges only in spatial problems, the results in Section 4.1 show something different. Looking at the internal structure of the configuration parameter we discover that the "translational" part of the vector of unknowns is a combination of the standard translational unknown and the functions of the rotational parameter. Since the interpolation of the rotational parameters in a non-consistent manner is the underlying source of non-invariance and path-dependence, this explains the possible reason for path-dependent results in Section 4.1 even in the planar case.

Since there are many analogies between the orientation matrix $\mathbf{\Lambda}$ and the configuration tensor $\mathbf{C}$, the idea of applying the methodology presented in [47, 51] as well as in the previous section, comes naturally. In this case, the rotational parameters (as well as the translational ones) are hidden inside the configurational spins $\Delta\boldsymbol{\varsigma}$.

5.3.1 Solution procedure

Decomposition of the configuration tensor

The configuration tensor $\mathbf{C}(x)$ is decomposed using a reference configuration tensor $\mathbf{C}_r$ which is unique for the whole beam and rigidly attached to it, and a configuration tensor defining a local 6D configuration vector, $\mathbf{\Phi}^l(x)$ between the reference configuration tensor and the total configuration tensor so that

$$\mathbf{C}(x) = \mathbf{C}_r \exp \widehat{\mathbf{\Phi}}^{lh}(x)\,. \tag{5.26}$$

The reference configuration tensor represents the configuration of one of the beam nodes. In the most general case, two nodes I and J are selected, and a relative configuration vector between these nodes is calculated using

$$\exp \widehat{\boldsymbol{\eta}}_{IJ} = \mathbf{C}_I^{-1}\mathbf{C}_J\,. \tag{5.27}$$

$\boldsymbol{\eta}_{IJ}$ is then extracted using a 6D version of Spurrier's algorithm which is described in Appendix A.4. The reference tensor $\mathbf{C}_r$ is defined as a midway configuration between $\mathbf{C}_I$ and $\mathbf{C}_J$ as

$$\mathbf{C}_r = \mathbf{C}_I \exp\left(\frac{1}{2}\widehat{\boldsymbol{\eta}}_{IJ}\right)\,. \tag{5.28}$$

The nodal configuration tensor $\mathbf{C}_i$ is evaluated from $\mathbf{C}_i = \exp \widehat{\Delta\boldsymbol{\varsigma}_i}\mathbf{C}_{i,\,\mathrm{old}}$. From (5.26) we extract the nodal values of the local configuration vector $\mathbf{\Phi}_i^l$ using

$$\exp \widehat{\mathbf{\Phi}}_i^l = \mathbf{C}_r^{-1}\mathbf{C}_i\,. \tag{5.29}$$

Then we interpolate the values of the local configuration vector along the beam reference axis using Lagrange polynomials

$$\mathbf{\Phi}^l(x) \doteq \mathbf{\Phi}^{lh}(x) = \sum_{k=1}^{N} I^k \mathbf{\Phi}_k^l \quad \text{and} \quad \mathbf{\Phi}^{l'}(x) \doteq \mathbf{\Phi}^{lh'}(x) = \sum_{k=1}^{N} I^{k'} \mathbf{\Phi}_k^l\,. \tag{5.30}$$

Finally we conclude that in order to compute the configuration tensor at integration points we only need (5.30) and (5.26). Again, interpolation (5.30) does not include rigid-body motion. The interpolation objectivity proof is given in Appendix A.5.

Generalised shape functions

The next step is deriving an appropriate interpolation for the configuration spins $\Delta\boldsymbol{\varsigma}$. Linearising the configuration tensor (5.26) we have

$$\Delta\mathbf{C} = \Delta\mathbf{C}_r \exp\widehat{\boldsymbol{\Phi}}^{lh}(x) + \mathbf{C}_r\Delta\left[\exp\widehat{\boldsymbol{\Phi}}^{lh}(x)\right] . \tag{5.31}$$

Substituting (2.66) into the above equation gives

$$\widehat{\Delta\boldsymbol{\varsigma}}\mathbf{C} = \widehat{\Delta\boldsymbol{\varsigma}}_r\mathbf{C}_r \exp\widehat{\boldsymbol{\Phi}}^{lh}(x) + \mathbf{C}_r\Delta\left[\exp\widehat{\boldsymbol{\Phi}}^{lh}(x)\right] .$$

Post-multiplying the above equation with $\mathbf{C}^{-1} = \left[\mathbf{C}_r \exp\widehat{\boldsymbol{\Phi}}^{lh}(x)\right]^{-1} = \left[\exp\widehat{\boldsymbol{\Phi}}^{lh}(x)\right]^{-1}\mathbf{C}_r^{-1}$ we obtain

$$\begin{aligned} &\widehat{\Delta\boldsymbol{\varsigma}} = \widehat{\Delta\boldsymbol{\varsigma}}_r + \mathbf{C}_r\Delta\left[\exp\widehat{\boldsymbol{\Phi}}^{lh}(x)\right]\left[\exp\widehat{\boldsymbol{\Phi}}^{lh}(x)\right]^{-1}\mathbf{C}_r^{-1} \\ \Rightarrow\quad &\Delta\boldsymbol{\varsigma} = \Delta\boldsymbol{\varsigma}_r + \mathbf{C}_r\mathbf{H}_{\mathbf{6}}(\boldsymbol{\Phi}^{lh}(x))\Delta\boldsymbol{\Phi}^{lh}(x) , \end{aligned} \tag{5.32}$$

due to (A.1) and the results of Appendix A.2.5. Next, we rewrite (5.32) for nodal values

$$\Delta\boldsymbol{\varsigma}_i = \Delta\boldsymbol{\varsigma}_r + \mathbf{C}_r\mathbf{H}_{\mathbf{6}}(\boldsymbol{\Phi}_i^l)\Delta\boldsymbol{\Phi}_i^l ,$$

and express $\Delta\boldsymbol{\Phi}_i^l$ from there as

$$\Delta\boldsymbol{\Phi}_i^l = \left[\mathbf{H}_{\mathbf{6}}(\boldsymbol{\Phi}_i^l)\right]^{-1}\mathbf{C}_r^{-1}(\Delta\boldsymbol{\varsigma}_i - \Delta\boldsymbol{\varsigma}_r) , \tag{5.33}$$

with $\left[\mathbf{H}_{\mathbf{6}}(\boldsymbol{\Phi}_i^l)\right]^{-1}$ given in (A.29). Writing (5.26) at node I we can express $\mathbf{C}_r$ as

$$\mathbf{C}_r = \mathbf{C}_I\left[\exp\left(\widehat{\boldsymbol{\Phi}}_I^l\right)\right]^{-1} ,$$

and equating it to (5.28) while using (A.18) we obtain

$$\exp\left(\frac{1}{2}\widehat{\boldsymbol{\eta}}_{IJ}\right) = \exp\left(-\widehat{\boldsymbol{\Phi}}_I^l\right) . \tag{5.34}$$

Analogously, for node J we obtain

$$\exp\left(\frac{1}{2}\widehat{\boldsymbol{\eta}}_{IJ}\right) = \underbrace{\mathbf{C}_I^{-1}\mathbf{C}_J}_{\exp\widehat{\boldsymbol{\eta}}_{IJ}}\exp\left(-\widehat{\boldsymbol{\Phi}}_J^l\right) = \exp\left(\widehat{\boldsymbol{\eta}}_{IJ}\right)\exp\left(-\widehat{\boldsymbol{\Phi}}_J^l\right) ,$$

which in turn gives

$$\exp\left(-\frac{1}{2}\widehat{\boldsymbol{\eta}}_{IJ}\right) = \exp\left(-\widehat{\boldsymbol{\Phi}}_J^l\right) , \tag{5.35}$$

i.e.

$$\exp\left(\frac{1}{2}\widehat{\boldsymbol{\eta}}_{IJ}\right) = \exp\left(\widehat{\boldsymbol{\Phi}}^l_J\right) . \tag{5.36}$$

Comparing (5.34) and (5.36) shows

$$\boldsymbol{\Phi}^l_J = -\boldsymbol{\Phi}^l_I . \tag{5.37}$$

Linearising (5.37) results in

$$\Delta\boldsymbol{\Phi}^l_J = -\Delta\boldsymbol{\Phi}^l_I , \tag{5.38}$$

while writing (5.33) for nodes I and J gives

$$\begin{aligned} I: \quad & \Delta\boldsymbol{\Phi}^l_I = \left[\mathbf{H_6}\left(\boldsymbol{\Phi}^l_I\right)\right]^{-1}\mathbf{C}_r^{-1}(\Delta\boldsymbol{\varsigma}_I - \Delta\boldsymbol{\varsigma}_r) , \\ J: \quad & \Delta\boldsymbol{\Phi}^l_J = \left[\mathbf{H_6}\left(\boldsymbol{\Phi}^l_J\right)\right]^{-1}\mathbf{C}_r^{-1}(\Delta\boldsymbol{\varsigma}_J - \Delta\boldsymbol{\varsigma}_r) , \end{aligned} \tag{5.39}$$

which can be related using (5.38) and (5.37) to obtain

$$\begin{aligned} \left[\mathbf{H_6}\left(\boldsymbol{\Phi}^l_I\right)\right]^{-1}\mathbf{C}_r^{-1}(\Delta\boldsymbol{\varsigma}_I - \Delta\boldsymbol{\varsigma}_r) &= -\left[\mathbf{H_6}\left(-\boldsymbol{\Phi}^l_I\right)\right]^{-1}\mathbf{C}_r^{-1}(\Delta\boldsymbol{\varsigma}_J - \Delta\boldsymbol{\varsigma}_r) \\ \left\{\left[\mathbf{H_6}\left(\boldsymbol{\Phi}^l_I\right)\right]^{-1} + \left[\mathbf{H_6}\left(-\boldsymbol{\Phi}^l_I\right)\right]^{-1}\right\}\mathbf{C}_r^{-1}\Delta\boldsymbol{\varsigma}_r &= \left[\mathbf{H_6}\left(\boldsymbol{\Phi}^l_I\right)\right]^{-1}\mathbf{C}_r^{-1}\Delta\boldsymbol{\varsigma}_I + \left[\mathbf{H_6}\left(-\boldsymbol{\Phi}^l_I\right)\right]^{-1}\mathbf{C}_r^{-1}\Delta\boldsymbol{\varsigma}_J . \end{aligned} \tag{5.40}$$

Finally, we can express $\Delta\boldsymbol{\varsigma}_r$ from (5.40), using (5.37) as well as (A.32) as

$$\begin{aligned} \Delta\boldsymbol{\varsigma}_r =& \mathbf{C}_r\left\{\left[\mathbf{H_6}\left(\boldsymbol{\Phi}^l_I\right)\right]^{-1} + \left[\mathbf{H_6}\left(-\boldsymbol{\Phi}^l_I\right)\right]^{-1}\right\}^{-1}\left[\mathbf{H_6}\left(\boldsymbol{\Phi}^l_I\right)\right]^{-1}\mathbf{C}_r^{-1}\Delta\boldsymbol{\varsigma}_I \\ &+ \mathbf{C}_r\left\{\left[\mathbf{H_6}\left(\boldsymbol{\Phi}^l_I\right)\right]^{-1} + \left[\mathbf{H_6}\left(-\boldsymbol{\Phi}^l_I\right)\right]^{-1}\right\}^{-1}\left[\mathbf{H_6}\left(-\boldsymbol{\Phi}^l_I\right)\right]^{-1}\mathbf{C}_r^{-1}\Delta\boldsymbol{\varsigma}_J \\ =& \mathbf{C}_r\left\{\left[\mathbf{H_6}\left(\boldsymbol{\Phi}^l_I\right)\right]^{-1} + \left[\mathbf{H_6}\left(-\boldsymbol{\Phi}^l_I\right)\right]^{-1}\right\}^{-1}\left[\mathbf{H_6}\left(\boldsymbol{\Phi}^l_I\right)\right]^{-1}\mathbf{C}_r^{-1}\Delta\boldsymbol{\varsigma}_I \\ &+ \mathbf{C}_r\left\{\left[\mathbf{H_6}\left(-\boldsymbol{\Phi}^l_J\right)\right]^{-1} + \left[\mathbf{H_6}\left(\boldsymbol{\Phi}^l_J\right)\right]^{-1}\right\}^{-1}\left[\mathbf{H_6}\left(\boldsymbol{\Phi}^l_J\right)\right]^{-1}\mathbf{C}_r^{-1}\Delta\boldsymbol{\varsigma}_J \\ &= \mathbf{C}_r\mathbf{b}_I\mathbf{C}_r^{-1}\Delta\boldsymbol{\varsigma}_I + \mathbf{C}_r\mathbf{b}_J\mathbf{C}_r^{-1}\Delta\boldsymbol{\varsigma}_J , \end{aligned} \tag{5.41}$$

with $\mathbf{b}_I$ and $\mathbf{b}_J$ as short-hand notations for

$$\mathbf{b}_j = \left(\mathbf{I} + \exp\widehat{\boldsymbol{\Phi}}^l_j\right)^{-1} = \begin{cases} \left[\mathbf{I} + \exp\left(-\frac{1}{2}\widehat{\boldsymbol{\eta}}_{IJ}\right)\right]^{-1} = \begin{bmatrix} \mathbf{v}_I & -\mathbf{v}_I\left[\mathbf{Q}(\frac{1}{2}\widehat{\boldsymbol{\eta}}_{IJ})\right]^T\mathbf{v}_I \\ \mathbf{0} & \mathbf{v}_I \end{bmatrix} & \text{if } j = I \\ \left[\mathbf{I} + \exp\left(\frac{1}{2}\widehat{\boldsymbol{\eta}}_{IJ}\right)\right]^{-1} = \begin{bmatrix} \mathbf{v}_J & -\mathbf{v}_J\left[\mathbf{Q}(\frac{1}{2}\widehat{\boldsymbol{\eta}}_{IJ})\right]\mathbf{v}_J \\ \mathbf{0} & \mathbf{v}_J \end{bmatrix} & \text{if } j = J \end{cases} \tag{5.42}$$

due to (5.34) and (5.36). Inserting (5.41) into (5.33) we obtain

$$\Delta\mathbf{\Phi}_i^l = \left[\mathbf{H_6}\left(\mathbf{\Phi}_i^l\right)\right]^{-1}\mathbf{C}_r^{-1}\left[\Delta\boldsymbol{\varsigma}_i - \mathbf{C}_r\left(\mathbf{b}_I\mathbf{C}_r^{-1}\Delta\boldsymbol{\varsigma}_I + \mathbf{b}_J\mathbf{C}_r^{-1}\Delta\boldsymbol{\varsigma}_J\right)\right] . \tag{5.43}$$

Inserting (5.43) and (5.30) into (5.32) we finally have

$$\Delta\boldsymbol{\varsigma}(x) = \sum_{j=1}^{N}\tilde{\mathbf{I}}_6^j(x)\Delta\boldsymbol{\varsigma}_j\,, \quad \Delta\boldsymbol{\varsigma}'(x) = \sum_{j=1}^{N}\tilde{\mathbf{I}}_6^{j'}(x)\Delta\boldsymbol{\varsigma}_j \tag{5.44}$$

as the interpolation for configurational spins, with $\tilde{\mathbf{I}}_6^j(x)$ as the 6D generalised shape function and $\tilde{\mathbf{I}}_6^{j'}(x)$ as its derivative, given as

$$\begin{aligned}\tilde{\mathbf{I}}_6^j = (\delta_I^j + \delta_J^j)\mathbf{C}_r&\left[\mathbf{I} - \mathbf{H}_6\left[\mathbf{\Phi}^{lh}(x)\right]\sum_{m=1}^{N} I^m(x)\mathbf{H}_6^{-1}(\mathbf{\Phi}_m^l)\right]\mathbf{b}_j\mathbf{C}_r^{-1}\\ &+\mathbf{C}_r\mathbf{H}_6\left[\mathbf{\Phi}^{lh}(x)\right]I^j(x)\mathbf{H}_6^{-1}(\mathbf{\Phi}_j^l)\mathbf{C}_r^{-1}\,, \end{aligned}\tag{5.45}$$

$$\begin{aligned}\tilde{\mathbf{I}}_6^{j'} = (\delta_I^j + \delta_J^j)\mathbf{C}_r&\sum_{m=1}^{N}\left\{-\mathbf{H}_6'\left[\mathbf{\Phi}^{lh}(x)\right]I^m(x)\mathbf{H}_6^{-1}(\mathbf{\Phi}_m^l)\right.\\ &\left.-\mathbf{H}_6\left[\mathbf{\Phi}^{lh}(x)\right]I^{m'}(x)\mathbf{H}_6^{-1}(\mathbf{\Phi}_m^l)\right\}\mathbf{b}_j\mathbf{C}_r^{-1}\\ &+\mathbf{C}_r\left\{\mathbf{H}_6'\left[\mathbf{\Phi}^{lh}(x)\right]I^j(x) + \mathbf{H}_6\left[\mathbf{\Phi}^{lh}(x)\right]I^{j'}(x)\right\}\mathbf{H}_6^{-1}(\mathbf{\Phi}_j^l)\mathbf{C}_r^{-1}\,, \end{aligned}\tag{5.46}$$

with $\mathbf{H}_6'(\mathbf{\Phi})$ defined as

$$\mathbf{H}_6'(\mathbf{\Phi}) = \begin{bmatrix}\mathbf{H}'(\mathbf{\Phi}_2) & \mathbf{B}'(\mathbf{\Phi})\\ \mathbf{0} & \mathbf{H}'(\mathbf{\Phi}_2)\end{bmatrix}, \tag{5.47}$$

which is evaluated using (5.15) and (A.33).

Configuration update

Here we limit our attention to the simplest case of these interpolating functions, when $I = J$ so that the reference node $I = \frac{N}{2}$ for even-noded elements and $I = \frac{N+1}{2}$ for odd-noded elements. In such a case the generalised shape functions given in (5.45) and (5.46) take the following explicit form

$$\tilde{\mathbf{I}}_6^j(x) = \begin{cases}\mathbf{I} - \mathbf{C}_I\mathbf{H_6}\left[\mathbf{\Phi}^{lh}(x)\right]\sum_{m=1}^{N}(1-\delta_I^m)I^m(x)\left[\mathbf{H_6}(\mathbf{\Phi}_m^l)\right]^{-1}\mathbf{C}_I^{-1}\,, & \text{if } j = I\,,\\ \mathbf{C}_I\mathbf{H_6}\left[\mathbf{\Phi}^{lh}(x)\right]I^j(x)\left[\mathbf{H_6}(\mathbf{\Phi}_j^l)\right]^{-1}\mathbf{C}_I^{-1}\,, & \text{if } j \neq I\,.\end{cases} \tag{5.48}$$

$$\tilde{\mathbf{I}}_6^{j'}(x) = \begin{cases} -\mathbf{C}_I \left\{ \mathbf{H_6}' \left[\mathbf{\Phi}^{lh}(x)\right] \sum_{m=1}^{N} (1-\delta_I^m) I^m(x) \left[\mathbf{H_6}(\mathbf{\Phi}_m^l)\right]^{-1} + \right. & \\ \left. + \mathbf{H_6} \left[\mathbf{\Phi}^{lh}(x)\right] \sum_{m=1}^{N} (1-\delta_I^m) I^{m'}(x) \left[\mathbf{H_6}(\mathbf{\Phi}_m^l)\right]^{-1} \right\} \mathbf{C}_I^{-1}\,, & \text{if } j = I\,, \\ \mathbf{C}_I \left\{ \mathbf{H_6}' \left[\mathbf{\Phi}^{lh}(x)\right] I^j(x) + \mathbf{H_6} \left[\mathbf{\Phi}^{lh}(x)\right] I^{j'}(x) \right\} \left[\mathbf{H_6}(\mathbf{\Phi}_j^l)\right]^{-1} \mathbf{C}_I^{-1}\,, & \text{if } j \neq I\,. \end{cases} \tag{5.49}$$

Implementation into the formulation given in Section 4.1 is straightforward (I^j is replaced with $\tilde{\mathbf{I}}_6^j$, although the fact that these functions are now matrices, not scalars, must be taken into account). Substituting (5.44) into (4.5) and (4.8) we obtain

$$\mathbf{K}_{ij}^{i} = \int_0^L I^{i'} \mathbf{C}^{-T} \left(\mathbf{D}\mathbf{C}^{-1} \tilde{\mathbf{I}}_6^{j'} - \overset{\triangledown}{\mathbf{S}} \mathbf{C}^{-1} \tilde{\mathbf{I}}_6^{j} \right) \mathrm{d}x\,, \tag{5.50}$$

$$\mathbf{K}_{ij}^{e,\,\mathrm{local}} = -\int_0^L I^i \overset{\triangledown}{\mathbf{s}}_e \begin{bmatrix} \mathbf{I} & -\widehat{\mathbf{r}} \\ \mathbf{0} & \mathbf{0} \end{bmatrix} \tilde{\mathbf{I}}_6^j \,\mathrm{d}x\,, \tag{5.51}$$

noting that the introduction of these interpolation functions has no effect on (4.16), i.e. we use the old expression for $\mathbf{K}_{ij}^{e,\,\mathrm{nodal}}$.

Evaluation of strain measures

In order to evaluate the material strain measures, $\mathbf{X}-\mathbf{X}_N$, we first need to find the approximated value of the material configuration parameter $\mathbf{X}^h$ at x using (3.49) and (5.26) as

$$\widehat{\mathbf{X}}^h = \left[\mathbf{C}_r \exp \widehat{\mathbf{\Phi}}^{lh}\right]^{-1} \left[\mathbf{C}_r \exp \widehat{\mathbf{\Phi}}^{lh}\right]' = \left[\exp \widehat{\mathbf{\Phi}}^{lh}\right]^{-1} \underbrace{\mathbf{C}_r^{-1}\mathbf{C}_r}_{\mathbf{I}} \left[\exp \widehat{\mathbf{\Phi}}^{lh}\right]'\,,$$

which, using Appendix A.2.5 turns into

$$\widehat{\widehat{\mathbf{X}}}^h = \overbrace{\mathbf{H_6}(\mathbf{\Phi}^{lh})\mathbf{\Phi}^{lh'}} \quad \Leftrightarrow \quad \mathbf{X}^h = \mathbf{H_6}(\mathbf{\Phi}^{lh})\mathbf{\Phi}^{lh'}\,, \tag{5.52}$$

from where it is clear that the strain measures evaluated in this way are strain-invariant because they depend only on the local configuration vectors $\mathbf{\Phi}^{lh}(x)$.

5.3.2 Numerical examples

In this section, all the numerical examples from Section 4.1.2 are repeated using the generalised formulation.

Increments	r_1	r_2
1 [4]	0	0
1	-8.7×10^{-12}	3.2×10^{-12}
2	-3.1×10^{-16}	-4.7×10^{-16}
5	6.4×10^{-16}	3.8×10^{-16}
10	3.3×10^{-11}	1.1×10^{-11}
20	7.3×10^{-14}	9.7×10^{-14}

Table 5.5: Pure cantilever bending: Tip position components obtained using different load incrementation

Formulation	Increments	u_1	u_2	u_3
Invariant [51]	3	13.48286	-23.47949	53.37152
GFP	3	-	-	-
GFP	7	13.46870	-23.47565	53.26603
GFP	10	13.46870	-23.47565	53.26603
GFP	20	13.46870	-23.47565	53.26603

Table 5.6: 45° cantilever bend: Tip displacement components using different load incrementation – the generalised approach

Cantilever beam subject to pure bending

As it is seen from Table 5.5, the results of this test are correct. The results do not depend on the load incrementation, i.e. they are path independent. This is in accordance with the assumption that the special group of rigid motions is not commutative in 2D.

45° cantilever bend

The results of this test given in Table 5.6 show that not only the results are path-independent, but also that the robustness of the procedure is improved by using the generalised approach compared. Compared to the results in Table 4.3 we see that the minimum number of load increments for the solution procedure to converge is reduced from ten to seven. This effect is analogous to generalised modified fixed-pole approach where robustness was also improved.

Chapter 6

Conclusions and future work

Fixed-pole formulation

In this thesis we have developed a new family of geometrically exact beam finite elements of arbitrary order based on the fixed-pole approach. Although in literature the configuration-tensor approach and the helicoidal interpolation usually go together, in this thesis we have made a distinction in order to analyse the implications of utilising the former approach. We have derived a new fixed-pole element from the principle of virtual work, which uses non-standard nodal unknowns. In contrast to the original formulation given by Bottasso and Borri, in this thesis we have interpolated the iterative changes of the configuration vector. The fact that these elements use non-standard system unknowns has two direct consequences: (i) imposing of the boundary conditions is more complex than in the usual approaches and (ii) the elements cannot be combined with the standard displacement-based finite element meshes, which has been the main motivation to derive and analyse a modified fixed-pole approach which uses the standard system unknowns.

Modified fixed-pole formulation

A modified approach has been derived by using the relationship between the fixed-pole and standard virtual quantities at a nodal level. such a modification of the fixed-pole approach has resulted in a definition of the nodal residual and stiffness matrix in which the position vector is present, and left us with an open question – how do we interpolate the position vector? From there we have considered three possible options. Interpolation option 1 has been motivated by our desire to utilise the same interpolation for the test and the trial functions. However, we have additionally decided to interpolate the position vector in the simplest possible way – using

Lagrange polynomials – which is of course not consistent with the chosen interpolation for the iterative changes. In Interpolation option 2, instead, we want to have consistent interpolation of the iterative changes which follows from the Lagrange interpolation of the nodal unknowns. In this case, though, different interpolations have been used for the test and the trial functions. Finally, Interpolation option 3 makes the most consistent choice with the character of the non-linear solution space, where the same interpolations have been used for the test and trial function and the interpolation of the position vector has been completely avoided and the position vector updated at the integration points.

Detection of non-invariance and path-dependence of proposed formulations

In Section 4.1.2 we have tested our fixed-pole formulation with respect to its accuracy, robustness and path-dependence using two numerical examples – one planar and one spatial. Path dependence is recognised in both examples, i.e. the fixed-pole formulation is path-dependent even in the planar case. Also, the robustness of the procedure is poorer in comparison to standard approaches. In Section 4.2.2 the proposed family of modified fixed-pole formulations is tested in two planar and two spatial examples. In the case of the planar example of pure bending, all three interpolation options provid accurate results. However, in the case of Lee's frame, Interpolation options 1 and 2 provide the same results as the standard elements and show no signs of path-dependence, while Interpolation option 3 yields what seemed as more accurate results, although being path-dependent. In the case of the two spatial examples, all three interpolation options exhibit strain non-invariant and path-dependent behaviour.

Strain-invariant and path independent family of modified fixed-pole elements

In the case of the modified fixed-pole formulations, non-invariance and path-dependence occur due to additive interpolation of rotational variables. A remedy for this problem is to implement the strain-invariant approach in the proposed interpolation options, i.e. (i) to interpolate only the relative rotations between two selected nodes and (ii) to implement the generalised shape functions derived by Jelenić and Crisfield. As demonstrated in Section 5.2.2, the results obtained using the generalised modified fixed-pole approach are now both strain-invariant and path-independent, although not for all the interpolation options, i.e. Interpolation option 3 still exhibits non-invariant and path-dependent behaviour which is now only due to the translational part (the translational strain measures remain non-invariant while the rotational strain measures

become invariant). The reason for this lies in the fact that within this option the displacements are *not* interpolated, but directly updated at integration points on the basis of a non-invariant interpolation of the iterative changes of the position vector and such an interpolation cannot be proven to be strain-invariant and path-independent.

A strain invariant approach in SR(6)

Bearing in mind that Interpolation option 3 is the most consistent choice (i.e. the one closest to the original fixed-pole approach, but still using the standard system unknowns) and observing the results obtained using the fixed-pole elements – the path-dependence and non-invariance come as no surprise. As already mentioned, the fixed-pole elements exhibit path-dependent behaviour even in the planar case.

This is due to the fact that even in the planar case the special group of rigid motions is not commutative. In order to fix this, a new generalised approach has been derived which generalises the interpolation of relative rotations to the relative configurations. Following the methodology given by Jelenić and Crisfield, we have managed to derive the 6D generalised shape functions along with the solution procedure in which only the relative configurations between nodes are interpolated. The result of this implementation is a strain-invariant and path-independent formulation. The objectivity proof shows that the interpolated strain measures in this way indeed are invariant to rigid-body motion.

Future work

In our future work, we first plan to solve the problem of reduced robustness of our formulations with respect to the standard approaches. Sonneville and co-workers have shown that using the helicoidal interpolation along with the configuration update consistent with the group yields not only strain-invariant and path-independent results, but also a very robust procedure. Unfortunately, the helicoidal interpolation was given only for two-noded elements, while our proposed formulations are given for an element of arbitrary order. However, Papa Dukić and co-workers have recently derived a generalisation of the helicoidal interpolation to an arbitrary order which we intend to implement into our proposed formulations. Furthermore, we will explore the implications of utilising the fixed-pole approach in non-linear dynamic analysis due to its energy and momentum conserving properties.

Appendix A

A little bit of algebra

A.1 Some properties of the configuration tensor

For any 6D vector $\mathbf{a} = \langle \mathbf{a}_1^T \ \mathbf{a}_2^T \rangle^T$, where $\mathbf{a}_1$, $\mathbf{a}_2$ are 3D vectors, the generalised cross-product $\hat{\mathbf{a}}$ is defined in (2.25). Evaluating $\mathbf{C}\hat{\mathbf{a}}\mathbf{C}^{-1}$ we have

$$\mathbf{C}\hat{\mathbf{a}}\mathbf{C}^{-1} = \begin{bmatrix} \mathbf{\Lambda} & \hat{\mathbf{r}}\mathbf{\Lambda} \\ \mathbf{0} & \mathbf{\Lambda} \end{bmatrix} \begin{bmatrix} \hat{\mathbf{a}}_2 & \hat{\mathbf{a}}_1 \\ \mathbf{0} & \hat{\mathbf{a}}_2 \end{bmatrix} \begin{bmatrix} \mathbf{\Lambda}^T & -\mathbf{\Lambda}^T\hat{\mathbf{r}} \\ \mathbf{0} & \mathbf{\Lambda}^T \end{bmatrix} = \begin{bmatrix} \mathbf{\Lambda}\hat{\mathbf{a}}_2\mathbf{\Lambda}^T & -\mathbf{\Lambda}\hat{\mathbf{a}}_2\mathbf{\Lambda}^T\hat{\mathbf{r}} + \mathbf{\Lambda}\hat{\mathbf{a}}_1\mathbf{\Lambda}^T + \hat{\mathbf{r}}\mathbf{\Lambda}\hat{\mathbf{a}}_2\mathbf{\Lambda}^T \\ \mathbf{0} & \mathbf{\Lambda}\hat{\mathbf{a}}_2\mathbf{\Lambda}^T \end{bmatrix}.$$

For any two skew-symmetric matrices $\hat{\mathbf{a}}_1, \hat{\mathbf{a}}_2 \in \mathrm{so}(3)$ the following relationships hold $\hat{\mathbf{a}}_1\hat{\mathbf{a}}_2 - \hat{\mathbf{a}}_2\hat{\mathbf{a}}_1 = \widehat{\mathbf{a}_1 \times \mathbf{a}_2}$, $\mathbf{\Lambda}\hat{\mathbf{a}}_1\mathbf{\Lambda}^T = \widehat{\mathbf{\Lambda}\mathbf{a}_1}$ which means that we can write the above result as

$$\mathbf{C}\hat{\mathbf{a}}\mathbf{C}^{-1} = \begin{bmatrix} \widehat{\mathbf{\Lambda}\mathbf{a}_2} & \widehat{\mathbf{\Lambda}\mathbf{a}_1} + \widehat{\mathbf{r} \times \mathbf{\Lambda}\mathbf{a}_2} \\ \mathbf{0} & \widehat{\mathbf{\Lambda}\mathbf{a}_2} \end{bmatrix} = \widehat{\mathbf{C}\mathbf{a}}. \tag{A.1}$$

To prove it, we immediately observe that the matrix in (A.1) has the form of the generalised cross-product (2.25) associated with the vector

$$\begin{Bmatrix} \mathbf{\Lambda}\mathbf{a}_1 + \hat{\mathbf{r}}\mathbf{\Lambda}\mathbf{a}_2 \\ \mathbf{\Lambda}\mathbf{a}_2 \end{Bmatrix} = \begin{bmatrix} \mathbf{\Lambda} & \hat{\mathbf{r}}\mathbf{\Lambda} \\ \mathbf{0} & \mathbf{\Lambda} \end{bmatrix} \begin{Bmatrix} \mathbf{a}_1 \\ \mathbf{a}_2 \end{Bmatrix} = \mathbf{C}\mathbf{a}.$$

Evaluating $\mathbf{C}^{-1}\hat{\mathbf{a}}\mathbf{C}$ gives

$$\mathbf{C}^{-1}\hat{\mathbf{a}}\mathbf{C} = \begin{bmatrix} \mathbf{\Lambda}^T & -\mathbf{\Lambda}^T\hat{\mathbf{r}} \\ \mathbf{0} & \mathbf{\Lambda}^T \end{bmatrix} \begin{bmatrix} \hat{\mathbf{a}}_2 & \hat{\mathbf{a}}_1 \\ \mathbf{0} & \hat{\mathbf{a}}_2 \end{bmatrix} \begin{bmatrix} \mathbf{\Lambda} & \hat{\mathbf{r}}\mathbf{\Lambda} \\ \mathbf{0} & \mathbf{\Lambda} \end{bmatrix} = \begin{bmatrix} \mathbf{\Lambda}^T\hat{\mathbf{a}}_2\mathbf{\Lambda} & \mathbf{\Lambda}^T\hat{\mathbf{a}}_2\hat{\mathbf{r}}\mathbf{\Lambda} + \mathbf{\Lambda}^T\hat{\mathbf{a}}_1\mathbf{\Lambda} - \mathbf{\Lambda}^T\hat{\mathbf{r}}\hat{\mathbf{a}}_2\mathbf{\Lambda} \\ \mathbf{0} & \mathbf{\Lambda}^T\hat{\mathbf{a}}_2\mathbf{\Lambda} \end{bmatrix},$$

which, using the properties of 3D skew-symmetric matrices yields

$$\mathbf{C}^{-1}\hat{\mathbf{a}}\mathbf{C} = \begin{bmatrix} \widehat{\mathbf{\Lambda}^T\mathbf{a}_2} & \widehat{\mathbf{\Lambda}^T\mathbf{a}_1} + \mathbf{\Lambda}^T\left(\hat{\mathbf{a}}_2\hat{\mathbf{r}} - \hat{\mathbf{r}}\hat{\mathbf{a}}_2\right)\mathbf{\Lambda} \\ \mathbf{0} & \widehat{\mathbf{\Lambda}^T\mathbf{a}_2} \end{bmatrix} = \begin{bmatrix} \widehat{\mathbf{\Lambda}^T\mathbf{a}_2} & \widehat{\mathbf{\Lambda}^T\mathbf{a}_1} + \widehat{\mathbf{\Lambda}^T(\mathbf{a}_2 \times \mathbf{r})} \\ \mathbf{0} & \widehat{\mathbf{\Lambda}^T\mathbf{a}_2} \end{bmatrix} = \widehat{\mathbf{C}^{-1}\mathbf{a}}, \tag{A.2}$$

because the matrix on the right-hand side of (A.2) has the form of the generalised cross product corresponding to the vector

$$\begin{Bmatrix} \mathbf{\Lambda}^T\mathbf{a}_1 + \mathbf{\Lambda}^T(\mathbf{a_2} \times \mathbf{r}) \\ \mathbf{\Lambda}^T\mathbf{a}_2 \end{Bmatrix} = \begin{bmatrix} \mathbf{\Lambda}^T & -\mathbf{\Lambda}^T\hat{\mathbf{r}} \\ \mathbf{0} & \mathbf{\Lambda}^T \end{bmatrix} \begin{Bmatrix} \mathbf{a}_1 \\ \mathbf{a}_2 \end{Bmatrix}.$$

For any 6D vector $\mathbf{a} = \langle \mathbf{a}_1^T \ \mathbf{a}_2^T \rangle^T$, where $\mathbf{a}_1$, $\mathbf{a}_2$ are 3D vectors, the generalised cross-product $\overset{\triangledown}{\mathbf{a}}$ is defined in (4.4). Evaluating $\mathbf{C}^{-T}\overset{\triangledown}{\mathbf{a}}\mathbf{C}^{-1}$ we have

$$\begin{aligned}\mathbf{C}^{-T}\overset{\triangledown}{\mathbf{a}}\mathbf{C}^{-1} &= \begin{bmatrix}\boldsymbol{\Lambda} & \mathbf{0}\\ \widehat{\mathbf{r}}\boldsymbol{\Lambda} & \boldsymbol{\Lambda}\end{bmatrix}\begin{bmatrix}\mathbf{0} & \widehat{\mathbf{a}}_1\\ \widehat{\mathbf{a}}_1 & \widehat{\mathbf{a}}_2\end{bmatrix}\begin{bmatrix}\boldsymbol{\Lambda}^T & -\boldsymbol{\Lambda}^T\widehat{\mathbf{r}}\\ \mathbf{0} & \boldsymbol{\Lambda}^T\end{bmatrix} = \begin{bmatrix}\mathbf{0} & \boldsymbol{\Lambda}\widehat{\mathbf{a}}_1\boldsymbol{\Lambda}^T\\ \boldsymbol{\Lambda}\widehat{\mathbf{a}}_1\boldsymbol{\Lambda}^T & -\boldsymbol{\Lambda}\widehat{\mathbf{a}}_1\boldsymbol{\Lambda}^T\widehat{\mathbf{r}} + \widehat{\mathbf{r}}\boldsymbol{\Lambda}\widehat{\mathbf{a}}_1\boldsymbol{\Lambda}^T + \boldsymbol{\Lambda}\widehat{\mathbf{a}}_2\boldsymbol{\Lambda}^T\end{bmatrix}\\ &= \begin{bmatrix}\mathbf{0} & \widehat{\boldsymbol{\Lambda}\mathbf{a}_1}\\ \widehat{\boldsymbol{\Lambda}\mathbf{a}_1} & \widehat{\mathbf{r}}\widehat{\boldsymbol{\Lambda}\mathbf{a}_1} - \widehat{\boldsymbol{\Lambda}\mathbf{a}_1}\widehat{\mathbf{r}} + \widehat{\boldsymbol{\Lambda}\mathbf{a}_2}\end{bmatrix} = \begin{bmatrix}\mathbf{0} & \widehat{\boldsymbol{\Lambda}\mathbf{a}_1}\\ \widehat{\boldsymbol{\Lambda}\mathbf{a}_1} & \widehat{\mathbf{r}\times\boldsymbol{\Lambda}\mathbf{a}_1} + \widehat{\boldsymbol{\Lambda}\mathbf{a}_2}\end{bmatrix} = \left(\overset{\triangledown}{\mathbf{C}^{-T}\mathbf{a}}\right). \end{aligned} \tag{A.3}$$

To prove it, we observe that the matrix in (A.3) has the form of a generalised cross-product $\overset{\triangledown}{(\bullet)}$ associated with the vector

$$\begin{Bmatrix}\boldsymbol{\Lambda}\mathbf{a}_1\\ \widehat{\mathbf{r}}\boldsymbol{\Lambda}\mathbf{a}_1 + \boldsymbol{\Lambda}\mathbf{a}_2\end{Bmatrix} = \begin{bmatrix}\boldsymbol{\Lambda} & \mathbf{0}\\ \widehat{\mathbf{r}}\boldsymbol{\Lambda} & \boldsymbol{\Lambda}\end{bmatrix}\begin{Bmatrix}\mathbf{a}_1\\ \mathbf{a}_2\end{Bmatrix} = \mathbf{C}^{-T}\mathbf{a}\,.$$

The inverse of the configuration tensor given in (2.23) can also be written as

$$\mathbf{C}^{-1} = \begin{bmatrix}\mathbf{0} & \mathbf{I}\\ \mathbf{I} & \mathbf{0}\end{bmatrix}\underbrace{\begin{bmatrix}\boldsymbol{\Lambda}^T & \mathbf{0}\\ -\boldsymbol{\Lambda}^T\widehat{\mathbf{r}} & \boldsymbol{\Lambda}^T\end{bmatrix}}_{\mathbf{C}^T}\begin{bmatrix}\mathbf{0} & \mathbf{I}\\ \mathbf{I} & \mathbf{0}\end{bmatrix} = \begin{bmatrix}-\boldsymbol{\Lambda}^T\widehat{\mathbf{r}} & \boldsymbol{\Lambda}^T\\ \boldsymbol{\Lambda}^T & \mathbf{0}\end{bmatrix}\begin{bmatrix}\mathbf{0} & \mathbf{I}\\ \mathbf{I} & \mathbf{0}\end{bmatrix} = \begin{bmatrix}\boldsymbol{\Lambda}^T & -\boldsymbol{\Lambda}^T\widehat{\mathbf{r}}\\ \mathbf{0} & \boldsymbol{\Lambda}^T\end{bmatrix}. \tag{A.4}$$

A.2 Variation of exp

A.2.1 Directional derivative of $\boldsymbol{\Lambda}$

$$\begin{aligned}\left.\frac{\mathrm{d}}{\mathrm{d}\epsilon}\right|_{\epsilon=0}\exp\left(\epsilon\widehat{\delta\boldsymbol{\vartheta}}\right) &= \left.\frac{\mathrm{d}}{\mathrm{d}\epsilon}\right|_{\epsilon=0}\left(\mathbf{I} + \frac{\sin\epsilon\delta\vartheta}{\epsilon\delta\vartheta}\epsilon\widehat{\delta\boldsymbol{\vartheta}} + \frac{1-\cos\epsilon\delta\vartheta}{(\epsilon\delta\vartheta)^2}\epsilon^2\widehat{\delta\boldsymbol{\vartheta}}^2\right)\\ &= \left(\cos(\epsilon\delta\vartheta)\widehat{\delta\boldsymbol{\vartheta}} + \frac{\sin(\epsilon\delta\vartheta)}{\delta\vartheta}\widehat{\delta\boldsymbol{\vartheta}}^2\right)\Bigg|_{\epsilon=0} = \widehat{\delta\boldsymbol{\vartheta}}\,.\end{aligned} \tag{A.5}$$

Variation of trigonometric coefficients

In order to simplify notation, (2.46) and (2.52) were introduced. Their variations are given as

$$\begin{aligned}\delta\alpha_1 = \left.\frac{\mathrm{d}}{\mathrm{d}\epsilon}\right|_{\epsilon=0}\alpha_1(\boldsymbol{\psi}+\epsilon\delta\boldsymbol{\psi}) &= \frac{\cos\psi-\alpha_1}{\psi^2}\left(\boldsymbol{\psi}^T\delta\boldsymbol{\psi}\right) = (\beta_2-\alpha_2)\left(\boldsymbol{\psi}^T\delta\boldsymbol{\psi}\right),\\ \delta\alpha_2 = \delta\beta_1 = \left.\frac{\mathrm{d}}{\mathrm{d}\epsilon}\right|_{\epsilon=0}\alpha_2(\boldsymbol{\psi}+\epsilon\delta\boldsymbol{\psi}) &= \frac{\alpha_1-2\alpha_2}{\psi^2}\left(\boldsymbol{\psi}^T\delta\boldsymbol{\psi}\right),\\ \delta\beta_2 = \left.\frac{\mathrm{d}}{\mathrm{d}\epsilon}\right|_{\epsilon=0}\beta_2(\boldsymbol{\psi}+\epsilon\delta\boldsymbol{\psi}) &= \frac{\alpha_2-3\beta_2}{\psi^2}\left(\boldsymbol{\psi}^T\delta\boldsymbol{\psi}\right).\end{aligned} \tag{A.6}$$

noting that $\delta\psi$ may be written as $\frac{\boldsymbol{\psi}^T\delta\boldsymbol{\psi}}{\psi}$.

A.2.2 Function $\mathbf{H}(\boldsymbol{\psi})$ and its properties

By equating (2.47) and (2.48) we have

$$\widehat{\delta\boldsymbol{\vartheta}}\boldsymbol{\Lambda} = \delta\left(\exp\widehat{\boldsymbol{\psi}}\right)\boldsymbol{\Lambda}_0\,,$$

which, using relationship (2.39) may be expressed as

$$\widehat{\delta\boldsymbol{\vartheta}} = \delta\left(\exp\widehat{\boldsymbol{\psi}}\right)\boldsymbol{\Lambda}_0\boldsymbol{\Lambda}^T = \delta\left(\exp\widehat{\boldsymbol{\psi}}\right)\underbrace{\boldsymbol{\Lambda}_0\boldsymbol{\Lambda}_0^T}_{\mathbf{I}}\left(\exp\widehat{\boldsymbol{\psi}}\right)^T . \tag{A.7}$$

The variation $\delta\left(\exp\widehat{\boldsymbol{\psi}}\right)$ is the directional derivative of $\exp\widehat{\boldsymbol{\psi}}$ in the direction of an infinitesimal superimposed perturbation $\delta\widehat{\boldsymbol{\psi}}$. Using (A.6) it is evaluated as

$$\begin{aligned}\delta\left(\exp\widehat{\boldsymbol{\psi}}\right) &= \left.\frac{\mathrm{d}}{\mathrm{d}\epsilon}\right|_{\epsilon=0}\exp(\widehat{\boldsymbol{\psi}}+\epsilon\delta\widehat{\boldsymbol{\psi}})\\ &= (\beta_2-\alpha_2)\left(\boldsymbol{\psi}^T\delta\boldsymbol{\psi}\right)\widehat{\boldsymbol{\psi}} + \alpha_1\delta\widehat{\boldsymbol{\psi}} + \frac{\alpha_1-2\alpha_2}{\psi^2}\left(\boldsymbol{\psi}^T\delta\boldsymbol{\psi}\right)\widehat{\boldsymbol{\psi}}^2 + \alpha_2\left(\delta\widehat{\boldsymbol{\psi}}\widehat{\boldsymbol{\psi}} + \widehat{\boldsymbol{\psi}}\delta\widehat{\boldsymbol{\psi}}\right)\end{aligned}$$

Noting that $\widehat{\boldsymbol{\psi}}^T = -\widehat{\boldsymbol{\psi}}$ yields $\left(\exp\widehat{\boldsymbol{\psi}}\right)^T = \exp(-\widehat{\boldsymbol{\psi}})$, the right-hand side of (A.7) can be written as

$$\begin{aligned}\delta\left(\exp\widehat{\boldsymbol{\psi}}\right)\left(\exp\widehat{\boldsymbol{\psi}}\right)^T &= (\beta_2-\alpha_2)\left(\boldsymbol{\psi}^T\delta\boldsymbol{\psi}\right)\widehat{\boldsymbol{\psi}} + \alpha_1\delta\widehat{\boldsymbol{\psi}} + \frac{\alpha_1-2\alpha_2}{\psi^2}\left(\boldsymbol{\psi}^T\delta\boldsymbol{\psi}\right)\widehat{\boldsymbol{\psi}}^2 + \alpha_2\left(\delta\widehat{\boldsymbol{\psi}}\widehat{\boldsymbol{\psi}} + \widehat{\boldsymbol{\psi}}\delta\widehat{\boldsymbol{\psi}}\right)\\ &\quad - \alpha_1(\beta_2-\alpha_2)\left(\boldsymbol{\psi}^T\delta\boldsymbol{\psi}\right)\widehat{\boldsymbol{\psi}}^2 - \alpha_1^2\delta\widehat{\boldsymbol{\psi}}\widehat{\boldsymbol{\psi}} - \alpha_1\frac{\alpha_1-2\alpha_2}{\psi^2}\left(\boldsymbol{\psi}^T\delta\boldsymbol{\psi}\right)\widehat{\boldsymbol{\psi}}^3\\ &\quad - \alpha_1\alpha_2\left(\widehat{\boldsymbol{\psi}}\delta\widehat{\boldsymbol{\psi}}\widehat{\boldsymbol{\psi}} + \delta\widehat{\boldsymbol{\psi}}\widehat{\boldsymbol{\psi}}^2\right) + \alpha_2(\beta_2-\alpha_2)\left(\boldsymbol{\psi}^T\delta\boldsymbol{\psi}\right)\widehat{\boldsymbol{\psi}}^3 + \alpha_1\alpha_2\delta\widehat{\boldsymbol{\psi}}\widehat{\boldsymbol{\psi}}^2\\ &\quad + \alpha_2\frac{\alpha_1-2\alpha_2}{\psi^2}\left(\boldsymbol{\psi}^T\delta\boldsymbol{\psi}\right)\widehat{\boldsymbol{\psi}}^4 + \alpha_2^2\left(\widehat{\boldsymbol{\psi}}\delta\widehat{\boldsymbol{\psi}}\widehat{\boldsymbol{\psi}}^2 + \delta\widehat{\boldsymbol{\psi}}\widehat{\boldsymbol{\psi}}^3\right)\end{aligned} \tag{A.8}$$

Since the left-hand side of (A.7) is skew-symmetric, (A.8) must also be skew-symmetric. To show it, we group the skew-symmetric members of (A.8) together

$$\begin{aligned}\left[\delta\left(\exp\widehat{\boldsymbol{\psi}}\right)\left(\exp\widehat{\boldsymbol{\psi}}\right)^T\right]_{\text{skew}} &= (\beta_2-\alpha_2)\left(\boldsymbol{\psi}^T\delta\boldsymbol{\psi}\right)\widehat{\boldsymbol{\psi}} + \alpha_1\delta\widehat{\boldsymbol{\psi}} - \alpha_1\frac{\alpha_1-2\alpha_2}{\psi^2}\left(\boldsymbol{\psi}^T\delta\boldsymbol{\psi}\right)\widehat{\boldsymbol{\psi}}^3\\ &\quad - \alpha_1\alpha_2\widehat{\boldsymbol{\psi}}\delta\widehat{\boldsymbol{\psi}}\widehat{\boldsymbol{\psi}} + \alpha_2(\beta_2-\alpha_2)\left(\boldsymbol{\psi}^T\delta\boldsymbol{\psi}\right)\widehat{\boldsymbol{\psi}}^3\\ &= \alpha_1\delta\widehat{\boldsymbol{\psi}} + \beta_2\left(\boldsymbol{\psi}^T\delta\boldsymbol{\psi}\right)\widehat{\boldsymbol{\psi}} .\end{aligned} \tag{A.9}$$

Then, we group together the symmetric members

$$\begin{aligned}\left[\delta\left(\exp\widehat{\boldsymbol{\psi}}\right)\left(\exp\widehat{\boldsymbol{\psi}}\right)^T\right]_{\text{sym}} &= \frac{\alpha_1-2\alpha_2}{\psi^2}\left(\boldsymbol{\psi}^T\delta\boldsymbol{\psi}\right)\widehat{\boldsymbol{\psi}}^2 + \alpha_2\left(\delta\widehat{\boldsymbol{\psi}}\widehat{\boldsymbol{\psi}} + \widehat{\boldsymbol{\psi}}\delta\widehat{\boldsymbol{\psi}}\right)\\ &\quad - \alpha_1(\beta_2-\alpha_2)\left(\boldsymbol{\psi}^T\delta\boldsymbol{\psi}\right)\widehat{\boldsymbol{\psi}}^2 + \alpha_2\frac{\alpha_1-2\alpha_2}{\psi^2}\left(\boldsymbol{\psi}^T\delta\boldsymbol{\psi}\right)\widehat{\boldsymbol{\psi}}^4 + \alpha_2^2\widehat{\boldsymbol{\psi}}\delta\widehat{\boldsymbol{\psi}}\widehat{\boldsymbol{\psi}}^2\\ &= \alpha_2\left(\delta\widehat{\boldsymbol{\psi}}\widehat{\boldsymbol{\psi}} + \widehat{\boldsymbol{\psi}}\delta\widehat{\boldsymbol{\psi}}\right) ,\end{aligned} \tag{A.10}$$

Finally we group the remaining members

$$\begin{aligned}\left[\delta\left(\exp\widehat{\boldsymbol{\psi}}\right)\left(\exp\widehat{\boldsymbol{\psi}}\right)^T\right]_{\text{non}} &= -\alpha_1^2\delta\widehat{\boldsymbol{\psi}}\widehat{\boldsymbol{\psi}} - \alpha_1\alpha_2\delta\widehat{\boldsymbol{\psi}}\widehat{\boldsymbol{\psi}}^2 + \alpha_1\alpha_2\delta\widehat{\boldsymbol{\psi}}\widehat{\boldsymbol{\psi}}^2 + \alpha_2^2\delta\widehat{\boldsymbol{\psi}}\widehat{\boldsymbol{\psi}}^3\\ &= (-\alpha_1^2-\psi^2\alpha_2^2)\delta\widehat{\boldsymbol{\psi}}\widehat{\boldsymbol{\psi}} .\end{aligned} \tag{A.11}$$

Adding (A.10) to (A.11) yields

$$\left[\delta\left(\exp\widehat{\boldsymbol{\psi}}\right)\left(\exp\widehat{\boldsymbol{\psi}}\right)^T\right]_{\text{sym+non}} = \alpha_2\left(\widehat{\boldsymbol{\psi}}\delta\widehat{\boldsymbol{\psi}} - \delta\widehat{\boldsymbol{\psi}}\widehat{\boldsymbol{\psi}}\right) = \alpha_2\widehat{\boldsymbol{\psi}\times\delta\boldsymbol{\psi}} , \tag{A.12}$$

which is a skew-symmetric matrix. Adding (A.9) and (A.12) gives

$$\widehat{\delta\boldsymbol{\vartheta}} = \delta\left(\exp\widehat{\boldsymbol{\psi}}\right)\left(\exp\widehat{\boldsymbol{\psi}}\right)^T = \alpha_1\delta\widehat{\boldsymbol{\psi}} + \beta_2\left(\boldsymbol{\psi}^T\delta\boldsymbol{\psi}\right)\widehat{\boldsymbol{\psi}} + \alpha_2\widehat{\boldsymbol{\psi}\times\delta\boldsymbol{\psi}}$$

which can now be written without superimposed hats because both sides are skew-symmetric as

$$\delta\boldsymbol{\vartheta} = \alpha_1\delta\boldsymbol{\psi} + \alpha_2\widehat{\boldsymbol{\psi}}\delta\boldsymbol{\psi} + \beta_2\boldsymbol{\psi}\boldsymbol{\psi}^T\delta\boldsymbol{\psi}\,,$$

and finally, noting that $\mathbf{a}\mathbf{a}^T = a^2\mathbf{I} + \widehat{\mathbf{a}}^2$ for any 3D vector $\mathbf{a}$, we obtain relationship (2.49), i.e.

$$\delta\boldsymbol{\vartheta} = \mathbf{H}(\boldsymbol{\psi})\delta\boldsymbol{\psi}\,.$$

Using the Sherman-Morrison formula [5], the inverse of (2.49) follows as (2.51), i.e.

$$\mathbf{H}^{-1}(\boldsymbol{\psi}) = \mathbf{I} + \gamma_1\widehat{\boldsymbol{\psi}} + \gamma_2\widehat{\boldsymbol{\psi}}^2\,,$$

with γ_1 and γ_2 given in (2.52). Evaluating $\mathbf{H}(\boldsymbol{\psi})\mathbf{H}^{-T}(\boldsymbol{\psi})$ gives

$$\begin{aligned}\mathbf{H}(\boldsymbol{\psi})\mathbf{H}^{-T}(\boldsymbol{\psi}) =& \left(\mathbf{I} + \beta_1\widehat{\boldsymbol{\psi}} + \beta_2\widehat{\boldsymbol{\psi}}^2\right)\left(\mathbf{I} + \frac{1}{2}\widehat{\boldsymbol{\psi}} + \gamma_2\widehat{\boldsymbol{\psi}}^2\right)\\ =&\mathbf{I} + \beta_1\widehat{\boldsymbol{\psi}} + \beta_2\widehat{\boldsymbol{\psi}}^2 + \frac{1}{2}\widehat{\boldsymbol{\psi}} + \frac{1}{2}\beta_1\widehat{\boldsymbol{\psi}}^2 + \frac{1}{2}\beta_2\widehat{\boldsymbol{\psi}}^3 + \gamma_2\widehat{\boldsymbol{\psi}}^2 + \beta_1\gamma_2\widehat{\boldsymbol{\psi}}^3 + \beta_2\gamma_2\widehat{\boldsymbol{\psi}}^4\,.\end{aligned}$$

Using (2.46) and (2.52) as well as the recursive properties of matrices in so(3) we get

$$\mathbf{H}(\boldsymbol{\psi})\mathbf{H}^{-T}(\boldsymbol{\psi}) = \mathbf{I} + \underbrace{\left(\beta_1 + \frac{1}{2} - \frac{1}{2}\psi^2\beta_2 - \psi^2\beta_1\gamma_2\right)}_{\alpha_1}\widehat{\boldsymbol{\psi}} + \underbrace{\left(\beta_2 + \frac{1}{2}\beta_1 + \gamma_2 - \psi^2\beta_2\gamma_2\right)}_{\alpha_2}\widehat{\boldsymbol{\psi}}^2 = \exp\widehat{\boldsymbol{\psi}}\,. \tag{A.13}$$

A.2.3 Relationship between $\mathbf{Q}(\boldsymbol{\nu})$, $\mathbf{H}(\boldsymbol{\psi})$ and $\boldsymbol{\rho}$

The first factor in (2.61) is

$$\widehat{\mathbf{H}(\boldsymbol{\psi})\boldsymbol{\rho}} = \widehat{\boldsymbol{\rho}} + \beta_1\widehat{\boldsymbol{\psi}\times\boldsymbol{\rho}} + \beta_2\widehat{\boldsymbol{\psi}\times(\boldsymbol{\psi}\times\boldsymbol{\rho})}\,,$$

which, using the fact that for any three 3D vectors $\mathbf{a}$, $\mathbf{b}$, $\mathbf{c}$, we have $\mathbf{a}\times(\mathbf{b}\times\mathbf{c}) = \mathbf{b}(\mathbf{a}\cdot\mathbf{c}) - \mathbf{c}(\mathbf{a}\cdot\mathbf{b})$ as well as $\widehat{\mathbf{a}\times\mathbf{b}} = \widehat{\mathbf{a}}\widehat{\mathbf{b}} - \widehat{\mathbf{b}}\widehat{\mathbf{a}}$, turns into

$$\begin{aligned}\widehat{\mathbf{H}(\boldsymbol{\psi})\boldsymbol{\rho}} &= \widehat{\boldsymbol{\rho}} + \beta_1\widehat{\boldsymbol{\psi}\times\boldsymbol{\rho}} + \beta_2\left[(\boldsymbol{\rho}\cdot\boldsymbol{\psi})\,\widehat{\boldsymbol{\psi}} - (\boldsymbol{\psi}\cdot\boldsymbol{\psi})\,\widehat{\boldsymbol{\rho}}\right]\\ &= \left(1 - \psi^2\beta_2\right)\widehat{\boldsymbol{\rho}} + \beta_2\,(\boldsymbol{\rho}\cdot\boldsymbol{\psi})\,\widehat{\boldsymbol{\psi}} + \beta_1\widehat{\boldsymbol{\psi}\times\boldsymbol{\rho}}\\ &= \alpha_1\widehat{\boldsymbol{\rho}} + \beta_2\,(\boldsymbol{\rho}\cdot\boldsymbol{\psi})\,\widehat{\boldsymbol{\psi}} + \beta_1\left(\widehat{\boldsymbol{\psi}}\widehat{\boldsymbol{\rho}} - \widehat{\boldsymbol{\rho}}\widehat{\boldsymbol{\psi}}\right)\,.\end{aligned} \tag{A.14}$$

Then, postmultiplying (A.14) by (2.45) yields

$$\begin{aligned}\widehat{\mathbf{H}(\boldsymbol{\psi})\boldsymbol{\rho}}\exp\widehat{\boldsymbol{\psi}} =&\alpha_1\widehat{\boldsymbol{\rho}} + \beta_2\,(\boldsymbol{\rho}\cdot\boldsymbol{\psi})\,\widehat{\boldsymbol{\psi}} + \beta_1\left(\widehat{\boldsymbol{\psi}}\widehat{\boldsymbol{\rho}} - \widehat{\boldsymbol{\rho}}\widehat{\boldsymbol{\psi}}\right)\\ &+ \alpha_1^2\widehat{\boldsymbol{\rho}}\widehat{\boldsymbol{\psi}} + \alpha_1\beta_2\,(\boldsymbol{\rho}\cdot\boldsymbol{\psi})\,\widehat{\boldsymbol{\psi}}^2 + \alpha_1\beta_1\left(\widehat{\boldsymbol{\psi}}\widehat{\boldsymbol{\rho}}\widehat{\boldsymbol{\psi}} - \widehat{\boldsymbol{\rho}}\widehat{\boldsymbol{\psi}}^2\right)\\ &+ \alpha_1\alpha_2\widehat{\boldsymbol{\rho}}\widehat{\boldsymbol{\psi}}^2 + \alpha_2\beta_2\,(\boldsymbol{\rho}\cdot\boldsymbol{\psi})\,\widehat{\boldsymbol{\psi}}^3 + \alpha_2\beta_1\left(\widehat{\boldsymbol{\psi}}\widehat{\boldsymbol{\rho}}\widehat{\boldsymbol{\psi}}^2 - \widehat{\boldsymbol{\rho}}\widehat{\boldsymbol{\psi}}^3\right)\,.\end{aligned}$$

Noting the recursive properties (2.41) of matrices in so(3) as well as $\widehat{\boldsymbol{\psi}}\widehat{\boldsymbol{\rho}}\widehat{\boldsymbol{\psi}} = -(\boldsymbol{\rho}\cdot\boldsymbol{\psi})\,\widehat{\boldsymbol{\psi}}$, the above equation turns into

$$\begin{aligned}\widehat{\mathbf{H}(\boldsymbol{\psi})\boldsymbol{\rho}}\exp\widehat{\boldsymbol{\psi}} =&\alpha_1\widehat{\boldsymbol{\rho}} + \alpha_2\widehat{\boldsymbol{\psi}}\widehat{\boldsymbol{\rho}} + \left(-\alpha_2+\alpha_1^2+\psi^2\alpha_2^2\right)\widehat{\boldsymbol{\rho}}\widehat{\boldsymbol{\psi}} + \left(\beta_2-\alpha_1\beta_1-\psi^2\alpha_2\beta_2\right)(\boldsymbol{\rho}\cdot\boldsymbol{\psi})\,\widehat{\boldsymbol{\psi}}\\ &+\left(\alpha_1\beta_2-\alpha_2^2\right)(\boldsymbol{\rho}\cdot\boldsymbol{\psi})\,\widehat{\boldsymbol{\psi}}^2\\ =&\alpha_1\widehat{\boldsymbol{\rho}} + \alpha_2(\widehat{\boldsymbol{\rho}}\widehat{\boldsymbol{\psi}}+\widehat{\boldsymbol{\psi}}\widehat{\boldsymbol{\rho}}) - (\alpha_2-\beta_2)(\boldsymbol{\rho}\cdot\boldsymbol{\psi})\,\widehat{\boldsymbol{\psi}} + \frac{\alpha_1-2\alpha_2}{\psi^2}(\boldsymbol{\rho}\cdot\boldsymbol{\psi})\,\widehat{\boldsymbol{\psi}}^2,\end{aligned}$$

which is equal to (2.60), which means that (2.61) holds.

A.2.4 Directional derivative of C

We first evaluate the variation of (2.61) as

$$\begin{aligned}\delta\mathbf{Q} =&\frac{\mathrm{d}}{\mathrm{d}\epsilon}\Big|_{\epsilon=0}\mathbf{Q}(\epsilon\delta\boldsymbol{\varsigma}) = \frac{\mathrm{d}}{\mathrm{d}\epsilon}\Big|_{\epsilon=0}\left[\frac{\sin\epsilon\delta\vartheta}{\epsilon\delta\vartheta}\epsilon\widehat{\delta\boldsymbol{\xi}} + \frac{1-\cos(\epsilon\delta\vartheta)}{(\epsilon\delta\vartheta)^2}\epsilon^2(\widehat{\delta\boldsymbol{\xi}}\widehat{\delta\boldsymbol{\vartheta}}+\widehat{\delta\boldsymbol{\vartheta}}\widehat{\delta\boldsymbol{\xi}})\right.\\ &-\left(\frac{1-\cos(\epsilon\delta\vartheta)}{(\epsilon\delta\vartheta)^2}-\frac{(\epsilon\delta\vartheta)-\sin(\epsilon\delta\vartheta)}{(\epsilon\delta\vartheta)^3}\right)\epsilon^3(\delta\boldsymbol{\xi}\cdot\delta\boldsymbol{\vartheta})\widehat{\delta\boldsymbol{\vartheta}}\\ &\left.-2\frac{1-\cos(\epsilon\delta\vartheta)}{(\epsilon\delta\vartheta)^2}\frac{1}{(\epsilon\delta\vartheta)^2}\left(1-\frac{1}{2}\frac{(\epsilon\delta\vartheta)\sin(\epsilon\delta\vartheta)}{1-\cos(\epsilon\delta\vartheta)}\right)\epsilon^4(\delta\boldsymbol{\xi}\cdot\delta\boldsymbol{\vartheta})\widehat{\delta\boldsymbol{\vartheta}}^2\right]\\ =&\cos(\epsilon\delta\vartheta)\Big|_{\epsilon=0}\widehat{\delta\boldsymbol{\xi}} + \frac{\sin\epsilon\delta\vartheta}{\delta\vartheta}\Big|_{\epsilon=0}(\widehat{\delta\boldsymbol{\xi}}\widehat{\delta\boldsymbol{\vartheta}}+\widehat{\delta\boldsymbol{\vartheta}}\widehat{\delta\boldsymbol{\xi}})\\ &-\frac{\epsilon\sin\epsilon\delta\vartheta}{\delta\vartheta}\Big|_{\epsilon=0}(\delta\boldsymbol{\xi}\cdot\delta\boldsymbol{\vartheta})\widehat{\delta\boldsymbol{\vartheta}} - \frac{1}{\delta\vartheta^3}\left(\sin\epsilon\delta\vartheta+\epsilon\delta\vartheta\cos\epsilon\delta\vartheta\right)\Big|_{\epsilon=0}(\delta\boldsymbol{\xi}\cdot\delta\boldsymbol{\vartheta})\widehat{\delta\boldsymbol{\vartheta}}^2\\ =&\widehat{\delta\boldsymbol{\xi}}\,.\end{aligned} \tag{A.15}$$

The variation of $\mathbf{C}$ then follows as

$$\delta\mathbf{C} = \begin{bmatrix}\widehat{\delta\boldsymbol{\vartheta}} & \widehat{\delta\boldsymbol{\xi}}\\ \mathbf{0} & \widehat{\delta\boldsymbol{\vartheta}}\end{bmatrix}\mathbf{C}\,, \tag{A.16}$$

where we recognise the generalised cross product

$$\widehat{\delta\boldsymbol{\varsigma}} = \begin{bmatrix}\widehat{\delta\boldsymbol{\vartheta}} & \widehat{\delta\boldsymbol{\xi}}\\ \mathbf{0} & \widehat{\delta\boldsymbol{\vartheta}}\end{bmatrix}.$$

The inverse of (2.59) is

$$(\exp\widehat{\boldsymbol{\nu}})^{-1} = \begin{bmatrix}\left(\exp\widehat{\boldsymbol{\psi}}\right)^T & -\left(\exp\widehat{\boldsymbol{\psi}}\right)^T\mathbf{Q}(\boldsymbol{\nu})\left(\exp\widehat{\boldsymbol{\psi}}\right)^T\\ \mathbf{0} & \left(\exp\widehat{\boldsymbol{\psi}}\right)^T\end{bmatrix} = \begin{bmatrix}\left(\exp\widehat{\boldsymbol{\psi}}\right)^T & [\mathbf{Q}(\boldsymbol{\nu})]^T\\ \mathbf{0} & \left(\exp\widehat{\boldsymbol{\psi}}\right)^T\end{bmatrix}, \tag{A.17}$$

because, using (2.61) it can be shown that

$$\begin{aligned}-\left(\exp\widehat{\boldsymbol{\psi}}\right)^T\mathbf{Q}(\boldsymbol{\nu})\left(\exp\widehat{\boldsymbol{\psi}}\right)^T =& -\left(\exp\widehat{\boldsymbol{\psi}}\right)^T\widehat{\mathbf{H}(\boldsymbol{\psi})\boldsymbol{\rho}}\exp\widehat{\boldsymbol{\psi}}\left(\exp\widehat{\boldsymbol{\psi}}\right)^T\\ =& -\left(\exp\widehat{\boldsymbol{\psi}}\right)^T\widehat{\mathbf{H}(\boldsymbol{\psi})\boldsymbol{\rho}} = \left[\widehat{\mathbf{H}(\boldsymbol{\psi})\boldsymbol{\rho}}\exp\widehat{\boldsymbol{\psi}}\right]^T = [\mathbf{Q}(\boldsymbol{\nu})]^T\,.\end{aligned}$$

We also note here that $\left(\exp\widehat{\boldsymbol{\psi}}\right)^T = \exp(-\widehat{\boldsymbol{\psi}})$ as well as $\mathbf{Q}(\boldsymbol{\nu})^T = \mathbf{Q}(-\boldsymbol{\nu})$. This means that

$$(\exp\widehat{\boldsymbol{\nu}})^{-1} = \exp(-\widehat{\boldsymbol{\nu}}). \tag{A.18}$$

Using (A.17) the variation of $\mathbf{C}^{-1}$ follows as

$$\delta\mathbf{C}^{-1} = \Big[\frac{\mathrm{d}}{\mathrm{d}\epsilon}\Big|_{\epsilon=0} \exp(\epsilon\delta\boldsymbol{\varsigma})\mathbf{C}\Big]^{-1} = \mathbf{C}^{-1}\frac{\mathrm{d}}{\mathrm{d}\epsilon}\Big|_{\epsilon=0}\begin{bmatrix}\left(\exp\epsilon\delta\widehat{\boldsymbol{\vartheta}}\right)^T & \mathbf{Q}(\epsilon\delta\boldsymbol{\varsigma})^T\\ \mathbf{0} & \left(\exp\epsilon\delta\widehat{\boldsymbol{\vartheta}}\right)^T\end{bmatrix} = -\mathbf{C}^{-1}\widehat{\delta\boldsymbol{\varsigma}}\,. \quad \text{(A.19)}$$

A.2.5 Function $\mathbf{H}_6(\boldsymbol{\nu})$ and its properties

By equating (2.66) and (2.67) we have

$$\widehat{\delta\boldsymbol{\varsigma}}\mathbf{C} = \delta\left(\exp\widehat{\boldsymbol{\nu}}\right)\mathbf{C}_0\,,$$

which, using relationship $\mathbf{C} = \exp\widehat{\boldsymbol{\nu}}\mathbf{C}_0$ may be expressed as

$$\widehat{\delta\boldsymbol{\varsigma}} = \delta\left(\exp\widehat{\boldsymbol{\nu}}\right)\underbrace{\mathbf{C}_0\mathbf{C}_0^{-1}}_{\mathbf{I}}\left(\exp\widehat{\boldsymbol{\nu}}\right)^{-1}\,. \quad \text{(A.20)}$$

The variation $\delta\left(\exp\widehat{\boldsymbol{\nu}}\right)$ is the directional derivative in the direction of an infinitesimal superimposed perturbation $\delta\widehat{\boldsymbol{\nu}}$ evaluated as

$$\delta\left(\exp\widehat{\boldsymbol{\nu}}\right) = \frac{\mathrm{d}}{\mathrm{d}\epsilon}\Big|_{\epsilon=0}\exp(\widehat{\boldsymbol{\nu}} + \epsilon\delta\widehat{\boldsymbol{\nu}}) = \begin{bmatrix}\delta\left(\exp\widehat{\boldsymbol{\psi}}\right) & \delta\mathbf{Q}(\boldsymbol{\nu})\\ \mathbf{0} & \delta\left(\exp\widehat{\boldsymbol{\psi}}\right)\end{bmatrix}. \quad \text{(A.21)}$$

Substituting (A.21) and (A.17) into (A.20) we obtain

$$\begin{aligned}\widehat{\delta\boldsymbol{\varsigma}} &= \begin{bmatrix}\widehat{\delta\boldsymbol{\vartheta}} & \widehat{\delta\boldsymbol{\xi}}\\ \mathbf{0} & \widehat{\delta\boldsymbol{\vartheta}}\end{bmatrix} = \begin{bmatrix}\delta\left(\exp\widehat{\boldsymbol{\psi}}\right) & \delta\mathbf{Q}(\boldsymbol{\nu})\\ \mathbf{0} & \delta\left(\exp\widehat{\boldsymbol{\psi}}\right)\end{bmatrix}\begin{bmatrix}\left(\exp\widehat{\boldsymbol{\psi}}\right)^T & [\mathbf{Q}(\boldsymbol{\nu})]^T\\ \mathbf{0} & \left(\exp\widehat{\boldsymbol{\psi}}\right)^T\end{bmatrix}\\ &= \begin{bmatrix}\delta\left(\exp\widehat{\boldsymbol{\psi}}\right)\left(\exp\widehat{\boldsymbol{\psi}}\right)^T & \delta\left(\exp\widehat{\boldsymbol{\psi}}\right)[\mathbf{Q}(\boldsymbol{\nu})]^T + \delta\mathbf{Q}(\boldsymbol{\nu})\left(\exp\widehat{\boldsymbol{\psi}}\right)^T\\ \mathbf{0} & \delta\left(\exp\widehat{\boldsymbol{\psi}}\right)\left(\exp\widehat{\boldsymbol{\psi}}\right)^T\end{bmatrix},\end{aligned}$$

where we recall relationships (2.49) and (2.61) to simplify the above result as

$$\begin{bmatrix}\widehat{\delta\boldsymbol{\vartheta}} & \widehat{\delta\boldsymbol{\xi}}\\ \mathbf{0} & \widehat{\delta\boldsymbol{\vartheta}}\end{bmatrix} = \begin{bmatrix}\widehat{\mathbf{H}(\boldsymbol{\psi})\delta\boldsymbol{\psi}} & -\widehat{\mathbf{H}(\boldsymbol{\psi})\delta\boldsymbol{\psi}}\widehat{\mathbf{H}(\boldsymbol{\psi})\boldsymbol{\rho}} + \delta\mathbf{Q}(\boldsymbol{\nu})\left(\exp\widehat{\boldsymbol{\psi}}\right)^T\\ \mathbf{0} & \widehat{\mathbf{H}(\boldsymbol{\psi})\delta\boldsymbol{\psi}}\end{bmatrix}. \quad \text{(A.22)}$$

At this point, let us assume that the relationship

$$\begin{Bmatrix}\delta\boldsymbol{\xi}\\ \delta\boldsymbol{\vartheta}\end{Bmatrix} = \begin{bmatrix}\mathbf{H}(\boldsymbol{\psi}) & \mathbf{B}(\boldsymbol{\nu})\\ \mathbf{0} & \mathbf{H}(\boldsymbol{\psi})\end{bmatrix}\begin{Bmatrix}\delta\boldsymbol{\rho}\\ \delta\boldsymbol{\psi}\end{Bmatrix}, \quad \text{(A.23)}$$

holds for some unknown $\mathbf{B}(\boldsymbol{\nu})$. Comparing (A.22) and (A.23) we see that this relationship is valid for the diagonal blocks. We now consider the remaining block which obviously, also must be skew-symmetric. From (A.23) we have

$$\delta\boldsymbol{\xi} = \mathbf{H}(\boldsymbol{\psi})\delta\boldsymbol{\rho} + \mathbf{B}(\boldsymbol{\nu})\delta\boldsymbol{\psi} \quad \Leftrightarrow \quad \widehat{\delta\boldsymbol{\xi}} = \widehat{\mathbf{H}(\boldsymbol{\psi})\delta\boldsymbol{\rho}} + \widehat{\mathbf{B}(\boldsymbol{\nu})\delta\boldsymbol{\psi}}\,, \quad \text{(A.24)}$$

while from (A.22) we have

$$\widehat{\delta\boldsymbol{\xi}} = -\widehat{\mathbf{H}(\boldsymbol{\psi})\delta\boldsymbol{\psi}}\widehat{\mathbf{H}(\boldsymbol{\psi})\boldsymbol{\rho}} + \delta\mathbf{Q}(\boldsymbol{\nu})\left(\exp\widehat{\boldsymbol{\psi}}\right)^T. \quad \text{(A.25)}$$

Varying both sides of $\mathbf{Q}(\boldsymbol{\nu})\left(\exp\widehat{\boldsymbol{\psi}}\right)^T = \widehat{\mathbf{H}(\boldsymbol{\psi})\boldsymbol{\rho}}$ gives

$$\delta\left[\mathbf{Q}(\boldsymbol{\nu})\left(\exp\widehat{\boldsymbol{\psi}}\right)^T\right] = \delta\left[\mathbf{Q}(\boldsymbol{\nu})\right]\left(\exp\widehat{\boldsymbol{\psi}}\right)^T + \mathbf{Q}(\boldsymbol{\nu})\delta\left(\exp\widehat{\boldsymbol{\psi}}\right)^T$$
$$\delta\left[\widehat{\mathbf{H}(\boldsymbol{\psi})\boldsymbol{\rho}}\right] = \widehat{\delta\mathbf{H}(\boldsymbol{\psi})\boldsymbol{\rho}} + \widehat{\mathbf{H}(\boldsymbol{\psi})\delta\boldsymbol{\rho}},$$

from where, noting that $\mathbf{Q}(\boldsymbol{\nu}) = \widehat{\mathbf{H}(\boldsymbol{\psi})\boldsymbol{\rho}}\exp\widehat{\boldsymbol{\psi}}$, there follows

$$\delta\mathbf{Q}(\boldsymbol{\nu})\left(\exp\widehat{\boldsymbol{\psi}}\right)^T = \widehat{\delta\mathbf{H}(\boldsymbol{\psi})\boldsymbol{\rho}} + \widehat{\mathbf{H}(\boldsymbol{\psi})\delta\boldsymbol{\rho}} - \widehat{\mathbf{H}(\boldsymbol{\psi})\boldsymbol{\rho}}\underbrace{\exp\widehat{\boldsymbol{\psi}}\,\delta\left(\exp\widehat{\boldsymbol{\psi}}\right)^T}_{\widehat{\mathbf{H}(\boldsymbol{\psi})\delta\boldsymbol{\psi}}^T = -\widehat{\mathbf{H}(\boldsymbol{\psi})\delta\boldsymbol{\psi}}}.$$

Equating (A.25) to (A.24) while substituting the above result we obtain

$$\begin{aligned}
\widehat{\mathbf{H}(\boldsymbol{\psi})\delta\boldsymbol{\rho}} + \widehat{\mathbf{B}(\boldsymbol{\nu})\delta\boldsymbol{\psi}} &= -\widehat{\mathbf{H}(\boldsymbol{\psi})\delta\boldsymbol{\psi}}\widehat{\mathbf{H}(\boldsymbol{\psi})\boldsymbol{\rho}} + \widehat{\delta\mathbf{H}(\boldsymbol{\psi})\boldsymbol{\rho}} + \widehat{\mathbf{H}(\boldsymbol{\psi})\delta\boldsymbol{\rho}} + \widehat{\mathbf{H}(\boldsymbol{\psi})\boldsymbol{\rho}}\widehat{\mathbf{H}(\boldsymbol{\psi})\delta\boldsymbol{\psi}} \\
\widehat{\mathbf{B}(\boldsymbol{\nu})\delta\boldsymbol{\psi}} &= \widehat{\delta\mathbf{H}(\boldsymbol{\psi})\boldsymbol{\rho}} + \widehat{\mathbf{H}(\boldsymbol{\psi})\boldsymbol{\rho}}\widehat{\mathbf{H}(\boldsymbol{\psi})\delta\boldsymbol{\psi}} - \widehat{\mathbf{H}(\boldsymbol{\psi})\delta\boldsymbol{\psi}}\widehat{\mathbf{H}(\boldsymbol{\psi})\boldsymbol{\rho}} \\
&= \widehat{\delta\mathbf{H}(\boldsymbol{\psi})\boldsymbol{\rho}} + \widehat{(\mathbf{H}(\boldsymbol{\psi})\boldsymbol{\rho})\times(\mathbf{H}(\boldsymbol{\psi})\delta\boldsymbol{\psi})} \\
\Rightarrow\quad \mathbf{B}(\boldsymbol{\nu})\delta\boldsymbol{\psi} &= \delta\mathbf{H}(\boldsymbol{\psi})\boldsymbol{\rho} + \widehat{\mathbf{H}(\boldsymbol{\psi})\boldsymbol{\rho}}\mathbf{H}(\boldsymbol{\psi})\delta\boldsymbol{\psi}\,. \qquad \text{(A.26)}
\end{aligned}$$

The variation of $\mathbf{H}(\boldsymbol{\psi})$ is

$$\delta\mathbf{H}(\boldsymbol{\psi}) = \frac{\alpha_1 - 2\alpha_2}{\psi^2}\left(\boldsymbol{\psi}^T\delta\boldsymbol{\psi}\right)\widehat{\boldsymbol{\psi}} + \beta_1\delta\widehat{\boldsymbol{\psi}} + \frac{\alpha_2 - 3\beta_2}{\psi^2}\left(\boldsymbol{\psi}^T\delta\boldsymbol{\psi}\right)\widehat{\boldsymbol{\psi}}^2 + \beta_2\left(\delta\widehat{\boldsymbol{\psi}}\widehat{\boldsymbol{\psi}} + \widehat{\boldsymbol{\psi}}\delta\widehat{\boldsymbol{\psi}}\right),$$

then the first term in (A.26) is

$$\begin{aligned}
\delta\mathbf{H}(\boldsymbol{\psi})\boldsymbol{\rho} =& \frac{\alpha_1 - 2\alpha_2}{\psi^2}\left(\boldsymbol{\psi}^T\delta\boldsymbol{\psi}\right)\boldsymbol{\psi}\times\boldsymbol{\rho} + \beta_1\delta\boldsymbol{\psi}\times\boldsymbol{\rho} + \frac{\alpha_2 - 3\beta_2}{\psi^2}\left(\boldsymbol{\psi}^T\delta\boldsymbol{\psi}\right)\boldsymbol{\psi}\times(\boldsymbol{\psi}\times\boldsymbol{\rho}) \\
&+ \beta_2\left[\delta\boldsymbol{\psi}\times(\boldsymbol{\psi}\times\boldsymbol{\rho}) + \boldsymbol{\psi}\times(\delta\boldsymbol{\psi}\times\boldsymbol{\rho})\right] \\
=& -\frac{\alpha_1 - 2\alpha_2}{\psi^2}\widehat{\boldsymbol{\rho}}\boldsymbol{\psi}\boldsymbol{\psi}^T\delta\boldsymbol{\psi} - \beta_1\widehat{\boldsymbol{\rho}}\delta\boldsymbol{\psi} - \frac{\alpha_2 - 3\beta_2}{\psi^2}\widehat{\boldsymbol{\psi}}\widehat{\boldsymbol{\rho}}\boldsymbol{\psi}\boldsymbol{\psi}^T\delta\boldsymbol{\psi} - \beta_2\left(\widehat{\boldsymbol{\psi}}\widehat{\boldsymbol{\rho}} - \widehat{\boldsymbol{\rho}}\widehat{\boldsymbol{\psi}}\right)\delta\boldsymbol{\psi} - \beta_2\widehat{\boldsymbol{\psi}}\widehat{\boldsymbol{\rho}}\delta\boldsymbol{\psi} \\
=& \left[(\alpha_2 - \alpha_1)\widehat{\boldsymbol{\rho}} + \frac{\alpha_2 - 3\beta_2}{\psi^2}(\boldsymbol{\rho}\cdot\boldsymbol{\psi})\widehat{\boldsymbol{\psi}}^2 + \beta_2\widehat{\boldsymbol{\rho}}\widehat{\boldsymbol{\psi}} + (\beta_2 - \alpha_2)\widehat{\boldsymbol{\psi}}\widehat{\boldsymbol{\rho}} - \frac{\alpha_1 - 2\alpha_2}{\psi^2}\widehat{\boldsymbol{\rho}}\widehat{\boldsymbol{\psi}}^2\right]\delta\boldsymbol{\psi}\,.
\end{aligned}$$

Next, we evaluate $\mathbf{H}(\boldsymbol{\psi})\boldsymbol{\rho}$ as

$$\mathbf{H}(\boldsymbol{\psi})\boldsymbol{\rho} = \boldsymbol{\rho} + \beta_1\boldsymbol{\psi}\times\boldsymbol{\rho} + \beta_2\boldsymbol{\psi}\times(\boldsymbol{\psi}\times\boldsymbol{\rho}),$$

from where we have

$$\begin{aligned}
\widehat{\mathbf{H}(\boldsymbol{\psi})\boldsymbol{\rho}} =& \widehat{\boldsymbol{\rho}} + \beta_1\widehat{\boldsymbol{\psi}\times\boldsymbol{\rho}} + \beta_2\widehat{\boldsymbol{\psi}\times(\boldsymbol{\psi}\times\boldsymbol{\rho})} \\
=& \widehat{\boldsymbol{\rho}} + \beta_1(\widehat{\boldsymbol{\psi}}\widehat{\boldsymbol{\rho}} - \widehat{\boldsymbol{\rho}}\widehat{\boldsymbol{\psi}}) + \beta_2\left[(\boldsymbol{\rho}\cdot\boldsymbol{\psi})\widehat{\boldsymbol{\psi}} - \psi^2\widehat{\boldsymbol{\rho}}\right] \\
=& \alpha_1\widehat{\boldsymbol{\rho}} + \beta_2(\boldsymbol{\rho}\cdot\boldsymbol{\psi})\widehat{\boldsymbol{\psi}} + \beta_1(\widehat{\boldsymbol{\psi}}\widehat{\boldsymbol{\rho}} - \widehat{\boldsymbol{\rho}}\widehat{\boldsymbol{\psi}})
\end{aligned}$$

Using the above results, the second term in (A.26) is

$$\begin{aligned}
\widehat{\mathbf{H}(\boldsymbol{\psi})\boldsymbol{\rho}}\mathbf{H}(\boldsymbol{\psi})\delta\boldsymbol{\psi} &= \left[\alpha_1\widehat{\boldsymbol{\rho}} + \beta_2(\boldsymbol{\rho}\cdot\boldsymbol{\psi})\widehat{\boldsymbol{\psi}} + \beta_1(\widehat{\boldsymbol{\psi}}\widehat{\boldsymbol{\rho}} - \widehat{\boldsymbol{\rho}}\widehat{\boldsymbol{\psi}})\right]\left(\delta\boldsymbol{\psi} + \beta_1\widehat{\boldsymbol{\psi}}\delta\boldsymbol{\psi} + \beta_2\widehat{\boldsymbol{\psi}}^2\delta\boldsymbol{\psi}\right) \\
&= \left[\alpha_1\widehat{\boldsymbol{\rho}} + \frac{\alpha_1 - 2\alpha_2}{\psi^2}(\boldsymbol{\rho}\cdot\boldsymbol{\psi})\widehat{\boldsymbol{\psi}} + \beta_1\widehat{\boldsymbol{\psi}}\widehat{\boldsymbol{\rho}} + \frac{\alpha_1 - 2\alpha_2}{\psi^2}\widehat{\boldsymbol{\rho}}\widehat{\boldsymbol{\psi}}^2\right]\delta\boldsymbol{\psi}\,.
\end{aligned}$$

Adding the two above expressions yields

$$\mathbf{B}(\boldsymbol{\nu})\delta\boldsymbol{\psi} = \left[\alpha_2\widehat{\boldsymbol{\rho}} + \frac{\alpha_1 - 2\alpha_2}{\psi^2}\left(\boldsymbol{\rho}\cdot\boldsymbol{\psi}\right)\widehat{\boldsymbol{\psi}} + \frac{\alpha_2 - 3\beta_2}{\psi^2}\left(\boldsymbol{\rho}\cdot\boldsymbol{\psi}\right)\widehat{\boldsymbol{\psi}}^2 + \beta_2\left(\widehat{\boldsymbol{\psi}}\widehat{\boldsymbol{\rho}} + \widehat{\boldsymbol{\rho}}\widehat{\boldsymbol{\psi}}\right)\right]\delta\boldsymbol{\psi}\,, \tag{A.27}$$

i.e. we obtain $\mathbf{B}(\boldsymbol{\nu})$ as given in (2.70) for which relationship (A.23) is valid. This relationship is written in a more compact form in (2.68) using the matrix in (A.23) as

$$\mathbf{H_6}(\boldsymbol{\nu}) = \begin{bmatrix}\mathbf{H}(\boldsymbol{\psi}) & \mathbf{B}(\boldsymbol{\nu}) \\ \mathbf{0} & \mathbf{H}(\boldsymbol{\psi})\end{bmatrix}. \tag{A.28}$$

The inverse of (2.69) follows as

$$\left[\mathbf{H_6}(\boldsymbol{\nu})\right]^{-1} = \begin{bmatrix}\mathbf{H}^{-1}(\boldsymbol{\psi}) & -\mathbf{H}^{-1}(\boldsymbol{\psi})\mathbf{B}(\boldsymbol{\nu})\mathbf{H}^{-1}(\boldsymbol{\psi}) \\ \mathbf{0} & \mathbf{H}^{-1}(\boldsymbol{\psi})\end{bmatrix}, \tag{A.29}$$

while the inverse of $\mathbf{H_6}(-\boldsymbol{\nu})$ is

$$\left[\mathbf{H_6}(-\boldsymbol{\nu})\right]^{-1} = \begin{bmatrix}\mathbf{H}^{-T}(\boldsymbol{\psi}) & -\mathbf{H}^{-T}(\boldsymbol{\psi})\mathbf{B}^T(\boldsymbol{\nu})\mathbf{H}^{-T}(\boldsymbol{\psi}) \\ \mathbf{0} & \mathbf{H}^{-T}(\boldsymbol{\psi})\end{bmatrix} =, \tag{A.30}$$

because $\mathbf{B}(-\boldsymbol{\nu}) = \mathbf{B}^T(\boldsymbol{\nu})$. Multiplying (A.28) and (A.30) gives

$$\begin{aligned}\mathbf{H_6}(\boldsymbol{\nu})\left[\mathbf{H_6}(-\boldsymbol{\nu})\right]^{-1} &= \begin{bmatrix}\mathbf{H}(\boldsymbol{\psi}) & \mathbf{B}(\boldsymbol{\nu}) \\ \mathbf{0} & \mathbf{H}(\boldsymbol{\psi})\end{bmatrix}\begin{bmatrix}\mathbf{H}^{-T}(\boldsymbol{\psi}) & -\mathbf{H}^{-T}(\boldsymbol{\psi})\mathbf{B}^T(\boldsymbol{\nu})\mathbf{H}^{-T}(\boldsymbol{\psi}) \\ \mathbf{0} & \mathbf{H}^{-T}(\boldsymbol{\psi})\end{bmatrix} \\ &= \begin{bmatrix}\mathbf{H}(\boldsymbol{\psi})\mathbf{H}^{-T}(\boldsymbol{\psi}) & -\mathbf{H}(\boldsymbol{\psi})\mathbf{H}^{-T}(\boldsymbol{\psi})\mathbf{B}^T(\boldsymbol{\nu})\mathbf{H}^{-T}(\boldsymbol{\psi}) + \mathbf{B}(\boldsymbol{\nu})\mathbf{H}^{-T}(\boldsymbol{\psi}) \\ \mathbf{0} & \mathbf{H}(\boldsymbol{\psi})\mathbf{H}^{-T}(\boldsymbol{\psi})\end{bmatrix},\end{aligned}$$

which turns into

$$\mathbf{H_6}(\boldsymbol{\nu})\left[\mathbf{H_6}(-\boldsymbol{\nu})\right]^{-1} = \exp\widehat{\boldsymbol{\nu}}\,, \tag{A.31}$$

due to (A.13) and direct calculation of the non-diagonal term which yields $\mathbf{Q}(\boldsymbol{\nu})$. The result (A.31) is useful for deriving the following relationship

$$\begin{aligned}\left(\left[\mathbf{H_6}(\boldsymbol{\nu})\right]^{-1} + \left[\mathbf{H_6}(-\boldsymbol{\nu})\right]^{-1}\right)^{-1}\left[\mathbf{H_6}(\boldsymbol{\nu})\right]^{-1} &= \left[\mathbf{H_6}(\boldsymbol{\nu})\left(\left[\mathbf{H_6}(\boldsymbol{\nu})\right]^{-1} + \left[\mathbf{H_6}(-\boldsymbol{\nu})\right]^{-1}\right)\right]^{-1} \\ &= \left(\mathbf{I} + \exp\widehat{\boldsymbol{\nu}}\right)^{-1}.\end{aligned} \tag{A.32}$$

Variation of $\mathbf{B}(\boldsymbol{\nu})$

Using results (A.6) we obtain the variation of $\mathbf{B}(\boldsymbol{\nu})$. The variation of the first factor in (2.70) yields

$$\delta\left(\alpha_2\widehat{\boldsymbol{\rho}}\right) = \delta\alpha_2\widehat{\boldsymbol{\rho}} + \alpha_2\delta\widehat{\boldsymbol{\rho}} = \frac{\alpha_1 - 2\alpha_2}{\psi^2}\left(\boldsymbol{\psi}\cdot\delta\boldsymbol{\psi}\right)\widehat{\boldsymbol{\rho}} + \alpha_2\delta\widehat{\boldsymbol{\rho}}\,.$$

Variation of the second factor in (2.70) is

$$\begin{aligned}\delta\left[\frac{\alpha_1 - 2\alpha_2}{\psi^2}\left(\boldsymbol{\rho}\cdot\boldsymbol{\psi}\right)\widehat{\boldsymbol{\psi}}\right] &= \delta\left(\frac{\alpha_1 - 2\alpha_2}{\psi^2}\right)\left(\boldsymbol{\rho}\cdot\boldsymbol{\psi}\right)\widehat{\boldsymbol{\psi}} + \frac{\alpha_1 - 2\alpha_2}{\psi^2}\left(\delta\boldsymbol{\rho}\cdot\boldsymbol{\psi} + \boldsymbol{\rho}\cdot\delta\boldsymbol{\psi}\right)\widehat{\boldsymbol{\psi}} + \\ &\quad \frac{\alpha_1 - 2\alpha_2}{\psi^2}\left(\boldsymbol{\rho}\cdot\boldsymbol{\psi}\right)\delta\widehat{\boldsymbol{\psi}} \\ &= \frac{\cos\psi - 5\alpha_1 + 8\alpha_2}{\psi^4}\left(\boldsymbol{\psi}\cdot\delta\boldsymbol{\psi}\right)\left(\boldsymbol{\rho}\cdot\boldsymbol{\psi}\right)\widehat{\boldsymbol{\psi}} +\end{aligned}$$

$$\frac{\alpha_1-2\alpha_2}{\psi^2}\left(\delta\boldsymbol{\rho}\cdot\boldsymbol{\psi}+\boldsymbol{\rho}\cdot\delta\boldsymbol{\psi}\right)\widehat{\boldsymbol{\psi}}+\frac{\alpha_1-2\alpha_2}{\psi^2}\left(\boldsymbol{\rho}\cdot\boldsymbol{\psi}\right)\delta\widehat{\boldsymbol{\psi}}\,.$$

Variation of the third factor in (2.70) gives

$$\begin{aligned}\delta\left[\frac{\alpha_2-3\beta_2}{\psi^2}\left(\boldsymbol{\rho}\cdot\boldsymbol{\psi}\right)\widehat{\boldsymbol{\psi}}^2\right]&=\delta\left(\frac{\alpha_2-3\beta_2}{\psi^2}\right)\left(\boldsymbol{\rho}\cdot\boldsymbol{\psi}\right)\widehat{\boldsymbol{\psi}}^2+\frac{\alpha_2-3\beta_2}{\psi^2}\left(\delta\boldsymbol{\rho}\cdot\boldsymbol{\psi}+\boldsymbol{\rho}\cdot\delta\boldsymbol{\psi}\right)\widehat{\boldsymbol{\psi}}^2+\\&\qquad\frac{\alpha_2-3\beta_2}{\psi^2}\left(\boldsymbol{\rho}\cdot\boldsymbol{\psi}\right)\left(\delta\widehat{\boldsymbol{\psi}}\widehat{\boldsymbol{\psi}}+\widehat{\boldsymbol{\psi}}\delta\widehat{\boldsymbol{\psi}}\right)\\&=\frac{\alpha_1-7\alpha_2+15\beta_2}{\psi^4}\left(\boldsymbol{\rho}\cdot\boldsymbol{\psi}\right)\left(\boldsymbol{\psi}\cdot\delta\boldsymbol{\psi}\right)\widehat{\boldsymbol{\psi}}^2+\\&\qquad\frac{\alpha_2-3\beta_2}{\psi^2}\left(\delta\boldsymbol{\rho}\cdot\boldsymbol{\psi}+\boldsymbol{\rho}\cdot\delta\boldsymbol{\psi}\right)\widehat{\boldsymbol{\psi}}^2+\frac{\alpha_2-3\beta_2}{\psi^2}\left(\boldsymbol{\rho}\cdot\boldsymbol{\psi}\right)\left(\delta\widehat{\boldsymbol{\psi}}\widehat{\boldsymbol{\psi}}+\widehat{\boldsymbol{\psi}}\delta\widehat{\boldsymbol{\psi}}\right),\end{aligned}$$

and finally, variation of the fourth factor in (2.70) is simply

$$\begin{aligned}\delta\left[\beta_2\left(\widehat{\boldsymbol{\psi}}\widehat{\boldsymbol{\rho}}+\widehat{\boldsymbol{\rho}}\widehat{\boldsymbol{\psi}}\right)\right]&=\delta\beta_2\left(\widehat{\boldsymbol{\psi}}\widehat{\boldsymbol{\rho}}+\widehat{\boldsymbol{\rho}}\widehat{\boldsymbol{\psi}}\right)+\beta_2\left(\delta\widehat{\boldsymbol{\psi}}\widehat{\boldsymbol{\rho}}+\widehat{\boldsymbol{\psi}}\delta\widehat{\boldsymbol{\rho}}+\delta\widehat{\boldsymbol{\rho}}\widehat{\boldsymbol{\psi}}+\widehat{\boldsymbol{\rho}}\delta\widehat{\boldsymbol{\psi}}\right)\\&=\frac{\alpha_2-3\beta_2}{\psi^2}\left(\boldsymbol{\psi}\cdot\delta\boldsymbol{\psi}\right)\left(\widehat{\boldsymbol{\psi}}\widehat{\boldsymbol{\rho}}+\widehat{\boldsymbol{\rho}}\widehat{\boldsymbol{\psi}}\right)+\beta_2\left(\delta\widehat{\boldsymbol{\psi}}\widehat{\boldsymbol{\rho}}+\widehat{\boldsymbol{\psi}}\delta\widehat{\boldsymbol{\rho}}+\delta\widehat{\boldsymbol{\rho}}\widehat{\boldsymbol{\psi}}+\widehat{\boldsymbol{\rho}}\delta\widehat{\boldsymbol{\psi}}\right).\end{aligned}$$

Therefore, adding the four expressions above we obtain the variation of $\mathbf{B}(\boldsymbol{\nu})$ as

$$\begin{aligned}\delta\mathbf{B}(\boldsymbol{\nu})=\frac{\alpha_1-2\alpha_2}{\psi^2}\left(\boldsymbol{\psi}\cdot\delta\boldsymbol{\psi}\right)\widehat{\boldsymbol{\rho}}+\alpha_2\delta\widehat{\boldsymbol{\rho}}+\frac{\cos\psi-5\alpha_1+8\alpha_2}{\psi^4}\left(\boldsymbol{\psi}\cdot\delta\boldsymbol{\psi}\right)\left(\boldsymbol{\rho}\cdot\boldsymbol{\psi}\right)\widehat{\boldsymbol{\psi}}+\\\frac{\alpha_1-2\alpha_2}{\psi^2}\left(\delta\boldsymbol{\rho}\cdot\boldsymbol{\psi}+\boldsymbol{\rho}\cdot\delta\boldsymbol{\psi}\right)\widehat{\boldsymbol{\psi}}+\frac{\alpha_1-2\alpha_2}{\psi^2}\left(\boldsymbol{\rho}\cdot\boldsymbol{\psi}\right)\delta\widehat{\boldsymbol{\psi}}+\frac{\alpha_1-7\alpha_2+15\beta_2}{\psi^4}\left(\boldsymbol{\rho}\cdot\boldsymbol{\psi}\right)\left(\boldsymbol{\psi}\cdot\delta\boldsymbol{\psi}\right)\widehat{\boldsymbol{\psi}}^2+\\\frac{\alpha_2-3\beta_2}{\psi^2}\left(\delta\boldsymbol{\rho}\cdot\boldsymbol{\psi}+\boldsymbol{\rho}\cdot\delta\boldsymbol{\psi}\right)\widehat{\boldsymbol{\psi}}^2+\frac{\alpha_2-3\beta_2}{\psi^2}\left(\boldsymbol{\rho}\cdot\boldsymbol{\psi}\right)\left(\delta\widehat{\boldsymbol{\psi}}\widehat{\boldsymbol{\psi}}+\widehat{\boldsymbol{\psi}}\delta\widehat{\boldsymbol{\psi}}\right)+\\\frac{\alpha_2-3\beta_2}{\psi^2}\left(\boldsymbol{\psi}\cdot\delta\boldsymbol{\psi}\right)\left(\widehat{\boldsymbol{\psi}}\widehat{\boldsymbol{\rho}}+\widehat{\boldsymbol{\rho}}\widehat{\boldsymbol{\psi}}\right)+\beta_2\left(\delta\widehat{\boldsymbol{\psi}}\widehat{\boldsymbol{\rho}}+\widehat{\boldsymbol{\psi}}\delta\widehat{\boldsymbol{\rho}}+\delta\widehat{\boldsymbol{\rho}}\widehat{\boldsymbol{\psi}}+\widehat{\boldsymbol{\rho}}\delta\widehat{\boldsymbol{\psi}}\right).\end{aligned}\tag{A.33}$$

A.2.6 Relationship between the standard and non-standard virtual quantities

Varying the configuration tensor blockwise

$$\delta\mathbf{C}=\begin{bmatrix}\delta\boldsymbol{\Lambda}&\delta\hat{\mathbf{r}}\boldsymbol{\Lambda}+\hat{\mathbf{r}}\delta\boldsymbol{\Lambda}\\\mathbf{0}&\delta\boldsymbol{\Lambda}\end{bmatrix}=\begin{bmatrix}\widehat{\delta\boldsymbol{\vartheta}}\boldsymbol{\Lambda}&\delta\hat{\mathbf{r}}\boldsymbol{\Lambda}+\hat{\mathbf{r}}\widehat{\delta\boldsymbol{\vartheta}}\boldsymbol{\Lambda}\\\mathbf{0}&\widehat{\delta\boldsymbol{\vartheta}}\boldsymbol{\Lambda}\end{bmatrix}=\begin{bmatrix}\widehat{\delta\boldsymbol{\vartheta}}&\delta\hat{\mathbf{r}}+\hat{\mathbf{r}}\widehat{\delta\boldsymbol{\vartheta}}\\\mathbf{0}&\widehat{\delta\boldsymbol{\vartheta}}\end{bmatrix}\begin{bmatrix}\boldsymbol{\Lambda}&\mathbf{0}\\\mathbf{0}&\boldsymbol{\Lambda}\end{bmatrix}\tag{A.34}$$

we obtain $\delta\mathbf{C}$ in terms of the standard virtual quantities $\delta\mathbf{r}$ and $\delta\boldsymbol{\vartheta}$. We can write (2.66) as

$$\delta\mathbf{C}=\widehat{\delta\boldsymbol{\varsigma}}\mathbf{C}=\begin{bmatrix}\widehat{\delta\boldsymbol{\vartheta}}&\widehat{\delta\boldsymbol{\xi}}\\\mathbf{0}&\widehat{\delta\boldsymbol{\vartheta}}\end{bmatrix}\begin{bmatrix}\mathbf{I}&\hat{\mathbf{r}}\\\mathbf{0}&\mathbf{I}\end{bmatrix}\begin{bmatrix}\boldsymbol{\Lambda}&\mathbf{0}\\\mathbf{0}&\boldsymbol{\Lambda}\end{bmatrix}=\begin{bmatrix}\widehat{\delta\boldsymbol{\vartheta}}&\widehat{\delta\boldsymbol{\vartheta}}\hat{\mathbf{r}}+\widehat{\delta\boldsymbol{\xi}}\\\mathbf{0}&\widehat{\delta\boldsymbol{\vartheta}}\end{bmatrix}\begin{bmatrix}\boldsymbol{\Lambda}&\mathbf{0}\\\mathbf{0}&\boldsymbol{\Lambda}\end{bmatrix}\tag{A.35}$$

Then, equating (A.34) to (A.35) yields

$$\begin{bmatrix}\widehat{\delta\boldsymbol{\vartheta}}&\delta\hat{\mathbf{r}}+\hat{\mathbf{r}}\widehat{\delta\boldsymbol{\vartheta}}\\\mathbf{0}&\widehat{\delta\boldsymbol{\vartheta}}\end{bmatrix}=\begin{bmatrix}\widehat{\delta\boldsymbol{\vartheta}}&\widehat{\delta\boldsymbol{\vartheta}}\hat{\mathbf{r}}+\widehat{\delta\boldsymbol{\xi}}\\\mathbf{0}&\widehat{\delta\boldsymbol{\vartheta}}\end{bmatrix}\tag{A.36}$$

where the diagonal blocks are obviously identically satisfied. Equating the remaining block results in

$$\widehat{\delta\boldsymbol{\xi}}=\delta\hat{\mathbf{r}}+\hat{\mathbf{r}}\widehat{\delta\boldsymbol{\vartheta}}-\widehat{\delta\boldsymbol{\vartheta}}\hat{\mathbf{r}}=\delta\hat{\mathbf{r}}+\widehat{\mathbf{r}\times\delta\boldsymbol{\vartheta}}\,,$$

i.e. $\delta\boldsymbol{\xi} = \delta\mathbf{r} + \mathbf{r} \times \delta\boldsymbol{\vartheta}$. Finally, the relationship between non-standard and standard virtual quantities follows as

$$\delta\boldsymbol{\varsigma} = \begin{Bmatrix} \delta\boldsymbol{\xi} \\ \delta\boldsymbol{\vartheta} \end{Bmatrix} = \begin{bmatrix} \mathbf{I} & \widehat{\mathbf{r}} \\ \mathbf{0} & \mathbf{I} \end{bmatrix} \begin{Bmatrix} \delta\mathbf{r} \\ \delta\boldsymbol{\vartheta} \end{Bmatrix} . \tag{A.37}$$

A.3 Material strain measures

Reissner [1] derived the material strain measures from the stipulation that the virtual work equation must be equal to the equations of motion integrated over the same domain. We use the same procedure here to obtain the material translational and rotational strain measures. Assuming a static case (i.e. $V_m = 0$), this is achieved by expressing the external loading from differential equations (3.19) in terms of the stress resultants as

$$\begin{aligned} \mathbf{n}_e &= -(\boldsymbol{\Lambda}\mathbf{N})' , \\ \mathbf{m}_e &= -\mathbf{r}' \times \boldsymbol{\Lambda}\mathbf{N} - (\boldsymbol{\Lambda}\mathbf{M})' , \end{aligned}$$

and substituting it in (3.35), which results in

$$\begin{aligned} V_e &= -\int_0^L \left[\delta\mathbf{r} \cdot (\boldsymbol{\Lambda}\mathbf{N})' + \delta\boldsymbol{\vartheta} \cdot \left(\mathbf{r}' \times \boldsymbol{\Lambda}\mathbf{N} + (\boldsymbol{\Lambda}\mathbf{M})'\right)\right] \mathrm{d}x \\ &\quad + \delta\mathbf{r}_0 \cdot \mathbf{F}_0 + \delta\boldsymbol{\vartheta}_0 \cdot \mathbf{M}_0 + \delta\mathbf{r}_L \cdot \mathbf{F}_L + \delta\boldsymbol{\vartheta}_L \cdot \mathbf{M}_L \\ &= \int_0^L \left(\delta\mathbf{r}' \cdot \boldsymbol{\Lambda}\mathbf{N} - \delta\boldsymbol{\vartheta} \cdot (\widehat{\mathbf{r}}'\boldsymbol{\Lambda}\mathbf{N}) + \delta\boldsymbol{\vartheta}' \cdot \boldsymbol{\Lambda}\mathbf{M}\right) \mathrm{d}x . \end{aligned} \tag{A.38}$$

because after integrating by parts, the boundary terms cancel out. Substituting (3.23) and (A.38) in $V_i - V_e = 0$ we have

$$\int_0^L \mathbf{N}^T \left(\delta\boldsymbol{\Gamma} - \boldsymbol{\Lambda}^T\delta\mathbf{r}' - \boldsymbol{\Lambda}^T\widehat{\mathbf{r}}'\delta\boldsymbol{\vartheta}\right) \mathrm{d}x + \int_0^L \mathbf{M}^T \left(\delta\mathbf{K} - \boldsymbol{\Lambda}^T\delta\boldsymbol{\vartheta}'\right) \mathrm{d}x = 0 , \tag{A.39}$$

which is non-trivially satisfied only for

$$\delta\boldsymbol{\Gamma} = \boldsymbol{\Lambda}^T \left(\delta\mathbf{r}' + \mathbf{r}' \times \delta\boldsymbol{\vartheta}\right) \quad \text{and} \quad \delta\mathbf{K} = \boldsymbol{\Lambda}^T\delta\boldsymbol{\vartheta}' ,$$

which is equivalent to (3.27) and (3.28). By using (2.47) we integrate the above equations as

$$\begin{aligned} \delta\boldsymbol{\Gamma} &= \boldsymbol{\Lambda}^T\delta\mathbf{r}' + \boldsymbol{\Lambda}^T\widehat{\delta\boldsymbol{\vartheta}}^T\mathbf{r}' = \boldsymbol{\Lambda}^T\delta\mathbf{r}' + \delta\boldsymbol{\Lambda}^T\mathbf{r}' = \delta(\boldsymbol{\Lambda}^T\mathbf{r}') , \\ \delta\widehat{\mathbf{K}} &= \boldsymbol{\Lambda}^T\widehat{\delta\boldsymbol{\vartheta}}'\boldsymbol{\Lambda} = \boldsymbol{\Lambda}^T(\widehat{\delta\boldsymbol{\vartheta}}\boldsymbol{\Lambda})' - \boldsymbol{\Lambda}^T\widehat{\delta\boldsymbol{\vartheta}}\boldsymbol{\Lambda}' = \boldsymbol{\Lambda}^T\delta\boldsymbol{\Lambda}' + \delta\boldsymbol{\Lambda}^T\boldsymbol{\Lambda}' = \delta(\boldsymbol{\Lambda}^T\boldsymbol{\Lambda}') . \end{aligned}$$

Since strain measures must be equal to zero at the initial configuration ($\mathbf{r}_0$, $\boldsymbol{\Lambda}_0$) the above equations are integrated, noting that $\mathbf{r}_0' = \mathbf{t}_{0,1}$ (i.e. the base vector in the initial configuration is directed along the initial centroid axis), to give

$$\boldsymbol{\Gamma} = \boldsymbol{\Lambda}^T\mathbf{r}' - \mathbf{E}_1 , \tag{A.40}$$

$$\widehat{\mathbf{K}} = \boldsymbol{\Lambda}^T\boldsymbol{\Lambda}' - \boldsymbol{\Lambda}_0^T\boldsymbol{\Lambda}_0' , \tag{A.41}$$

which, in case of an initially horizontal beam, turn into (3.4) and (3.5).

A.4 Algorithm for extracting $\boldsymbol{\Phi}$ from $\exp \boldsymbol{\Phi}$

First we define $\boldsymbol{\eta}_{IJ} = \left\langle \boldsymbol{\mu}_{IJ}^T \, \boldsymbol{\phi}_{IJ}^T \right\rangle^T$. From (5.27) we have

$$\exp \widehat{\boldsymbol{\eta}}_{IJ} = \mathbf{C}_I^{-1} \mathbf{C}_J$$
$$\begin{bmatrix} \exp \widehat{\boldsymbol{\phi}}_{IJ} & \boldsymbol{Q}(\boldsymbol{\eta}_{IJ}) \\ \mathbf{0} & \exp \widehat{\boldsymbol{\phi}}_{IJ} \end{bmatrix} = \begin{bmatrix} \boldsymbol{\Lambda}_I^T \boldsymbol{\Lambda}_J & \boldsymbol{\Lambda}_I^T \left(\widehat{\mathbf{r}}_J - \widehat{\mathbf{r}}_I \right) \boldsymbol{\Lambda}_J \\ \mathbf{0} & \boldsymbol{\Lambda}_I^T \boldsymbol{\Lambda}_J \end{bmatrix},$$

where we recognise relationship (5.7) in the diagonal terms. Using (5.7) and (2.61), the remaining terms give

$$\widehat{\mathbf{H}(\boldsymbol{\phi}_{IJ}) \boldsymbol{\mu}_{IJ}} \exp \widehat{\boldsymbol{\phi}}_{IJ} = \boldsymbol{\Lambda}_I^T \left(\widehat{\mathbf{r}}_J - \widehat{\mathbf{r}}_I \right) \boldsymbol{\Lambda}_I \exp \boldsymbol{\phi}_{IJ} \,,$$

i.e.

$$\widehat{\mathbf{H}(\boldsymbol{\phi}_{IJ}) \boldsymbol{\mu}_{IJ}} = \widehat{\boldsymbol{\Lambda}_I^T \left(\mathbf{r}_J - \mathbf{r}_I \right)} \quad \Rightarrow \boldsymbol{\mu}_{IJ} = \left[\mathbf{H}(\boldsymbol{\phi}_{IJ}) \right]^{-1} \boldsymbol{\Lambda}_I^T \left(\mathbf{r}_J - \mathbf{r}_I \right) . \tag{A.42}$$

Since during computation we only need the final result, i.e. the value of $\boldsymbol{\eta}_{IJ}$, any configuration tensor $\mathbf{M}$ is represented as

$$\begin{bmatrix} \mathbf{M}_{\text{rot}} & \mathbf{M}_{\text{comp}} \\ \mathbf{0} & \mathbf{M}_{\text{rot}} \end{bmatrix} .$$

Then, $\boldsymbol{\phi}_{IJ}$ is extracted using Spurrier's algorithm from $\mathbf{M}_{\text{rot}}$, while the value of $\boldsymbol{\mu}_{IJ}$ is obtained via

$$\boldsymbol{\mu}_{IJ} = \left[\mathbf{H}(\boldsymbol{\phi}_{IJ}) \right]^{-1} \text{axial} \left(\mathbf{M}_{\text{comp}} \right) . \tag{A.43}$$

A.5 Interpolation objectivity proof

As shown in Section 5.1, we can superimpose a rigid translation and rotation $\mathbf{C}_R$ to a configuration $\mathbf{C}$ to obtain a new configuration $\underline{\mathbf{C}}$ as $\underline{\mathbf{C}} = \mathbf{C}_R \mathbf{C}$. Using (5.26) we will prove that this relationship is valid for the approximated values of $\mathbf{C}^h(x)$ at integration points as well for the interpolation scheme employed in this work. Using (5.26) we write $\mathbf{C}^h(x)$ and $\underline{\mathbf{C}}^h(x)$ as

$$\mathbf{C}^h(x) = \mathbf{C}_r \exp \widehat{\boldsymbol{\Phi}}^{lh}(x) \,, \tag{A.44}$$
$$\underline{\mathbf{C}}^h(x) = \underline{\mathbf{C}}_r \exp \widehat{\underline{\boldsymbol{\Phi}}}^{lh}(x) \,. \tag{A.45}$$

Noting that $\underline{\mathbf{C}}_r = \mathbf{C}_R \mathbf{C}_r$, we see that

$$\underline{\mathbf{C}}^h = \mathbf{C}_R \mathbf{C}_r \exp \widehat{\underline{\boldsymbol{\Phi}}}^{lh} \,, \tag{A.46}$$

as well as

$$\mathbf{C}_R \mathbf{C}^h = \mathbf{C}_R \mathbf{C}_r \exp \widehat{\boldsymbol{\Phi}}^{lh} . \tag{A.47}$$

Comparing (A.46) and (A.47) we see that in order for $\underline{\mathbf{C}}^h = \mathbf{C}_R \mathbf{C}^h$ to hold true, the following equation must be satisfied

$$\exp \widehat{\underline{\boldsymbol{\Phi}}}^{lh} \stackrel{?}{=} \exp \widehat{\boldsymbol{\Phi}}^{lh}$$
$$\exp \left(I^i(x) \widehat{\underline{\boldsymbol{\Phi}}}_i^l \right) \stackrel{?}{=} \exp \left(I^i(x) \widehat{\boldsymbol{\Phi}}_i^l \right) ,$$

which obviously suggests that the material local nodal configuration vectors must be equal, i.e. $\underline{\mathbf{\Phi}}_i^l = \mathbf{\Phi}_i^l$. In order to check this we use (5.29) to obtain these nodal values

$$\begin{aligned}
\exp \widehat{\mathbf{\Phi}}_i^l &= \mathbf{C}_r^{-1}\mathbf{C}_i \to \mathbf{\Phi}_i^l \\
\exp \widehat{\underline{\mathbf{\Phi}}}_i^l &= \underline{\mathbf{C}}_r^{-1}\underline{\mathbf{C}}_i \\
&= \mathbf{C}_r^{-1}\mathbf{C}_R^{-1}\mathbf{C}_R\mathbf{C}_i \\
&= \mathbf{C}_r^{-1}\mathbf{C}_i = \exp \widehat{\mathbf{\Phi}}_i^l \to \mathbf{\Phi}_i^l \,,
\end{aligned}$$

which means that two configurations differing only by rigid-body motion have the same local configuration vectors. This also means that the approximated values of the configuration tensor are indeed objective.

Bibliography

[1] E. Reissner. On one-dimensional finite-strain beam theory: The plane problem. *Zeitschrift für Angew. Math. und Phys.*, 23(5):795–804, 1972.

[2] J. C. Simo. A finite strain beam formulation. The three-dimensional dynamic problem. Part I. *Comput. Methods Appl. Mech. Eng.*, 49(1):55–70, 1985.

[3] B. Hall. *Lie Groups, Lie Algebras, and Representations: An Elementary Introduction.* Springer-Verlag, New York, 2003.

[4] J. C. Simo and L. Vu-Quoc. A three-dimensional finite-strain rod model. Part II: Computational aspects. *Comput. Methods Appl. Mech. Eng.*, 58(1):79–116, 1986.

[5] A. Cardona and M. Geradin. A beam finite element non-linear theory with finite rotations. *Int. J. Numer. Methods Eng.*, 26(11):2403–2438, 1988.

[6] A. Ibrahimbegović, F. Frey, and I. Kožar. Computational aspects of vector-like parametrization of three-dimensional finite rotations. *Int. J. Numer. Methods Eng.*, 38(21):3653–3673, 1995.

[7] M. Borri and C. L. Bottasso. An intrinsic beam model based on a helicoidal approximation—Part I: Formulation. *Int. J. Numer. Methods Eng.*, 37(13):2267–2289, 1994.

[8] C. L. Bottasso and M. Borri. Energy preserving/decaying schemes for non-linear beam dynamics using the helicoidal approximation. *Comput. Methods Appl. Mech. Eng.*, 143(3-4):393–415, 1997.

[9] C. L. Bottasso and M. Borri. Energy preserving/decaying schemes for non-linear beam dynamics using the helicoidal approximation. *Comput. Methods Appl. Mech. Eng.*, 143(3-4):393–415, 1997.

[10] C. L. Bottasso and M. Borri. Integrating finite rotations. *Comput. Methods Appl. Mech. Eng.*, 164(3-4):307–331, 1998.

[11] M. Borri, L. Trainelli, and C. L. Bottasso. On Representations and Parameterizations of Motion. *Multibody Syst. Dyn.*, 4(2-3):129–193, 2000.

[12] T. Merlini and M. Morandini. The helicoidal modeling in computational finite elasticity. Part I: Variational formulation. *Int. J. Solids Struct.*, 41(18-19):5351–5381, 2004.

[13] T. Merlini and M. Morandini. The helicoidal modeling in computational finite elasticity. Part II: Multiplicative interpolation. *Int. J. Solids Struct.*, 41(18-19):5383–5409, 2004.

[14] M. Borri and C. L. Bottasso. An intrinsic beam model based on a helicoidal approximation—Part II: Linearization and finite element implementation. *Int. J. Numer. Methods Eng.*, 37(13):2291–2309, 1994.

[15] E. Papa Dukić, G. Jelenić, and M. Gaćeša. Configuration-dependent interpolation in higher-order 2D beam finite elements. *Finite Elem. Anal. Des.*, 78:47–61, 2014.

[16] O. A. Bauchau. On the Modeling of Friction and Rolling in Flexible Multi-Body Systems. *Multibody Syst. Dyn.*, 3(3):209–239, 1999.

[17] M. Borri, C. L. Bottasso, and L. Trainelli. An invariant-preserving approach to robust finite-element multibody simulation. *Zeitschrift für Angew. Math. und Mech.*, 83(10):663–676, 2003.

[18] O. A. Bauchau, C. L. Bottasso, and L. Trainelli. Robust integration schemes for flexible multibody systems. *Comput. Methods Appl. Mech. Eng.*, 192(3-4):395–420, 2003.

[19] O. A. Bauchau. Modeling Rotorcraft Dynamics With Finite Element Multibody Procedures. In *Vol. 4 7th Int. Conf. Multibody Syst. Nonlinear Dyn. Control. Parts A, B C*, pages 31–40. ASME, January 2009.

[20] O. A. Bauchau. On the modeling of prismatic joints in flexible multi-body systems. *Comput. Methods Appl. Mech. Eng.*, 181(1-3):87–105, 2000.

[21] O. A. Bauchau and C. L. Bottasso. Contact Conditions for Cylindrical, Prismatic, and Screw Joints in Flexible Multibody Systems. *Multibody Syst. Dyn.*, 5(3):251–278, 2001.

[22] O. A. Bauchau and J. Rodriguez. Simulation of Wheels in Nonlinear, Flexible Multibody Systems. *Multibody Syst. Dyn.*, 7(4):407–438, 2002.

[23] O. A. Bauchau and J. Rodriguez. Modeling of joints with clearance in flexible multibody systems. *Int. J. Solids Struct.*, 39(1):41–63, 2002.

[24] O. A. Bauchau, J. Y. Choi, and C. L. Bottasso. On the Modeling of Shells in Multibody Dynamics. *Multibody Syst. Dyn.*, 8(4):459–489, 2002.

[25] O. A. Bauchau, J. Y. Choi, and C. L. Bottasso. Time integrators for shells in multibody dynamics. *Comput. Struct.*, 80(9-10):871–889, 2002.

[26] C. L. Bottasso, O. A. Bauchau, and J. Y. Choi. An energy decaying scheme for nonlinear dynamics of shells. *Comput. Methods Appl. Mech. Eng.*, 191(27-28):3099–3121, 2002.

[27] P. Krysl. Dynamically equivalent implicit algorithms for the integration of rigid body rotations. *Commun. Numer. Methods Eng.*, 24(2):141–156, 2006.

[28] M. Borri, C. L. Bottasso, and L. Trainelli. Integration of elastic multibody systems by invariant conserving/dissipating algorithms. I. Formulation. *Comput. Methods Appl. Mech. Eng.*, 190(29-30):3669–3699, 2001.

[29] C. L. Bottasso, M. Borri, and L. Trainelli. Integration of elastic multibody systems by invariant conserving/dissipating algorithms. II. Numerical schemes and applications. *Comput. Methods Appl. Mech. Eng.*, 190(29-30):3701–3733, 2001.

[30] A. Ibrahimbegovic and S. Mamouri. Energy conserving/decaying implicit time-stepping scheme for nonlinear dynamics of three-dimensional beams undergoing finite rotations. *Comput. Methods Appl. Mech. Eng.*, 191(37-38):4241–4258, 2002.

[31] C. L. Bottasso and L. Trainelli. An Attempt at the Classification of Energy Decaying Schemes for Structural and Multibody Dynamics. *Multibody Syst. Dyn.*, 12(2):173–185, 2004.

[32] L. Noels, L. Stainier, and J. P. Ponthot. On the use of large time steps with an energy momentum conserving algorithm for non-linear hypoelastic constitutive models. *Int. J. Solids Struct.*, 41(3-4):663–693, 2004.

[33] P. Betsch and S. Leyendecker. The discrete null space method for the energy consistent integration of constrained mechanical systems. Part II: multibody dynamics. *Int. J. Numer. Methods Eng.*, 67(4):499–552, 2006.

[34] L. Noels, L. Stainier, and J. P. Ponthot. An energy momentum conserving algorithm using the variational formulation of visco-plastic updates. *Int. J. Numer. Methods Eng.*, 65(6):904–942, 2006.

[35] M. Gams, I. Planinc, and M. Saje. Energy conserving time integration scheme for geometrically exact beam. *Comput. Methods Appl. Mech. Eng.*, 196(17-20):2117–2129, 2007.

[36] O. Brüls and P. Eberhard. Sensitivity analysis for dynamic mechanical systems with finite rotations. *Int. J. Numer. Methods Eng.*, 74(13):1897–1927, 2008.

[37] L. Noels, L. Stainier, and J. P. Ponthot. A first-order energy-dissipative momentum-conserving scheme for elasto-plasticity using the variational updates formulation. *Comput. Methods Appl. Mech. Eng.*, 197(6-8):706–726, 2008.

[38] E. V. Lens and A. Cardona. A nonlinear beam element formulation in the framework of an energy preserving time integration scheme for constrained multibody systems dynamics. *Comput. Struct.*, 86(1-2):47–63, 2008.

[39] J. C. Simo, N. Tarnow, and M. Doblare. Non-linear dynamics of three-dimensional rods: Exact energy and momentum conserving algorithms. *Int. J. Numer. Methods Eng.*, 38(9):1431–1473, 1995.

[40] G. Jelenić and M. A. Crisfield. Stability and convergence characteristics of conserving algorithms for dynamics of 3D rods. Technical report, Imperial College London, Department of Aeronautics, Aero report 99-02, 1999.

[41] G. Jelenić and M. A. Crisfield. Energy–momentum dynamic integrator for geometrically exact 3D beams: Attempt at a strain-invariant solution. Technical report, Imperial College London, Department of Aeronautics, Aero report 99-04, 1999.

[42] G. Jelenić and M. A. Crisfield. Problems associated with the use of Cayley transform and tangent scaling for conserving energy and momenta in the Reissner-Simo beam theory. *Commun. Numer. Methods Eng.*, 18(10):711–720, 2002.

[43] V. Sonneville and O. Brüls. Sensitivity analysis for multibody systems formulated on a Lie group. *Multibody Syst. Dyn.*, 31(1):47–67, 2013.

[44] V. Sonneville, A. Cardona, and O. Brüls. Geometrically exact beam finite element formulated on the special Euclidean group. *Comput. Methods Appl. Mech. Eng.*, 268:451–474, 2014.

[45] V. Sonneville and O. Brüls. A Formulation on the Special Euclidean Group for Dynamic Analysis of Multibody Systems. *J. Comput. Nonlinear Dyn.*, 9(4):041002, 2014.

[46] V. Sonneville, A. Cardona, and O. Brüls. Geometric Interpretation of a Non-Linear Beam Finite Element on The Lie Group SE(3). *Arch. Mech. Eng.*, 61(2):305–329, 2014.

[47] M. A. Crisfield and G. Jelenić. Objectivity of strain measures in the geometrically exact three-dimensional beam theory and its finite-element implementation. *Proc. R. Soc. A Math. Phys. Eng. Sci.*, 455(1983):1125–1147, 1999.

[48] G. Jelenić and M. Saje. A kinematically exact space finite strain beam model — finite element formulation by generalized virtual work principle. *Comput. Methods Appl. Mech. Eng.*, 120(1-2):131–161, 1995.

[49] G. Jelenić and M. A. Crisfield. Interpolation of rotational variables in nonlinear dynamics of 3D beams. *Int. J. Numer. Methods Eng.*, 43(7):1193–1222, 1998.

[50] I. Romero. The interpolation of rotations and its application to finite element models of geometrically exact rods. *Comput. Mech.*, 34(2):121–133, 2004.

[51] G. Jelenić and M. A. Crisfield. Geometrically exact 3D beam theory: implementation of a strain-invariant finite element for statics and dynamics. *Comput. Methods Appl. Mech. Eng.*, 171(1-2):141–171, 1999.

[52] A. Ibrahimbegović and R.L. Taylor. On the role of frame-invariance in structural mechanics models at finite rotations. *Comput. Methods Appl. Mech. Eng.*, 191(45):5159–5176, 2002.

[53] S. Ghosh and D. Roy. A frame-invariant scheme for the geometrically exact beam using rotation vector parametrization. *Comput. Mech.*, 44(1):103–118, 2009.

[54] S. Ghosh and D. Roy. Consistent quaternion interpolation for objective finite element approximation of geometrically exact beam. *Comput. Methods Appl. Mech. Eng.*, 198(3-4):555–571, 2008.

[55] H. Zhong, R. Zhang, and N. Xiao. A quaternion-based weak form quadrature element formulation for spatial geometrically exact beams. *Arch. Appl. Mech.*, 84(12):1825–1840, 2014.

[56] P. Betsch and P. Steinmann. Frame-indifferent beam finite elements based upon the geometrically exact beam theory. *Int. J. Numer. Methods Eng.*, 54(12):1775–1788, 2002.

[57] I. Romero and F. Armero. An objective finite element approximation of the kinematics of geometrically exact rods and its use in the formulation of an energy-momentum conserving scheme in dynamics. *Int. J. Numer. Methods Eng.*, 54(12):1683–1716, 2002.

[58] D. Zupan and M. Saje. Finite-element formulation of geometrically exact three-dimensional beam theories based on interpolation of strain measures. *Comput. Methods Appl. Mech. Eng.*, 192(49-50):5209–5248, 2003.

[59] D. Zupan and M. Saje. The three-dimensional beam theory: Finite element formulation based on curvature. *Comput. Struct.*, 81(18-19):1875–1888, 2003.

[60] C. Sansour and W. Wagner. Multiplicative updating of the rotation tensor in the finite element analysis of rods and shells - a path independent approach. *Comput. Mech.*, 31(1-2):153–162, May 2003.

[61] O. A. Bauchau, A. Epple, and S. Heo. Interpolation of finite rotations in flexible multi-body dynamics simulations. *Proc. Inst. Mech. Eng. Part K J. Multi-body Dyn.*, 222(4):353–366, 2008.

[62] M. C. Saravia, S. P. Machado, and V. H. Cortínez. A consistent total Lagrangian finite element for composite closed section thin walled beams. *Thin-Walled Struct.*, 52:102–116, 2012.

[63] R. W. Ogden. *Non-Linear Elastic Deformations*. Dover Publications, Mineola, New York, 1997.

[64] J. E. Marsden and T. J. R. Hughes. *Mathematical Foundations of Elasticity*. Dover, Mineola, New York, 1994.

[65] A. Ibrahimbegović. Stress resultant geometrically nonlinear shell theory with drilling rotations—Part I. A consistent formulation. *Comput. Methods Appl. Mech. Eng.*, 118(3-4):265–284, 1994.

[66] L. Meirovitch. *Methods of Analytical Dynamics*. Dover, Mineola, New York, 2012.

[67] L. Sciavicco and B. Siciliano. *Modelling and Control of Robot Manipulators*. Springer Science & Business Media, London, 2000.

[68] V. G. Ivančević and T. T. Ivančević. Lecture Notes in Lie Groups. Technical report, Land Operations Division, Defence Science & Technology Organisation, Edinburgh, Australia, 2011.

[69] O. A. Bauchau and L. Trainelli. The Vectorial Parameterization of Rotation. *Nonlinear Dyn.*, 32(1):71–92, 2003.

[70] T. R. Kane. *Dynamics. Holt, Rinehart and Winston*. Holt, Rinehart and Winston, New York, 1968.

[71] A. Ibrahimbegović. On the choice of finite rotation parameters. *Comput. Methods Appl. Mech. Eng.*, 149(1-4):49–71, 1997.

[72] J. S. Dai. An historical review of the theoretical development of rigid body displacements from Rodrigues parameters to the finite twist. *Mech. Mach. Theory*, 41(1):41–52, 2006.

[73] J. Argyris. An excursion into large rotations. *Comput. Methods Appl. Mech. Eng.*, 32(1-3):85–155, 1982.

[74] T. J. R. Hughes. *The Finite Element Method*. Prentice-Hall, Inc., Englewood Cliffs, New Jersey, 1987.

[75] F. Irgens. *Continuum Mechanics*. Springer Science & Business Media, 2008.

[76] M. Gaćeša and G. Jelenić. Modified fixed-pole approach in geometrically exact spatial beam finite elements. *Finite Elem. Anal. Des.*, 99:39–48, 2015.

[77] O. C. Zienkiewicz, R. L. Taylor, and J. Z. Zhu. *The Finite Element Method: its Basis and Fundamentals*. Elsevier, 2005.

[78] R. A. Spurrier. Comment on "Singularity-Free Extraction of a Quaternion from a Direction-Cosine Matrix". *J. Spacecr. Rockets*, 15(4):255–255, 1978.

List of Figures

List of Tables